

SUSTAINABLE CROSS-COUPPLINGS FOR PHARMACEUTICAL SCALE-UP USING ARYLDIAZONIUM SALTS



GlaxoSmithKline / University of Strathclyde Industrial PhD Programme

Aymeric Pierre Colleville

Thesis

submitted in partial fulfilment of the requirements for the degree of
Doctor of Philosophy

March 2016

GlaxoSmithKline Medicines Research Centre
Global API Chemistry & Analysis
Platform Technology & Science
Gunnel Woods Road, SG1 2NY
Stevenage, Herts
United Kingdom

University of Strathclyde
Department of Pure and Applied Chemistry
Thomas Graham Building
295 Cathedral Street, G1 1XL
Glasgow
United Kingdom

ABSTRACT**SUSTAINABLE CROSS-COUPPLINGS FOR PHARMACEUTICAL SCALE-UP
USING ARYLDIAZONIUM SALTS**

Aymeric Pierre Colleville

GlaxoSmithKline / University of Strathclyde industrial PhD programme

Cross-coupling reactions are some of the most important tools to form aryl-aryl bonds in modern organic chemistry because of the predominance of this motif in pharmaceuticals, agrochemicals and materials. In this context, aryldiazonium salts are very promising building blocks owing to their ability to release benign by-products (nitrogen gas, which represents 80% of the composition of the atmosphere). This characteristic makes them very attractive from a pharmaceutical development point of view and their high reactivity provides a unique opportunity to develop new types of reactivity involving transition metal catalysis. However, this high reactivity can also translate into instability, potentially to explosivity and as a consequence their use is not well established. This thesis aims to render aryldiazonium salts more accessible by presenting results of studies on preparation, stability and couplings focused on the sustainability, efficiency and novelty of the processes. The use of aryldiazonium salts as arylating agents was investigated from a process chemistry perspective and were found to be efficient in both palladium catalysed cross-couplings and radical C-H arylations. Both methodologies were optimised using statistical tools (Design of Experiment, Orthogonal Partial Least Square regression) and optimal reaction conditions were applied to a range of functionalised substrates. Ultimately, a full scale-up study was conducted for the kilogram-scale synthesis of a selected aryldiazonium salts and the subsequent palladium-mediated coupling to generate a valuable intermediate involved in the synthesis of important angiotensin II inhibitors. Valuable mechanistic insights were also obtained for the radical C-H arylation of *N*-oxide heterocycles through IR monitoring and X-ray crystallography which allowed the identification of a triazene intermediate and refuted the role of ascorbic acid as radical initiator in this transformation.

TABLE OF CONTENTS

ABSTRACT	2
TABLE OF CONTENTS	3
ACKNOWLEDGMENTS	6
ABBREVIATIONS	7
CHAPTER I INTRODUCTION	9
I.1 INTRODUCTION TO THE CONCEPT OF GREEN CHEMISTRY	9
I.2 THE STRUCTURE OF ARYLDIAZONIUM SALTS	11
I.3 PREPARATION OF ARYLDIAZONIUM SALTS	11
I.4 STABILITY OF ARYLDIAZONIUM SALTS	16
<i>I.4.i Stability-impacting factors</i>	<i>16</i>
<i>I.4.ii Managing the risks associated with the handling of aryldiazonium salts ...</i>	<i>17</i>
I.5 THE REACTIVITY OF ARYLDIAZONIUM SALTS	19
<i>I.5.i The versatility of aryldiazonium salts</i>	<i>19</i>
<i>I.5.ii Nucleophilic substitution on the carbon-diazonium bond</i>	<i>21</i>
<i>I.5.iii Halogenation, sulfonylation and trifluoromethylation reactions</i>	<i>23</i>
<i>I.5.iv Borylation reactions</i>	<i>26</i>
<i>I.5.v Aryldiazonium salts as superelectrophilic cross-coupling partners</i>	<i>29</i>
<i>I.5.vi Transition metal promoted arylation: The Meerwein reaction</i>	<i>37</i>
<i>I.5.vii Base-mediated arylations : The Gomberg-Bachmann reaction</i>	<i>40</i>
<i>I.5.viii Organocatalytic transformations</i>	<i>42</i>
<i>I.5.ix Miscellaneous transformations involving aryldiazonium salts</i>	<i>44</i>
I.6 DRAWBACKS AND ADVANTAGES OF ARYLDIAZONIUM SALTS	46
CHAPTER II AIMS	48
CHAPTER III RESULTS & DISCUSSION	50
III.1 SYNTHESIS, ISOLATION AND THERMAL STABILITY ASSESSMENT OF ARYLDIAZONIUM SALTS	50
<i>III.1.i Synthesis and isolation of aryldiazonium tetrafluoroborate salts</i>	<i>50</i>
<i>III.1.ii Synthesis and isolation of aryldiazonium tosylate salts</i>	<i>55</i>
<i>III.1.iii Synthesis and isolation of aryldiazonium dihydrogen phosphate salts ...</i>	<i>57</i>
<i>III.1.iv Synthesis and isolation of a benzyne precursor</i>	<i>59</i>
<i>III.1.v Thermal stability assessment of aryldiazonium salts</i>	<i>60</i>
<i>III.1.vi Scale-up study</i>	<i>65</i>
III.2 ARYLDIAZONIUM SALTS AS GREEN AND EFFICIENT COUPLING PARTNERS FOR THE SUZUKI-MIYAJIMA REACTION	67
<i>III.2.i Reducing the cost of palladium catalysis in the pharmaceutical industry .</i>	<i>67</i>
<i>III.2.ii Investigating the impact of the palladium catalyst properties</i>	<i>69</i>
<i>III.2.iii Identifying the optimal solvent through OPLS and PCA analysis</i>	<i>71</i>
<i>III.2.iv Optimisation of the reaction conditions through Design of Experiments .</i>	<i>75</i>
<i>III.2.v Exploring the scope of the reaction</i>	<i>79</i>

III.2.vi Designing the process for industrial scale	81
III.2.vii Comparison with existing methodologies	84
III.2.viii End game – synthesis of Valsartan.....	85
III.2.ix Preliminary work towards flow chemistry	86
III.2.x Reaction mechanism.....	90
III.2.xi Conclusion & future work.....	91
III.3 RADICAL ARYLATION OF HETEROCYCLES.....	91
III.3.i From metal catalysis to organocatalysis.....	91
III.3.ii Screening of N-oxide heterocycles	92
III.3.iii Identifying the optimal solvent through OPLS and PCA analysis	95
III.3.iv Optimising the reaction conditions through Design of Experiments	99
III.3.v Investigating the role of ascorbic acid.....	102
III.3.vi Scale-up and calorimetry study	112
III.3.vii Scope of the metal-free, ascorbic acid-free arylation	114
III.3.viii Formal synthesis of SB222200	116
III.3.ix Future work	117
CHAPTER IV CONCLUSION	118
CHAPTER V EXPERIMENTAL	120
V.1 GENERAL EXPERIMENTAL	120
V.2 SYNTHESIS AND ISOLATION OF ARYLDIAZONIUM SALTS	124
V.2.i General diazotisation procedure 1 using boron trifluoride – THF complex	124
V.2.ii General diazotisation procedure 2 using PTSA.....	131
V.2.iii Synthesis of 4-bromo-benzenediazonium dihydrogen phosphate 195..	132
V.2.iv Synthesis of 2-carboxylate-benzenediazonium 163	133
V.2.v Scale-up of 2-Cyano-benzenediazonium tetrafluoroborate 182	134
V.3 CROSS-COUPLING OF ARYLDIAZONIUM SALTS	135
V.3.i Catalyst and solvent screening procedure	135
V.3.ii Design of Experiments Reactions	136
V.3.iii General cross-coupling procedure for substrate scope	136
V.3.iv Control reactions for safety assessment	141
V.3.v Cross-coupling scale-up procedure	142
V.3.vi Synthesis of N-((2'-Cyanobiphenyl-4-yl)-methyl)-(L)-valine methyl ester 225	142
V.3.vii Synthesis of N-Pentanoyl-N-((2'-cyanobiphenyl-4-yl)-methyl)-(L)-valine methyl ester 227	144
V.3.viii Synthesis of (S)-3-methyl-2-(N-{{2'-(2H-1,2,3,4-tetrazol-5-yl)biphenyl-4-yl}methyl}pentanamido)butanoic acid (Valsartan) 166.....	145
V.3.ix One-pot synthesis of ethyl 4-(benzofuran-2'-yl) benzoate 228.....	147
V.3.x Control reactions for oxidative coupling	148
V.3.xi Sequential diazotisation / cross-coupling reaction.....	149
V.3.xii Sequential diazotisation / cross-coupling reaction	149
V.4 RADICAL ARYLATION OF HETEROCYCLES	151
V.4.i General procedure for the screening of N-oxide heterocycles and solvents	151

TABLE OF CONTENTS

V.4.ii Design of Experiments Reactions	154
V.4.iii Synthesis of (3R,4S)-4-hydroxy-2-oxotetrahydrofuran-3-yl-2-(2-(4'-(trifluoromethyl)phenyl)hydrazinyl)-2-oxoacetate 261.....	155
V.4.iv Procedure for IR and LC/MS monitoring experiment	156
V.4.v Synthesis of 1,3 bis(4'-trifluoromethyl-phenyl)-triazene 264	157
V.4.vi Control reactions – synthesis of ethyl 4-(furan-2'-yl)-benzoate 267	158
V.4.vii Scale-up and calorimetry study	159
V.4.viii General procedure for the C-H arylation of N-oxide heterocycles	160
V.4.ix Synthesis of 4-(methoxycarbonyl)-quinoline N-oxide 272.....	167
V.4.x Synthesis of 2-phenyl-4-(carboxy-(S)- α -ethylbenzylamine)-quinoline N-oxide 285.....	168
V.4.xi Synthesis of 2-phenyl-4-(carboxy-(S)- α -ethylbenzylamine)-quinoline	169
REFERENCES	171
APPENDIX 1 – Crystal data	178
APPENDIX 2 – Calibration curve	184
APPENDIX 3 – Calibration curve	185
APPENDIX 4 – Crystal data	186

ACKNOWLEDGMENTS

I would like to take this opportunity to thank all the people who have contributed to my enjoyment during the last three and a half years on the industrial PhD programme:

Dr Richard Horan and Prof Nicholas Tomkinson for their advice, inspiration and enthusiasm in this industrial PhD programme. Special thanks to Dr Katherine Wheelhouse for your involvement in the projects, valuable advice and supply of catalysts. Thanks for your support and for sharpening my interest in cutting edge organic chemistry.

GlaxoSmithKline and the University of Strathclyde for funding.

Prof Harry Kelly from GlaxoSmithKline and Prof William Kerr from the University of Strathclyde for allowing me to be part of this programme and for your support.

The Global API Chemistry & Analysis department at GlaxoSmithKline as well as the Tomkinson group at the University of Strathclyde for their warm welcome and for all the good times spent together.

Sandrine Olazabal for her assistance with the statistical methods (PCA, OPLS and DoE) and Andrew Payne from the Process Safety Group at GlaxoSmithKline for his precious advice regarding the thermal stability assessment of chemicals (DSC).

Dawn Peel for her assistance with travel bookings.

The Analytical Department staff at GlaxoSmithKline (Alec Simpson, Anne-Sophie Bretonnet, Ian Lynch and Dr William Leavens) for assisting me in generating accurate analytical data.

My family for their unconditional support and their inspiration.

Emilie for everything.

ABBREVIATIONS

Ac	Acetyl
Adj	Adjusted
aq	aqueous
ARC	Accelerated Rate Calorimetry
Bn	Benzyl
Boc	<i>tert</i> -Butyloxycarbonyl
bpy	Bi-pyridine
C	Charcoal
Cat	Catalyst / catalytic
Cp	Cyclopentyl
CPME	Cyclopentyl methyl ether
DABAI-Me ₃	Bis(trimethylaluminum)-1,4-diazabicyclo[2.2.2]-octane
dba	Dibenzylideneacetone
DCE	Dichloroethane
DMF	Dimethyl formamide
DMSO	Dimethyl sulfoxide
DNA	Deoxyribonucleic acid
DoE	Design of Experiments
DSC	Differential scanning calorimetry
Et	Ethyl
equiv	equivalents
HPLC	High-performance liquid chromatography
HRMS	High-resolution mass spectrometry
<i>i</i> -amyl	<i>iso</i> -pentyl
ICP	Inductively coupled plasma
<i>i</i> -Pr	<i>iso</i> -propyl
IR	Infrared
MCPBA	<i>meta</i> -Chloroperoxybenzoic acid
Me	Methyl
MP	Melting point
MW	Microwave
N.A.	Not applicable
N.D.	Not detected

ABBREVIATIONS

NHC	<i>N</i> -Heterocyclic carbene
NMP	<i>N</i> -Methyl-2-pyrrolidone
NMR	Nuclear magnetic resonance
N.R.	Not reported
Nu	Nucleophile
OPLS	Orthogonal projection to latent structures
O.S.	Oxidation state
PCA	Principal component analysis
Ph	Phenyl
Pred	Predicted
PTSA	<i>para</i> -Toluylsulfonic acid
Red	Reductant
rt	room temperature
SET	Single electron transfer
SN _{Ar}	Aromatic nucleophilic substitution
SPhos	2-Dicyclohexylphosphino-2',6'-dimethoxybiphenyl
T	Temperature
t	time
TBME	<i>tert</i> -Butyl methyl ether
TEMPO	2,2,6,6-Tetramethylpiperidine-1-oxyl
TFA	Trifluoroacetic acid
THF	Tetrahydrofuran
TMEDA	<i>N,N,N,N</i> -Tetramethylethylenediamine
UV	Ultraviolet
vol	Volumes of solvents (mL/g)

CHAPTER I INTRODUCTION

I.1 Introduction to the concept of Green Chemistry

As the reduction of the human impact on the environment has increasingly become a priority due to the necessity to preserve our planet, new concepts leading to a more sustainable world have arisen in almost all the fields concerned by this environmental challenge. Amongst them, the pharmaceutical industry is directly concerned by this effort as working on low volume and high complexity pharmaceuticals results in a high carbon footprint and a lot of effort is still required to improve this situation. As a consequence, chemists have developed the concept of Green Chemistry¹ which is based on 12 principles described as follows:¹

1. Prevention: It is better to prevent waste than to treat or clean up waste after it has been created.
2. Atom economy: Synthetic methods should be designed to maximise the incorporation of all materials used in the process into the final product.
3. Less hazardous chemical syntheses: Wherever practicable, synthetic methods should be designed to use and generate substances that possess little or no toxicity to human health and the environment.
4. Designing safer chemicals: Chemical products should be designed to effect their desired function while minimising their toxicity.
5. Safer solvents and auxiliaries: The use of auxiliary substances (e.g., solvents, separation agents, etc.) should be made unnecessary wherever possible and innocuous when used.
6. Designing for energy efficiency: Energy requirements of chemical processes should be recognized for their environmental and economic impacts and should be minimised. If possible, synthetic methods should be conducted at ambient temperature and pressure.
7. Use of renewable feedstocks: A raw material or feedstock should be renewable rather than depleting whenever technically and economically practicable.

8. Reduce derivatives: Unnecessary derivatisation (use of blocking groups, protection/ deprotection, temporary modification of physical/chemical processes) should be minimised or avoided if possible, because such steps require additional reagents and can generate waste.

9. Catalysis: Catalytic reagents (as selective as possible) are superior to stoichiometric reagents.

10. Design for degradation: Chemical products should be designed so that at the end of their function they break down into innocuous degradation products and do not persist in the environment.

11. Real-time analysis for pollution prevention: Analytical methodologies need to be further developed to allow for real-time, in-process monitoring and control prior to the formation of hazardous substances.

12. Inherently safer chemistry for accident prevention: Substances and the form of a substance used in a chemical process should be chosen to minimise the potential for chemical accidents, including releases, explosions, and fires.

These principles were designed to increase the sustainability of chemical processes by reducing and ultimately preventing waste generation as well as reducing the costs and being ethically good.

The aryl group is ubiquitous across chemistry and reactions to bring together commercial aryl substrates are among the most widely used in the industry.² Because of their wide use, this class of reactions has received significant attention to render them greener.³ As a consequence, aryldiazonium salts have recently seen a resurgence in popularity as the release of nitrogen gas (a non ozone depleting substance) associated with their reactivity provides a strong driving force for reactions. Hence, minimal amounts of catalysts or additives such as ligands can be employed in the transformations involving these species. According to these assertions, aryldiazonium salts may prove an interesting alternative for the ever more challenging development of Green Chemistry.

I.2 The structure of aryldiazonium salts

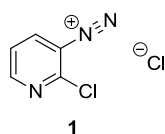


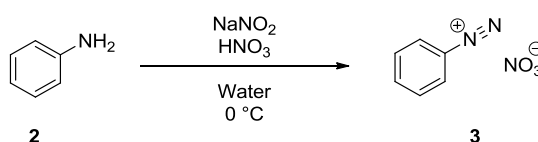
Figure 1: Aryldiazonium salt used in the synthesis of Zibotentan®⁴

Aryldiazonium salts are a class of organic compounds composed of an aromatic ring covalently bound to a positively charged diazo group, combined with a negatively charged counter-ion. Figure 1 shows an example of an aryldiazonium salt used in the preparation of Zibotentan®, an anti-cancer candidate from Astra Zeneca.⁴ These molecular entities comprise three important parts:

- The aromatic ring: Can be all carbon or heterocyclic, with or without substituents. Its electronic and steric properties have a pronounced impact on the stability and therefore the reactivity of the salt. This is the component which can be functionalised or coupled to a second component by reaction of the carbon-diazonium bond.
- The carbon-diazonium bond: This is where reactions take place driven by the release of nitrogen. This bond can react through several pathways including nucleophilic aromatic substitution, single electron transfer reduction and metal insertion (*vide infra*).
- The counter-ion: The complementary part of the aryldiazonium compound influences the stability of the salt by affecting the electronics and sterics of the diazonium bond and hence its reactivity.

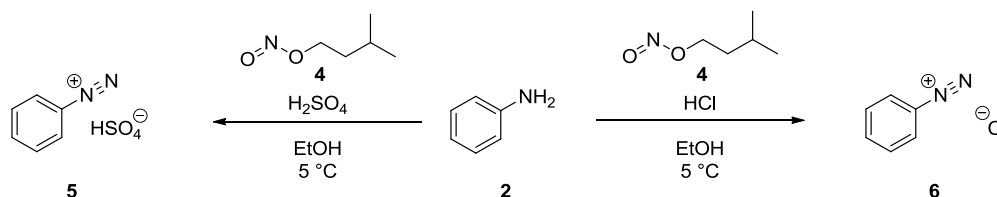
I.3 Preparation of aryldiazonium salts

The first preparation of an aryldiazonium salt was reported by Griess in 1867, forming the benzenediazonium nitrate salt **3** by reacting aniline **2** with nitric acid and sodium nitrite in water (Scheme 1).⁵



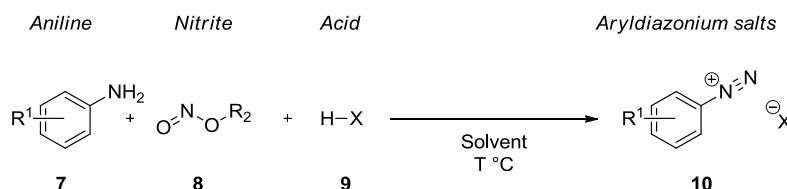
Scheme 1: First reported aryl diazotisation by Griess

The compound **3** exhibited very poor stability, as described by the author: “*Heated even below 100 °C, they explode with unparalleled violence, far surpassing that of fulminating mercury or iodide of nitrogen. About a gramme of this substance causes by its explosion a concussion like that produced by firing a pistol*”. Inspired by this first report on the preparation of an aryldiazonium salt, Knoevenagel detailed the synthesis and the isolation of the relatively more stable benzene diazonium hydrogen sulfate **5** and benzenediazonium chloride **6** in 1890, thereby reporting the first use of an alkyl nitrite **4** for the diazotisation of aniline **2** (Scheme 2).⁶



Scheme 2: Synthesis of benzenediazonium salts by Knoevenagel

Although these preparations were disclosed more than a century ago, it is worth mentioning that almost all aryldiazonium salts are still made through these processes. Through these first reports on aryldiazonium salt formation, the diazotisation reaction could be identified as a three component process: the aniline **7**, the nitrite **8** and the acid **9** (Scheme 3).



Scheme 3: Diazotisation as a three-component process

- **Aniline:** The substrate of the reaction. The amino group is transformed into a diazonium moiety and the core can be elaborated through this functionality.
- **Nitrite:** Can be either mineral (NaNO_2) or organic (alkylNO_2). Although the mineral nitrites are cheaper, organic nitrites are more convenient to handle as they are liquids, have a better solubility in organic solvents and are generally less toxic.
- **Acid:** Can be either Brønsted or Lewis acids. This component activates the nitrite to allow the diazotisation to proceed and also provides the counter-ion of the aryldiazonium salt.

These key components interact together following the mechanism detailed in Figure 2. The acid **9** activates the nitrite **8** to form the nitrosating agent **11** which, upon nucleophilic substitution by the aniline **7**, triggers the cascade of proton exchange and water release leading to the formation of aryldiazonium salt **10**.⁷

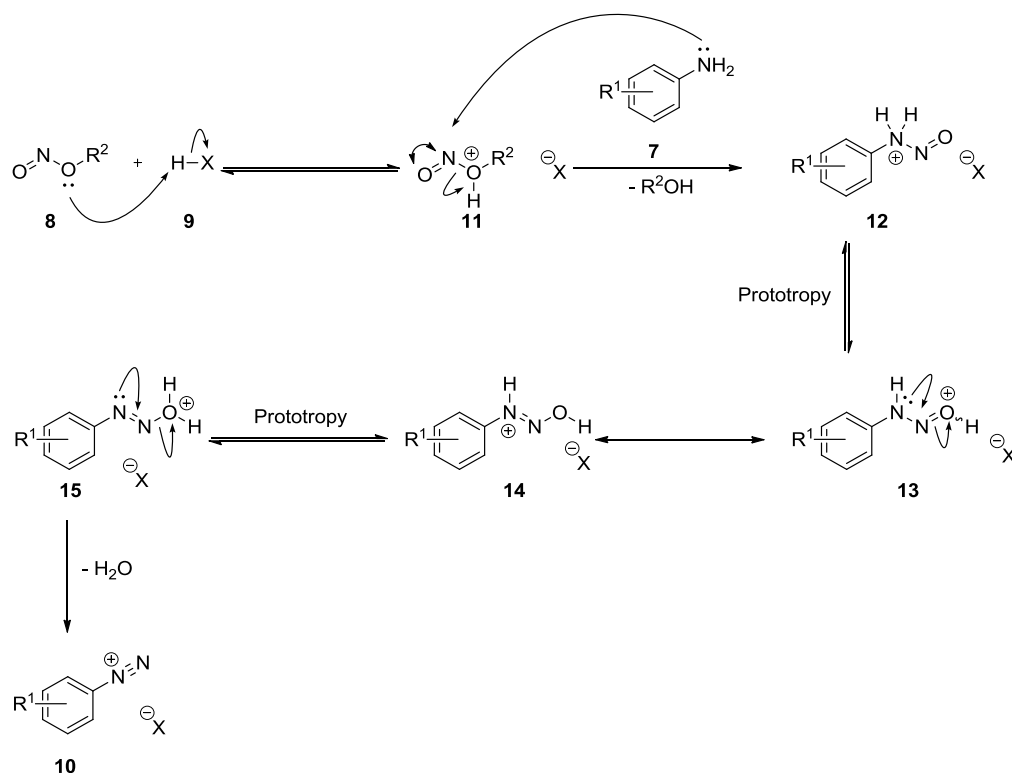
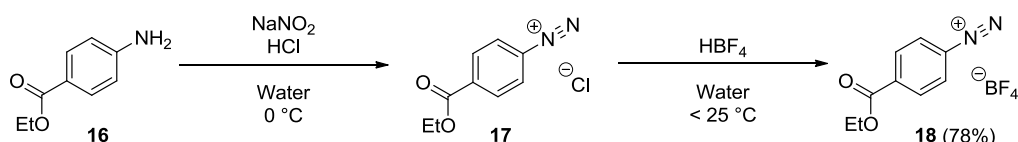


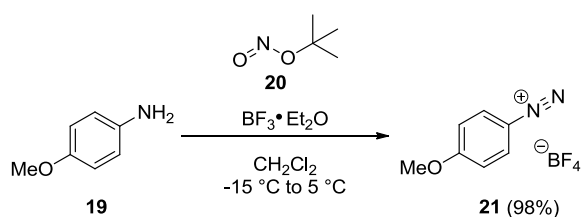
Figure 2: Diazotisation mechanism

The product of such reactions can also be easily isolated by precipitation through careful choice of the solvent. Hence aryldiazonium salts can easily be prepared from anilines through this modular approach and as a consequence, a wide range of functionalised aryl diazonium salts / counter-ion combinations have been prepared over the intervening decades.^{5,6,8-11} This approach was used by Schiemann and Winkel Müller in their synthesis of the first aryldiazonium tetrafluoroborate salt **18** in 1933 through the formation of the chloride salt **17** followed by an anion exchange with tetrafluoroboric acid in water (Scheme 4).¹²



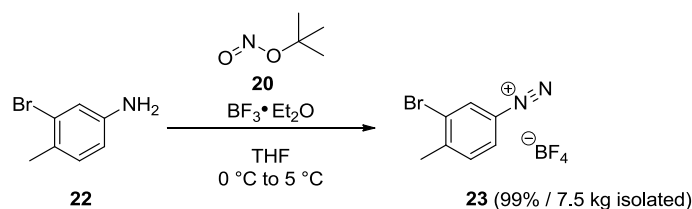
Scheme 4: First reported aryldiazonium tetrafluoroborate preparation

More recently, Doyle and co-workers described a direct synthesis of aryldiazonium tetrafluoroborate salts through the use of boron trifluoride etherate complex as a tetrafluoroborate source (Scheme 5).⁹



Scheme 5: Modern synthesis of aryldiazonium tetrafluoroborate salts

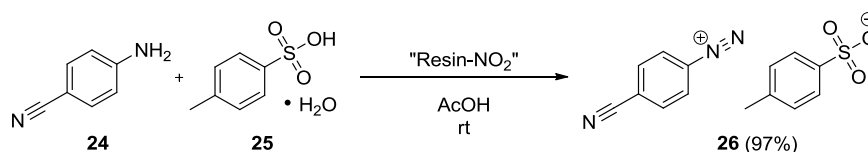
Early examples of the preparation of aryldiazonium salts often required water miscible solvents in order to dissolve inorganic nitrite (NaNO_2) or acid. In the Doyle procedure, all components were soluble in organic reaction media, adding to the flexibility of the transformation. It is thus possible to select an optimal solvent in which the starting aniline will be soluble but the aryldiazonium tetrafluoroborate product will precipitate, allowing facile isolation by filtration. Precipitating the product also provides an additional driving force for the reaction and prevents further reactions which may lead to the decomposition of the product. Recent large-scale preparation of these salts attests to the popularity of this method (Scheme 6).¹³



Scheme 6: Kilogramme-scale preparation of an aryldiazonium tetrafluoroborate salt

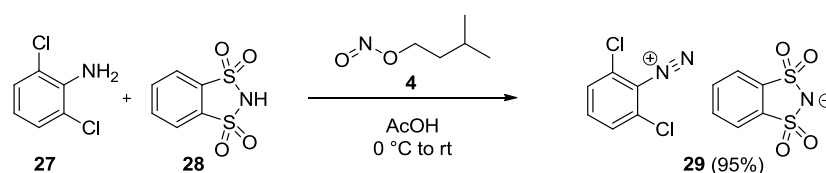
These reports on aryldiazonium tetrafluoroborate salt formation emphasise the ease of preparation from cost-effective reagents, the simple isolation by filtration and safe handling of these species on large scale (*vide infra*, section II.1). It is hence possible to associate aryldiazonium salts with a multitude of counter-ions in order to tune stability, reactivity and solubility properties. As a consequence, alternative syntheses involving more elaborate counter-ions and focusing on the stability of these salts have arisen. In one of these efforts, aryldiazonium tosylate salts **26** were prepared by Filimonov and co-workers using an innovative polymer-supported nitrite and PTSA **25** (Scheme 7).¹¹ Whilst this approach is fluoride free, acetic acid is required for the reaction to proceed as only low yields were obtained in water with

PTSA **25** as sole acid. It is noteworthy that the precise reason for the need of the second acid was not clear from this report.



Scheme 7: Synthesis of aryldiazonium tosylate salts

Promising stability data were obtained for **26** when assessed by differential scanning calorimetry. In a similar manner, Barbero and co-workers isolated 1,2-benzenedisulfonimidate salts by reacting anilines with iso-amyl nitrite **4** in the presence of 1,2-benzenedisulfonimide **28** in acetic acid (Scheme 8).¹⁰



Scheme 8: Synthesis of aryldiazonium 1,2-benzenedisulfonimidate salts

1,2-Benzenedisulfonimidate salts **29** also proved to be relatively stable as these species could be stored at room temperature for months without decomposing and led to non-violent decomposition when heated at high temperature, both in solution and in the solid-state.

Aryldiazonium salts can therefore be prepared from anilines through a very modular and efficient three-component diazotisation which is compatible with a wide variety of reaction media. It is thus possible to telescope this step with subsequent reactions or to isolate the aryldiazonium salt product through a judicious choice of counter-ion / solvent combination. The counter-ion can also be tuned to influence properties such as stability, reactivity and solubility, affording enormous flexibility for downstream processing.

I.4 Stability of aryldiazonium salts

I.4.i Stability-impacting factors

Historically, diazo-compounds suffer from a bad reputation among chemists because of publications reporting unexpected and uncontrolled reactions which have led to explosion and damage.^{14,15} These reports confirm that the nature of the counter-ion has a strong influence on the solid-state stability of the aryldiazonium salt and emphasise the need to assess and understand the stability of these high-energy compounds. The kinetic stability may be influenced by nucleophilic counter-ions such as azides, sulfides, xanthates, carboxylates and picrates which can attack the aryldiazonium unit whereas the thermodynamic stability may be altered by counter-ions adding an enthalpic energy to the system such as chromates, nitrates, triiodides and perchlorates.¹⁴ While scientific data on the stabilisation of aryldiazonium species are empirical and limited, crystal structures of previously reported stable aryldiazonium chloride **6**,^{14,16} tetrafluoroborate **30**,^{14,16,17} tosylate **26**¹¹ and 1,2-benzenedisulfonimide **29**¹⁰ showed that the stabilising effect of these counter-ions was due to their highly coordinating nature (Table 1).^{10,11,17,18}

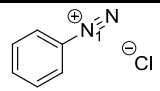
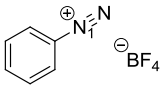
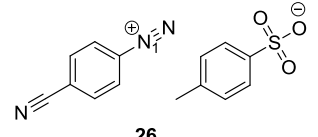
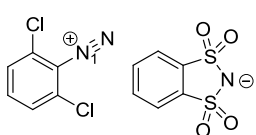
Entry	Aryldiazonium salt	Van der Waals Radii (Å)	N ₁ – X (Å)	N ₁ – N ₂ (Å)	N ₁ – C (Å)
1	 6	N + Cl = 3.30	3.24 (Cl)	1.097	1.385
2	 30	N + F = 3.02	2.83 (F)	1.083	1.415
3	 26	N + O = 3.07	2.77 (O)	1.094	1.417
4	 29	N + N = 3.10	2.98 (N)	1.088	1.387

Table 1: Selected bond lengths from aryldiazonium salt crystal structures

As shown by the data presented in Table 1, the counter-ion was always closely coordinated to the diazo bond (Table 1, N₁-N distance smaller than Van der Waals radii), suggesting that their electron donor properties were involved in an electronic density modification of the diazo bond while being non-nucleophilic (Figure 3).¹⁷

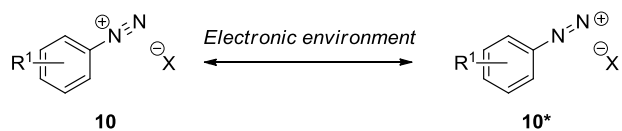


Figure 3: Positive charge transfer between nitrogen atoms

This electron-rich environment surrounding the diazonium group is believed to increase the ability of the diazo bond to share the positive charge between the two nitrogen atoms and hence increases its stability. This ability has been found to be a key mechanism for the stabilisation of aryldiazonium salts.¹⁷

While counter-ions play an important role in the stabilisation of these salts, it has also been reported that the nature of the substituents on the aromatic ring can influence the overall stability of the salt.¹⁹ The explosive character of these species is indeed enhanced by high-energy substituents (*i.e.* functional groups with high nitrogen content in a high oxidation state which would release nitrogen gas upon decomposition such as the nitro group)²⁰ on the aromatic core whereas a higher molecular weight decreases the energy per mass unit and contributes therefore to the stabilisation of the whole entity.

Although the nature of the counter-ion and ring substituents were found to have a direct impact on the stability of aryldiazonium salts, it is rarely possible to derive any structure-based rules given the complex interactions involved between the key stabilising factors. As a consequence it must be borne in mind that such salts are potentially explosive and their stability must therefore be assessed on a case-by-case basis.

1.4.ii Managing the risks associated with the handling of aryldiazonium salts

The relative instability of aryldiazonium salts also translates into a high synthetic potential and it is thus desirable and possible to manage the risks associated with the preparation and handling of these species through the consideration of the three key concepts: Knowledge, Substitution and Design (Figure 4).

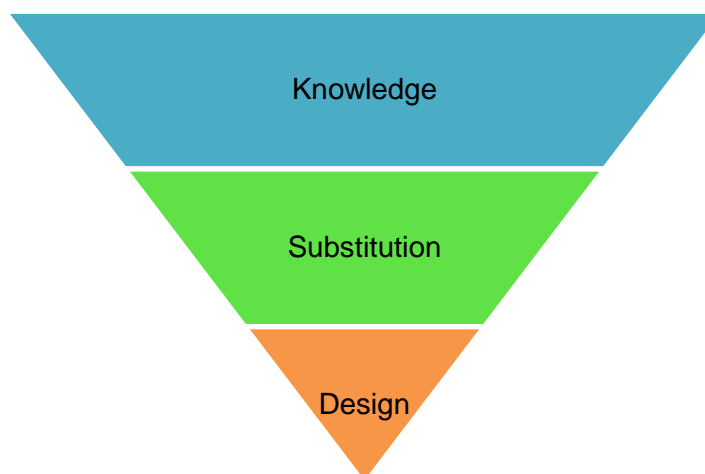


Figure 4: Hierarchical order of safety concepts

- Knowledge: Being aware of the hazards associated with any chemical involved in a reaction not only prepares the operator to deal with the risk associated with this chemical in the case of an accident but also allows for its substitution by a less hazardous reagent or to design a different process. In addition to the literature, the knowledge of the chemical hazards can be acquired through a variety of analytical techniques such as drop test, DSC and ARC for isolated materials and computer-assisted calorimetry reactors for reaction mixtures.
- Substitution: Substituting a hazardous reagent by a less hazardous chemical increases the overall safety of a reaction. The unique reactivity of aryldiazonium salts comes from their inherent structure and as a consequence it is not always possible to substitute them with safer alternatives. As discussed previously, the counter-ion plays an important role in their solid-state stability and as long as this component is not required for the subsequent reaction to proceed, it is preferable to substitute low-stabilising counter-ions by more stable alternatives when their isolation is intended. If the purpose of the aryldiazonium salt is to be reacted *in-situ*, the use of low-hazard and non-nucleophilic solvents should be investigated.
- Design: Some reactions can only be achieved by hazardous chemicals and it is still possible to considerably reduce the risks identified in the knowledge phase to an acceptable level by carefully designing the process operations. Appropriate process controls may be the slow addition of one of the reagents, the use of flow technologies or running the reaction on a small scale.²¹

The aim of this framework is not to deliver a totally safe process as it is not possible to eliminate all the risks associated with a chemical reaction but to reduce the risks associated with the use of aryldiazonium salts to an acceptable level. By following these guidelines, it is therefore possible to exploit the full synthetic potential of aryldiazonium salts in a safe environment.

I.5 The reactivity of aryldiazonium salts

I.5.i The versatility of aryldiazonium salts

Aryldiazonium salts can react through a variety of pathways, with or without the enthalpic and entropic release of nitrogen, to provide to a wide range of products. These different pathways were indexed by Zollinger in 1973 and thereby provided a first insight on the versatility of these species.²²

One of the types of reactivity associated with the diazo bond is the reaction of nucleophiles at the β -nitrogen to form a diazo-compound (Figure 5). In this transformation, various types of nucleophile can be used and the process is often referred to as the azo-coupling for the preparation of diazo-dyes **31** with nucleophilic aromatic rings.²³

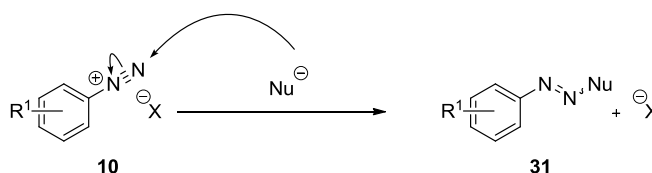


Figure 5: Nucleophilic attack at the β -nitrogen

An alternative nucleophilic addition path can also occur at the carbon bound to the diazonium group through a formal S_{N_Ar} mechanism (Figure 6). It is noteworthy that the regioselectivity of nucleophilic additions is dictated by the nature of the nucleophile as well as by the reaction conditions employed.²²

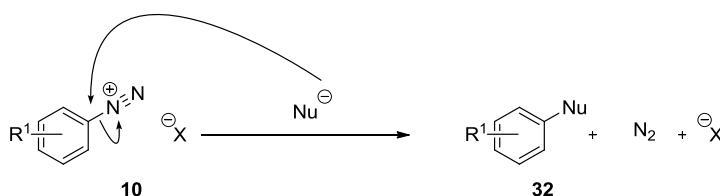


Figure 6: Heterolytic dediazotisation – nucleophilic substitution

In contrast with the previous heterolytic processes, the carbon-diazonium bond can also undergo a homolytic cleavage through a single-electron transfer with a reductant to form an aryl radical **33** through the entropically favoured release of nitrogen (Figure 7). This extremely reactive radical can then be involved in a large variety of transformations ranging from halide abstraction to attack on π -systems and is thus considered as a major reactive intermediate in the chemistry of aryldiazonium salts.²²

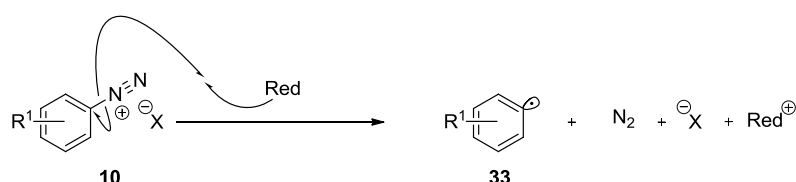


Figure 7: Single Electron Transfer dediazotisation

The reactivity of the carbon-diazonium bond can also be enabled by the oxidative insertion of a transition metal catalyst (often palladium) leading to the formation of an organometallic complex **36** (Figure 8).²⁴ Such complexes are designed to undergo cross-coupling reactions which are of central importance to organic synthesis, particularly in industry, as acknowledged by the Nobel Prize for Chemistry in 2010.²⁵

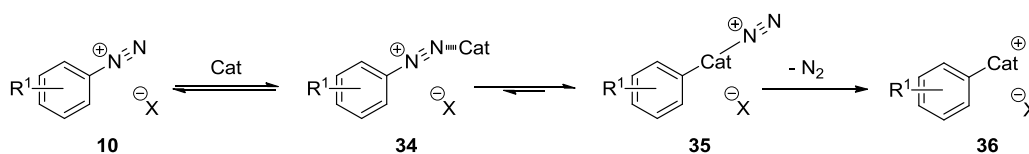


Figure 8: Catalyst insertion into the carbon-diazonium bond

While the previous reactivities were the results of extra-molecular interactions, intra-molecular decomposition of aryldiazonium salts bearing an electrofugal leaving group in the *ortho*-position has also been observed (Figure 9).²⁶ Such decompositions lead to the formation of nitrogen as well as reactive aryne intermediates **37** which are efficient partners for cyclo-addition reactions.²⁷

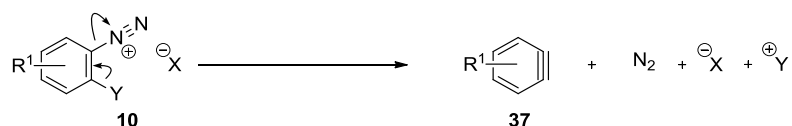


Figure 9: Aryne formation through intra-molecular decomposition

The synthetic power of aryldiazonium salts therefore comes from their ability to afford a wide range of skeletally different products through the tunable reactivity of the diazo-group. As a consequence, a number of synthetically useful transformations involving these species have been developed, including those based on aromatic ring functionalisation with halide, cyanide, thiol, trifluoromethyl, amide, boronic ester as well as carbon based species. A selection of products arising from the reaction of an aryldiazonium salt **10** replacing the C-N bond is shown on Figure 10. In the following section, each of these reactions will be described in more detail.

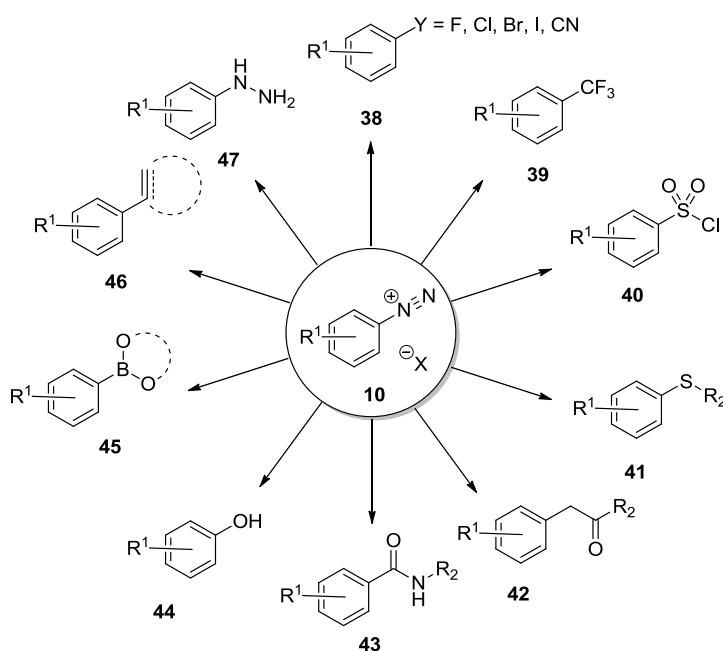
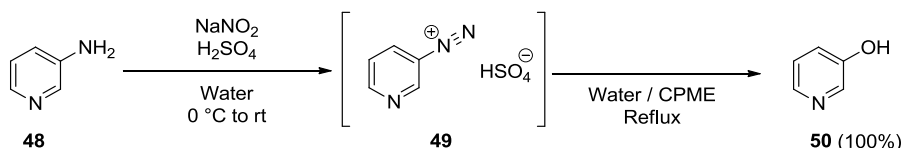


Figure 10: Versatility of aryldiazonium salts

1.5.ii Nucleophilic substitution on the carbon-diazonium bond

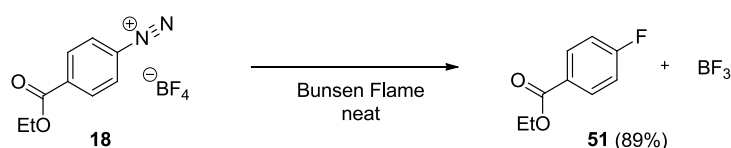
The direct nucleophilic substitution on the carbon-diazonium bond was exemplified by Tanigushi *et al.* who reported aryldiazonium salts to be efficient phenol precursors by reaction with water (Scheme 9).²⁸



Scheme 9: Hydrolysis of aryldiazonium salt in a biphasic system

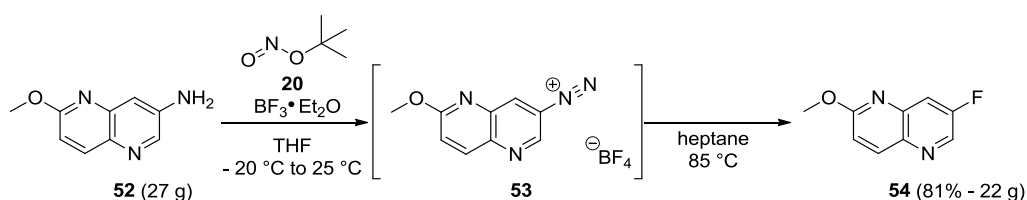
Interestingly, this reaction was found to proceed better when a biphasic system consisting of CPME and water was employed as it minimised the formation of tar products. Considering the co-products (sodium sulfate, water and nitrogen) as well as the reagents employed, this reaction is arguably a model sustainable method to afford phenolic compounds.

Another example of this class of reactivity is the fluorination of aryldiazonium tetrafluoroborate salts. In 1933, Schiemann and Winkelmueller reported the direct displacement of the diazonium group by fluoride through the thermal degradation of these species (Scheme 10).¹²



Scheme 10: Schiemann synthesis of fluoro-aryl derivatives

While this method may be considered as extreme, the concept of using the tetrafluoroborate counter-ion as a cheap source of fluoride remains attractive and as a consequence, industrial chemists from Actelion Pharmaceuticals have applied this transformation to the synthesis of a relevant drug intermediate **54** under more practical and controlled conditions (Scheme 11).²⁹



Scheme 11: Synthesis of a relevant drug intermediate through fluorodediazotisation

It is noteworthy that hydrogen fluoride was also found to be suitable for the conversion of an aniline to an aryl fluoride as it provides an acidic environment for the diazotisation of the aniline **52** while being a source of fluoride for the displacement of the diazonium group and similar yields were reported for the synthesis of fluoro-naphthyridine **54** (90% yield). Even though fluorine is the only halide able to be introduced through direct nucleophilic substitution, other halides such as chlorine, bromine and iodine can also be introduced through another type of reactivity.

1.5.iii Halogenation, sulfonylation and trifluoromethylation reactions

Aryl halides are an important class of molecules in medicinal chemistry thanks to their unique bonding abilities^{30,31} and their reactivity in cross-coupling reactions to afford more elaborated products. The most common preparation of these compounds through electrophilic halogenation is challenging as regioselectivity issues are often observed and harsh reaction conditions frequently required. An alternative approach to this method is the Sandmeyer reaction which has been used since the 19th century to prepare aryl halide species from aryl diazonium precursors through a copper-catalysed process (Figure 11).^{32–34}

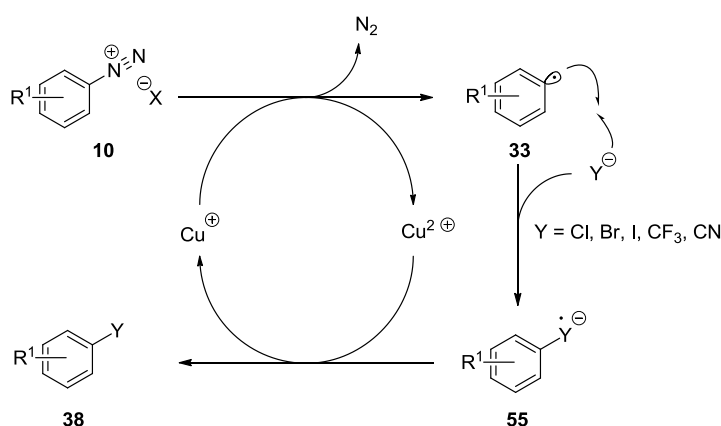
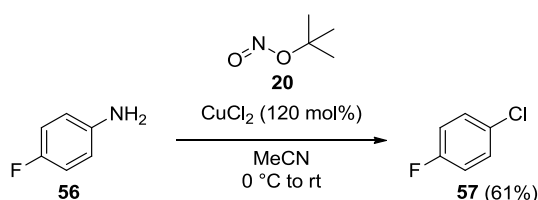


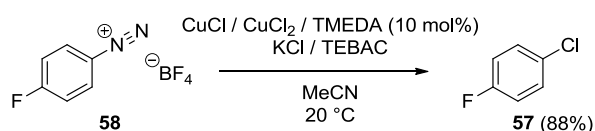
Figure 11: Mechanism of the Sandmeyer reaction

Aryldiazonium **10** is reduced by a copper(I) halide through a single electron transfer to generate nitrogen and a very reactive aryl radical **33** which then combines with the halide to give the corresponding aryl halide **56** after oxidation by copper(II) to regenerate copper(I). This named reaction has been extensively studied over the past century³⁵ by many research groups, including by Doyle and co-workers who telescoped the diazotisation step with the halogen exchange reaction in a one-pot process (Scheme 12).³⁶



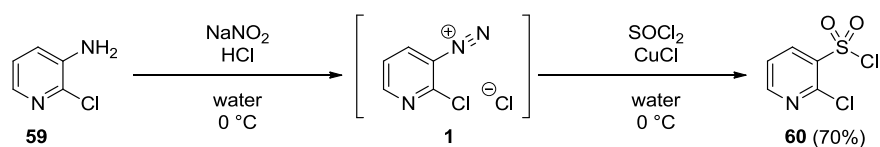
Scheme 12: One-pot diazotisation / chloro-dediazotisation reaction

Although this process is formally catalytic in copper, this procedure as well as many others require a stoichiometric amount of copper(II) halide to proceed. It was found by Beletskaya *et al.*³⁷ that a substoichiometric amount of this transition metal could be employed in this transformation when ligands such as TMEDA or phenanthroline were added to the reaction mixture (Scheme 13).



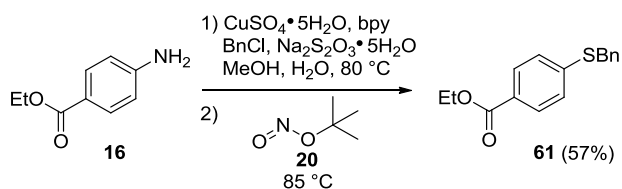
Scheme 13: Sandmeyer reaction in the presence of a ligand

It is also noteworthy that the use of isolated aryldiazonium tetrafluoroborate salts gave more control in the halogenation reaction as the impurities resulting from the diazotisation step were removed and thus higher yields were observed for this individual transformation (compare Schemes 12 and 13). As a consequence, bromide, chloride and iodide substituents can be introduced on aromatic rings through the copper-catalysed Sandmeyer reaction and in an effort to expand the scope of this well-established process, Hogan and Cox demonstrated⁴ its application to the synthesis of aryl sulfonyl chloride derivatives (Scheme 14). The process was initiated by the preparation of the pyridyldiazonium chloride salt **1** in the presence of sodium nitrite and hydrochloric acid in water. The resulting slurry was added at low temperature to an aqueous solution of thionyl chloride and copper(I) chloride to generate the corresponding pyridyl sulfonyl chloride **60**. It is noteworthy that precipitation of sulfonyl chloride derivative **60** from water prevents its hydrolysis and explains the high yield obtained.



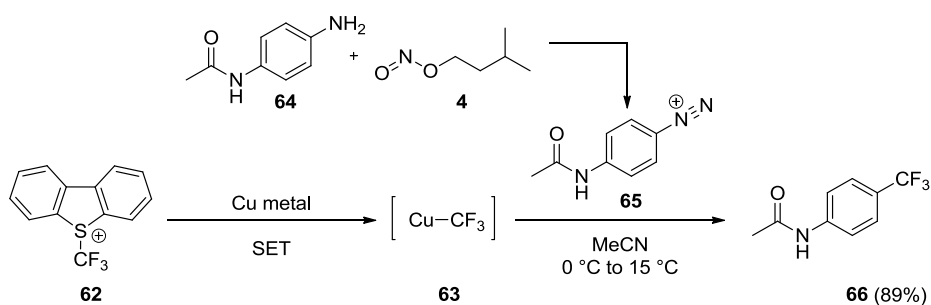
Scheme 14: Sandmeyer sulfonylation of aryldiazonium salts

Similarly, copper catalysis also allows for the introduction of sulfide substituents by using sodium thiosulfate as sulfurating agent in the presence of an aryldiazonium salt formed *in situ* (Scheme 15).³⁸ It is noteworthy that this three-component procedure avoids the handling of odorous thiols for the synthesis of these aromatic sulfide compounds.

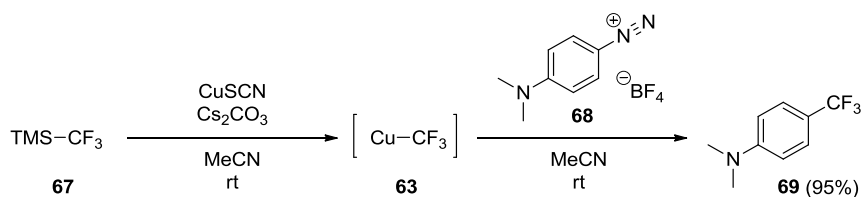


Scheme 15: Sandmeyer sulfuration of aryl diazonium salts

The scope of this copper-catalysed functionalisation was later expanded further by two groups led by Fu³⁹ and Goossen⁴⁰ who reported the synthesis of pharmaceutically relevant⁴¹ trifluoromethyl aryl derivatives (Schemes 16 & 17).



Scheme 16: Sandmeyer trifluoromethylation developed by Fu et al.



Scheme 17: Sandmeyer trifluoromethylation developed by Goossen et al.

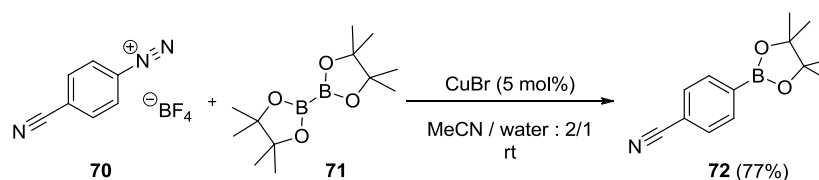
Both methods infer to the *in-situ* preparation of the copper-based trifluoromethylation agent **63**. In contrast with the strategy developed by Fu which proceeds through a single electron transfer between metallic copper and Umemoto's reagent **62** to generate trifluoromethyl copper(I) **63**, Goossen's preparation of this intermediate is a combination of the Ruppert – Prakash reagent **67** with a source of copper(I) in the presence of a caesium base. The reactivity of this copper-based intermediate towards aryl diazonium salts is thus similar to that observed in the Sandmeyer reaction and therefore leads to the corresponding trifluoromethyl aryl compounds.

This synthetic method provides a low-cost and sustainable framework for the radical bromination, chlorination, iodination, sulfonylation and trifluoromethylation of aryl diazonium salts. The scope of this reaction can also be extended to the synthesis of aryl cyanide derivatives¹⁹ as well as to pinacol aryl boronate

compounds,⁴² providing a robust and reliable method to introduce variety of highly relevant functional groups directly from an aniline.

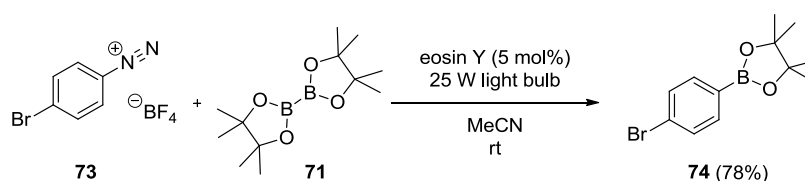
1.5.iv Borylation reactions

Beyond the synthesis of aryl halides from aryldiazonium salts, the Sandmeyer conditions can also be used to prepare their nucleophilic counter-part in the Suzuki-Miyaura cross-coupling reaction.^{43–45} Borylation reactions have therefore received a great deal of attention over the last decade with the desire to develop sustainable methods to access these valuable compounds. Yu and co-workers reported the synthesis of pinacol aryl boronate derivatives through the action of copper(I) bromide on aryldiazonium tetrafluoroborate salts and the use of bis(pinacolato)diboron **71** as boron source (Scheme 18).⁴²



Scheme 18: Sandmeyer borylation of aryldiazonium salts

This radical approach can also be exploited in the absence of a transition metal catalyst with the recent development and implementation of photochemical methodologies.⁴⁶ Among them, a metal-free borylation of aryldiazonium salts induced by visible light in combination with eosin Y was disclosed by Yu and co-workers in 2012 (Scheme 19).⁴⁷



Scheme 19: Metal-free, visible light-induced borylation reaction reported by Yu et al.

The mechanism of this photo-catalysed transformation is shown in Figure 12.⁴⁷ Visible-light irradiation of eosin Y generates an excited state increasing its reduction potential. This reacts with the aryldiazonium salt **10** to generate a reactive aryl radical **33** which is trapped by bis(pinacolato)diboron **71** to form the desired pinacol aryl boronate derivative **45**.

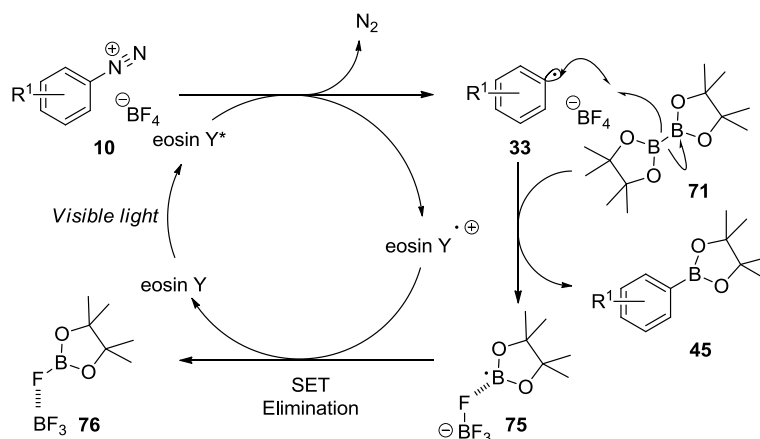
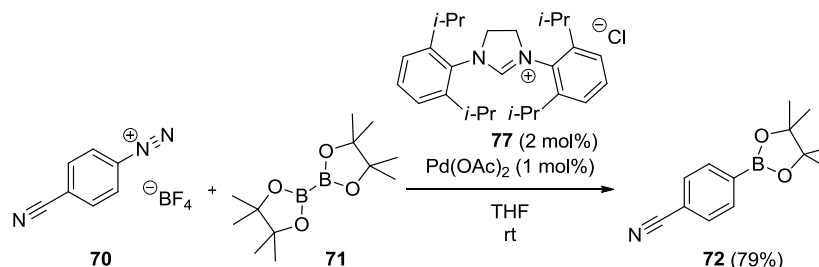


Figure 12: Mechanism of the photocatalysed borylation of aryldiazonium salts

This reaction is achieved with exquisite selectivity over halide substituents (Scheme 20) which are usually reacted in the more traditional palladium-catalysed borylation methods⁴⁸ such as the Miyaura borylation.⁴⁹ In this well-established transformation, the palladium catalyst inserts into the carbon-halide bond which can also be performed under similar conditions on carbon-diazonium bonds as reported by Andrus and co-workers (Scheme 20).⁵⁰ The borylation process is catalysed by a NHC-type ligand **77** – palladium complex and as observed previously, the bis(pinacolato)diboron **71** constitutes the source of pinacol boronate.



Scheme 20: Miyaura borylation of aryldiazonium salts

The mechanism of this transformation is shown in Figure 13. As discussed previously, the palladium inserts into the carbon-diazonium bond to generate an organometallic complex **36** and nitrogen by action of acetate anion. The complex then undergoes transmetalation with the diboron reagent to generate the pinacol aryl boronate derivative **45** by reductive elimination.

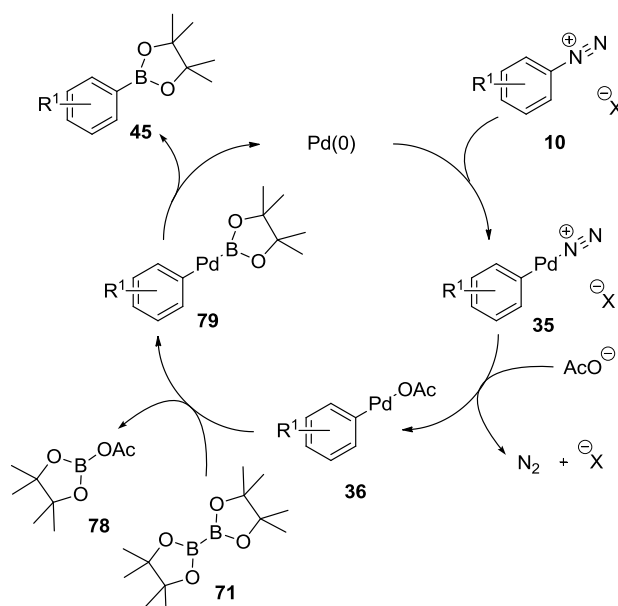
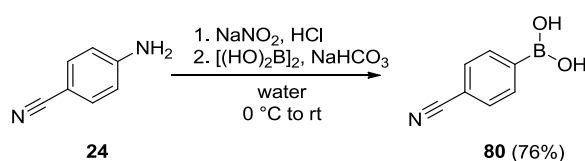


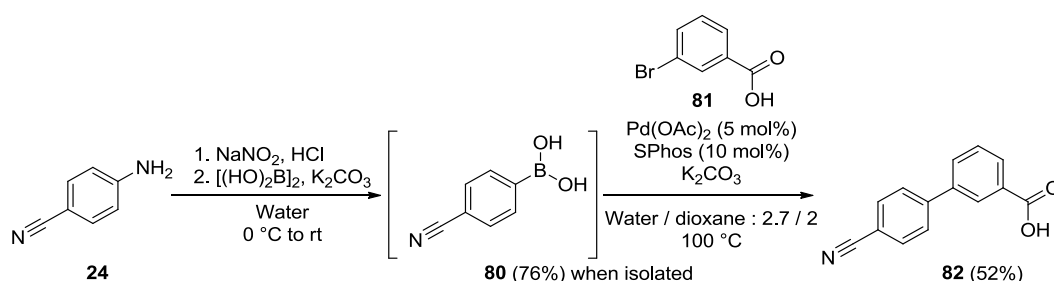
Figure 13: Miyaura borylation of aryldiazonium salts

Although pinacol aryl boronate derivatives are used in cross-coupling methodologies, it has previously been established that aryl boronic acids are more reactive species in such transformations^{48,51,52} and their synthesis was thus investigated by Blanchet *et al.* (Scheme 21).⁵³



Scheme 21: Aryl boronic acid synthesis from aryldiazonium salts

This methodology avoids the potentially challenging removal of the pinacol group and this activated coupling partner can thus be reacted without isolation in the subsequent palladium-catalysed Suzuki-Miyaura reaction with aryl halide derivatives (Scheme 22).⁵⁴



Scheme 22: Telescoped borylation / Suzuki-Miyaura cross-coupling in water

1.5.v Aryldiazonium salts as superelectrophilic cross-coupling partners

As discussed previously, aryldiazonium salts are relevant precursors for the preparation of both coupling partners involved in the palladium-catalysed Suzuki reaction⁴³⁻⁴⁵ (aryl halides and aryl boronic derivatives). As stated above, transition metals such as palladium also insert into the carbon-diazonium bond in a similar manner to aryl halides.⁵⁵ Consequently the direct cross-coupling of aryldiazonium species provides numerous advantages: expelling nitrogen offers a sustainable framework while by-passing the preparation of the corresponding aryl halide spares valuable resources such as time and cost (Figure 14).

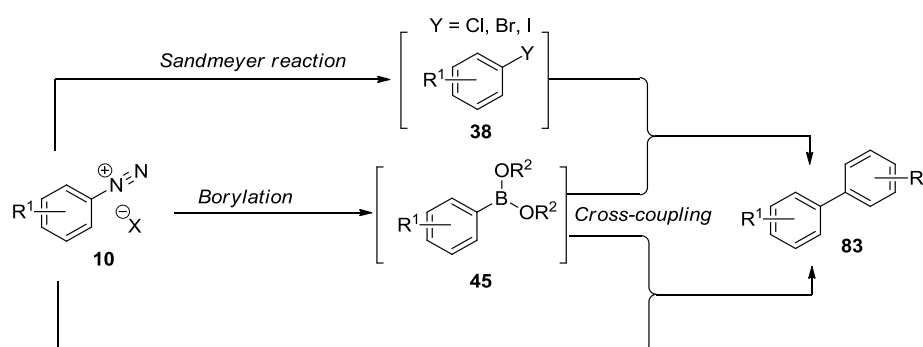
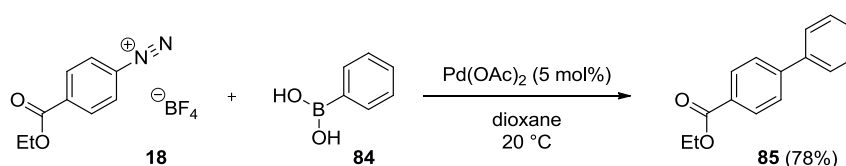


Figure 14: Cross-coupling strategies of aryldiazonium salts

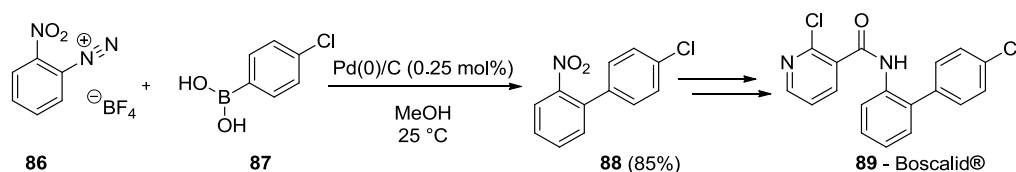
Given the importance of cross-coupling reactions, the direct cross-coupling of aryldiazonium species has been extensively studied over the last decades by a number of different groups.⁵⁶ Among them, Genet and co-workers⁵⁷ were the first to report the successful palladium-mediated coupling of aryldiazonium tetrafluoroborate salts with aryl boronic acids in 1996 (Scheme 23).



Scheme 23: Suzuki coupling of aryldiazonium salts with aryl boronic acids

The coupling was found to work at room temperature, no ligands were required to activate the catalyst and the procedure allowed the formation of bi-aryl systems in high yields. In contrast with standard cross-coupling conditions,^{43,44} the addition of a base such as triethylamine was found to be detrimental for the reaction as it led to the decomposition of the aryldiazonium salt. Hence, a different transmetalation

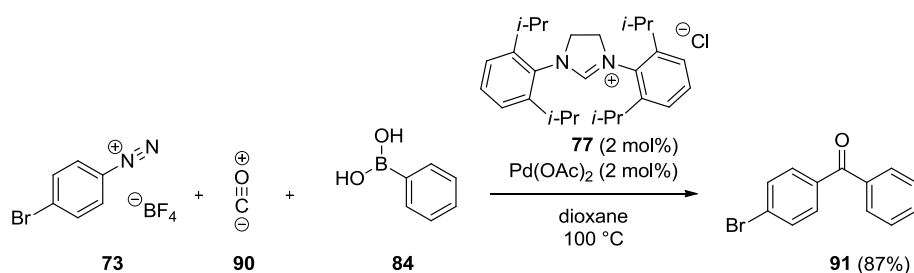
mechanism should be involved in this transformation.⁵² However, few in-depth studies of the process have been reported in the literature. Amongst them, Felpin and co-workers investigated the impact of the catalyst properties on the reaction and delivered the first optimised conditions for this transformation.⁵⁸ While a variety of catalysts possessing different properties were evaluated, simple palladium(0) on charcoal was found to perform best under the experimental conditions and was therefore retained to demonstrate the synthetic power of this methodology through the total synthesis of Boscalid® **89**, a potent agrochemical (Scheme 24).⁵⁸



Scheme 24: Suzuki cross-coupling of aryldiazonium salt for Boscalid® preparation

Palladium on charcoal can be recycled through simple filtration of the reaction mixture and it is noteworthy that in this case, the catalyst could be recycled up to three times, albeit with rapidly decreasing yields (Run 1: 82% yield; Run 2: 35% yield; Run 3: 16% yield).

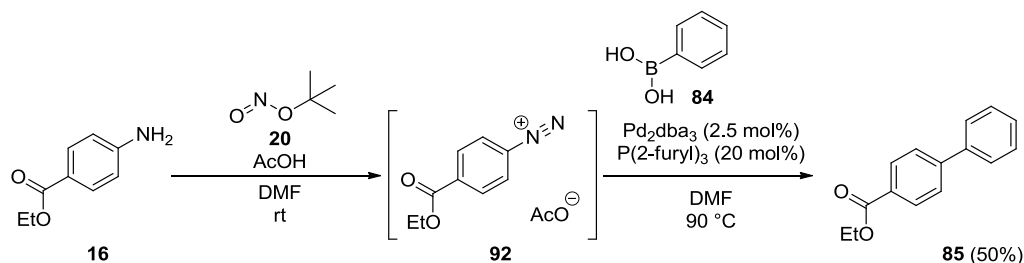
Palladium catalysed cross-coupling was found to be compatible with the insertion of carbon monoxide **90** to yield bis aryl ketone derivatives. While the carbonylative Suzuki reaction employed pre-formed aryldiazonium tetrafluoroborate salts as for the previous cross-couplings, a palladium(II) – NHC **77** combination was required to catalyse the process (Scheme 25).⁵⁹



Scheme 25: Carbonylative Suzuki coupling of aryldiazonium tetrafluoroborate salts

As highlighted previously, the isolation of potentially unstable and high-energy species such as aryldiazonium salts is not always desirable due to the safety risks associated with their handling in the dry state. Therefore it would be preferable to exploit their synthetic potential in domino reactions in which they are prepared *in-situ*

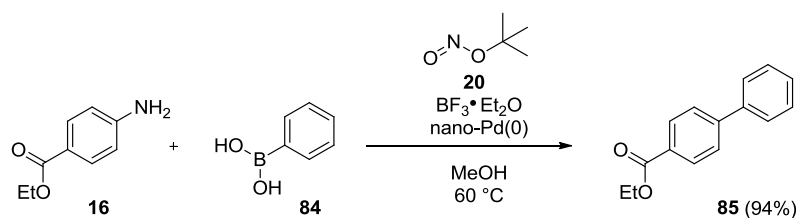
before being reacted, thus avoiding their isolation. With this concept in mind, Wang and co-workers have reported a one-pot cross-coupling of anilines with aryl boronic acids through the *in-situ* formation of an aryldiazonium intermediate with *tert*-butyl nitrite **20** and acetic acid (Scheme 26).⁶⁰



Scheme 26: Sequential diazotisation / Suzuki cross-coupling from anilines

While this method avoids the isolation of potentially unstable compounds, the yields observed are lower compared to those reported with isolated aryldiazonium salts. This yield loss is presumably due to the complexity introduced by the telescoping of the two steps as well as the thermal degradation of the intermediate. This two-step process indeed operates at an elevated temperature (90 °C) which may result in the decomposition of the aryldiazonium salt **92** and, depending on its profile, to a safety hazard. Moreover, a ligand is required to activate the palladium metal in this methodology whereas Felpin's procedure only required low-cost palladium on charcoal catalyst at room temperature.⁵⁸

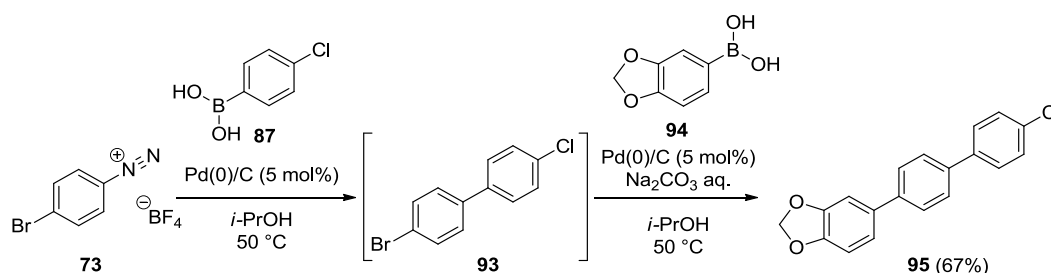
To improve the efficiency of the one-pot coupling process, Sun, Jiang and co-workers developed magnetic palladium nano-particles to catalyse the cross-coupling of aryldiazonium salts generated *in-situ* from anilines.⁶¹ In contrast with the previous sequence, the diazotisation was performed in the presence of *tert*-butyl nitrite and boron trifluoride and the cross-coupling was achieved at lower temperature, thus providing a significantly better reaction protocol (Scheme 27).



Scheme 27: One-pot diazotisation / Suzuki cross-coupling from anilines

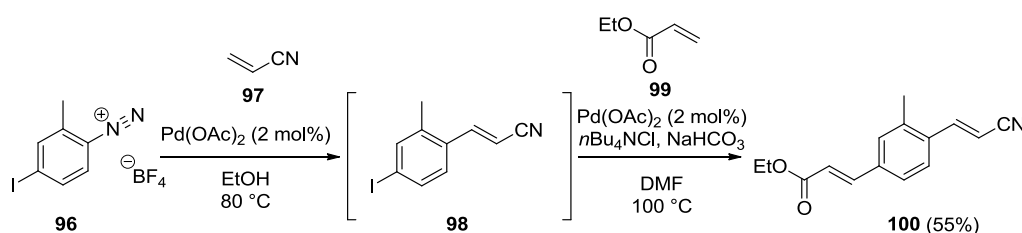
It is noteworthy that the magnetic palladium nano-particles could be recovered and recycled up to four times with similar yields, increasing the attractiveness of this one-pot process.

The superior reactivity of nitrogen as the nucleofuge over classic halides in cross-coupling methodologies has enabled the development of chemoselective and sequential transformations allowing the formation of polyarylated systems in a regioselective manner (Scheme 28).⁶²



Scheme 28: Chemoselective and sequential Suzuki couplings

In this system, the first coupling takes place at the more reactive carbon-diazonium bond and the addition of sodium carbonate then enables the coupling at the previously unreactive carbon-bromide bond. While aryl substituents were employed to exemplify the chemoselective functionalisation of aromatic rings, the differing reactivities of aryl halides and aryldiazonium species has also proved to be compatible with the introduction of different alkene substituents through the Heck reaction (Scheme 29).⁶³



Scheme 29: Chemoselective and sequential Heck couplings

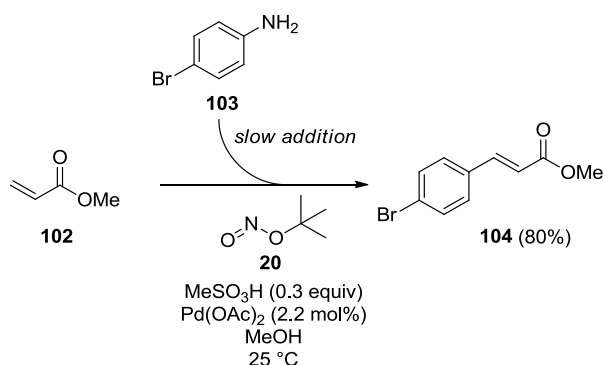
While the Suzuki coupling requires a boronate derivative to substitute planar sp^2 -hybridized carbon atoms, the Heck reaction allows for the formation of similar systems from unsubstituted alkenes and aryl halide substrates.^{64–66} The potential of reacting unfunctionalised alkenes with aryldiazonium salts to form sp^2 – sp^2 carbon-carbon bonds while releasing nitrogen has encouraged the development of

this low-waste process by the synthetic community. Among them, Kikukawa and Matsuda were the first to propose a procedure for the palladium-catalysed olefination of aryldiazonium salts (Scheme 30).^{67,68}



Scheme 30: Heck coupling of aryldiazonium salts

The impact of the palladium oxidation state was investigated and palladium(II) species were found to proceed better under the mild reaction conditions compared to palladium(0) complexes bearing triphenyl phosphine ligands. This result is allegedly due to the metal-stabilising phosphine which is known to react with aryldiazonium species.⁶⁹ The proof of concept was thus established and recent advances for the olefination of diazo compounds has focused on its adaptation to domino reactions involving the diazotisation of the aniline substrate followed directly by a palladium-catalysed process. In one of these efforts, Felpin and co-workers reported a bi-catalytic system requiring substoichiometric amounts of palladium and acid (Scheme 31).



Scheme 31: One-pot diazotisation / Heck coupling of aryldiazonium salts

This bicatalytic system shown on Figure 15 initiates with the diazotisation of the aniline **7** by action of *tert*-butyl nitrite **20** and acid **9** (Figure 15). The resulting aryldiazonium **10** is then engaged in the palladium catalytic cycle leading to the arylated alkene **107** and the regeneration of acid **9** which is used in the subsequent diazotisation cycle.

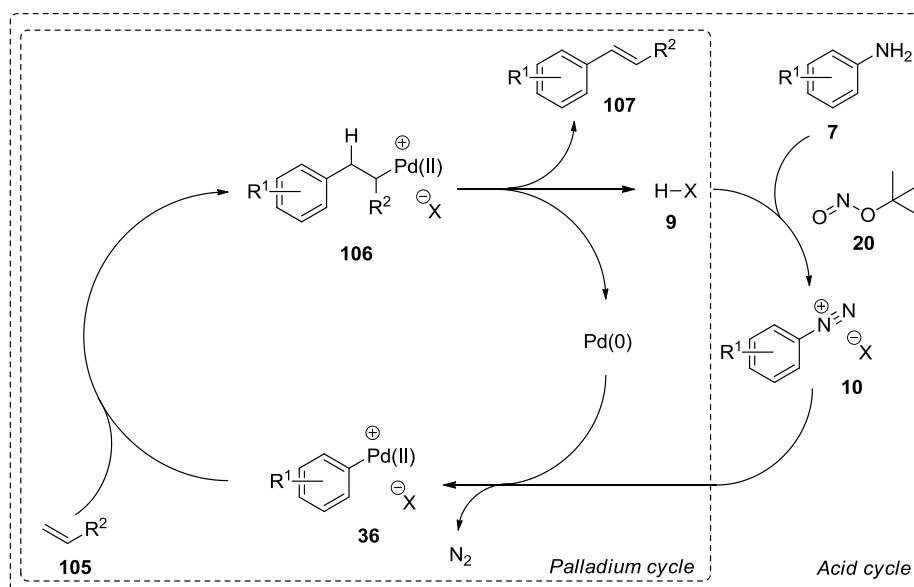
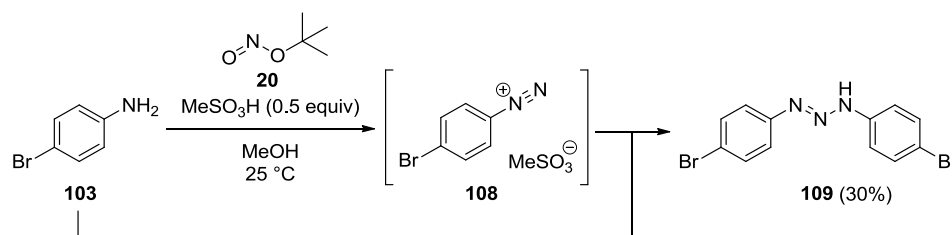


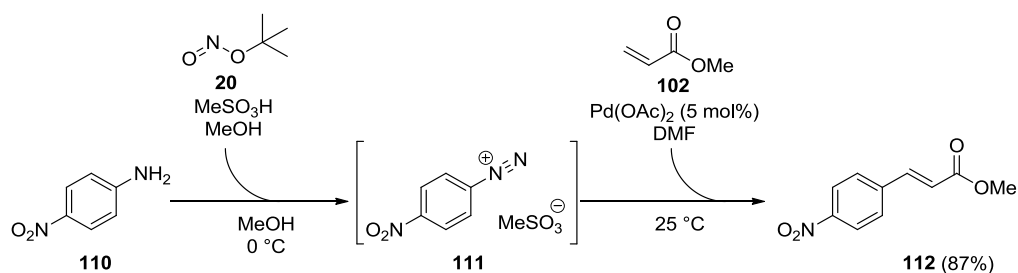
Figure 15: Mechanism of the bi-catalytic Heck coupling of aryldiazonium salts

It is noteworthy that this double process requires the slow addition of the aniline in order to minimise the formation of the triazene impurity **109** resulting from the attack of the parent aniline **103** on the aryldiazonium salt **108** in the absence of stoichiometric quantities of acid (Scheme 32).

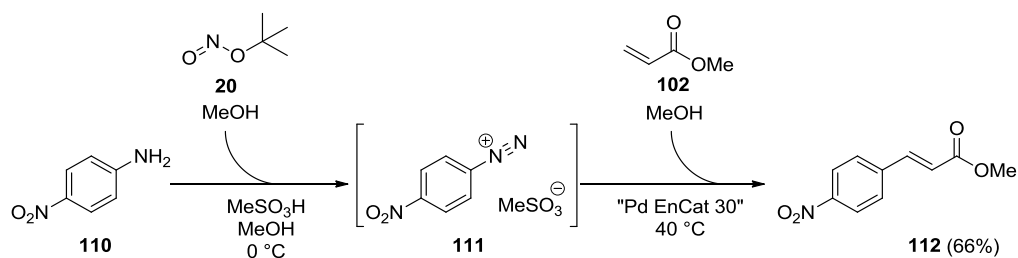


Scheme 32: Formation of the triazene impurity in the absence of acid

While the previous one-pot diazotisation / Heck reaction study was conducted in batch, McGuire and co-workers⁷⁰ as well as Felpin's group⁷¹ have both successfully adapted this system to flow technology. The flow chemistry design is similar for both reports: As the flowing solution of aniline is diazotised in a first reactor with *tert*-butyl nitrite and methanesulfonic acid, the subsequent Heck coupling occurs in a second reactor in the presence of palladium and an alkene **102** to generate styrene derivatives (Schemes 33 and 34).



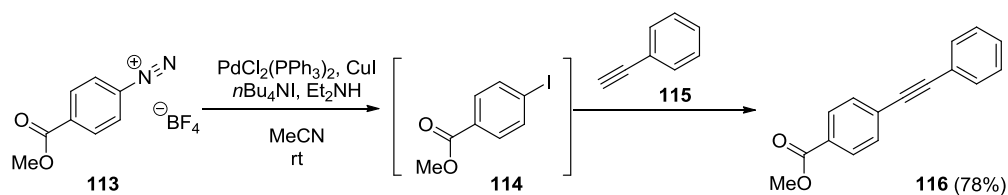
Scheme 33: Flow diazotisation / Heck reaction developed by McGuire *et al.*



Scheme 34: Flow diazotisation / Heck reaction developed by Felpin *et al.*

The divergence between the two methodologies comes from the type of palladium catalysis employed: As McGuire and co-workers were pumping a solution of alkene and palladium(II) acetate into the second reactor, Felpin *et al.* used a column packed with polymer-encapsulated palladium "Pd EnCat 30", which allows the recycling of the palladium and increases the attractiveness of the overall process, albeit the overall reactions proceed in lower yields.

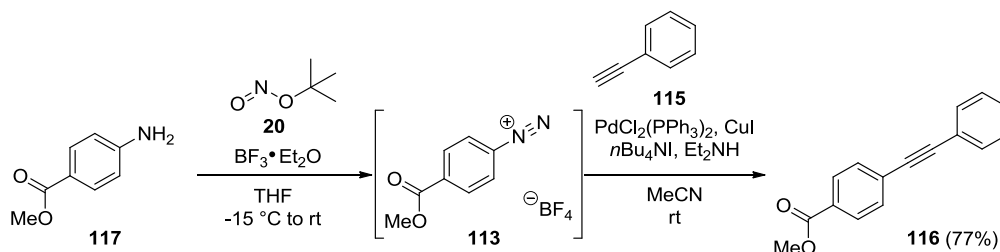
While the palladium-mediated formation of sp^2 – sp^2 carbon–carbon bonds from aryldiazonium salts has been extensively investigated, the related formation of sp^2 – sp carbon–carbon bond discovered by Sonogashira^{72,73} has only received limited attention. Cacchi and co-workers⁷⁴ reported the first palladium-mediated alkynylation of aryldiazonium salts in the presence of a base and copper(I) iodide (Scheme 35).



Scheme 35: Sonogashira coupling of aryldiazonium salts

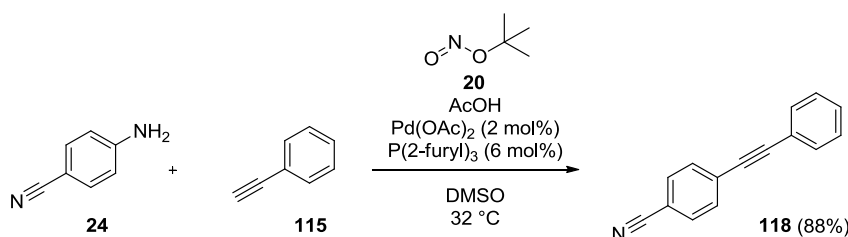
The successful strategy adopted for this transformation consists of a domino Sandmeyer iododediazotisation with copper(I) iodide followed by a palladium and copper-mediated Sonogashira coupling. The reaction conditions were first applied to

a range of aryldiazonium tetrafluoroborate salts as substrates to obtain the corresponding arylacetylene products in good to excellent yields before adapting the protocol to the sequential diazotisation / iododediazotisation / alkyne coupling (Scheme 36).⁷⁴



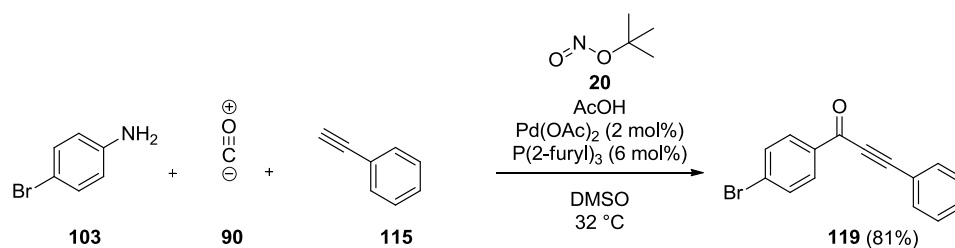
Scheme 36: Sequential diazotisation / Sonogashira coupling of anilines

As an alternative to this strategy, Beller *et al.* designed a one-pot alkyne coupling of aniline through *in-situ* diazotisation by *tert*-butyl nitrite and acetic acid in DMSO (Scheme 37).⁷⁵ This approach towards the synthesis of arylacetylene derivatives employed a different strategy to the one used by Cacchi *et al.* as the Sandmeyer conditions were not required for the coupling to proceed, rendering the process copper-free and halide-free.



Scheme 37: One-pot diazotisation / Sonogashira coupling of anilines

This methodology was extended to the formation of aryl alkynyl ketones through the insertion of carbon monoxide in a similar manner to the carbonylative Suzuki-Miyaura coupling (Scheme 25). This three-component process was reported by the group of Beller⁷⁶ shortly after their study of the one-pot methodology and the reaction conditions remained therefore unchanged apart from the addition of carbon monoxide **90** (Scheme 38).



Scheme 38: Carbonylative Sonogashira coupling of anilines

Aryldiazonium salts have proved to be efficient and sustainable cross-coupling partners in a wide range of palladium-mediated transformations. Their superior reactivity compared to the more commonly used aryl halides has led to breakthroughs such as chemoselective cross-coupling methodologies as well as the development of milder reaction conditions in comparison with standard processes.

1.5.vi Transition metal promoted arylation: The Meerwein reaction

While a number of palladium-based methodologies have arisen in the light of its unique ability to insert into carbon-halide or carbon-diazonium bonds, the supply of this scarce and expensive metal may prove problematic in the future because of geo-political considerations.⁷⁷ As an alternative, the reactivity of more earth-abundant transition metals such as copper and iron have become of high interest⁷⁸ for the development of new methodologies involving aryldiazonium salts. In a similar manner to the Sandmeyer reaction,^{32,33,35} Meerwein and co-workers⁷⁹ exploited the ability of copper to generate aryl radicals **33** from aryldiazonium salts **10** to arylate sp^2 hybridised systems **124** (Figure 16).^{34,80}

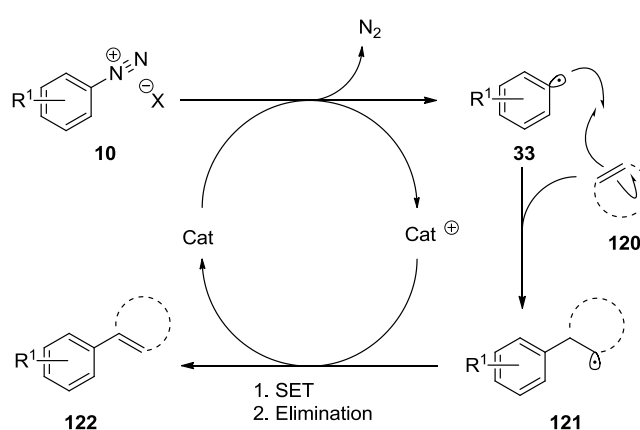
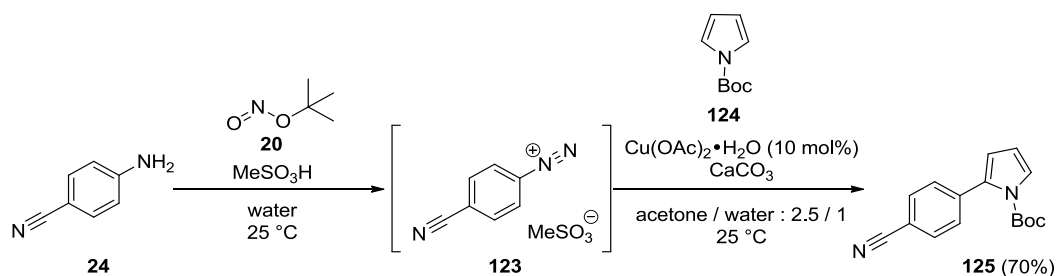


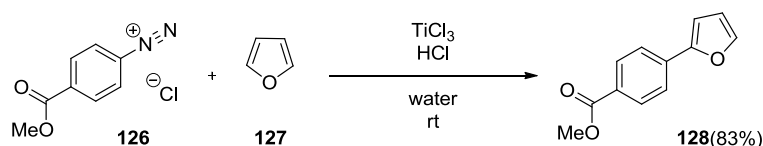
Figure 16: Mechanism of the Meerwein arylation

This reactivity was highlighted by Felpin and his group who developed the arylation of *N*-Boc protected pyrroles with anilines using a catalytic amount of copper (Scheme 39).⁸¹ The one-pot process encompassed the diazotisation of the aniline with *tert*-butyl nitrite **20** and methanesulfonic acid followed by a Meerwein arylation in the presence of copper(II) acetate hydrate and *N*-Boc protected pyrrole **124**. While furan derivatives could also be arylated in good yields,^{80,82} thiophene substrates exhibited a lower reactivity⁸³ in similar copper-catalysed methodologies as only moderate yields were observed.



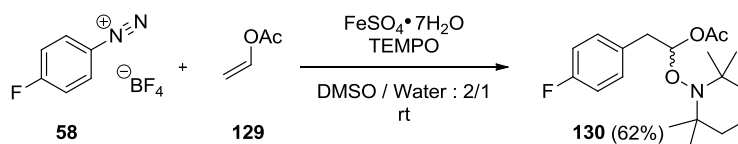
Scheme 39: Meerwein arylation of *N*-Boc protected pyrrole

Titanium was also found to promote the heteroarylation of diazonium salts by Heinrich and co-workers⁸⁴ who reported that stoichiometric amounts of metal were needed, even though the Meerwein reaction was catalytic. This method gives access to arylated phenol and furan derivatives from the corresponding aryldiazonium chloride salts (Scheme 40).⁸⁴



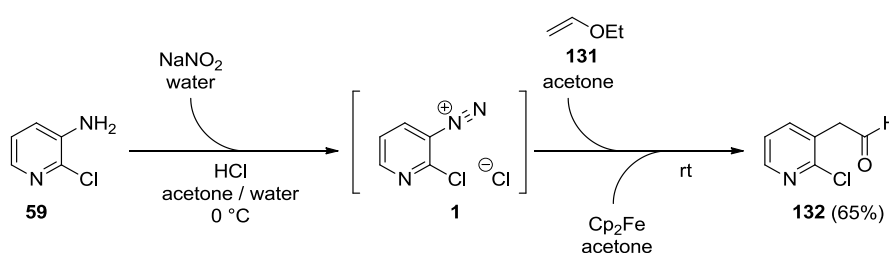
Scheme 40: Titanium-catalysed Meerwein arylation

While the Meerwein reaction proved to be convenient for the synthesis of bi-aryl systems,⁸⁴ other sp^2 hybridised systems such as α -aryl methyl carbonyls can be afforded through this methodology. As an example, Heinrich and co-workers used iron(II) sulfate to promote a radical cascade to afford alkylated aromatic rings from aryldiazonium substrates (Scheme 41).⁸⁵ The trapping of the radical intermediate **121** by TEMPO in the reaction mixture also gives extra evidence to support the radical nature of this transformation.



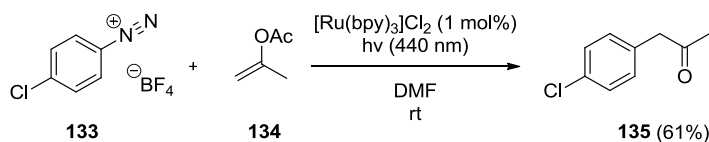
Scheme 41: Iron-catalysed Meerwein arylation

This methodology was later extended by Buchwald and Chernyak who telescoped the radical arylation with the aryldiazonium salt formation using flow technology.⁸⁶ As the flowing solution of aniline **59** is diazotised in the first reactor under acidic conditions at low temperature, the subsequent Meerwein arylation occurs in the second reactor in the presence of ferrocene and ethyl vinyl ether **131** to generate valuable mono aryl acetaldehyde derivatives such as **132** (Scheme 42).



Scheme 42: Flow synthesis of mono aryl acetaldehyde derivatives

In addition to copper, titanium and iron, ruthenium has also been used to catalyse the arylation of enol acetate **134** to access synthetically relevant α -aryl methyl ketones **135** under photo-catalytic conditions (Scheme 43).⁸⁷



Scheme 43: Photo-catalysed Meerwein arylation of enol acetate

Earth-abundant transition metal have been shown to reveal the arylation potential of aryldiazonium salts to functionalise their aromatic core with a variety of pharmaceutically and synthetically useful substituents. In the search for even more sustainable and low-cost arylation methodologies avoiding transition metals, base-mediated processes, discovered in 1924 by Gomberg and Bachmann,⁸⁸ have also been developed for this transformation. There is however a confusion in the literature with regards to the delineation between the two reaction concepts and for the sake of clarity within this review, transition metal processes will be referred to as

Sandmeyer reactions or Meerwein arylations while base-mediated processes will be referred to as Gomberg-Bachmann arylations.

1.5.vii Base-mediated arylations : The Gomberg-Bachmann reaction

While the mechanism of the arylation reaction under basic conditions remains similar to the Meerwein reaction, it involves a key aryl diazo anhydride intermediate **137** formed *in-situ* by the action of a base on two equivalents of aryl diazonium salt in water (Figure 17).⁸⁹ This unstable intermediate **137** undergoes a spontaneous radical decomposition to give nitrogen and an aryl radical **33** which will arylate the alkene **120** and form the arylated product **122** after subsequent electron transfer and deprotonation.

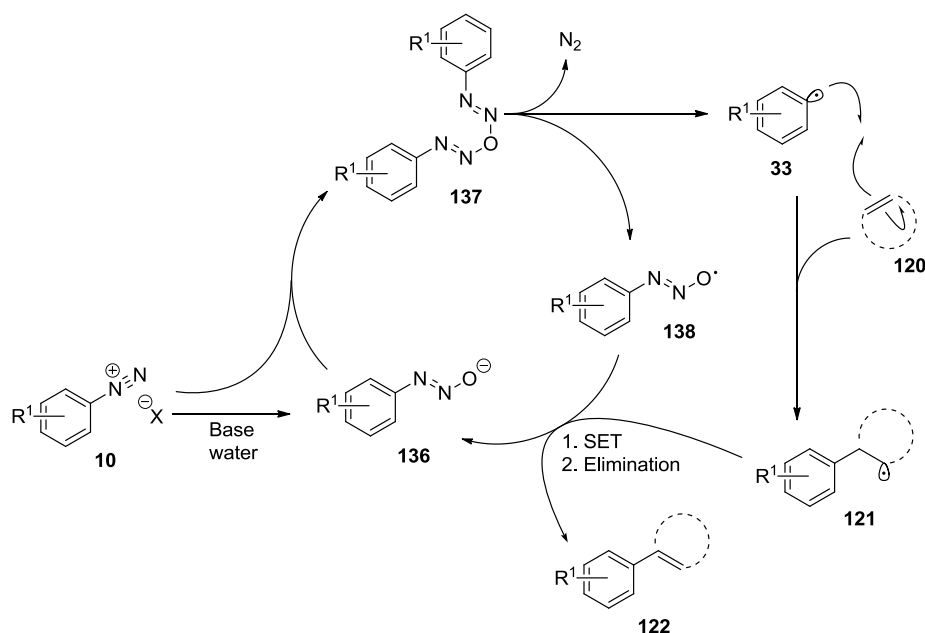
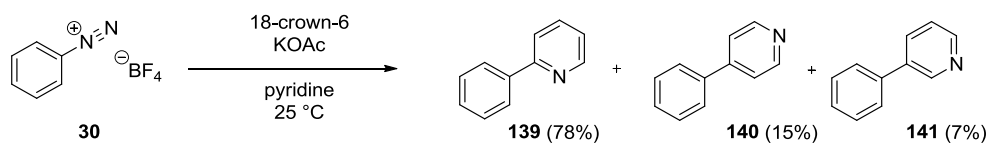


Figure 17: Base-mediated Meerwein arylation mechanism

Like the Meerwein reaction discussed earlier, this base-mediated arylation permits access to arylated sp^2 hybridised systems. The first report of this process by Gomberg and Bachmann⁸⁸ exploited the specific reactivity to form unsymmetrical bi-aryl systems by trapping the radical intermediate generated under basic conditions with a second aryl group. While this reaction presents obvious advantages such as simplicity and sustainability, the very high reactivity of the intermediate aryl radicals led to poor control over chemo- and regioselectivity impacting the yield and giving mixtures of products. In order to address these issues, Gokel and co-workers showed that crown ethers were efficient phase-transfer catalysts for the arylation of

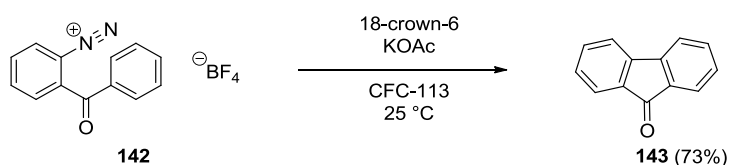
phenyl derivatives under the basic environment provided by potassium acetate (Scheme 44).⁹⁰



Scheme 44: Phase-transfer catalysed Gomberg-Bachmann arylation

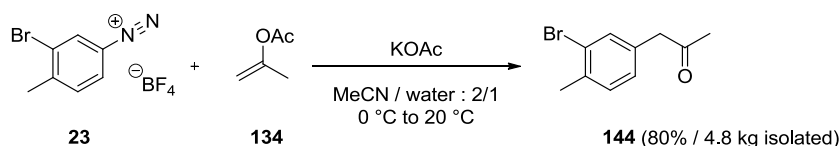
The phase-transfer-catalysed arylation allowed the full conversion of the starting benzenediazonium tetrafluoroborate **30** into the regioisomeric biaryl products **139**, **140** and **141** at the expense of using the aromatic substrate as solvent. It is noteworthy that given the radical nature of this transformation and the absence of functional groups to guide the reactivity, the regioselectivity of this transformation remains a challenge for the synthetic community.

The intramolecular variant of the Gomberg-Bachmann arylation, the Pschorr cyclisation, overcomes all of the previous issues and leads to a unique tricyclic product as the regioselectivity is dictated by the close environment of the reactive aryl radical (Scheme 45).⁹⁰



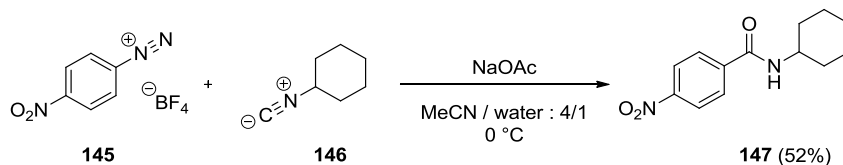
Scheme 45: Phase-transfer catalysed Pschorr cyclisation

Similarly to the Meerwein reaction discussed earlier, other sp^2 hybridised systems such as α -aryl methyl carbonyls can be prepared through this methodology. As an example, Molinaro and co-workers reported the synthesis of kilogram quantities of the pharmaceutical intermediate **144** by the action of potassium acetate on aryldiazonium tetrafluoroborate salt **23** (Scheme 46).⁹¹ The scale of this example is representative of the relevance and scalability of the process.

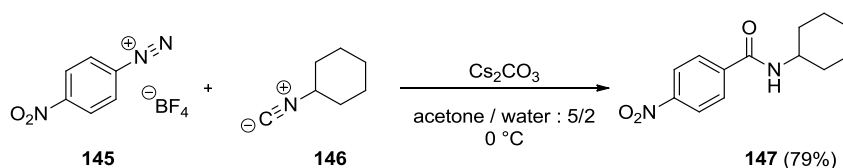


Scheme 46: Kilogram-scale Gomberg-Bachmann arylation

The ability of acetate anion to induce the formation of aryl radicals from aryldiazonium salts was extended to other radical acceptors by the groups of El Kaim⁹² and Zhu⁹³ who have independently reported the use of isonitriles as reaction partners to give amide products under similar conditions (Schemes 47 and 48).



Scheme 47: Base-mediated amide bond formation developed by El Kaim et al.

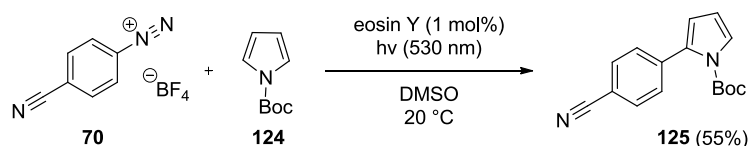


Scheme 48: Base-mediated amide bond formation developed by Zhu et al.

While the base-mediated processes presented in this section were found to be a viable alternative to the metal-catalysed arylations for regiospecific substrates, these methods proved to be chaotic when simple aromatic cores were employed as substrates. Hence metal-free and regioselective biaryl generating methods were developed through an organocatalytic approach.

1.5.viii Organocatalytic transformations

Aryl radicals can be generated from aryldiazonium salts following three very different methodologies: Transition metal catalysis (Sandmeyer and Meerwein reactions, *vide supra*),⁷⁸ base mediated decomposition (Gomberg-Bachmann reaction, *vide supra*)⁸⁹ and using organocatalysis.⁴⁶ The latter method is superior to the two other alternatives from a green chemistry perspective as it only requires a catalytic amount of an organic molecule (transition metal-free) while using mild reaction conditions (base-free). In a similar manner to the Meerwein and the Gomberg-Bachmann reactions, the trapping of the aryl radical **33** by sp^2 hybridised systems such as **120** leads to similar products **122** (Figure 16, *vide supra*). As an example, eosin Y was found by König and co-workers⁹⁴ to catalyse the selective 2-arylation of 5-membered heterocyclic substrates such as furan, *N*-Boc protected pyrrole **124** and thiophene under visible-light activation (Scheme 49).



Scheme 49: Photo-catalysed arylation of N-Boc protected pyrrole

It is noteworthy that this methodology overcomes the poor reactivity of thiophene substrates when compared to the copper-catalysed transformations (*vide supra*) as the corresponding arylated thiophenes could be obtained in acceptable yields (up to 70%). The mechanism of this transformation is shown on Figure 18.^{46,94}

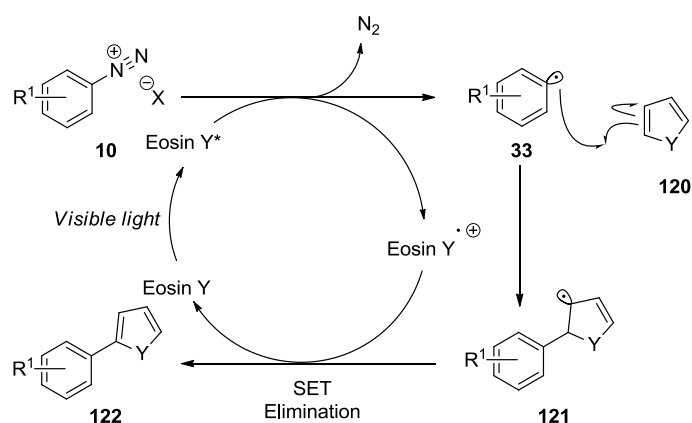


Figure 18: Mechanism of the photocatalytic arylation of aryl diazonium salts

While this mechanism requires the assistance of light to enable the reduction potential of eosin Y to reduce the aryl diazonium salt, 4-amino-morpholine **148** was recently found^{95,96} to generate an aryl radical from diazo compounds through the formation of the unstable tetrazene intermediate **149** (Figure 19).⁹⁷

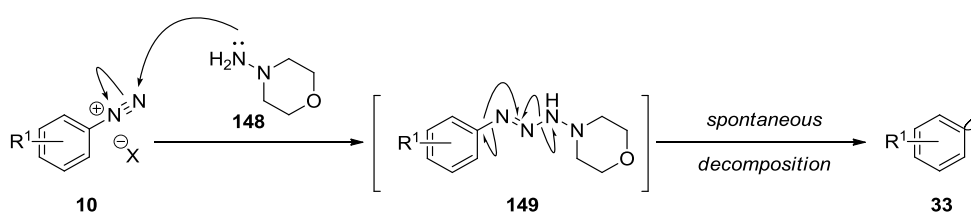
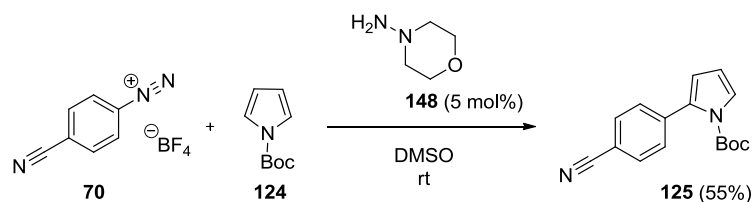
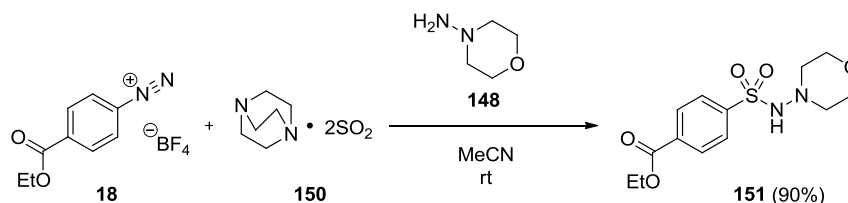


Figure 19: Radical decomposition of aryl diazonium salts by 4-amino-morpholine

4-Amino-morpholine **148** was employed as a transition metal surrogate in a variety of radical-mediated transformations such as the Meerwein-type arylation (Scheme 50)⁹⁶ and the Sandmeyer-like sulfonylation (Scheme 51).⁹⁵



Scheme 50: Organocatalysed Meerwein-type arylation

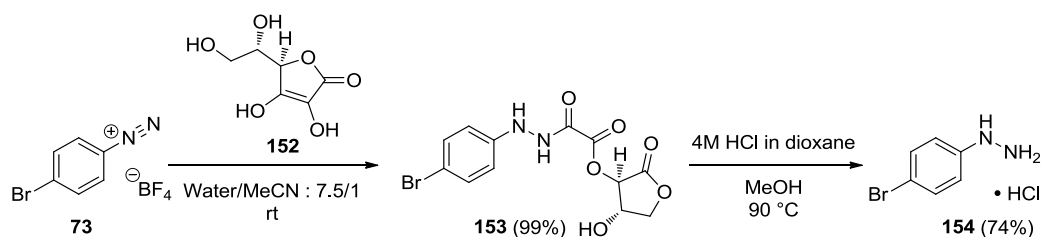


Scheme 51: Radical-mediated sulfonylation of aryldiazonium tetrafluoroborate salts

The organocatalytic methods developed in this section emphasised the recent resurgence of interest in aryldiazonium salts as these transformations were developed as a more sustainable alternative to the methodologies developed by Sandmeyer and Meerwein in the XIXth century.

1.5.ix Miscellaneous transformations involving aryldiazonium salts

While all of the previously discussed methodologies took advantage of the entropically favoured release of nitrogen as a reaction driving force, aryldiazonium salts are also important precursors to hydrazines. Historically, such reductions were performed by employing supra-stoichiometric quantities of tin(II) chloride as reducing agent⁹⁸ but given the health and environmental hazards associated with the use of this metal, novel reduction methods were required. Arguably the most sustainable way of achieving this transformation is by using ascorbic acid **156** as the reducing agent.⁹⁹ Ley and co-workers demonstrated that reduction of the aryldiazonium species to the corresponding hydrazines using ascorbic acid **156** proceeded through the formation of an hydrazine amide intermediate **157** before being hydrolysed under acidic conditions to deliver the desired hydrazine **158** as the hydrochloride salt (Scheme 52).



Scheme 52: Ascorbic acid-mediated reduction of aryldiazonium salts

The structure of the hydrazine amide intermediate **153** was investigated by the same group and it was brought to light that a Japp-Klingemann rearrangement occurred between the aryldiazonium substrate **10** and ascorbic acid **152** (Figure 20).

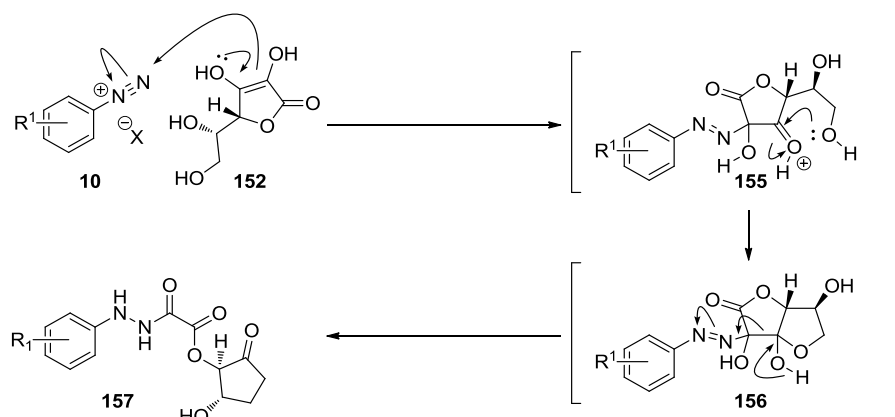
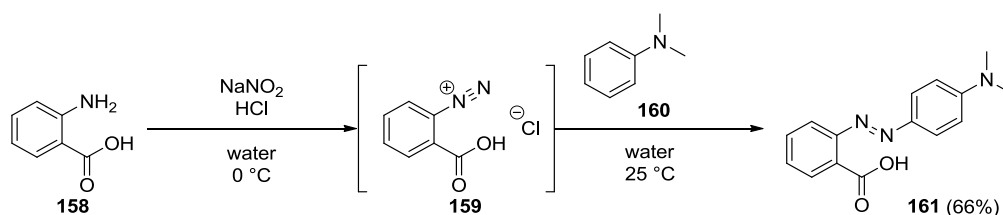


Figure 20: Japp-Klingemann rearrangement for hydrazine formation

It is noteworthy that the first step of this rearrangement, a nucleophilic attack on the β -nitrogen of the diazonium group is also a commonly used transformation in the preparation of diazo-dye compounds²³ as exemplified by the preparation of Methyl Red **161** (Scheme 53).¹⁰⁰



Scheme 53: Preparation of Methyl Red

In the preparation of this pH indicator, anthranilic acid **158** is diazotised before being reacted with electron-rich *N,N*-dimethyl aniline **160** via an azo-coupling (Figure 21).²³

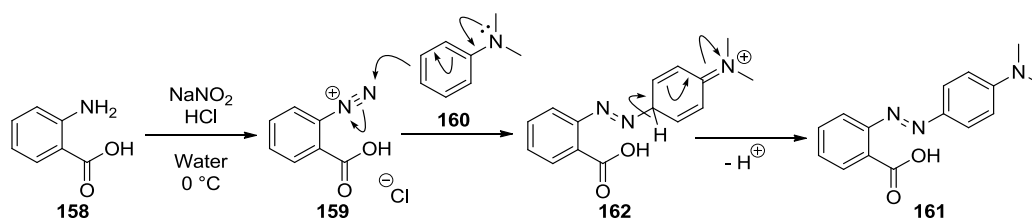
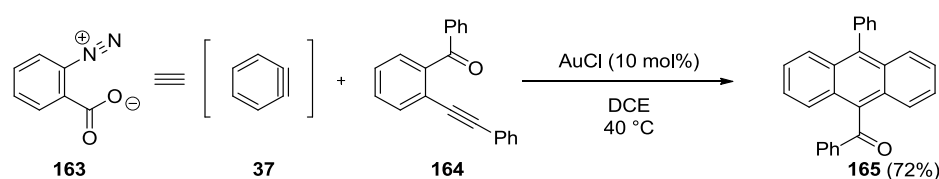


Figure 21: Azo-coupling mechanism

Specific diazotisation conditions¹⁰¹ can lead anthranilic acid **158** to the formation of zwitterion benzenediazonium carboxylate **163** which is an effective precursor to aryne intermediates **37** in cycloaddition reactions (*vide supra*).²⁶ This type of reactivity was reported by Asao and Sato in the gold-catalysed synthesis of anthracene derivatives **165** (Scheme 54).²⁷



Scheme 54: Anthracene synthesis through cycloaddition of aryne

These miscellaneous transformations are representative of the versatility of aryldiazonium salts and only represent a fraction of their synthetic potential and it is believed that many other reactions are still to be discovered.

I.6 Drawbacks and advantages of aryldiazonium salts

The classes of reaction discussed have shown the breadth of reactivity of aryldiazonium salts and have highlighted how challenging it is to find suitable conditions to react these species in a selective manner with other substrates. Nevertheless, their synthetic potential in organic chemistry is colossal and remains underexploited due to the reputation of these salts among the chemistry community. The potentially violent decomposition of aryldiazonium compounds is entropically favoured through nitrogen expulsion and along with concerns about the quality of the product, this decomposition may lead to damage and even casualties.^{15,16}

Understanding the critical parameters influencing the stability of aryldiazonium salts and implementing safety protocols to handle these species in a controlled environment could potentially increase their use in sustainable processes for the

preparation of valuable pharmaceutical compounds. It is these principal factors that drove the research described within this thesis.

CHAPTER II AIMS

As patients, regulatory authorities and other organisations are requesting ever cheaper drugs,³ price and sustainability have become increasingly important factors in route design.¹⁰² While the time in plant and the costs of goods (substrates, metal and ligand) must be taken into consideration when scouting a new route, the removal of the catalyst, the number of steps and the yields obtained are also of interest as these parameters impact the sustainability of the process.¹⁰³ Furthermore, cost and sustainability are related through regulatory measures which encourages the pharmaceutical industry to develop greener processes in counterpart of tax modulation.¹⁰⁴

In this context, there is a significant interest and desire to develop sustainable and green chemistry within the Chemical Development department at GlaxoSmithKline. This is due to the strong desire to deliver quality drugs for the patient and to minimise the waste stream. Hence the aim of this PhD was to contribute to this effort through the discovery and the investigation of efficient and sustainable methodologies.

As discussed in the previous chapter, reactions with aryldiazoniums release nitrogen as by-product by acting as an electrophile, providing an outstanding opportunity to uncover novel Green carbon-carbon bond formations as discussed in the introduction. Key amongst these are the aryl-aryl cross-couplings as numerous pharmaceuticals present this motif in their structure (Figure 22)^{2,105} and the importance of this transformation was recognised by the award of the Nobel prize for Chemistry in 2010.²⁵

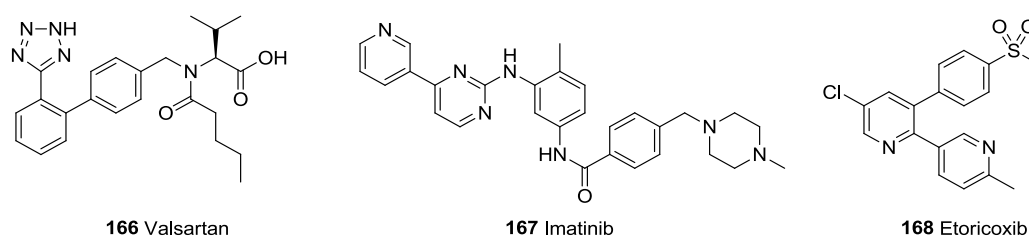


Figure 22: biaryl-containing pharmaceuticals

While a variety of methods preparing such systems are available in the literature,^{106–108} the work presented in this thesis will focus on the exploration, the optimisation

and the implementation of cross-couplings employing aryldiazonium salts as substrates for pharmaceutical scale-up. Initial investigations will focus on the preparation and safety assessment of various salts of aryldiazonium species by DSC before moving on to the coupling reactions (Figure 23).

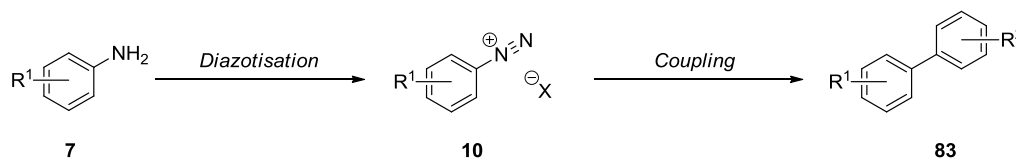


Figure 23: Aims of the project

Appropriate statistical methods including PCA (Principal Component Analysis), DoE (Design of Experiment) and OPLS (Orthogonal Partial Least Squares) regression will be used to develop the processes which would ultimately be demonstrated on a multimolar scale.

CHAPTER III RESULTS & DISCUSSION

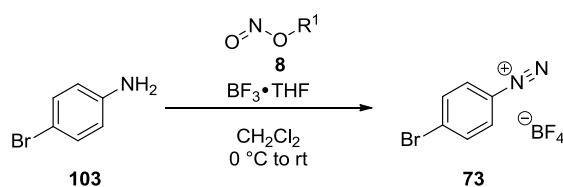
III.1 Synthesis, isolation and thermal stability assessment of aryldiazonium salts

While commercially available chemicals may be stable for months or years and therefore conveniently stored for long periods of time, aryldiazonium salts must be freshly prepared to prevent quality issues arising from their expected slow decomposition over time. As discussed in the introduction, these species can be conveniently prepared under a variety of conditions involving the following *triumvirate*: aniline **7**, nitrite **8** and acid **9**. Even though diazotisation conditions are available in the literature, it was decided to investigate the most relevant methods in order to acquire the expertise required for their safe formation and handling in an industrial framework. While the ease of preparation and isolation of various aryldiazonium salts will be investigated, their thermal stability will also be thoroughly assessed.

III.1.i Synthesis and isolation of aryldiazonium tetrafluoroborate salts

The industrial appeal for aryldiazonium tetrafluoroborate salts emanates from their relative stability as these species were reported to be amongst the most stable diazo compounds.^{14,16,17} As a consequence, their preparation from commercially available aniline derivatives, alkyl nitrites and boron trifluoride was investigated to understand the impact of each component involved in this transformation. The boron trifluoride is commercialised as a complex with either diethyl ether or THF and the latter was indeed preferred given its increased ease of handling compared to the diethyl etherate complex which is known to be moisture sensitive.¹⁰⁹

As a starting point of this study, the impact of the nitrite component was the first to be investigated and three different alkyl nitrites were screened (Table 2).



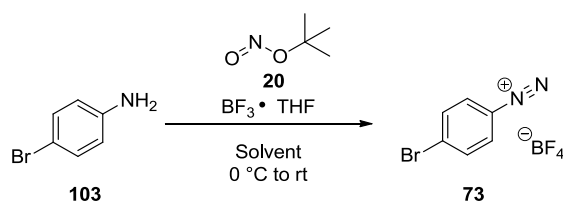
Entry	Alkyl nitrite	% Solid purity ^a	% Isolated yield
1	<i>tert</i> -butyl nitrite 20	>99	86
2	<i>iso</i> -butyl nitrite 169	>99	83
3	<i>iso</i> -amyl nitrite 4	>99	87

^aDetermined by HPLC (%Area)

Table 2: Alkyl nitrite screening for diazotisation reaction

The original reaction conditions reported by Doyle and Bryker⁹ were used with regards to the reagent stoichiometry and the choice of solvent for this screening. The reactions proceeded as expected and the product precipitated spontaneously from the reaction mixture leading to extremely similar yields for each nitrite examined after filtration and drying of the product. Hence the residual alcohol coming from the consumption of the alkyl nitrite **8** during the course of the reaction was not found to significantly impact the reaction outcome.

The industrial appeal of this transformation also comes from the ease of the product isolation by filtration. The solubility of the starting material and the insolubility of the product in the reaction medium were therefore expected to be key to this transformation and a solvent screen was performed to gain a better understanding and to identify suitable reaction media. Solvents were selected by consideration of the GlaxoSmithKline solvent selection guide¹¹⁰ (solvents ranked according to their sustainability) and a Principal Component Analysis (PCA) model of solvent properties.¹¹¹ The use of such tools led to the selection of solvents exhibiting diverse properties. Accordingly, 4-bromo-aniline **103** was reacted with *tert*-butyl nitrite **20** and boron trifluoride – THF complex in the selected solvents (Table 3).



Entry	Solvent	Precipitation	% Mixture ^a		% Solid ^b		% Yield ^c
			103	73	103	73	
1	Acetone	Yes ^d	0	>99	0	>99	45
2	Chlorobenzene	Yes	0	>99	0	>99	96
3	Dichloromethane	Yes	0	>99	0	>99	90
4	EtOAc	Yes	0	>99	1	99	89
5	<i>i</i> -AmylOH	Yes	0	>99	0	>99	90
6	<i>i</i> -PrOH	Yes	0	>99	0	>99	81
7	Me-cyclohexane	Yes	58	42	41	59	56
8	NMP	No	32	68	N.A.	N.A.	n.a.
9	<i>p</i> -Cymene	Yes	0	>99	0	>99	91
10	Propylene carbonate	No	0	>99	N.A.	N.A.	n.a.
11	TBME	Yes	6	94	4	96	94
12	Water	No	0	>99	N.A.	N.A.	n.a.

^aRatio of **103** and **73** in solution determined by HPLC (%Area); ^bPurity of the precipitate determined by HPLC (%Area); ^cIsolated yield after filtration and drying.

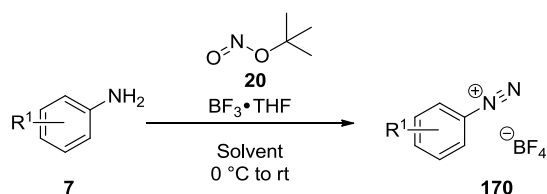
^dAfter TBME addition

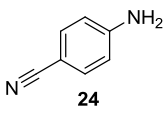
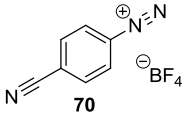
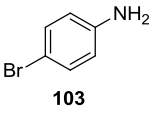
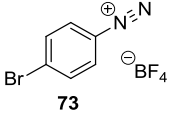
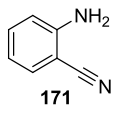
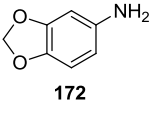
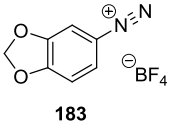
Table 3: Solvent screen for aryldiazonium tetrafluoroborate salt formation

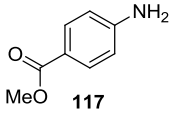
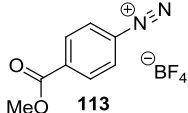
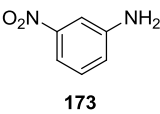
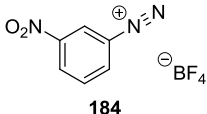
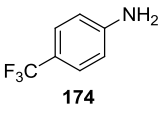
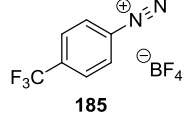
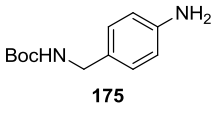
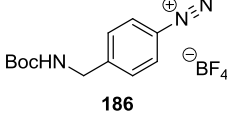
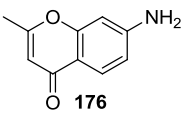
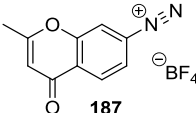
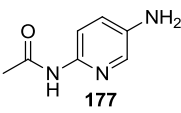
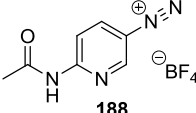
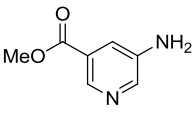
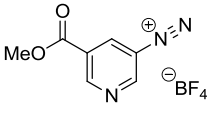
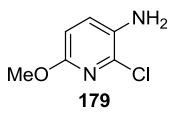
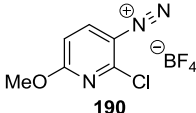
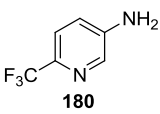
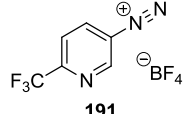
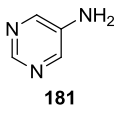
While the use of very polar solvents (Table 3, entries 8, 10 and 12) led to the formation of the aryldiazonium **73** in moderate to excellent yields, their precipitation as the tetrafluoroborate salt could not be achieved, even after the addition of TBME. Conversely, the use of very apolar solvents (Table 3, entries 7 and 11) resulted in the precipitation of an impure solid composed of both the product **73** and the starting aniline **103**, highlighting a poor solubility of the starting material in such solvents. The most interesting results were obtained when solvents having a medium polarity (Table 3, entries 3, 4, 5 and 6) were employed. Such solvents were indeed sufficiently polar to solubilise the starting aniline **103** while being sufficiently apolar to allow the precipitation of the aryldiazonium tetrafluoroborate salt **73**. It is noteworthy that aromatic solvents (Table 3, entries 2 and 9) also delivered interesting results, presumably due to increased solubility of the starting material

compared to the ionic product. As a result, several strategies taking advantage of the previous observations may be employed for the diazotisation step: polar solvents may be used for telescoped reactions whereas apolar solvents may be preferred when the isolation of the aryldiazonium intermediate is required. These results epitomise the flexibility of this transformation as the diazotisation appeared to work in most of the solvents examined.

The last component to investigate in this diazotisation reaction was the impact of the substituents present on the aniline substrates. As the nature of the substituents directly influenced the solubility of the starting aniline derivative, different solvents were employed in line with our previous observations in order to solubilise the starting material and isolate the product by filtration. Many drugs contain heterocyclic structures and as a consequence, it was important to check that the diazotisation conditions were compatible with these motifs. It is noteworthy that heteroaryldiazonium tetrafluoroborate salts were not extensively reported in the literature.



Entry	Starting Material	Solvent	Product	%Yield ^a
1	 24	EtOAc	 70	84
2	 103	EtOAc	 73	89
3	 171	EtOH	 182	86
4	 172	2-MeTHF	 183	87

Entry	Starting Material	Solvent	Product	%Yield ^a
5	 117	THF	 113	77
6	 173	THF	 184	73
7	 174	TBME	 185	79
8	 175	<i>i</i> -PrOH	 186	90
9	 176	EtOH	 187	91
10	 177	EtOH	 188	91
11	 178	THF	 189	84
12	 179	THF	 190	89
13	 180	EtOH	 191	70
14	 181	<i>i</i> -PrOH	Decomposition	0

^aIsolated yield after filtration.

Table 4: Synthesis of aryldiazonium tetrafluoroborate salts

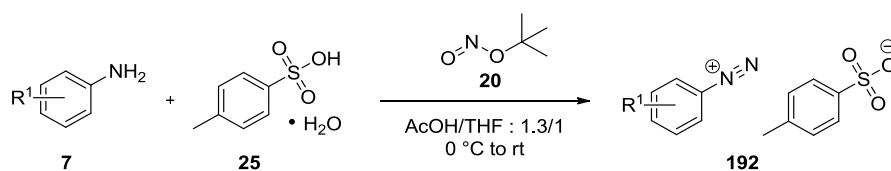
A variety of anilines **24**, **103**, **117**, **171-181** participated in the diazotisation reaction, affording the corresponding aryldiazonium tetrafluoroborate salts **70**, **73**, **113**,

182-191, with tolerance of a variety of functional groups and excellent purity. Electron-withdrawing substituents such as halides (Table 4, entries 1, 6 and 12), nitrile (Table 4, entries 2 and 3), ester (Table 4, entries 5 and 10) and amides (Table 4, entry 9) were as compatible with the diazotisation conditions as electron-donating substituents such as protected amines and alcohols (Table 4, entries 4, 7 and 11) as good to excellent yields were observed in both cases. It is noteworthy that a *N*-Boc protected amino group (Table 4, entry 4) remained intact during the transformation although Lewis acid promoted deprotection was conceivable in this particular case. Pyridine derivatives also proved to be compatible with the reaction (Table 4, entries 9 to 13). To further investigate the scope of this transformation, the procedure was evaluated on 5-amino-pyrimidine **181**, however the HPLC analysis of the reaction mixture clearly showed degradation products. This result may be due to the complexation of one or both of the endocyclic nitrogen atoms by the Lewis acid, providing an opportunity for nucleophilic attack on the pyrimidine ring.

The formation and isolation of aryldiazonium tetrafluoroborate salts using alkyl nitrites and boron trifluoride – THF complex in various solvents was successfully achieved and were found to be compatible with an industrial framework (ease of preparation, isolation by precipitation). While this method tolerates a variety of functional groups, some limitations were observed for heterocyclic substrates and the presence of fluoride in the counter-anion may be a source of concern for process chemists due to its etching properties¹² and waste disposal. These issues may be addressed by investigating other diazotisation methods involving non-coordinating, non-nucleophilic and non-halogenated counter-ions.

III.1.ii Synthesis and isolation of aryldiazonium tosylate salts

In the search for stable, non halogenated and easy to prepare aryldiazonium salts, Filimonov and co-workers reported¹¹ aryldiazonium tosylates as a viable alternative to the tetrafluoroborate salts. Hence their formation using *tert*-butyl nitrite **20** and PTSA hydrate **25** in a mixture of THF and acetic acid was investigated (Table 5).



Entry	Starting Material	Product	%Yield ^a
1	24	26	73
2	103	193	63

^aIsolated yield after precipitation with TBME and filtration.

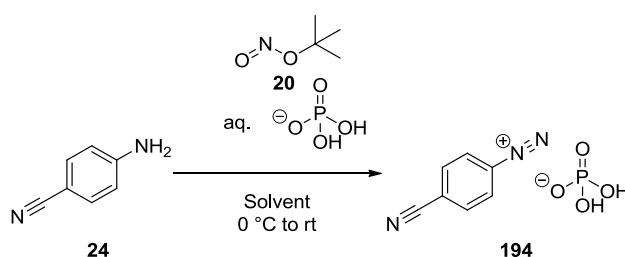
Table 5: Aryldiazonium tosylate salt synthesis

As PTSA **25** should be acidic enough to promote the diazotisation, the reaction was initially attempted in the absence of acetic acid. Although the formation of the aryldiazonium was observed by HPLC, the reaction was not complete and addition of acetic acid to the reaction mixture drove the reaction to completion. In line with our previous observations regarding the behaviour of aryldiazonium salts in very polar solvents, the tosylate salts did not precipitate spontaneously from the acetic acid / THF mixture and TBME was added as an anti-solvent to precipitate the products and allow their isolation by filtration.

This procedure was therefore found to be efficient to generate aryldiazonium species *in situ* even though their isolation proved problematic. Tosylate salts **26** and **193** were both isolated in moderate to good yields and these results might be explained by their high solubility in acetic acid. Moreover, the heavy tosylate counter-ion is not desirable in terms of atom efficiency as it represents nearly half of the weight of the entire salt. Finally, no advantages in terms of stability were observed by DSC for the tosylate salts when compared with the equivalent tetrafluoroborate salts which were found easier to prepare (*vide infra*, section II.1.v). These observations exemplify the need for an ideal counter-ion meeting the following criteria: low-weight, inexpensive, non-halogenated, non-toxic and easy to isolate.

III.1.iii Synthesis and isolation of aryldiazonium dihydrogen phosphate salts

With the objective of exploring more atom-economical and benign counter-ions, it was decided to investigate the synthesis of aryldiazonium dihydrogen phosphate salts. Dihydrogen phosphate indeed fulfils all of the desired requirements and an initial solvent screen focusing on the solubility of the starting material and the insolubility of the product was undertaken. The diazotisation was carried out using *tert*-butyl nitrite **20** and aqueous phosphoric acid in water-miscible solvents (Table 6).

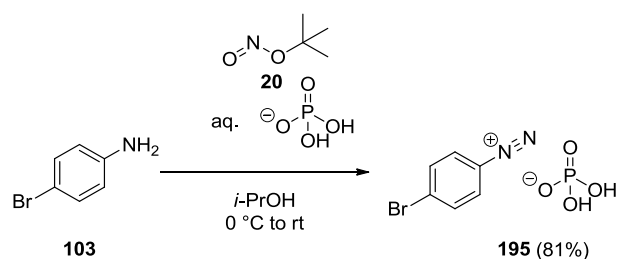


Entry	Solvent	Precipitation	% Mixture ^a		% Yield
			24	194	
1	THF	No	0	0	N.A.
2	MeCN	No	0	>99	N.A.
3	AcOH	No	0	>99	N.A.
4	Water	No	0	>99	N.A.
5	EtOH	No	0	0	N.A.

^aRatio of **24** and **192** in solution determined by HPLC (%Area).

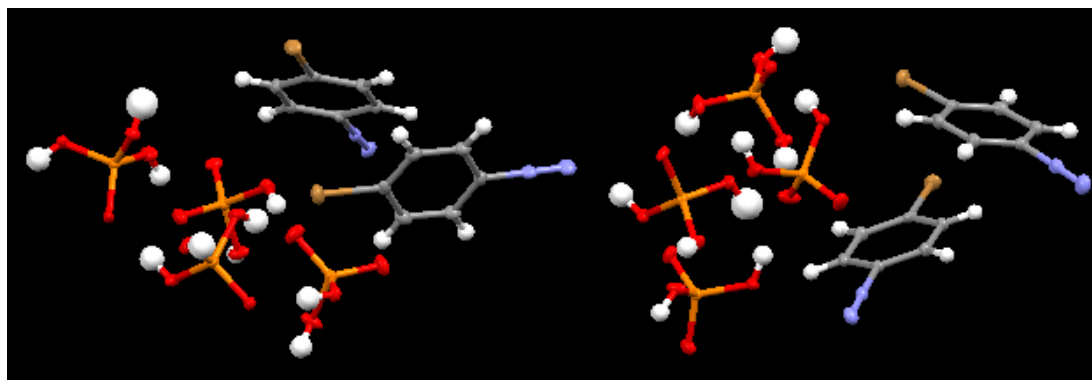
Table 6: Solvent screen for aryldiazonium dihydrogen phosphate formation

While the reaction proceeded as expected in acetonitrile, acetic acid and water (Table 6, entries 2, 3 and 4), the reactions performed in THF and ethanol exclusively led to a by-product believed to be the triazene derivative, as previously observed by Felpin *et al* with methanesulfonic acid in methanol.¹¹³ It is noteworthy that the dihydrogen phosphate salt **194** did not precipitate, even after addition of TBME as anti-solvent, and the product could not be isolated. In spite of these issues, a successful isolation of the analogous 4-bromo-benzenediazonium dihydrogen phosphate **195** could be achieved by switching the substrate to 4-bromo aniline **103** and the solvent to *iso*-propanol (Scheme 55).



Scheme 55: Synthesis of 4-bromo-benzenediazonium dihydrogen phosphate 193

The product precipitated spontaneously from the reaction mixture and was isolated in 81% yield. As no literature reports describing the formation of such salts were found, the precipitate was fully characterised, including by X-ray crystallography, to confirm its composition (Figure 24). Crystals of **195** were grown by slow diffusion of diethyl ether into a saturated solution of the previously obtained precipitate in acetic acid.



Grey: carbon; White: hydrogen; Blue: nitrogen; Brown: bromine; Red: oxygen; Orange: phosphorus

Figure 24: X-Ray data of 4-bromo benzenediazonium dihydrogen phosphate 195

While the X-ray crystal structure confirmed the presence of the dihydrogen phosphate motif, it also showed an extra dihydrogen phosphate unit which is presumably present to fill a gap in the crystal structure. This observation is believed to be an artefact of the structure packing within the crystal and may not be representative of the initially isolated material.

Although phosphoric acid was found to be efficient to generate aryldiazonium species *in situ*, the various advantages exhibited by the dihydrogen phosphate counter-ion could not overcome their isolation problem and as a consequence, it was decided not to pursue their investigation and to focus on more specific substrates.

III.1.iv Synthesis and isolation of a benzyne precursor

As discussed in the introduction (*vide supra*), 2-carboxylate benzenediazonium **163** is a specific compound which has the ability to decompose into benzyne **37** through the generation of carbon dioxide and nitrogen (Figure 25).

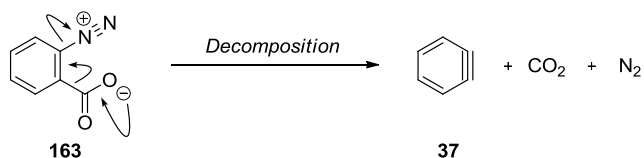
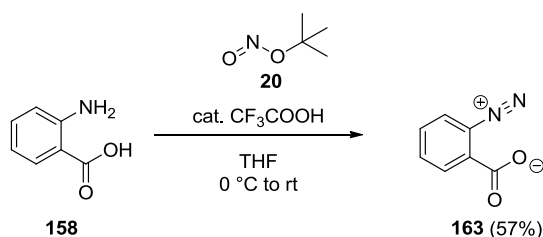


Figure 25: Decomposition of 2-carboxylate benzenediazonium **163**

Unlike the previously examined aryldiazonium salts in which the diazonium compound and the counter-ion were two separate entities, this zwitterion does not leave a latent counter-ion during subsequent reactions. Hence the formation of this benzyne intermediate under these conditions was attractive from an industrial point of view as it could potentially lead to new sustainable pathways releasing exclusively benign gases compared to other benzyne-based methodologies.^{114,115} As a consequence, this compound was prepared and isolated by adapting a procedure reported by Logullo *et al* (Scheme 56).



Scheme 56: Preparation of 2-carboxylate benzenediazonium **163**

Accordingly, anthranilic acid **158** was reacted with *tert*-butyl nitrite **20** in the presence of a catalytic amount of TFA to form the zwitterion **163** which precipitated spontaneously from the reaction mixture and was isolated in 57% yield by filtration. Logullo *et al* described the molecule as being highly explosive when dry and this observation was verified with the material detonating under friction or heat (*vide infra*). As a consequence, this area of research was not pursued further due to safety concerns and legal restrictions related to the preparation of explosive compounds.

III.1.v Thermal stability assessment of aryldiazonium salts

As observed with 2-carboxylate benzenediazonium **163** which detonated under friction or heat, aryldiazonium salts may prove to be unstable under certain circumstances and therefore suffer from a bad reputation among chemists. While the data reported in the literature are qualitative rather than quantitative, the work presented in this section aims to provide quantitative data about the thermal and mechanical stability of aryldiazonium salts to ultimately reach a correlation between structure and stability. In addition, process safety requires numerical data to assess the behaviour of these species in chemical processes.

It was necessary to first establish the following safety protocol to assess the stability of these compounds: Initial tests were designed to establish if the material would detonate under impact, friction or exposure to temperatures as high as 300 °C to assess if the material would behave as a detonator under specific conditions. These preliminary and qualitative tests were also designed to protect the Differential Scanning Calorimetry device, a sensitive piece of equipment which is used in the subsequent step for the quantitative evaluation of non-detonating compounds. Apart from 2-carboxylate benzenediazonium **163** which detonated under friction or heat, none of the previously isolated aryldiazonium salts exhibited a positive result and a DSC analysis was conducted for each of these compounds. This thermoanalytical technique allows the detection of energetic events such as melting point (endothermic phenomenon) or decomposition (exothermic phenomenon) and the temperatures at which they occur. This study was conducted by comparing the energy of a sample sealed in gold crucible with a standard reference upon gradual heating. An energetic event is represented by a peak which is defined by a left limit (temperature at which the phenomenon starts), a right limit (temperature at which the phenomenon stops) and the area under the curve (which gives the total energy of the phenomenon). Figure 25 exhibits both phenomena: an endothermic event starts at 136 °C and finishes at 149 °C while an exothermic event starts at 149 °C and finishes at 202 °C. It is noteworthy that both events are overlapping in this particular case.

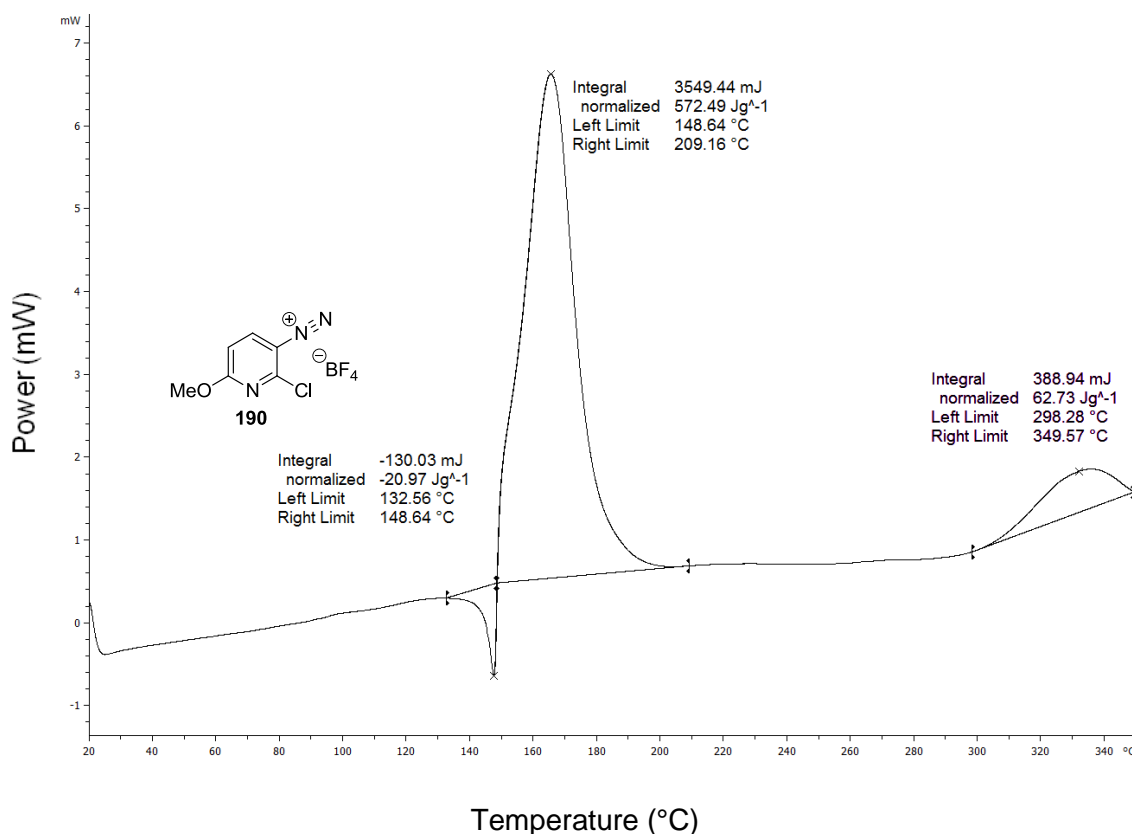
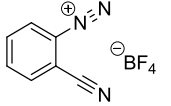
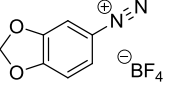
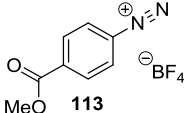
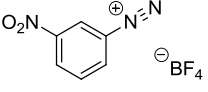
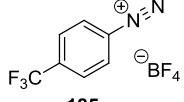
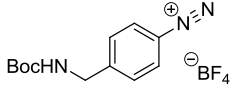
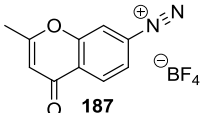
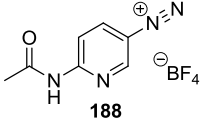
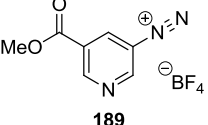
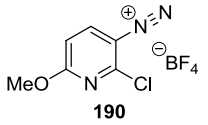
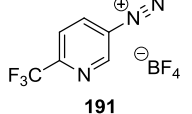


Figure 25: DSC analysis of compound **174**

The maximum recommended operating temperature T_{MR} , expressed in °C, was thus obtained from the formula $T_{MR} = 0.7T_o - 46$ in which T_o is the onset temperature (left limit) arising from the DSC evaluation.¹¹⁶ As discussed in the introduction, the knowledge brought by this safety protocol provided a scientific basis for the safe handling of these species. Accordingly, all the previously isolated aryldiazonium salts were evaluated by DSC and the results are reported in table 7.

Entry	Compound	T_o	Normalised Energy	T_{MR}
1		80 °C	425.81 J.g ⁻¹	16 °C
2		114 °C	98.62 J.g ⁻¹	34 °C

Entry	Compound	T ₀	Normalised Energy	T _{MR}
3	 182	143 °C	352.29 J.g ⁻¹	54 °C
4	 183	93 °C	674.97 J.g ⁻¹	19 °C
5	 113	72 °C	225.79 J.g ⁻¹	4 °C
6	 184	124 °C	493.78 J.g ⁻¹	41 °C
7	 185	77 °C	162.70 J.g ⁻¹	8 °C
8	 186	75 °C	242.66 J.g ⁻¹	7 °C
9	 187	104 °C	365.85 J.g ⁻¹	27 °C
10	 188	110 °C	418.17 J.g ⁻¹	31 °C
11	 189	72 °C	445.80 J.g ⁻¹	4 °C
12	 190	133 °C	571.56 J.g ⁻¹	47 °C
13	 191	63 °C	423.86 J.g ⁻¹	- 2 °C

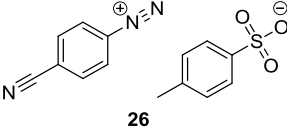
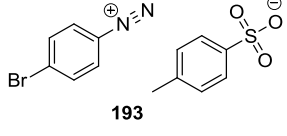
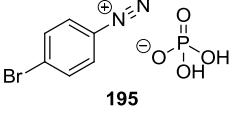
Entry	Compound	T _o	Normalised Energy	T _{MR}
14	 26	90 °C	429.44 J.g ⁻¹	17 °C
15	 193	90 °C	314.62 J.g ⁻¹	17 °C
16	 195	105 °C	243.86 J.g ⁻¹	28 °C

Table 7: DSC analysis of aryldiazonium salts

Unsurprisingly, a significant exothermic event between 63 °C and 202 °C was detected for all the aryldiazonium salts screened, with energies ranging from 98.62 J.g⁻¹ (Table 7, entry 2) to 674.97 J.g⁻¹ (Table 7, entry 4). After determination of the recommended maximum operating temperature T_{MR} for each compound it is noteworthy that only a very few of them may be used above 30 °C under totally safe conditions (Table 7, entries 2, 3, 6, 10 and 12), thus emphasising the limited stability of these salts.

The only emerging trend observed from these DSC data comes from the structure of the aryldiazonium core. Comparison of pyridinyldiazonium salts with the corresponding phenyldiazonium salts showed that the decomposition energies were much higher for pyridinyldiazonium species while the onset temperatures remained similar (Table 7, entries 5 and 7 vs entries 11 and 13). This observation confirmed that the presence of nitrogen atoms in the ring increases the enthalpic energy of such compounds.

The last component to be investigated in this stability study was the counter-ion of the aryldiazonium salt as it is believed to have an impact on the stabilisation of the diazonium group as discussed in the introduction. In order to conduct this study, previously prepared 4-bromo benzenediazonium tetrafluoroborate **73**, tosylate **193** and dihydrogenphosphate **195** salts were subjected to DSC analysis (Figure 26).

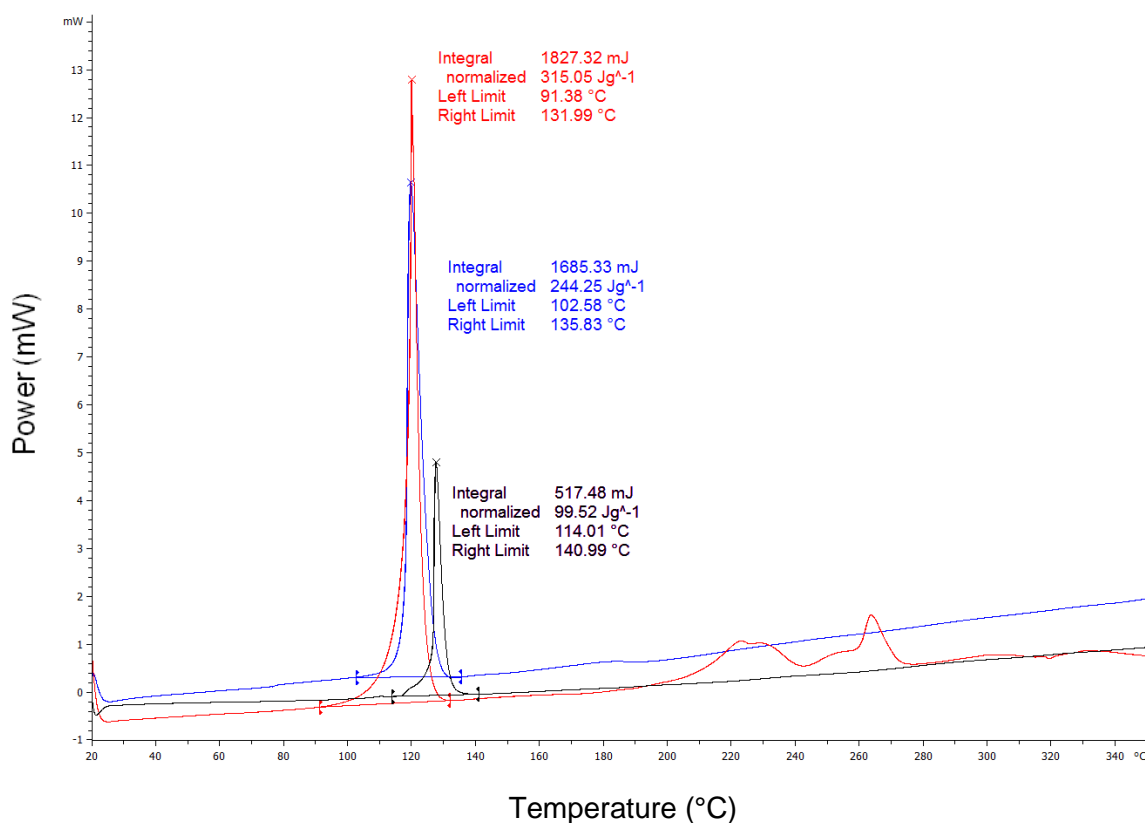


Figure 26: DSC data comparison of different 4-bromo benzenediazonium salts. Black: tetrafluoroborate salt; Red: tosylate salt; Blue: dihydrogen phosphate salt

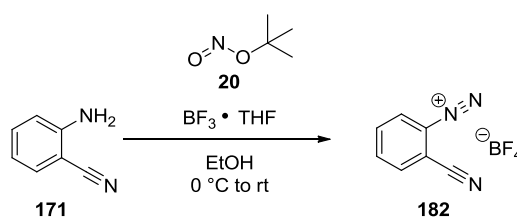
While the onset temperature of both the dihydrogen phosphate salt **195** and tosylate salt **193** were almost identical (ca. 100 °C), the onset temperature of the tetrafluoroborate salt **73** was higher (114 °C), exhibiting an increased stability of this salt. The decomposition energy was also found to be considerably lower for the tetrafluoroborate salt **73** (Table 7, entry 2) compared to the dihydrogen phosphate salt **195** (Table 7, entry 15) and the tosylate salt **193** (Table 7, entry 14). The quantitative results obtained by DSC analysis thus showed that if the kinetic stability was dependent on the nature of the aryldiazonium part, the counter-ion was found to influence the thermodynamic decomposition of these species as similar kinetic stabilities were observed in this case. Among the counter-ions investigated, tetrafluoroborate salts were found to provide the best stability as reported in the literature through empirical statements.^{17,16} It is also worth mentioning that an exothermic event was detected for the tosylate salt **193** despite the report by Filimonov *et al.* stating that “no explosive phenomenon” was recorded when the compound was analysed between 0 °C and 600 °C under a nitrogen atmosphere.¹¹

This inconsistency suggests that oxygen could play a role in the decomposition of these species by acting as a radical initiator.

The results obtained clearly supported the hypothesis that the counter-ion is a key component of aryldiazonium salt stability and among them, the tetrafluoroborate salt proved to be the most stable entity. Aryldiazonium salts were not found to be unstable beyond reason and in order to help break down the perception that these species cannot be handled on industrial scale, it was decided to scale-up the synthesis of 2-cyano-benzenediazonium tetrafluoroborate salt **182**.

III.1.vi Scale-up study

Prior to embarking on scale-up, the thermal stability of *tert*-butyl nitrite **20**, 2-cyano benzenediazonium tetrafluoroborate salt **182** and the reaction mixture were evaluated by DSC to confirm that the diazotisation conditions were compatible with the intended process of running the reaction from 0 °C to room temperature (Table 8).



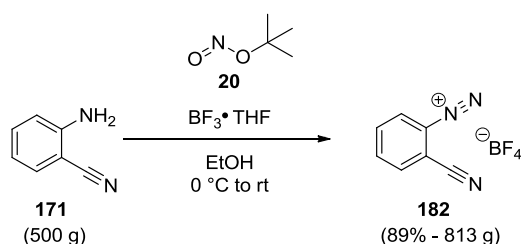
Entry	Compound	T _O	Normalised Energy	T _{MR}
1	 20	160 °C	270.44 J.g ⁻¹	66 °C
2	 182	143 °C	352.29 J.g ⁻¹	54 °C
3	Reaction mixture	56 °C	72.66 J.g ⁻¹	N.A. ^a

^aNot applicable due to the low energy (<100 J.g⁻¹), see text.

Table 8: Thermal stability assessment of the diazotisation process

While all the diazotisation components revealed an exothermic event by DSC analysis, these events only occur at elevated temperatures T_O (160 °C and 143 °C, Table 8, entries 1 and 2) and the corresponding maximum processing temperatures

T_{MR} (66 °C and 54 °C, Table 8, entries 1 and 2) were found to be compatible with the intended process of running the reaction from 0 °C to room temperature. It is also worth mentioning that the low amplitude decomposition of the reaction mixture (72.66 J.g^{-1} , Table 8, entry 3) could be absorbed through the substantial heat capacity of the solvent ($112.4 \text{ J.mol}^{-1}.\text{K}^{-1}$) and hence this event was not considered hazardous. These results allowed the scale-up of the diazotisation of 2-cyano-aniline **171** between 0 °C and room temperature under safe conditions (Scheme 57).



Scheme 57: Multimolar-scale diazotisation reaction

The reaction was carried out by pumping *tert*-butyl nitrite **20** through a peristaltic pump into a 20 L reactor maintained at 0 °C containing 2-cyano-aniline **171** and boron trifluoride – THF complex in 20 volumes of ethanol (Figure 24). The product, 2-cyano benzenediazonium tetrafluoroborate salt **182**, precipitated spontaneously from the reaction mixture and could be isolated by simple filtration in 89% yield after drying. It is noteworthy that using less than 20 volumes of ethanol decreased the purity of the precipitate as the starting aniline co-precipitated with the product under these conditions.

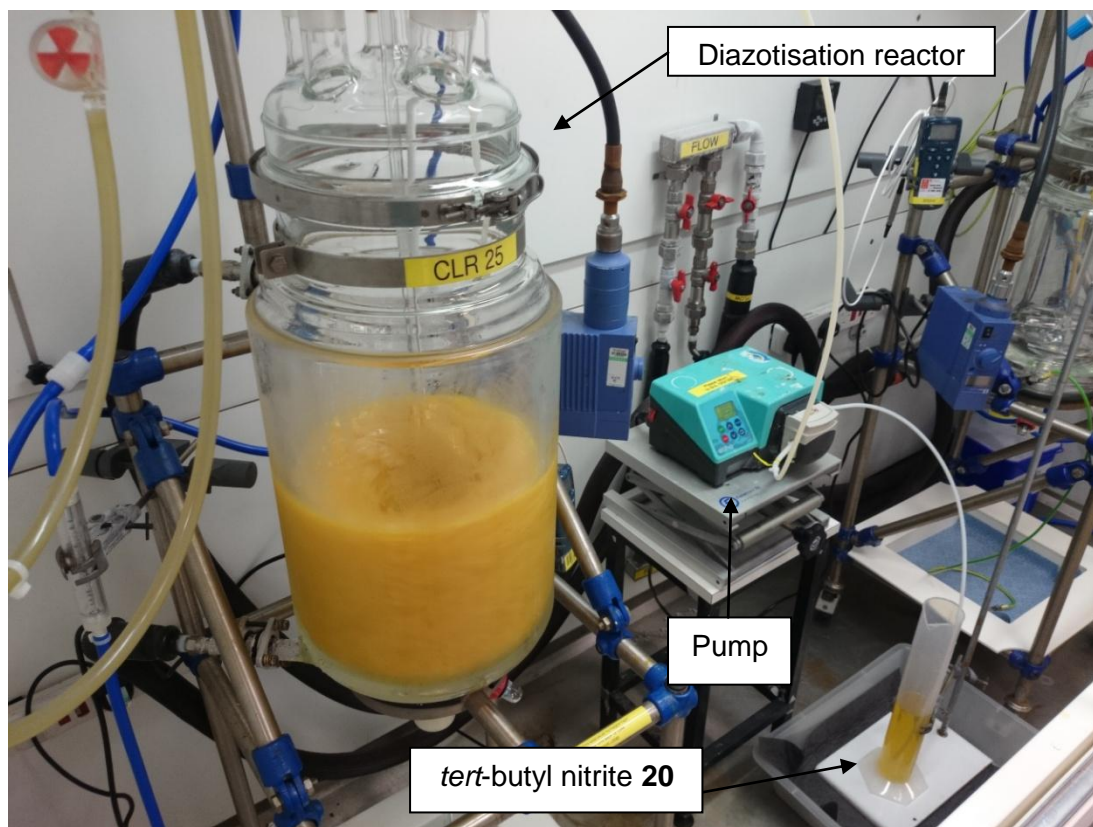


Figure 27: Kilogram-scale diazotisation set-up

By converting a cheap and readily available aniline into a high value and sustainable cross-coupling partner in a limited amount of solvent under safe conditions, this process emphasised the easy and safe preparation of aryldiazonium salts on an industrial scale. These species will now be investigated in new downstream reactions in order to improve their sustainability and cost-effectiveness.

III.2 Aryldiazonium salts as green and efficient coupling partners for the Suzuki-Miyaura reaction

III.2.i Reducing the cost of palladium catalysis in the pharmaceutical industry

The expertise acquired in the preparation, isolation and safety assessment of aryldiazonium salts is intended to handle these species under the safest conditions possible, including in synthetically relevant transformations. Among them, the Suzuki-Miyaura cross-coupling is central to organic synthesis, particularly in Industry, as recognised by the award of the Nobel prize for Chemistry in 2010.²⁵ Metal catalysis indeed exhibits numerous advantages such as efficiency and

sustainability as elaborated systems can be afforded through the use of a substoichiometric metal-ligand combination. Hence the place of catalysis in the pharmaceutical industry has grown up together with its associated challenges.¹⁰³

In this context, pharmaceutical companies including GlaxoSmithKline are committed to develop sustainable and catalytic processes while controlling the associated costs. In one of these efforts, the preference of aryl chlorides over more reactive aryl iodides and aryl bromides in cross-coupling methodologies is driven by their reduced costs, their wider availability and their better stability to other chemistry.¹¹⁷ However, these substrates frequently require more forcing conditions together with more active and expensive catalyst – ligand systems for the reaction when compared to analogous bromide and iodide derivatives. As discussed in the introduction, all these substrates could be effectively prepared from aryldiazonium salts through the Sandmeyer reaction^{32,33,35} (among other methodologies) and as a consequence, the direct cross-coupling of these species could shorten the synthesis while reducing the cost associated with the preparation of this valuable coupling partner (Figure 28).

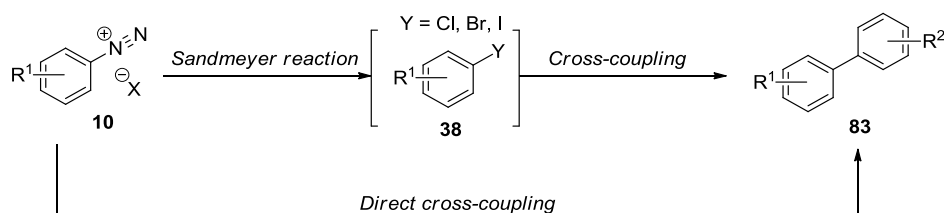


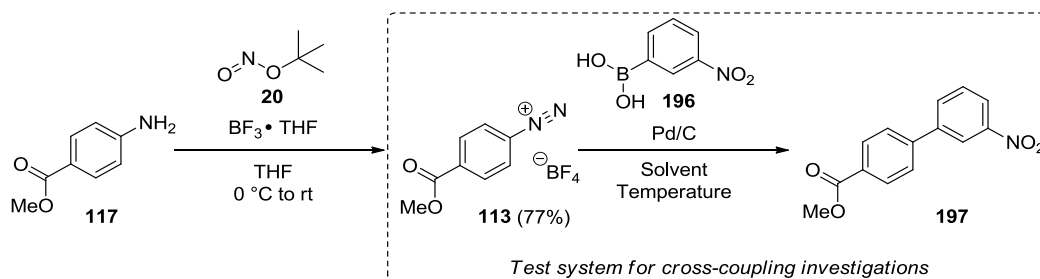
Figure 28: Shortening the synthesis of biaryl systems by direct cross-coupling

This entropically favourable release of nitrogen also provides an important driving force for the reaction, meaning that less active and low-cost palladium catalysts are potentially able to promote such couplings. Among them, palladium on charcoal provides a potential ligand-free option while allowing a simple recovery of this precious metal by filtration and therefore represents an attractive alternative to homogeneous palladium sources.¹¹⁸

While the combination of aryldiazonium salts with palladium on charcoal has proved to be successful in Suzuki-Miyaura reactions on laboratory scale,⁵⁸ an in-depth study of this system was required in order to develop an industrially viable process for the synthesis of biaryl-containing drugs.

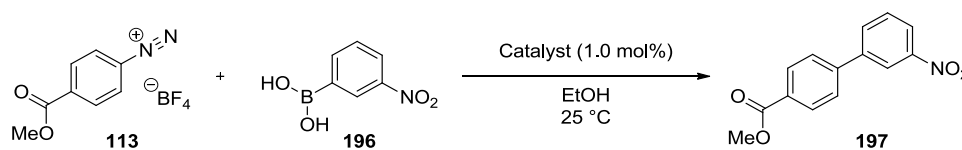
III.2.ii Investigating the impact of the palladium catalyst properties

As demonstrated in the previous section, aryldiazonium tetrafluoroborate salts can be reliably isolated through direct precipitation from the reaction medium and showed improved stability over other counter-ions. As a consequence, methyl 4-diazonium benzoate tetrafluoroborate **113** was selected as a model substrate to react with 3-nitro-phenylboronic acid **196** in the presence of catalytic amounts of palladium of charcoal (Scheme 58).



Scheme 58: Preparation of aryldiazonium tetrafluoroborate **113** and model system

Initial investigations focused on the choice of palladium catalyst and the properties which impact reaction efficiency, including metal loading, distribution, oxidation state and moisture content. While the characterisation of palladium on charcoal requires specific and advanced techniques,¹¹⁹ these data could not be obtained in-house and were provided by the different manufacturers to allow the selection and screening of a wide range of catalysts in our model system using previously reported reaction conditions⁵⁸ (Table 9). It is noteworthy that due to intellectual property reasons, some relevant parameters such as the source of charcoal employed or the preparation methods used were not disclosed by the suppliers and could therefore not be evaluated in this study.



Entry	Catalyst	O.S. ^a	Structure ^b	Water content	HPLC yield ^c	Isolated yield ^d
1	Johnson Matthey 5% Pd/C type 394	2	Egg shell	56.70%	>99%	95%
2	Johnson Matthey 10% Pd/C type 394	2	Egg shell	47.00%	85%	91%
3	Johnson Matthey 5% Pd/C type 58	0	Intermediate	48.00%	88%	79%

Entry	Catalyst	O.S. ^a	Structure ^b	Water content	HPLC yield ^c	Isolated yield ^d
4	Johnson Matthey 10% Pd/C type 58	0	Intermediate	58.10%	51%	52%
5	BASF 3% Pd CP M/R Code 00029	0	N.R.	56.68%	42%	44%
6	BASF 5% Pd CP M/R Code 00031	0	N.R.	57.22%	61%	64%
7	BASF 10% Pd CP M/R Code 00033	0	N.R.	54.91%	55%	68%
8	Johnson Matthey 5% Pd/C type 58	0	Intermediate	2.20%	83%	79%
9	Johnson Matthey 5% Pd/C type 39	2	Egg shell	58.10%	64%	73%
10	Johnson Matthey 10% Pd/C type 39	2	Egg shell	56.90%	75%	76%
11	Degussa 5% Pd/C E196 R/W 5%	0	Egg shell	56.30%	31%	37%
12	Degussa 10% Pd/C E196 XNN/W	0	Egg shell	53.20%	68%	66%
13	Degussa 5% Pd/C E101 O/W	2	Uniform	53.20%	45%	49%
14	BASF 3% Pd CP M/UR Code 00030	2	N.R.	57.86%	84%	82%
15	BASF 5% Pd CP M/UR Code 00032	2	N.R.	58.65%	90%	85%
16	BASF 10% Pd CP M/UR Code 00034	2	N.R.	59.70%	90%	86%
17	Sigma-Aldrich Pd(OAc) ₂	2	N.A.	N.R.	>99%	97%
18	Johnson Matthey 3% Rh/C + 2% Ru/C	0	Intermediate	2.10%	N.D.	-
19	Johnson Matthey 5% Ru/C type 97	0	Intermediate	59.00%	N.D.	-
20	Sigma-Aldrich 3% Cu/C	N.R.	N.R.	N.R.	N.D.	-

^aOxidation state of the metal species. ^bEggshell shows palladium located on the exterior surface; Intermediate shows palladium located deeper within charcoal pores; Uniform shows palladium evenly dispersed throughout the charcoal. ^cHPLC yield calculated with calibration curve. ^dReactions were repeated at least in duplicate and average isolated yield after chromatography is shown.

Table 9: Screening of different catalysts

As expected, all of the palladium catalysts examined promoted the transformation to give the desired biaryl product **197**, albeit in variable yields. While the cross-coupling proceeded generally better in the presence of palladium(II) species (Table 9, entries 1, 2, 9, 10, 13, 14, 15, 16 and 17) compared to palladium(0) metal (Table 9,

entries 3, 4, 5, 6, 7, 8 and 11), the minor difference observed in the reaction yields could unfortunately not lead to a definitive conclusion regarding the influence of the oxidation state on this transformation. Other catalyst properties, including moisture content, metal loading and distribution were also not found to have a significant impact on the reaction efficiency as no clear trends could be observed from the catalyst screening (Table 9, compare entries 3 and 8 for moisture; entries 1 and 2 for metal loading; entries 4 and 12 for metal distribution). In contrast with palladium species, alternative transition metals including rhodium, ruthenium and copper supported on charcoal did not enable the coupling as the product **197** could not be detected in the presence of these catalysts (Table 9, entries 18, 19 and 20). Finally, soluble palladium(II) acetate delivered the biaryl system **197** in 97% isolated yield (Table 9, entry 17) and therefore constitutes a useful alternative to supported catalysts depending on the intended isolation protocol.

The evaluation of a wide range of catalysts in the coupling of aryl diazonium tetrafluoroborate salts with aryl boronic acids showed that catalysts with nominally similar properties behaved in a markedly different manner. While no catalyst properties could be identified as critical, the elevated yields obtained in this screening highlighted the cost-effectiveness of the transformation in accordance with the objectives of the study.

III.2.iii Identifying the optimal solvent through OPLS and PCA analysis

As discussed in section II.1.i, costs and sustainability are the two pillars of process development and both factors can be impacted by the choice of the solvent. The identification of a solvent providing both reaction efficiency and compatibility with downstream isolation as well as green credentials was crucial, especially when scale-up is envisaged.¹⁰² As a consequence, two efficient heterogeneous catalysts presenting different properties (Johnson Matthey 5% Pd/C type 394 and Johnson Matthey 5% Pd/C type 58) and soluble palladium(II) acetate were used in a screen of common organic solvents selected from a PCA model (Figure 29).¹¹¹

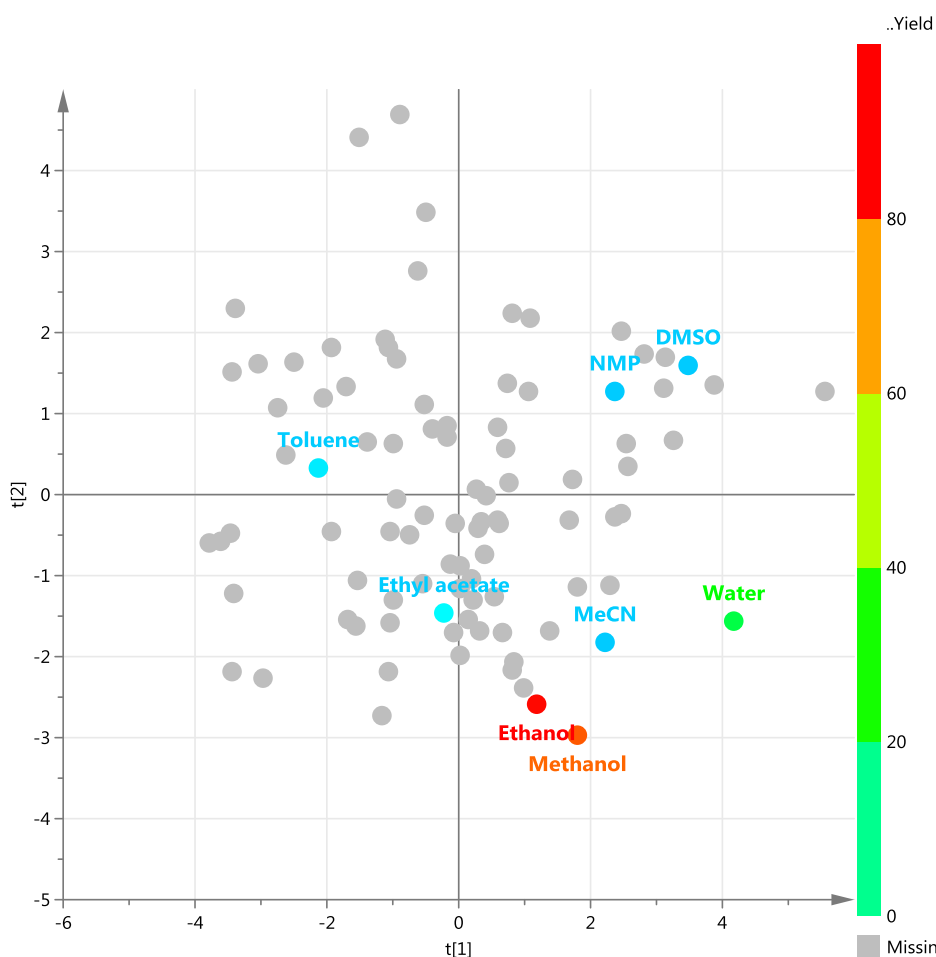
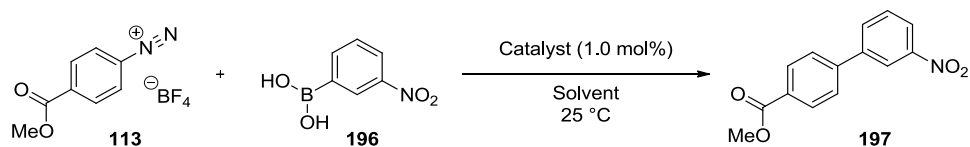


Figure 29: PCA solvent model with reported yields (by Sandrine Olazabal)

These reaction media were selected according to their difference in terms of physico-chemical properties, also referred to as solvent descriptors. These inherent descriptors were identified and reported by Carlson and co-workers¹¹¹ to describe each solvent through numerical values in nine dimensions: melting point, boiling point, dielectric constant, dipole moment, refractive index, normalised Reichardt-Dimroth parameter, lipophilicity (logP) and water solubility. The spatial position of a solvent in the PCA solvent model is hence representative of the combination of its inherent descriptors. The thus selected solvents were evaluated using the previously established model reaction in the presence of the different catalysts and their performance is shown in Table 10.



Entry	Solvent	Catalyst reference	HPLC yield ^a	Isolated Yield ^b
1		Johnson Matthey 5% Pd/C type 394	6%	-
2	EtOAc	Johnson Matthey 5% Pd/C type 58	4%	-
3		Sigma-Aldrich Pd(OAc) ₂	81%	83%
4		Johnson Matthey 5% Pd/C type 394	29%	30%
5	Water	Johnson Matthey 5% Pd/C type 58	11%	-
6		Sigma-Aldrich Pd(OAc) ₂	54%	54%
7		Johnson Matthey 5% Pd/C type 394	4%	-
8	Toluene	Johnson Matthey 5% Pd/C type 58	2%	-
9		Sigma-Aldrich Pd(OAc) ₂	22%	21%
10		Johnson Matthey 5% Pd/C type 394	N.D.	-
11	DMSO	Johnson Matthey 5% Pd/C type 58	N.D.	-
12		Sigma-Aldrich Pd(OAc) ₂	N.D.	-
13		Johnson Matthey 5% Pd/C type 394	89%	95%
14	MeOH	Johnson Matthey 5% Pd/C type 58	73%	82%
15		Sigma-Aldrich Pd(OAc) ₂	84%	91%
16		Johnson Matthey 5% Pd/C type 394	>99%	95%
17	EtOH	Johnson Matthey 5% Pd/C type 58	81%	79%
18		Sigma-Aldrich Pd(OAc) ₂	>99%	97%
19		Johnson Matthey 5% Pd/C type 394	N.D.	-
20	NMP	Johnson Matthey 5% Pd/C type 58	N.D.	-
21		Sigma-Aldrich Pd(OAc) ₂	3%	-
22		Johnson Matthey 5% Pd/C type 394	N.D.	-
23	MeCN	Johnson Matthey 5% Pd/C type 58	N.D.	-
24		Sigma-Aldrich Pd(OAc) ₂	N.D.	-

^aHPLC yield calculated with calibration curve. ^bReactions were repeated at least in duplicate and average isolated yield after chromatography is shown.

Table 10: Screening of different solvents

While the low levels of water present in the catalyst did not prove to affect the reaction, only low to moderate yields were obtained when using water as the sole solvent. Nitrogen-containing reaction media such as NMP and acetonitrile (Table 10, entries 19 to 24) as well as DMSO (Table 10, entries 10 to 12) failed to enable the cross-coupling and this observation is believed to be due to the ability of these solvents to complex the palladium metal.¹²⁰ Considering the low reaction temperature used, the complexation of these solvents to the metal may prevent the oxidative insertion of the aryldiazonium salt. As expected from previous

reports,^{56,58,62,121,122} polar and protic reaction media such as ethanol (Table 10, entries 16 to 18) and methanol (Table 10, entries 13 to 15) provided the highest yields. It is noteworthy that significant amounts of methyl 4-methoxybenzoate were also observed by LC/MS in the crude reaction mixture, arising from the displacement of the diazonium group when methanol was used as solvent.¹²³ In order to obtain a deeper insight on the influence of the previously discussed solvent descriptors, an OPLS ¹²⁴ regression model was built (collaboration with Sandrine Olazabal) describing reaction yield as a function of solvent properties with Johnson Matthey 5% Pd/C type 394 as catalyst. This regression method aims to find the multidimensional direction in the solvent descriptors space that explains the maximum variance in the yield (Figure 30).

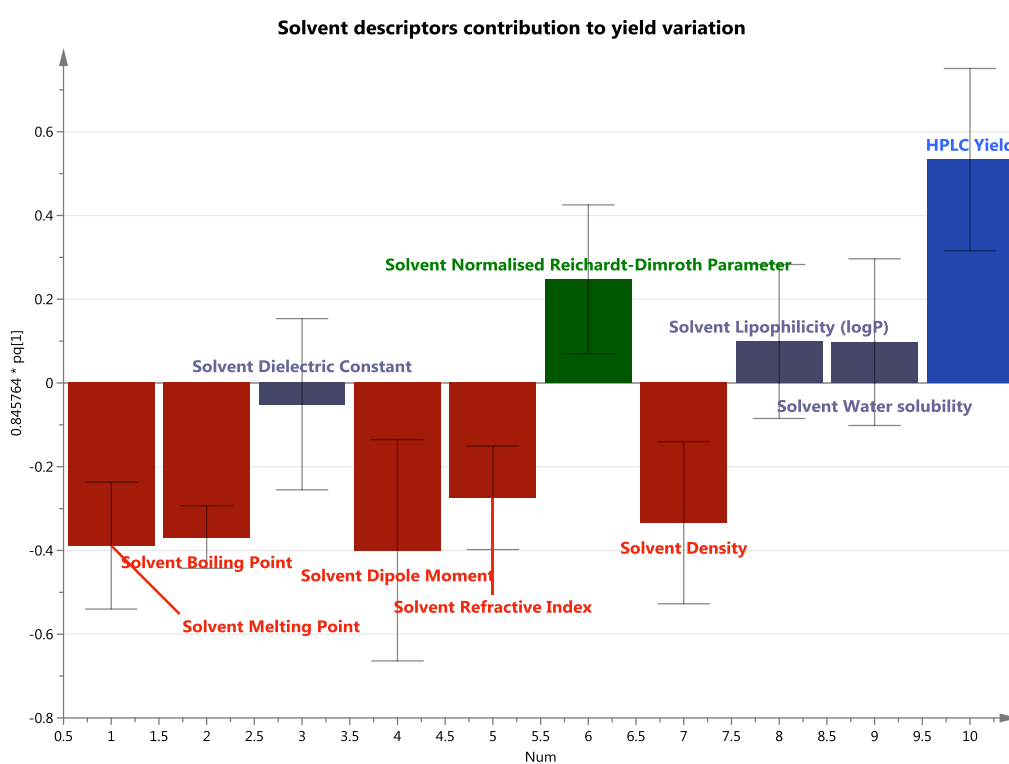


Figure 30: OPLS regression model (by Sandrine Olazabal)

Descriptors highlighted in green show a statistically-significant positive correlation with reaction yield; those in red show a statistically-significant negative correlation with reaction yield; and those in dark blue/grey show a correlation that is not statistically significant (95% confidence interval). The model ($R^2X=97.6\%$, $R^2Y=98.7\%$, $Q^2=91.1\%$) revealed that solvents with high normalised Reichardt-Dimroth parameter (polarisability)¹²⁵ resulted in high yield whereas

increased solvent melting point, boiling point, dipole moment, refractive index and density were detrimental to the reaction. With the identification of the critical solvent properties in hand, it is then possible to predict potentially improved yields in other solvents according to the PCA model data (Figure 31).

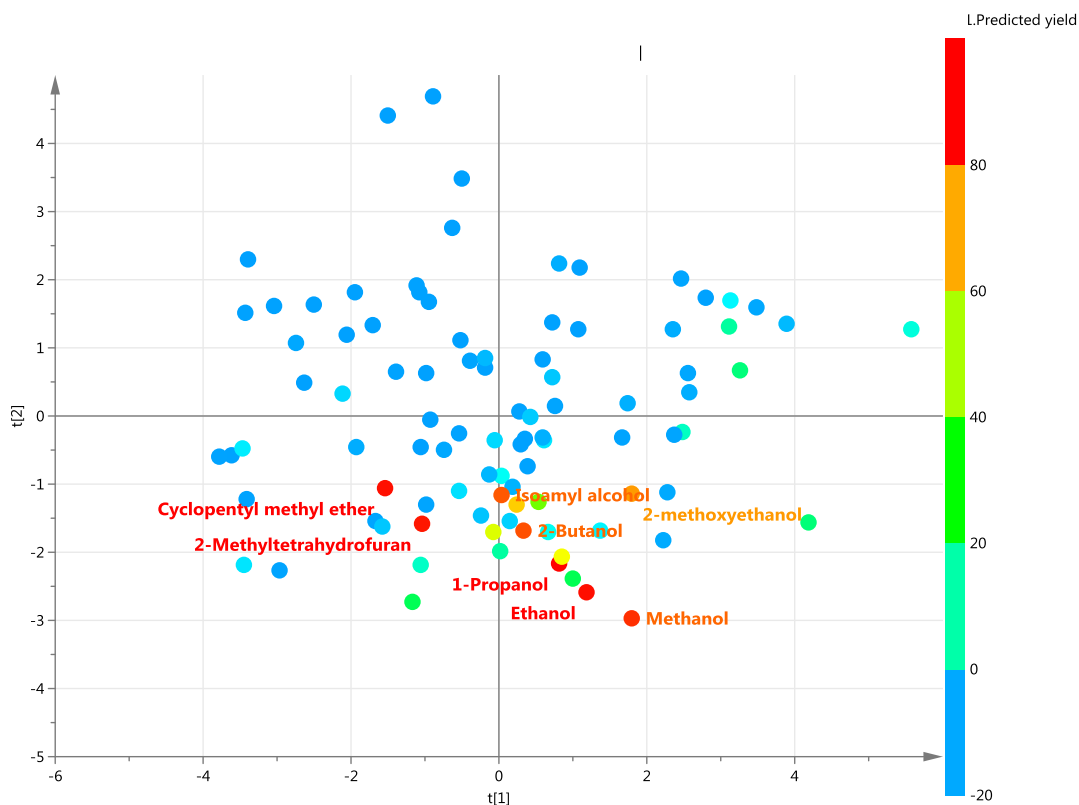


Figure 31: PCA solvent model with predicted yield (by Sandrine Olazabal)

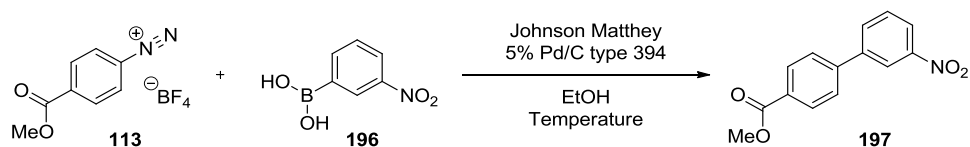
While the model surprisingly predicted CPME and 2-MeTHF as potential alternatives to alcohols, the known insolubility of aryldiazonium tetrafluoroborate salts in these reaction media led to the adoption of ethanol as best possible solvent for this transformation. The use of this relatively inexpensive solvent is compliant with the sustainability objectives of this work.

III.2.iv Optimisation of the reaction conditions through Design of Experiments

Design of experiments is a multifactorial analysis technique allowing the identification of key reaction parameters within a previously defined space¹²⁶ and is heavily used in industry for process optimisation.¹²⁷ Given the relative simplicity of this cross-coupling system, all of the critical parameters could be investigated, including aryldiazonium salt **113** equivalents (A), temperature (B), palladium

RESULTS & DISCUSSION

loading (C), volumes of solvent (with respect to **196**, D) and ethanol content (%v/v with respect to water, E) through 20 runs (16 factorial and 4 centre points) using a fractional factorial two level resolution V with HPLC yield as the response (Table 11).

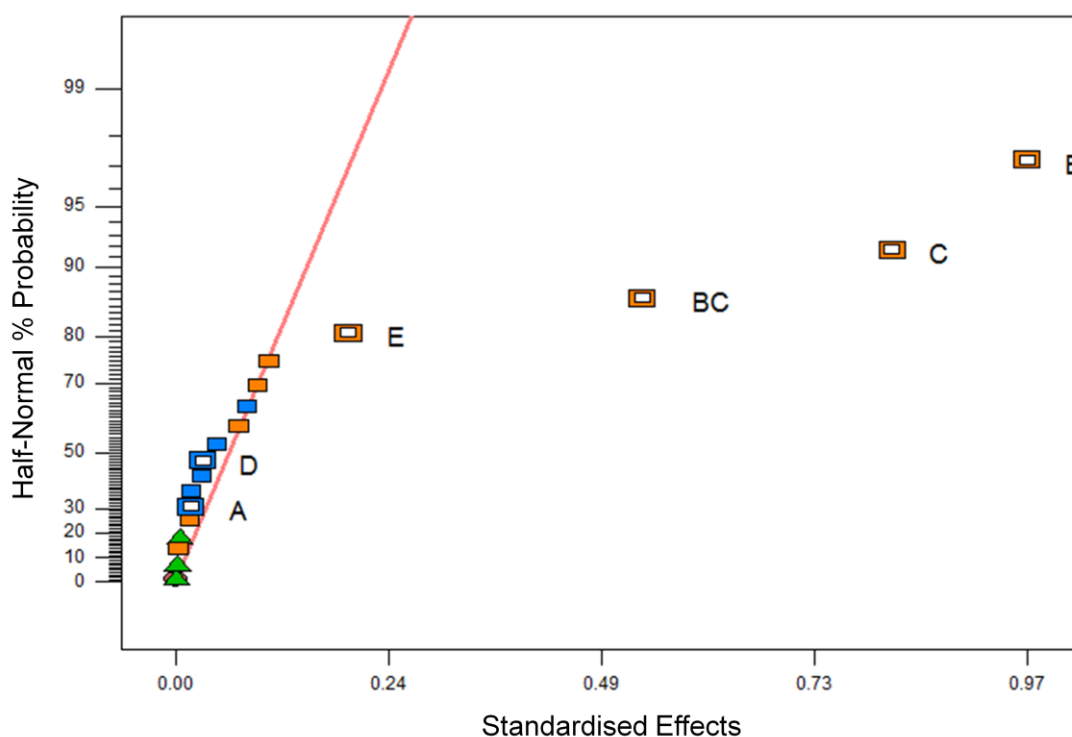


Run	Aryldiazonium Equivalent (equiv.) (A)	Temperature (°C) (B)	Palladium Loading (mol%) (C)	Solvent volumes (D)	Ethanol vs water (%v/v) (E)	HPLC Yield ^a (%)
1	1.25	20	1.05	55	75	25
2	1.25	20	1.05	55	75	29
3	1	0	2	100	100	1
4	1.5	0	0.1	100	100	0
5	1.5	0	2	10	100	2
6	1	40	2	10	100	69
7	1.5	40	0.1	10	100	3
8	1.5	40	0.1	100	50	1
9	1	0	0.1	100	50	0
10	1.25	20	1.05	55	75	31
11	1	40	0.1	10	50	1
12	1	40	0.1	100	100	5
13	1.5	40	2	100	100	92
14	1.25	20	1.05	55	75	28
15	1.5	40	2	10	50	61
16	1	40	2	100	50	54
17	1.5	0	0.1	10	50	0
18	1.5	0	2	100	50	1
19	1	0	2	10	50	1
20	1	0	0.1	10	100	1

^aHPLC yield calculated with calibration curve. Red: centre points.

Table 11: Design of Experiment runs

While Table 11 gives the detailed results of the thus designed runs, the data were interpreted in the software Design-Expert (version 7.1.1, Stat-Ease, Inc.) using a \log_{10} transformation with 0.92 as constant and an accurate model could be obtained ($R^2 = 0.9806$, $\text{Adj } R^2 = 0.9751$, $\text{Pred } R^2 = 0.9591$). The resulting half-normal plot shown in Figure 32 indicated that elevated temperature (B) as well as high catalyst loading (C) delivered increased reaction yields whereas neither the number of aryldiazonium salts (A) equivalents nor the solvent volumes (D) were found to influence the reaction outcome within the ranges investigated. It is noteworthy that while low moisture content in the catalyst could be tolerated by the transformation, the presence of water (E) proved to be slightly detrimental to the transformation.



Orange: positive effects; Blue: negative effects; Green: error from replicates

Figure 32: Half-normal plot using HPLC yield as response

The interaction temperature-palladium loading (BC) was also found to be important as Figure 33 showed that the effect of temperature was negligible at low catalyst loading (Figure 33, black line) whereas the reaction yield proved to increase together with the temperature in a non-linear manner at high catalyst loading (Figure 33, red line).

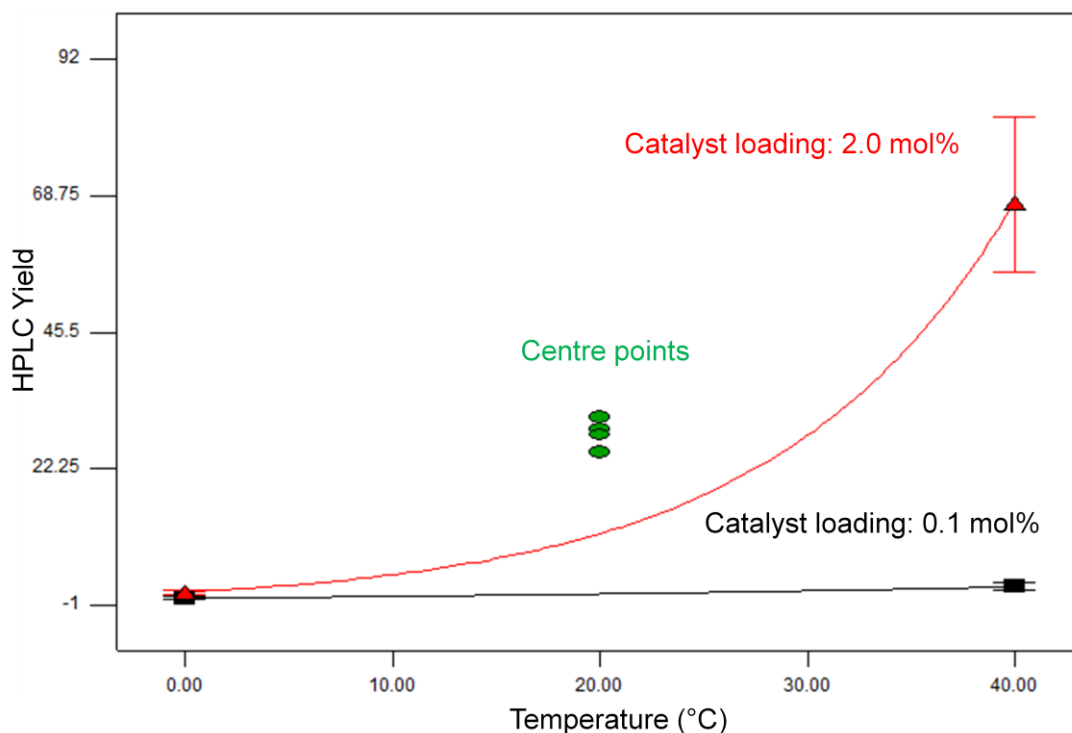


Figure 33: Interaction temperature – palladium loading (BC)

As a consequence of this optimisation study and in accordance with the objective set in terms of cost-effectiveness and sustainability, the optimal reaction conditions were selected as shown in Table 12, entry 4 which involved a minimum amount of valuable aryldiazonium salt **113** (1.1 equiv) in a concentrated solution of ethanol (10 vol) at 30 °C in the presence of 1.0 mol% of palladium catalyst.

Entry	Settings	Aryldiazonium	T	Palladium	Solvent	Ethanol
		Equivalent (equiv) (A)	(°C) (B)	Loading (mol%) (C)	volumes (D)	vs water (%v/v) (E)
1	Minimum	1.0	0	0.1	10	50
2	Centre	1.25	20	1.05	55	75
3	Maximum	1.5	40	2	100	100
4	Selected	1.1	30	1.0	10	100

Table 12: Design of Experiment summary with optimised conditions

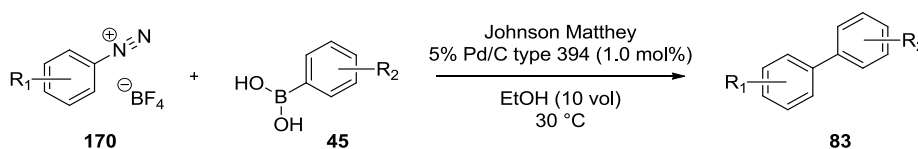
It is noteworthy that these results are in contrast with a previous study performed by Felpin *et al*⁶⁸ who found that with 0.1 mol% of palladium on charcoal, 100 volumes

of solvent were optimal and 1.5 equivalents of aryldiazonium tetrafluoroborate salt was required to give increased yields.

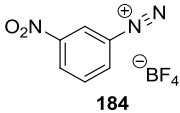
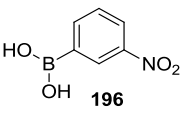
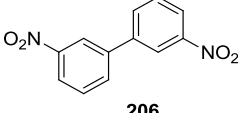
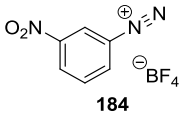
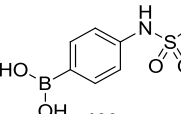
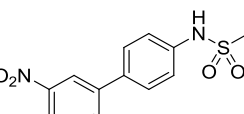
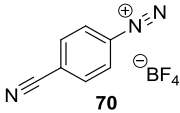
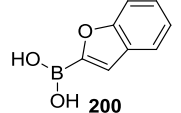
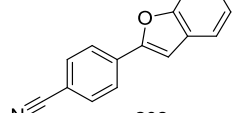
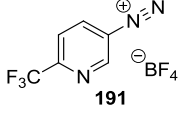
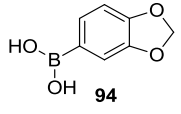
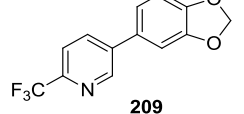
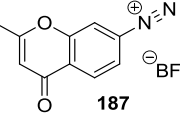
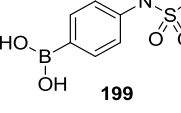
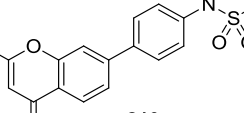
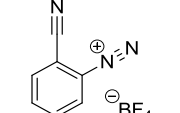
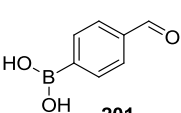
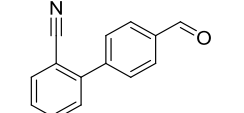
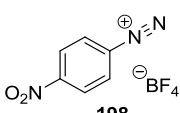
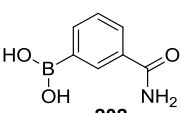
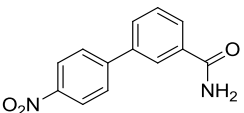
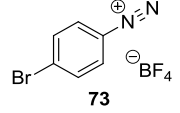
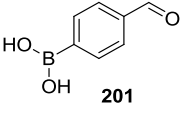
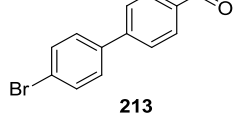
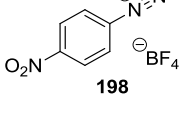
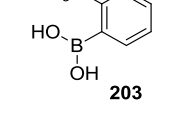
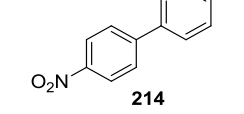
Hence the use of OPLS and DoE, two powerful statistical methods, enabled the rapid optimisation and understanding of this cross-coupling methodology while addressing the factors discussed in section II.1.i.

III.2.v Exploring the scope of the reaction

In order to implement this process into the portfolio of cross-coupling reactions, it was crucial to apply the previously selected reaction conditions to a challenging range of coupling partners in order to identify both compatible and incompatible functionalities (Table 13). While the aryl boronic acids investigated were commercially available, the requisite aryldiazonium tetrafluoroborate species were prepared using the methods developed in the first chapter. As a consequence, their thermal stability was also evaluated by DSC and their recommended maximum operating temperature T_{MR} is reported in Table 13. In the cases where the recommended maximum operating temperature T_{MR} was found to be below ambient temperature, the reaction was still run at 30 °C as the risks associated were minimal and manageable given the relatively small scale of the reactions. However, a full risk assessment must be carried out when handling any aryldiazonium species, especially on large scale.



Entry	T_{MR}^a	Aryldiazonium salt	Aryl boronic acid	Product	Isolated yield ^b
1	19 °C	 183	 196	 204	6%
2	41 °C	 184	 94	 204	90%
3	19 °C	 183	 94	 205	0%

Entry	T _{MR} ^a	Aryldiazonium salt	Aryl boronic acid	Product	Isolated yield ^b
4	41 °C	 184	 196	 206	94%
5	41 °C	 184	 199	 207	90%
6	16 °C	 70	 200	 208	35%
7	-2 °C	 191	 94	 209	7% (35%) ^c
8	27 °C	 187	 199	 210	92%
9	54 °C	 182	 201	 211	18% (72%) ^c
10	38 °C	 198	 202	 212	72%
11	34 °C	 73	 201	 213	42%
12	38 °C	 198	 203	 214	0% (0%) ^c

^aRecommended Maximum Processing Temperature. ^bIsolated yield after chromatography. ^cYield in parentheses refers to the reaction using Pd(OAc)₂ (1.0 mol%) as catalyst.

Table 13: Scope of the cross-coupling with aryldiazonium tetrafluoroborate salts

As a starting point of this scoping study, initial reactions were designed to understand the impact of the electronic properties of each coupling partner on the reaction outcome (Table 13, entries 1 to 4). Although electron rich aryldiazonium

salts failed to deliver the biaryl product (Table 13, entries 1 and 3) with unreacted starting materials observed by LC/MS, electron-deficient aryldiazonium salts proved to be efficient coupling partners under these conditions (Table 13, entries 2 and 4). The electronics of the aryl boronic acid were not found to significantly influence the process as both electron-rich (Table 13, entries 2, 5 and 8) and electron-deficient (Table 13, entries, 4, 9 and 10) substrates gave good conversion.

Depending on the purpose of the biaryl product, its substitution pattern is frequently designed either to allow further functionalisation of the core or to introduce biological activity / selectivity. In both cases, it was important to evaluate the compatibility of this new process with a range of functional groups. Hence, further substrate expansion showed that the reaction was compatible with a range of functional groups such as nitro (Table 13, entries 2, 4, 5 and 10), acetal (Table 13, entry 2), sulfonamide (Table 13, entry 5 and 8), aldehyde (Table 13, entries 9 and 11), nitrile (Table 13, entries 6 and 9), amide (Table 13, entry 10) and ester (Table 9). Unfortunately, pyridinyldiazonium species did not perform well in this process as the main by-product, 2-trifluoromethyl pyridine (as observed by LC/MS), arose from the protodediazotisation of the starting material. The corresponding pyridyl-aryl product **209** was therefore isolated in only 7% yield which improved to 35% when palladium(II) acetate was used, indicating that alternative catalysts may facilitate the coupling of this class of reaction partner (Table 13, entry 7).

The last aspect to be investigated in the reaction scope was the influence of the steric hindrance of both coupling partners. While the aryldiazonium species tolerated the relatively small 2-cyano group, albeit with diminished yield (Table 13, entry 9), the more bulky 2-trifluoromethyl group on the aryl boronic acid **203** was not tolerated and returned starting material (Table 13, entry 12). It is noteworthy that previous reports on similar methodologies appears to be highly dependent on the reaction conditions employed.⁵⁶

III.2.vi Designing the process for industrial scale

The purpose of this research was to implement this process to the existing portfolio of cross-coupling reactions for the production of active pharmaceutical ingredients and hence it was important to break down the perception that aryldiazonium salts could not be handled on larger scale. In line with the multimolar scale diazotisation

discussed in section III.1.vi, a similar thermal stability study was conducted prior to embarking on scale-up. Compound **211** (Table 13, entry 9) was selected as model substrate as it was a relevant pharmaceutical intermediate involved in the synthesis of important angiotensin II inhibitors, including Losartan **215**, Valsartan **166**, Irbesartan **216** and Telmisartan **217** (Figure 34).

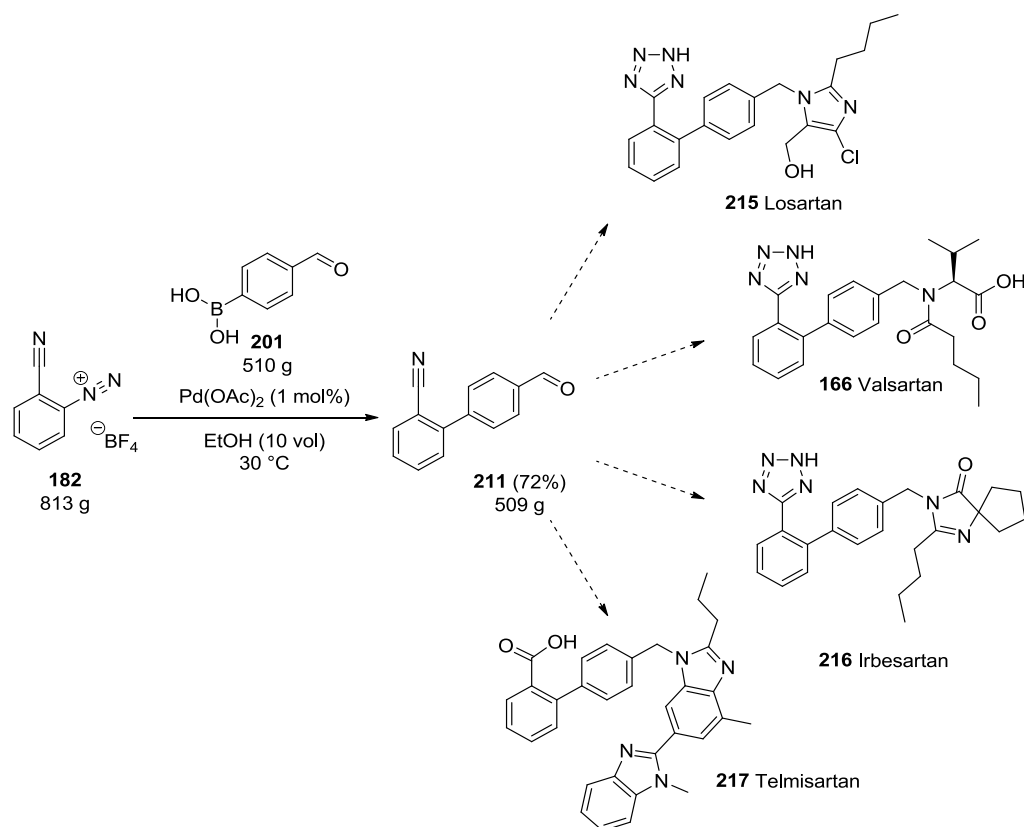


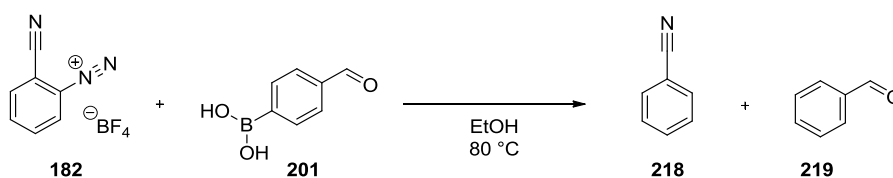
Figure 34: Scale-up of biaryl **211**, a precursor of angiotensin II inhibitors

2-Cyano-benzenediazonium tetrafluoroborate **182** and 4-formyl-phenyl boronic acid **201** both showed exothermic decompositions, with onset temperatures of 142 °C and 164 °C respectively (Table 14). As previously mentioned, the formula $T_{MR} = 0.7 \cdot T_O - 46$ set the recommended maximum operating temperature to 54 °C for aryldiazonium **181** and 69 °C for the boronic acid **201** (Table 14, entry 2). It is noteworthy that the DSC analysis of the coupling product **211** only revealed a negligible exothermic event (+27.65 J.g⁻¹) which was not considered hazardous given its low intensity (Table 14, entry 3). Finally, the mixture of **182** and **201** in ethanol exhibited an exothermic onset starting at 40 °C (Table 14, entry 4) with a relatively low severity (+194.50 J.g⁻¹) which could be absorbed through the substantial heat capacity of ethanol (112.4 J.mol⁻¹.K⁻¹).

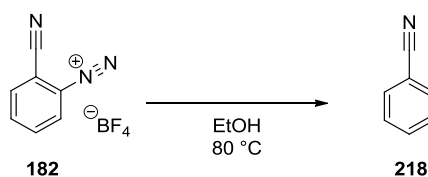
Entry	Sample	Onset temperature	Intensity	T _{MR}
1	182	142 °C – 194 °C	+352.29 J.g ⁻¹	54 °C
2	201	164 °C – 238 °C	-133.88 J.g ⁻¹ / +334.35 J.g ⁻¹	69 °C
3	211	111 °C – 171 °C	+27.65 J.g ⁻¹ / -119.28 J.g ⁻¹	None
4	182 + 201 in EtOH	40 °C – 92 °C	+194.50 J.g ⁻¹	N.A.

Table 14: Thermal stability assessment of cross-coupling components

This last result suggested the intriguing possibility that the reaction might take place under thermal conditions without the assistance of a catalyst. As a consequence, two control reactions were carried out on a small scale in order to minimise the consequences of an uncontrolled decomposition (Schemes 59 and 60).



Scheme 59: Control reaction without palladium catalyst



Scheme 60: Control reaction without palladium catalyst and without boronic acid

While the thermal reactions at 80 °C did not deliver the desired biaryl product **211**, the proto-dediazotised and proto-deborylated products **218** and **219** were observed by LC/MS, whose identity were confirmed by comparison with commercial samples. In addition, heating of 2-cyano-benzenediazonium tetrafluoroborate **182** in ethanol at 80 °C resulted in the formation of benzonitrile **218** which is in accordance with other reports of this type¹²⁸ and confirmed the need for palladium catalysis to achieve the reaction. The thermal stability study of this transformation showed that both coupling partners were compatible with the intended process of running the reaction at 30 °C with minimal risks. The reaction was carried out between 2-cyano-benzenediazonium tetrafluoroborate **182** (813 g, 1.00 equiv) and 4-formylphenyl boronic acid **201** (510 g, 0.91 equiv) in the presence of 1.0 mol% of palladium(II) acetate in 10 volumes of ethanol (Figure 34). After 24 hours, the reaction was

treated with an aqueous solution of *N*-acetyl-cysteine in order to scavenge the metal and help to precipitate the product which was then filtered, washed and dried to give 509 g (72% yield) of the valuable biaryl product **211** which was found to contain 1900 ppm of palladium by ICP analysis.

III.2.vii Comparison with existing methodologies

This methodology proved to be efficient for the preparation of biaryl containing drugs, even on large scale, and therefore constitutes a serious alternative in the portfolio of cross-coupling reactions. It was thus decided to compare the performance of this cross-coupling with similar methodologies published in the literature for the preparation of the valuable pharmaceutical intermediate **211** (Table 15).

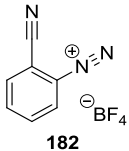
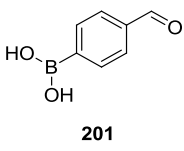
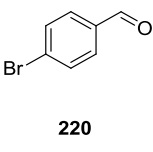
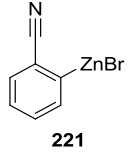
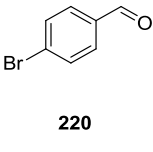
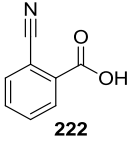
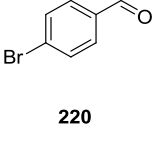
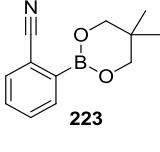
Entry	Electrophile	Nucleophile	Conditions	Yield
1	 182	 201	Pd(OAc) ₂ (1.0 mol%) EtOH (10 vol) 30 °C	72%
2 ¹²⁹	 220	 221	PdCl ₂ (PPh ₃) ₂ (2.0 mol%) THF (30 vol) MW, 160 °C	77%
3 ¹³⁰	 220	 222	PdBr ₂ (2.0 mol%), PPh ₃ (3.0 mol%) CuCO ₃ , K ₂ CO ₃ , Phenanthroline Quinoline (9 vol) 170 °C	50%
4 ¹³¹	 220	 223	Pd(PPh ₃) ₄ (3.0 mol%), K ₂ CO ₃ Toluene / EtOH (12 vol) 100 °C	73%

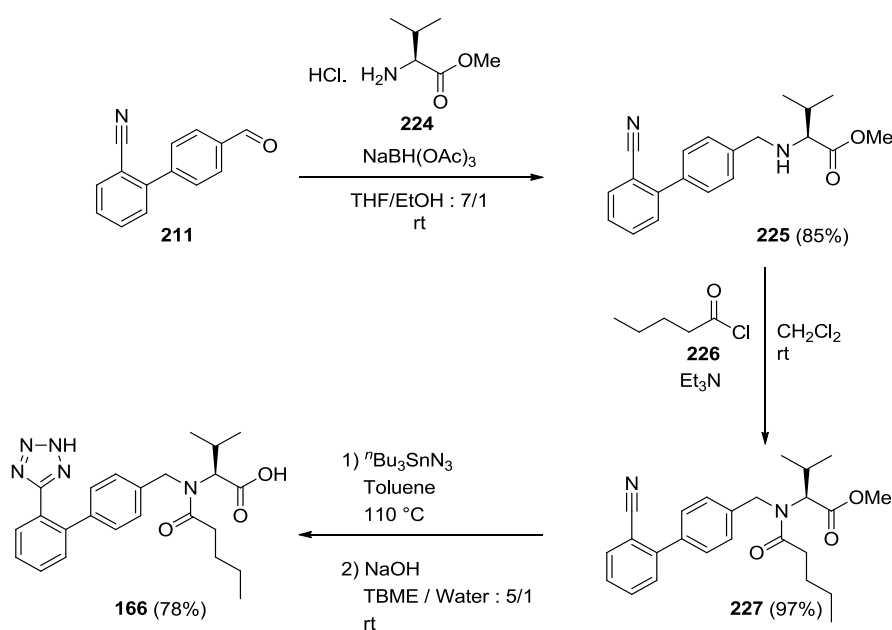
Table 15: Comparison with existing methodologies

While extremely similar yields were obtained with the cross-coupling of aryldiazonium salts (72%, Table 15, entry 1) in comparison with similar palladium-catalysed reactions including Negishi reaction (77%, Table 15, entry 2) and Suzuki reaction (73%, Table 15, entry 4), the reaction conditions optimised in this work proved to be less aggressive and more sustainable for a similar result. It is

noteworthy that the decarboxylative cross-coupling of 2-cyanobenzoic acid **222** with 4-bromo-benzaldehyde **220** delivered the target product in moderate yield (50%, Table 15, entry 3) with the authors suggesting that this was due to the decomposition of the sensitive aldehyde functionality under elevated temperature, thus highlighting the importance of mild reaction conditions.

III.2.viii End game – synthesis of Valsartan

Although the substrate **211** was prepared to demonstrate the scalability of this particular transformation, the short sequence left to complete the synthesis of Valsartan **166** was also carried out (Scheme 61).^{130,132}



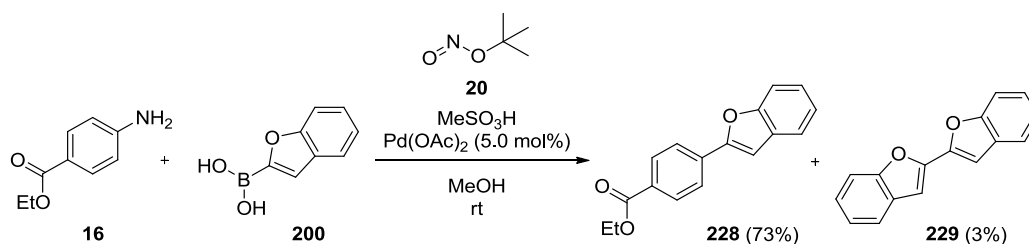
Scheme 61: End game synthesis of Valsartan **166**

The synthesis started with a reductive amination of aldehyde **211** with L-valine methyl ester hydrochloride **224** in the presence of sodium tris-acetoxyborohydride as reducing agent. The resulting amine **225** (85%) was then acylated by valeroyl chloride **226** in 97% yield to deliver the tertiary amide **227**. Finally, a [3+2] cycloaddition between the nitrile group of **228** and tri-butyl tin azide followed by ester hydrolysis during the work-up with sodium hydroxide led to Valsartan **166**. It is noteworthy that all of these steps were high-yielding.

III.2.ix Preliminary work towards flow chemistry

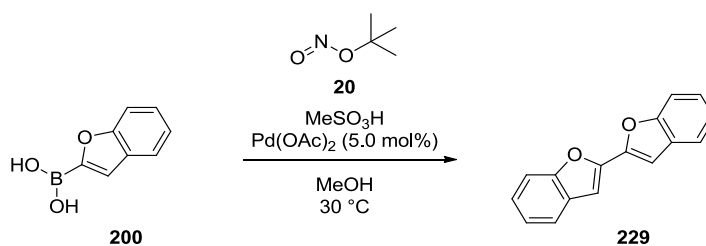
While this optimised methodology enabled the efficient and sustainable synthesis of biaryl systems including a relevant intermediate for the synthesis of angiotensin II inhibitors, the requirement for an isolated aryldiazonium salts was not ideal for the various reasons discussed in the introduction. It was thus decided to investigate the one-pot diazotisation / cross-coupling under mild conditions with the ultimate aim to perform this sequence in a flow reactor.

The model reaction used to investigate this opportunity was designed according to the knowledge acquired during the aryldiazonium synthesis and the cross-coupling studies: As methanol provided a better solubility for aryldiazonium salts while allowing the cross-coupling to proceed, electron-deficient benzocaine **16** and electron-rich benzofuran-2-boronic acid **200** were selected as cross-coupling partners. Finally, boron trifluoride – THF complex was replaced by methanesulfonic acid with the objective of removing any halogenated product and to generate a soluble aryldiazonium intermediate (Scheme 62).



Scheme 62: One-pot diazotisation / cross-coupling

The proof of concept could be established as the biaryl product **228** was obtained in 73% yield while 2,2'-bisbenzofuran **229**, arising from the homocoupling of the aryl boronic acid **200**, was isolated in 3% yield. This intriguing result warranted further investigation of this one-pot transformation in order to increase process understanding. Hence, the control reactions shown in Table 16 were designed to clarify the role of *tert*-butyl nitrite **20** as it could act as an oxidant for the palladium metal.



Entry	Conditions	Yield
1	Without palladium(II) acetate	Traces
2	Without <i>tert</i> -butyl nitrite 20	3%
3	Without methanesulfonic acid	47%

Table 16: Control reactions for the one-pot process

While very low yields of 2,2'-bisbenzofuran **229** were observed in the absence of either palladium(II) acetate or *tert*-butyl nitrite **20** (Table 16, entries 1 and 2), the reaction of benzofuran-2-boronic acid **200** in the presence of these two components led to the formation of the homocoupled product in 47% yield, thus revealing the oxidative properties of the nitrite species (Figure 34).

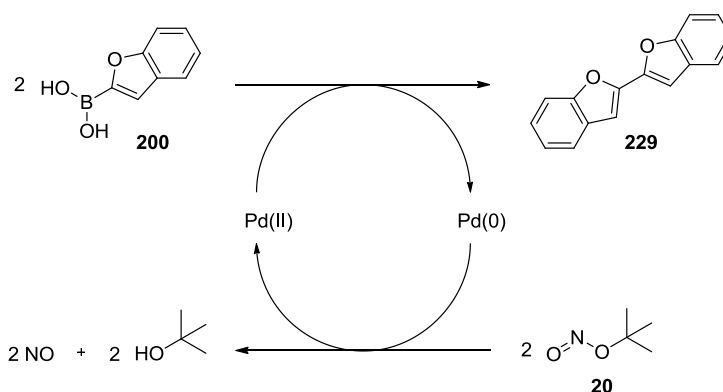
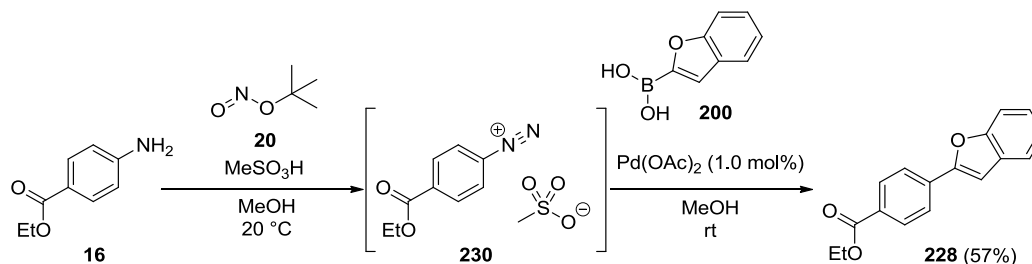


Figure 34: Mechanism of the oxidative homocoupling of aryl boronic acids

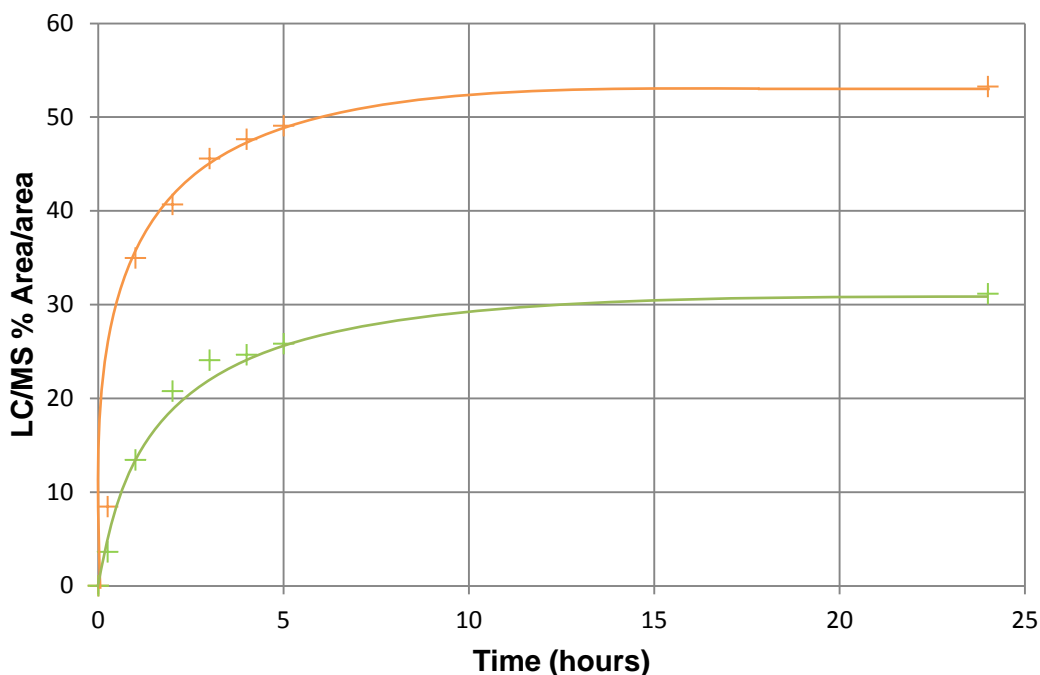
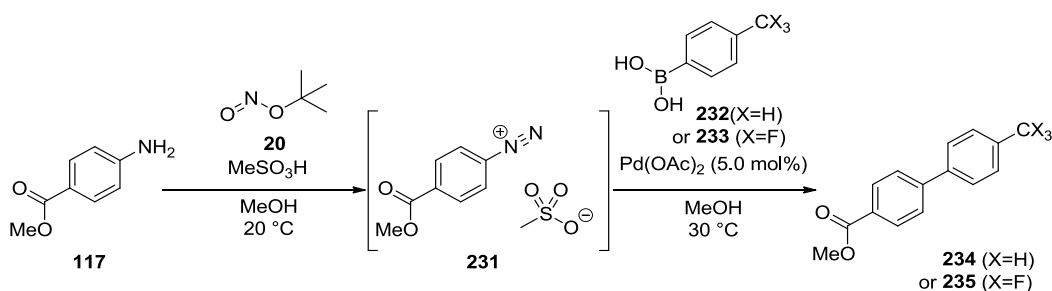
According to previous reports,^{133,134} aryl boronic acid derivatives can undergo double transmetallation on the palladium(II) metal, thus releasing the homocoupled product together with palladium(0) upon reductive elimination. The zerovalent palladium is then oxidised to palladium(II) through the action of *tert*-butyl nitrite **20**, thus rendering the process catalytic in palladium. Hence, two competitive reaction pathways (homo-coupling vs cross-coupling) were evident in the one-pot methodology and the strategy adopted to prevent the homo-coupling pathway was to perform the transformation in a sequential manner in which the diazotisation step was performed prior to the Suzuki reaction. In this process, the cross-coupling

components palladium(II) acetate and the aryl boronic acid **200** were added to the diazotisation mixture once the *tert*-butyl nitrite **20** had been consumed (Scheme 63).



Scheme 63: Sequential diazotisation / cross-coupling

However, this strategy did not prove to be more efficient as the coupling product **228** was isolated in 57% yield. As the diazotisation step was not found to be problematic in this sequence, it was believed that the transmetallation could be the rate-determining step of the cross-coupling, thus affecting the outcome of the reaction. This hypothesis was assessed through the monitoring of two control reactions performed in the presence of an electron-rich 4-toluy boronic acid **232** and an electron-deficient 4-trifluoromethyl-phenyl boronic acid **233** in order to compare the transmetallation rate of both species (Figure 35).



Entry	Conditions	Yield ^a
1	4-Tolyl boronic acid 232	41%
2	4-Trifluoromethyl-phenyl boronic acid 233	17%

^aIsolated yield after chromatography. **232** or **233** and Pd(OAc)₂ were added at t = 0 min.

Figure 35: Control reactions for the study of the transmetallation step

4-Trifluoromethyl-phenyl boronic acid **233** proved to be less efficient compared to 4-tolyl boronic acid **232** as shown by the different reaction rates revealed in Figure 35. This observation could be due to two factors: the less favoured transmetallation of **233** compared to **232** due to the difference in terms of electronic properties and the lack of transmetallation auxiliary such as a base. Better yields were indeed expected from both reactions given the electron-deficient nature of the aryl diazonium coupling partner (II.1.v, *vide supra*). While the only major difference between the two sets of reaction conditions employed was the counter-ion employed

(tetrafluoroborate vs methanesulfonate), it was assumed that this component could be playing a role in the transmetallation process.

III.2.x Reaction mechanism

From the observations made from this work, it was believed that an auxiliary assisting the transmetallation of the aryl boronic acid coupling partner was required for the transformation to proceed in acceptable yields. In line with the work of Amatore, Le Duc and Jutand,^{135,136} fluoride from the tetrafluoroborate counter-ion may be involved in the catalytic cycle in a similar manner to the Baltz-Schiemann reaction^{12,29} in which fluoride is able to displace from the stable tetrafluoroborate to form aryl fluoride derivatives. The postulated reaction mechanism is shown in Figure 36.

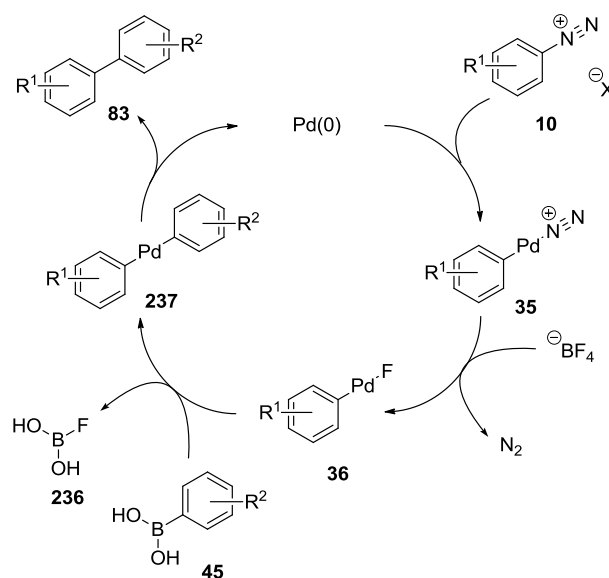


Figure 36: Postulated reaction mechanism

In this catalytic cycle, the palladium inserts first into the carbon-diazonium bond to give the intermediate **35**. The diazonium group is then displaced by a fluoride from the tetrafluoroborate counter-ion to form the intermediate **36**. It has been previously observed by Amatore, Le Duc and Jutand that the palladium-fluoride complex **36** undergoes transmetalation with the aryl boronic acid through the formation of a strong boron-fluoride bond which is the driving force of this step.¹³⁵ Finally, the biaryl product **83** is obtained through standard reductive elimination of complex **237**.

III.2.xi Conclusion & future work

The cross-coupling of aryldiazonium tetrafluoroborate salts with aryl boronic acids was found to be an economical and sustainable alternative to existing methodologies in this class of reaction and this methodology was published to provide a viable cross-coupling alternative for the development of better processes.¹³⁷

While this class of cross-coupling displayed undeniable advantages, unstable aryldiazonium tetrafluoroborate salts must still be isolated. In an effort to address this issue, preliminary work towards developing a flow chemistry method was carried out and despite the lower yields obtained, a better mechanistic understanding was gained. The future work in this field should consist in screening of alternative Brønsted or Lewis acids compatible with the diazotisation in flow (*i.e.* a soluble aryldiazonium salts) and the transmetallation of the aryl boronate species.

The second setback of this methodology lies in the incompatibility of heterocyclic coupling partners with the transformation. This issue could be addressed by screening a variety of palladium and ligand combinations, however, the associated costs would inevitably increase which is not in accordance with the objectives set (II.1.i, *vide supra*). Alternatively, different types of reactivity may be investigated and may afford similar heterocyclic bi-aryl systems.

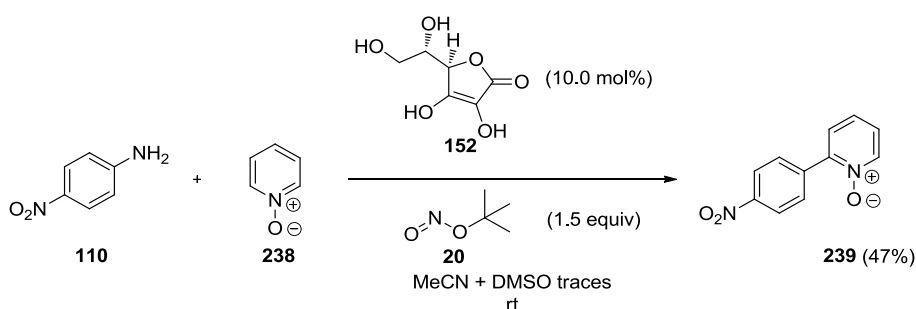
III.3 Radical arylation of heterocycles

III.3.i From metal catalysis to organocatalysis

While the previous palladium-mediated methodology proved to be efficient for the coupling of carbon-core substrates, heterocycles were unfortunately found to be incompatible with this reaction. Given the abundance of nitrogen-based cores in medicinally relevant molecules,^{2,105} a suitable method allowing the coupling of these species with aryldiazonium salts was desired. Furthermore, the previous cross-coupling still required the use of a transition metal catalyst, the long-term sustainability of which was an area of considerable concern.⁷⁷

As discussed in the introduction, a potentially more sustainable approach was the direct arylation of aromatic rings employing an aryl radical species generated *in situ*

from an aryldiazonium salt. While such arylations of 5-membered heterocycles is regioselective for the 2-position,⁷⁸ similar methodologies on 6-membered heterocycles leads to chaotic additions and mixtures of regioisomeric products.^{88,90} However, the introduction of an *N*-oxide auxiliary was reported in the literature to influence the regiochemical outcome of the radical attack through the modification of the electronic properties of the heterocycle,¹³⁸ hence offering the intriguing opportunity to selectively prepare a single regioisomer.^{139–142} Among them, Carrillo *et al* described an elegant method telescoping a diazotisation and a radical-mediated arylation reaction using ascorbic acid **152** as the sole putative promoter for both steps (Scheme 64).¹⁴³



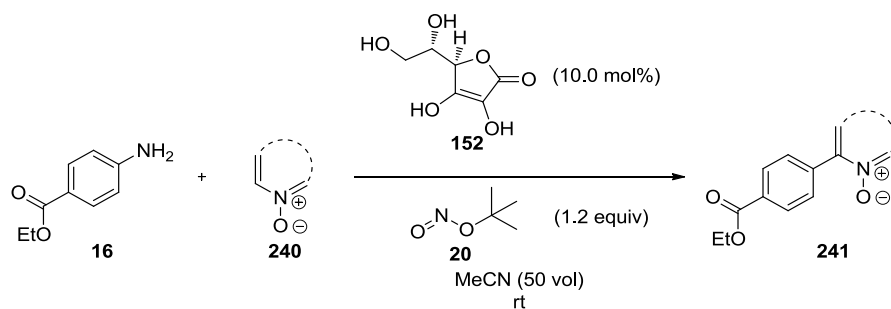
Scheme 64: Radical-mediated arylation of pyridine N-oxide 238

As well as 5-membered heterocycles which underwent selective addition of an aryl radical at the 2-position, it was also shown that pyridine *N*-oxide **238** underwent a regioselective attack by the same radical to yield the biaryl **239** through this single example in the literature (Scheme 64).¹⁴³ The *in situ* generation of the aryldiazonium from the cheap and readily available aniline helps to address safety concerns around the isolation of these species, while the use of inexpensive and benign ascorbic acid **152** provides an important alternative to standard metal-catalysed couplings. As a consequence, it was decided to develop, optimise and expand this methodology to other pharmaceutically relevant nitrogen heterocycles in order to deliver a viable process of relevance to the pharmaceutical industry.

III.3.ii Screening of *N*-oxide heterocycles

As a starting point of this study, a series of *N*-oxide containing heterocycles of relevance to the pharmaceutical industry were reacted with benzocaine **16** in order to identify suitable substrates for this arylation. While the *N*-oxide group was shown to stabilise free radicals and may be used in tumorous cells to break DNA

strands,^{144,145} the real interest of the compounds bearing this functionality came from their unoxidised form (*vide infra*). For the initial screening process the reaction conditions reported by Carrillo *et al*¹⁴³ were adapted, reducing the excess of *tert*-butyl nitrite **20** to 1.2 equivalents and omitting the DMSO cosolvent (Table 17).



Entry	Substrate	Product	Yield ^a
1			22%
2			19%
3			Traces ^b
4			Traces ^b
5			60%
6			71%
7			Traces ^b

^aIsolated yield after purification by column chromatography. ^bA mixture of regioisomers was observed by LC/MS.

Table 17: Screening of heterocyclic N-oxides

The reaction was found to be remarkably substrate specific for both single and fused ring systems. While only traces of the arylated product could be observed by LC/MS when pyridazine *N*-oxide **243** (Table 17, entry 3), pyrimidine *N*-oxide **244** (Table 17, entry 4) and isoquinoline *N*-oxide **247** (Table 17, entry 7) were evaluated as potential substrates, pyridine *N*-oxide **238** and pyrazine *N*-oxide **242** could be arylated with outstanding regioselectivity but disappointing yield (Table 17, entries 1 and 2). The most promising results were obtained from fused ring systems as both quinoline *N*-oxide **245** (Table 17, entry 5) and quinoxaline *N*-oxide **246** (Table 17, entry 6) were arylated in yields higher than 60% under these standard conditions. As a result, this initial screening displayed a number of interesting trends that warranted further investigation.

III.3.iii Identifying the optimal solvent through OPLS and PCA analysis

In line with the previously discussed cross-coupling reaction, it was decided to carry out the identification of potentially greener alternatives to acetonitrile through OPLS analysis.¹²⁴ The solvent screening results required by this statistical method were obtained through the evaluation of inexpensive benzocaine **16** and commercially available quinoline *N*-oxide **245** as model substrates for this transformation in a series of common organic solvents (Table 18) selected from a PCA model (Figure 36).¹¹¹

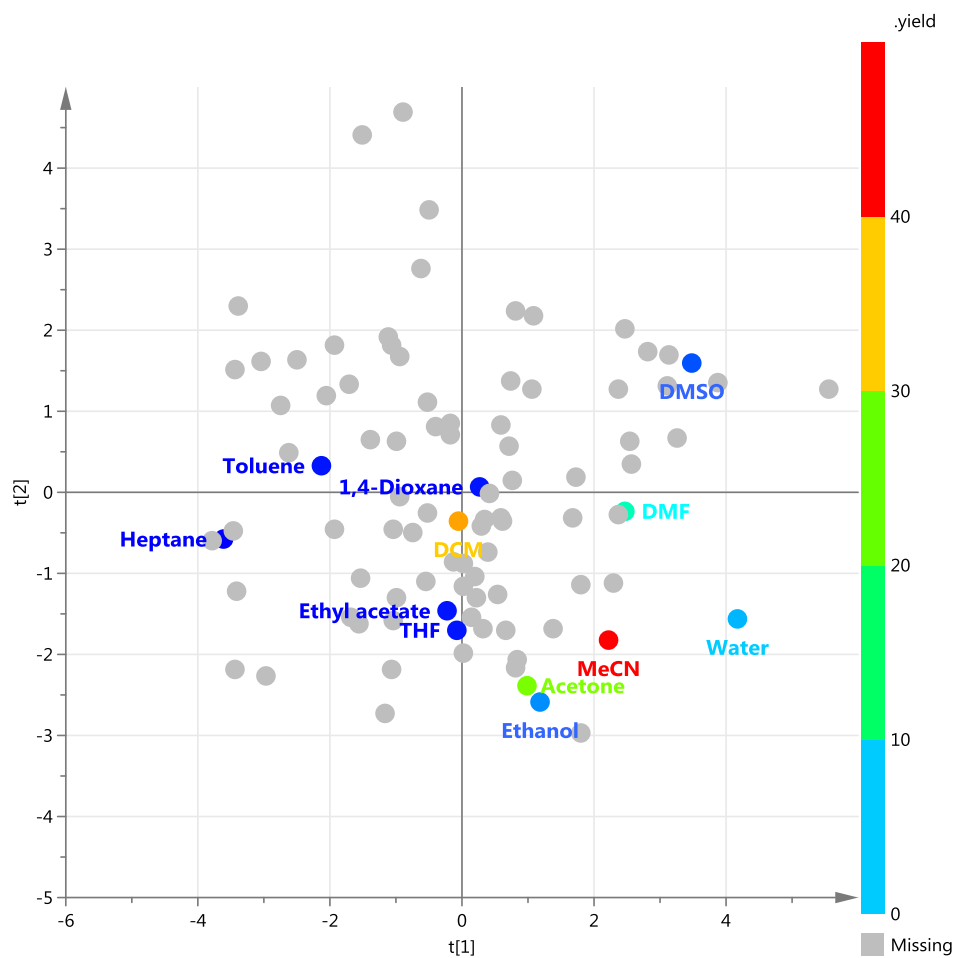
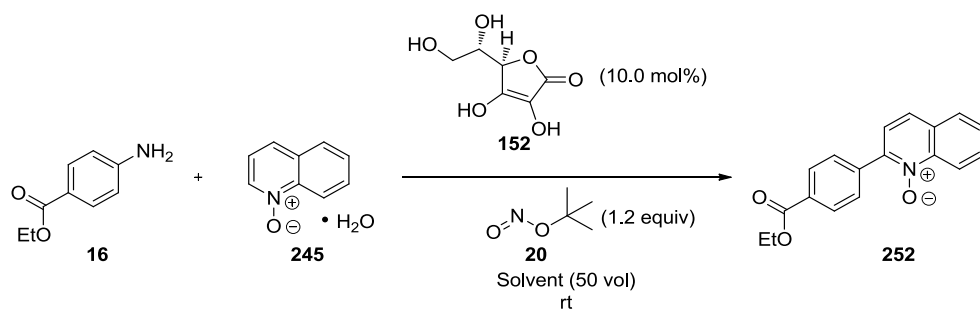
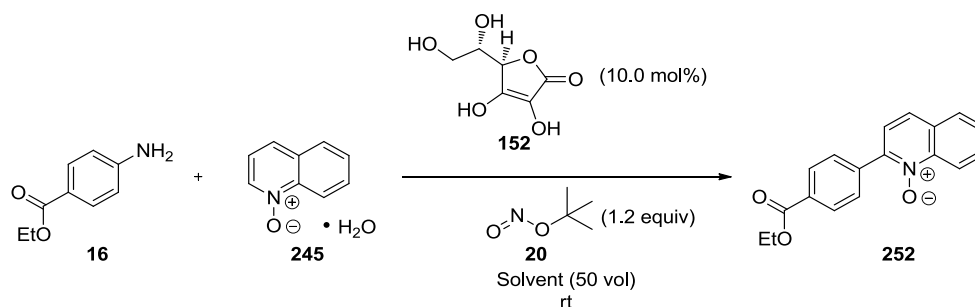


Figure 36: PCA solvent model with reported yields (by Sandrine Olazabal)

These reaction media were selected according to their difference in terms of physico-chemical properties, as discussed in section III.2.iii (*vide infra*).



Entry	Solvent	HPLC yield ^a	Isolated yield ^b
1	Heptane	N.D.	-
2	Toluene	1%	-
3	1,4-dioxane	1%	-
4	THF	1%	-
5	EtOAc	1%	-
6	DMSO	4%	-
7	EtOH	7%	-
8	Water	9%	-
9	DMF	16%	19%
10	Acetone	31%	33%
11	CH ₂ Cl ₂	42%	40%
12	MeCN	50%	60%

^aHPLC yield calculated with calibration curve. ^bIsolated yield after purification by column chromatography.

Table 18: Solvent screening for the radical arylation of quinoline N-oxide **245**

The reaction did not proceed well in heptane, toluene, 1,4-dioxane, tetrahydrofuran, ethyl acetate, DMSO, ethanol and water as only low yields were observed by HPLC (Table 18, entries 1 to 8). DMF, acetone and dichloromethane gave 16%, 31% and 42% yield of the biaryl product **252** respectively (Table 18, entries 9-11). Among all the solvents screened, acetonitrile gave the product in 60% isolated yield (Table 18, entry 7). As mentioned previously, these screening results were used to build the OPLS regression model describing reaction yield as a function of solvent properties in order to increase process understanding. This regression method aims to find the multidimensional direction in the solvent descriptors space that explains the maximum variance in the yield (Figure 37).

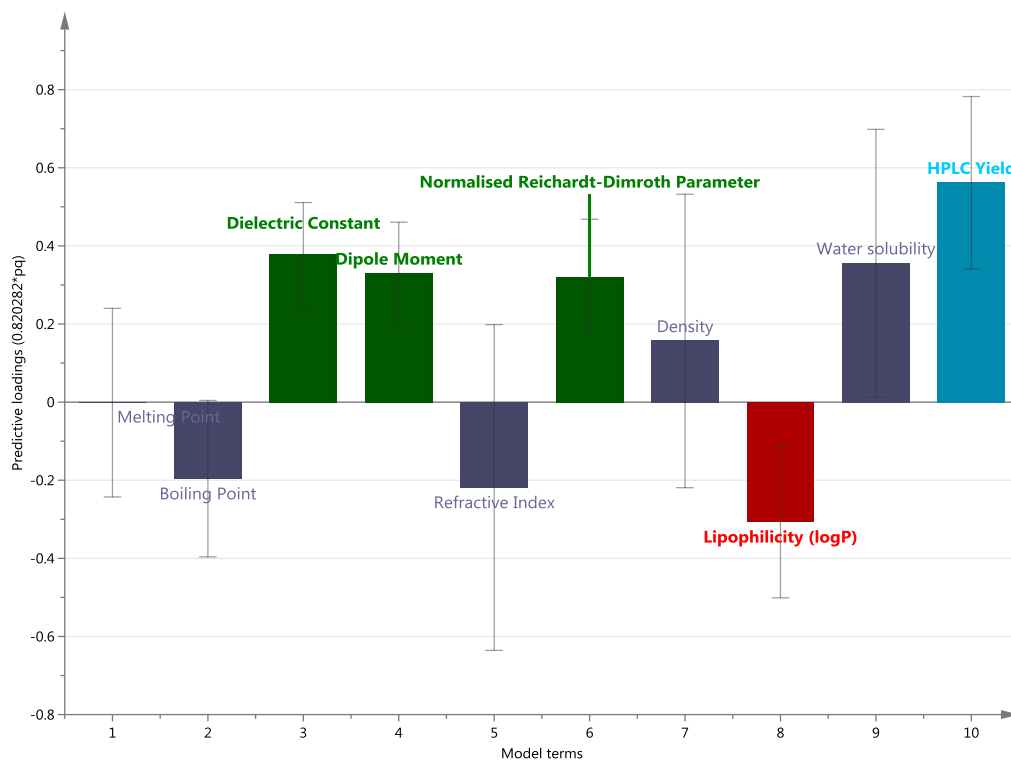
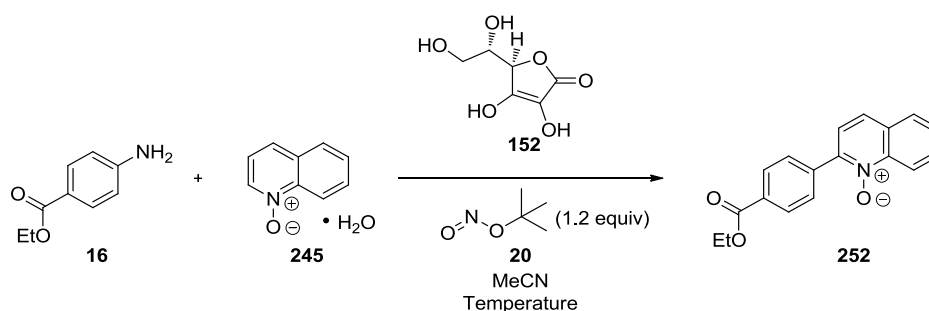


Figure 37: OPLS regression model (by Sandrine Olazabal)

Descriptors highlighted in green show a statistically-significant positive correlation with reaction yield; those in red show a statistically-significant negative correlation with reaction yield; and those in dark blue/grey show a correlation that is not statistically significant (95% confidence interval). The model ($R^2X=63.9\%$, $R^2Y=74.8\%$, $Q^2=43.7\%$) revealed that solvents with high dipole moment, dielectric constant and normalised Reichardt-Dimroth¹²⁵ parameters resulted in high yield whereas increased lipophilicity of the solvent was detrimental to the yield (Figure 37). Accordingly, this model highlights the clear affinity of the reaction for polar, polarisable solvents, which is consistent with the large number of charged intermediates involved in the transformation (*vide infra*). Although the PCA model used contains a wide variety of “green” alternatives, the only solvents predicted to give similar or better yields than acetonitrile were nitromethane and trifluoroethanol, both less desirable from a sustainability perspective. Therefore acetonitrile was chosen for the further development of this transformation through Design of Experiment methodology.

III.3.iv Optimising the reaction conditions through Design of Experiments

Design of experiments is a multifactorial analysis technique allowing the identification of key reaction parameters within a previously defined space. With suitable solvent and model substrates established, it was decided to evaluate the impact of other reaction parameters, including the ascorbic acid **152** loading (A), the number of equivalents of quinoline *N*-oxide **245** (B), the solvent volumes (C) and the temperature (D) through 20 runs (16 factorials and 4 centre points) using a full factorial model where HPLC yield was used as the response (Table 19).



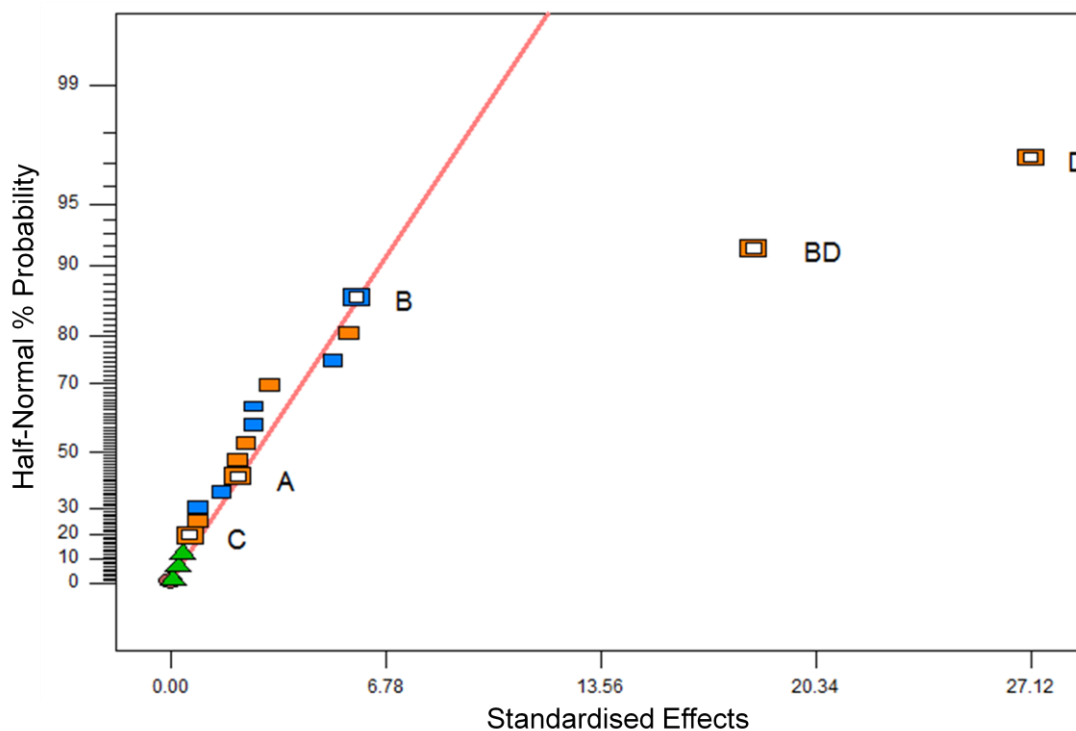
Entry	Ascorbic Acid	Quinoline <i>N</i> -Oxide	Solvent	Temperature	HPLC Yield ^a
	Loading	Equivalents	Volumes	(°C)	
	(mol%)	(equiv)	(vol)	(D)	
	(A)	(B)	(C)		
1	20	3	10	40	48
2	1	3	10	0	14
3	10.5	2	55	20	44
4	1	1	10	0	18
5	1	3	100	40	50
6	20	3	100	40	52
7	1	1	100	0	24
8	1	3	100	0	1
9	10.5	2	55	20	46
10	20	3	100	0	2
11	10.5	2	55	20	46
12	1	1	100	40	38
13	1	3	10	40	50
14	20	1	10	0	34
15	20	1	100	40	38

Entry	Ascorbic Acid	Quinoline <i>N</i> -Oxide	Solvent	Temperature	HPLC Yield ^a
	Loading	Equivalents	Volumes	(°C)	
	(mol%)	(equiv)	(vol)	(D)	
	(A)	(B)	(C)	(D)	
16	20	1	100	0	39
17	20	1	10	40	36
18	1	1	10	40	38
19	10.5	2	55	20	37
20	20	3	10	0	1

^aHPLC yield calculated with calibration curve. Red: centre points.

Table 19: Design of Experiments runs

The results presented in Table 19 were thus interpreted using Design-Expert (version 7.1.1, Stats-Ease, Inc) software without transformation in order to obtain the half-normal plot (Figure 38) of this accurate but not predictive model ($R^2 = 0.9104$, Adj $R^2 = 0.8760$, Pred $R^2 = 0.7795$).



Orange: positive effects; Blue: negative effects; Green: error from replicates

Figure 38: Half-normal plot using HPLC yield as response

The half-normal plot revealed that the temperature (D) had the greatest influence as reactions performed at elevated temperatures gave the best results (Table 19, entries 1, 5, 6, 12, 13 and 15). This study also revealed that the interaction between the amount of quinoline *N*-oxide **245** (B) and the temperature (D) also had a significant impact on the reaction (Figure 39): whilst a high loading of quinoline *N*-oxide **245** was beneficial to the reaction at high temperature (red line), it was found to be detrimental at low temperature (black line). Although this result does not seem intuitive, it was reproducible and was believed to be indicative of the mechanistic complexity of the reaction.

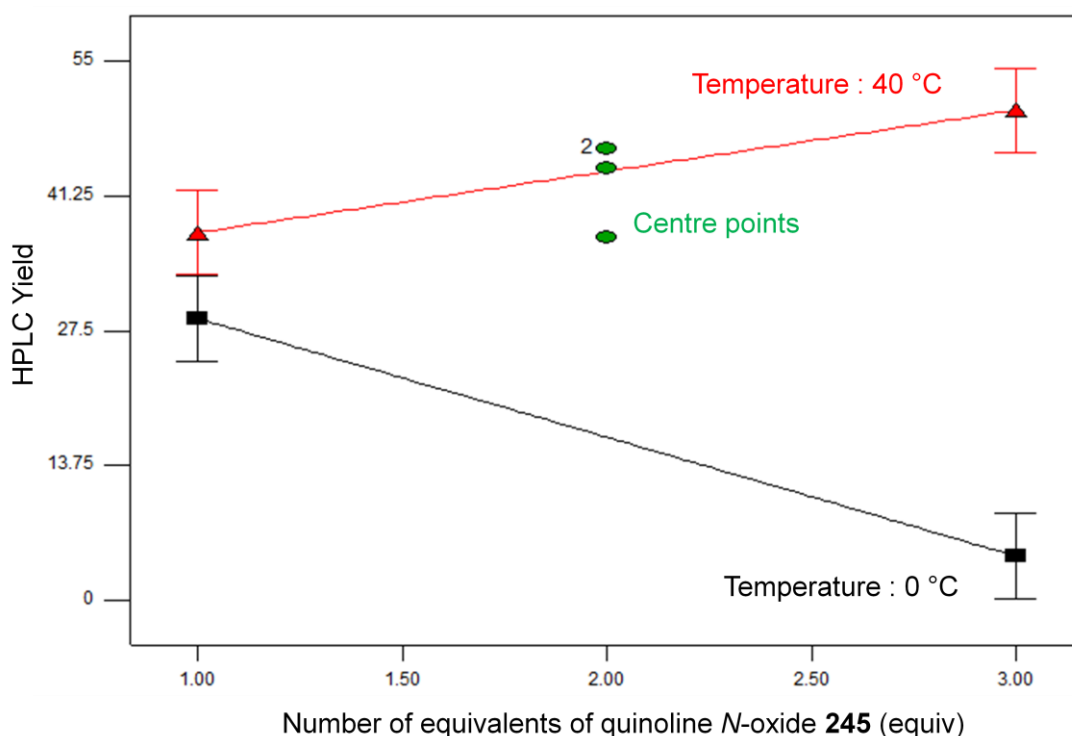


Figure 39: Quinoline-*N*-oxide equivalents / Temperature Interaction Plot

While the amount of quinoline *N*-oxide (B) and the temperature (D) were found to have a pronounced impact on the yield, the number of solvent volumes (C) and more surprisingly, the loading of ascorbic acid **152** (A) had no impact on the reaction outcome within the ranges studied and as a consequence of these results, minimum quantities of these reagents could be used to render this metal-free process even more sustainable. A compromise consisting of using two equivalents of the *N*-oxide heterocycle at 40 °C in 10 volumes of solvent was selected as exhibited in Table 20, entry 4. The intriguing result obtained in this study with regards to the impact of

ascorbic acid **152** (A) on this transformation warranted further investigation of its role in this radical arylation.

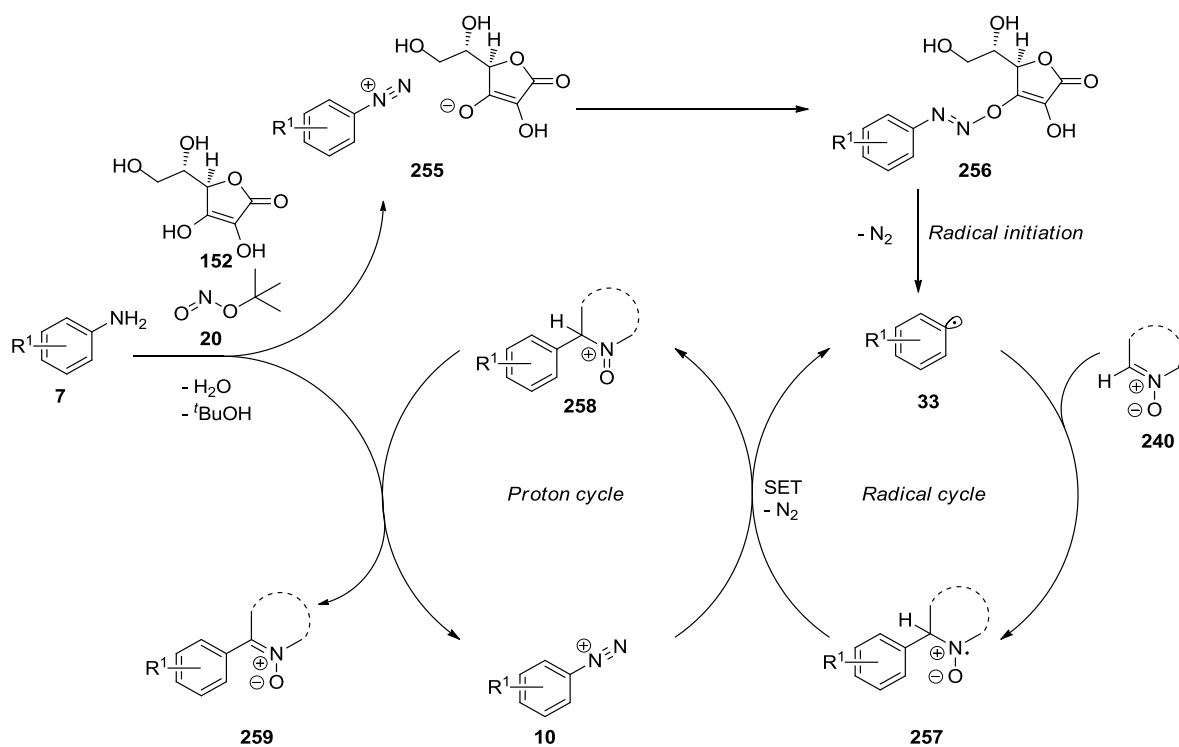
Entry	Settings	Ascorbic acid (mol %) (A)	Quinoline <i>N</i> -oxide (equiv) (B)	Solvent volumes (vol) (C)	Temperature (°C) (D)
1	Minimum	1%	1.0	10	0 °C
2	Centre	10.5%	2.0	55	20 °C
3	Maximum	20%	3.0	100	40 °C
4	Selected	N.A. ^a	2.0	10	40 °C

^aSee further discussion below.

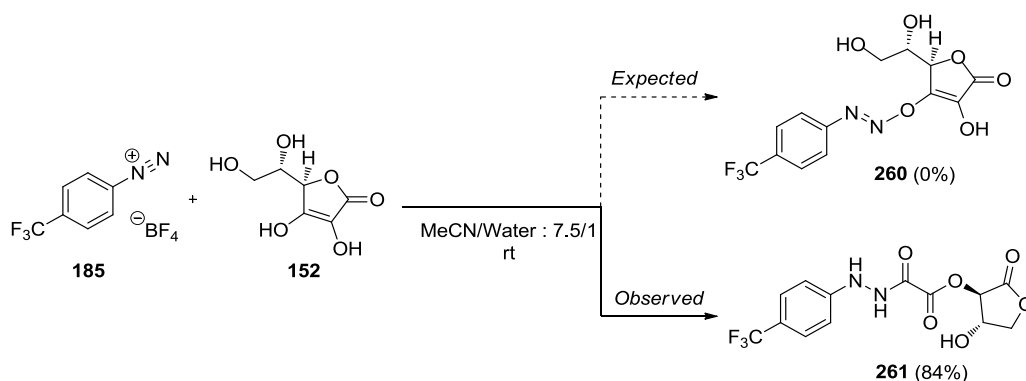
Table 20: Design of Experiment summary with optimised conditions

III.3.v Investigating the role of ascorbic acid

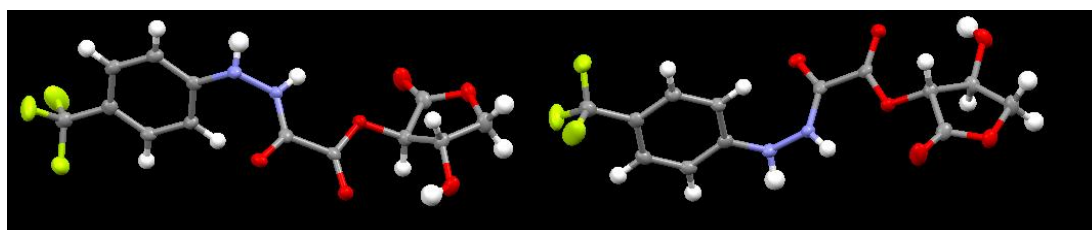
The Design of Experiments study suggested that the loading of ascorbic acid had no impact on the yield of the reaction and it was decided to investigate to what extent this observation could be verified and ultimately if this component was required at all. Carrillo and co-workers¹⁴³ hypothesised the possible role of ascorbic acid in this radical arylation of heterocycles as shown on Figure 40.



In this proposal, aniline **7** was diazotised in the presence of *tert*-butyl nitrite **20** and ascorbic acid **152** to form the aryldiazonium ascorbate salt **10** which reacted to generate the intermediate **256**. Diazo ether **256** was believed to be a key intermediate, able to generate aryl radicals **33** through spontaneous dediazotisation and generation of a stable ascorbate radical.¹⁴⁶ It was thus decided to prepare the compound **260** according to the method published by Doyle and co-workers¹⁴⁷ and to study its behaviour in the reaction mixture in order to confirm this hypothesis (Scheme 64).



The reaction of 4-trifluoromethyl benzenediazonium tetrafluoroborate **185** with ascorbic acid **152** in aqueous acetonitrile led to the formation of a precipitate which was isolated by filtration. While standard analysis of the precipitate by ^1H NMR, ^{13}C NMR and mass spectrometry were consistent with the reported structure **260**,¹⁴⁷ the IR spectrum exhibited three distinct bands in the carbonyl region (1781 cm^{-1} , 1760 cm^{-1} and 1694 cm^{-1}) which did not match the single carbonyl functionality of **261**. As a consequence, crystals of the precipitate were grown by diffusion of chloroform in a saturated solution of acetone and analysed by X-Ray diffraction to confirm the structure of the product (Figure 41).



Grey: carbon; White: hydrogen; Blue: nitrogen; Red: oxygen; Green: fluorine

Figure 41: X-ray crystal structure of compound **261**
(collected by the National Crystallography Service)

While this result was unexpected, a recent publication⁹⁹ from Ley's group confirmed this observation as their detailed study clearly discredited the formation of diazoether **256** under these reaction conditions as similar acylated hydrazine derivatives arising from a Japp-Klingemann rearrangement were isolated instead (Figure 42).

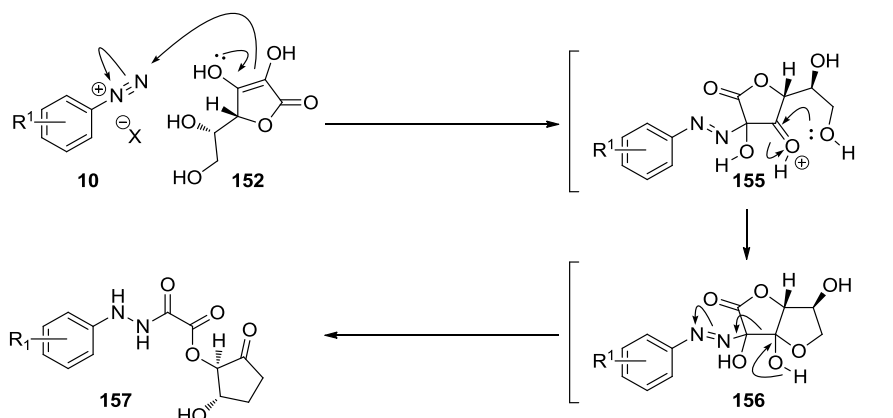
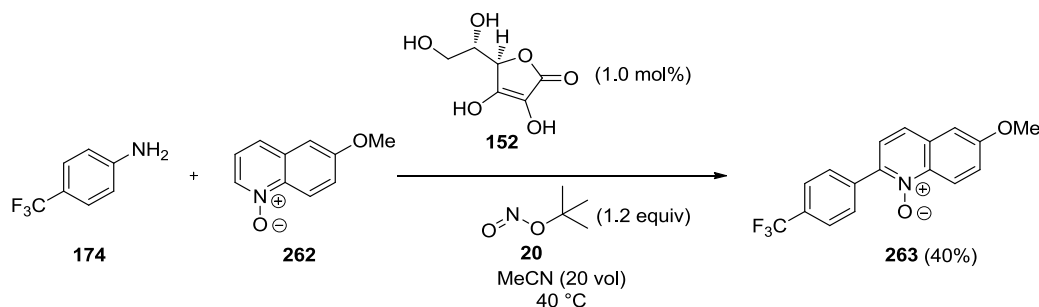


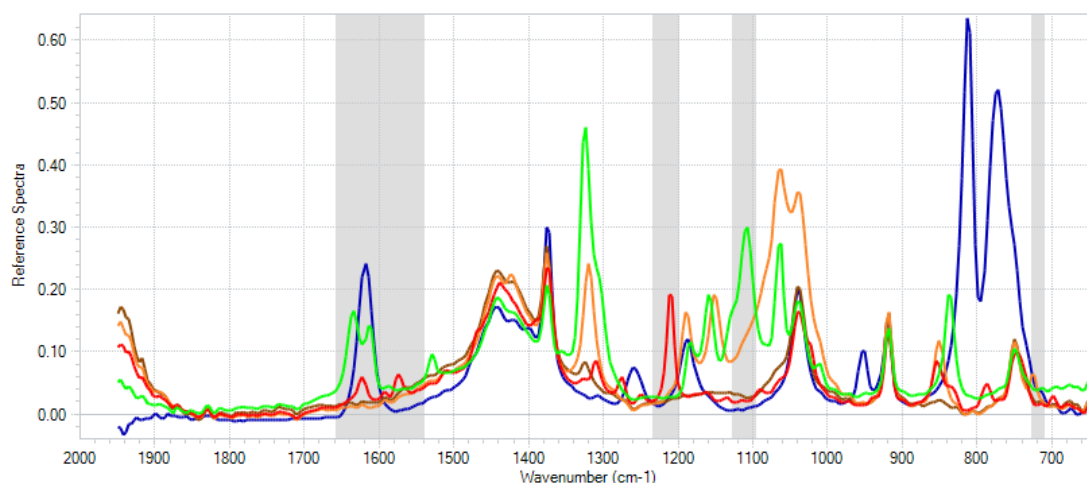
Figure 42: Japp-Klingemann rearrangement for hydrazine formation⁹⁹

Hence, the proposal from Carrillo *et al*¹⁴³ involving the formation of a key diazoether intermediate¹⁴⁶ was incorrect and it was decided to monitor the reaction by an infrared probe and LC/MS in order to identify potential reaction intermediates. Optimal reaction conditions previously established through DoE were thus adapted with minimal amounts of ascorbic acid used (1.0 mol%) in a reaction where the product could be easily isolated by precipitation and filtration (Scheme 65).



Scheme 65: Reaction for IR and LC/MS monitoring

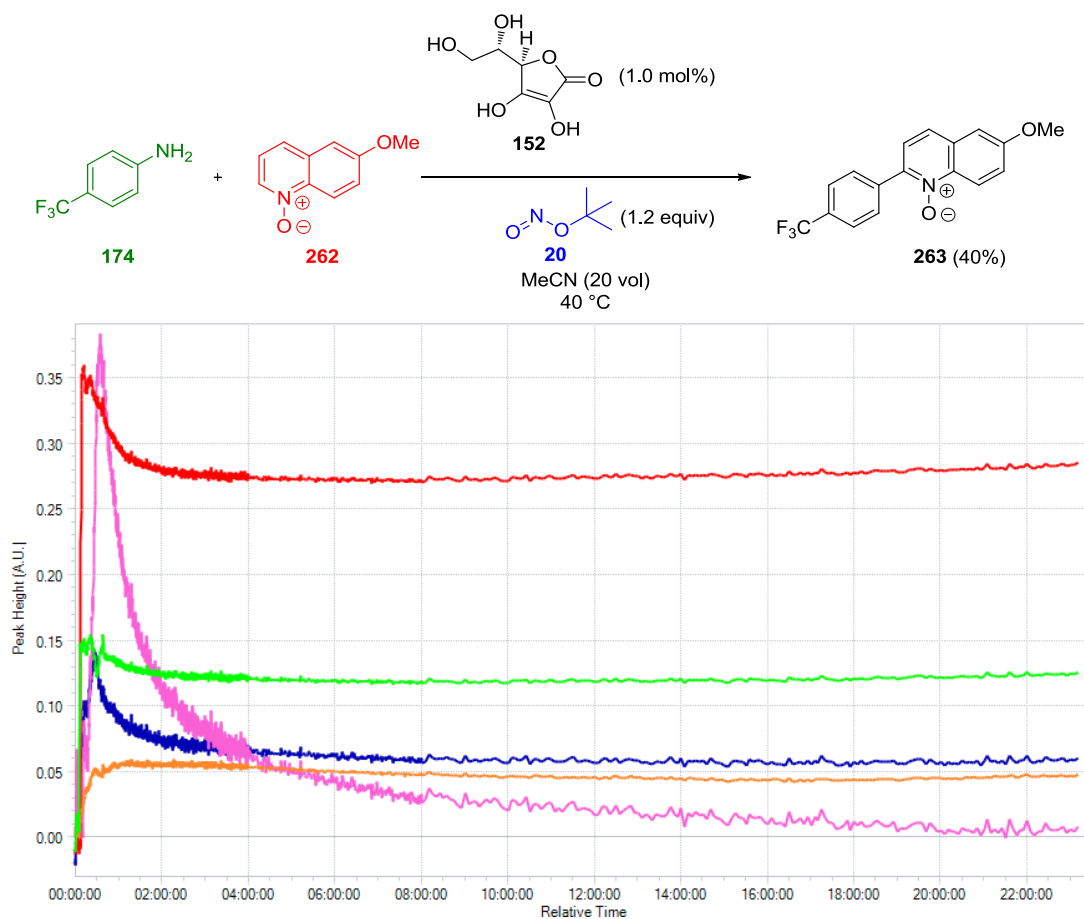
The infrared trace of the reaction mixture was analysed with software iC IR (version 4.3, Mettler Toledo) with the attribution of representative wavenumber for every component involved in this arylation, except for the product **263** as no characteristic band could be identified to monitor its formation (Figure 43).



Entry	Component	Wavenumber
1	4-Trifluoromethyl-aniline 174	1125 to 1097 cm ⁻¹
2	4-Trifluoromethyl benzenediazonium 185	725 to 711 cm ⁻¹
3	6-Methoxy quinoline <i>N</i> -oxide 262	1232 to 1199 cm ⁻¹
4	<i>tert</i> -Butyl nitrite 20	1656 to 1540 cm ⁻¹
5	2-(4-Trifluoromethyl-phenyl)-6-methoxy quinoline <i>N</i> -oxide 263	No characteristic band observed

Figure 43: IR absorption spectra of reaction components in acetonitrile

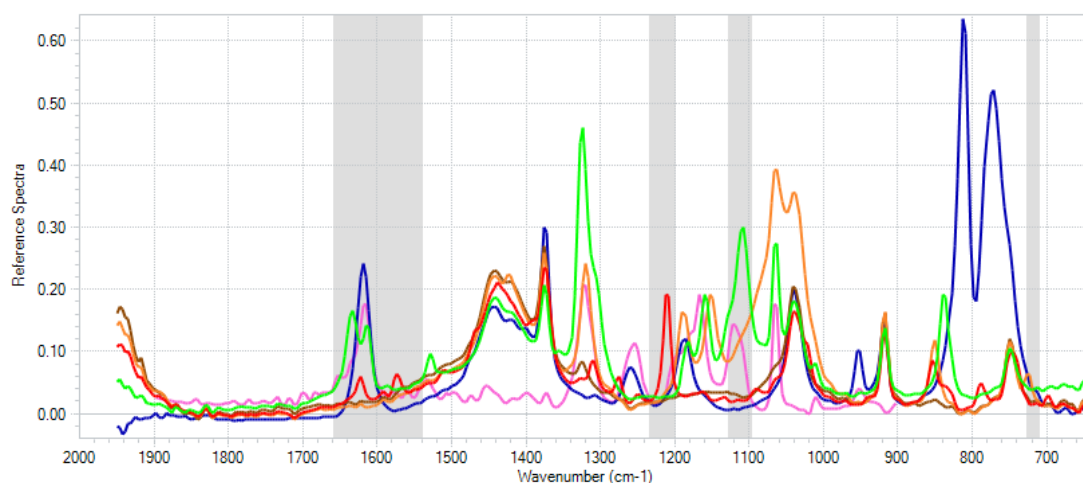
The identification of characteristic wavenumbers for each reagent allowed the monitoring of their behaviour over the course of the reaction (Figure 44). As expected, 4-trifluoromethyl aniline **174**, 6-methoxy quinoline *N*-oxide **262** and *tert*-butyl nitrite **20** were consumed while the formation of 4-trifluoromethyl benzenediazonium intermediate **185** was observed. Further analysis of the infrared spectra collected during this experiment by the software iC IR (version 4.3, Mettler Toledo) allowed the identification of a potential intermediate with a 99.2% fit through the predicative function ConclIRT (pink line, Figure 44). It is noteworthy that the trend observed for this predicted intermediate is consistent with the behaviour of a reaction intermediate as it is formed and consumed at the same time.



Entry	Component	Wavenumber
1	4-Trifluoromethyl-aniline 174	1125 to 1097 cm^{-1}
2	4-Trifluoromethyl benzenediazonium 185	725 to 711 cm^{-1}
3	6-Methoxy quinoline <i>N</i> -oxide 265	1232 to 1199 cm^{-1}
4	<i>tert</i> -Butyl nitrite 20	1656 to 1540 cm^{-1}
5	Simulated intermediate	Calculated

Figure 44: Wavenumbers monitoring and potential intermediate identification

In addition to the prediction of possible intermediates involved in the mechanism of the transformation, the software was able to generate a predicted infrared spectrum for this intermediate (Figure 45, pink line).



Entry	Component	Wavenumber
1	4-Trifluoromethyl-aniline 174	1125 to 1097 cm ⁻¹
2	4-Trifluoromethyl benzene diazonium 185	725 to 711 cm ⁻¹
3	6-Methoxy quinoline <i>N</i> -oxide 262	1232 to 1199 cm ⁻¹
4	<i>tert</i> -Butyl nitrite 20	1656 to 1540 cm ⁻¹
5	2-(4-Trifluoromethyl-phenyl)-6-methoxy quinoline <i>N</i> -oxide 263	No characteristic band observed
6	Simulated intermediate	Calculated

Figure 45: IR absorption spectra of reaction components in acetonitrile

Furthermore, a compound exhibiting a similar behaviour to the intermediate identified through ReactIR analysis (Figure 44) was also detected by LC/MS with a molecular weight of MW = 333 g.mol⁻¹ (Figure 46).

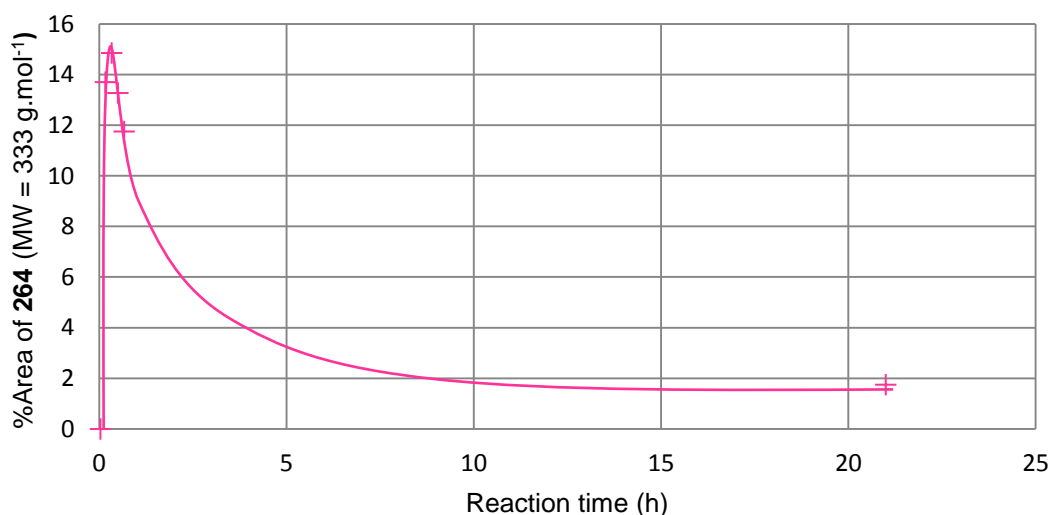


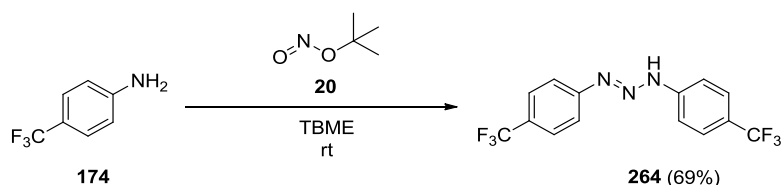
Figure 46: Detection of reaction intermediate by LC/MS

As similarities were observed between both infrared spectra (Figure 47, bands at 1616 cm^{-1} , 1320 cm^{-1} , 1168 cm^{-1} , 1116 cm^{-1} and 1062 cm^{-1}), a structure derived from the starting 4-trifluoromethyl aniline **174** was envisaged for this intermediate. In addition to this observation, the molecular weight obtained by LC/MS led to postulate that this intermediate was the triazene **264**, arising from the reaction of aryldiazonium **185** with the aniline **174** (Scheme 66).



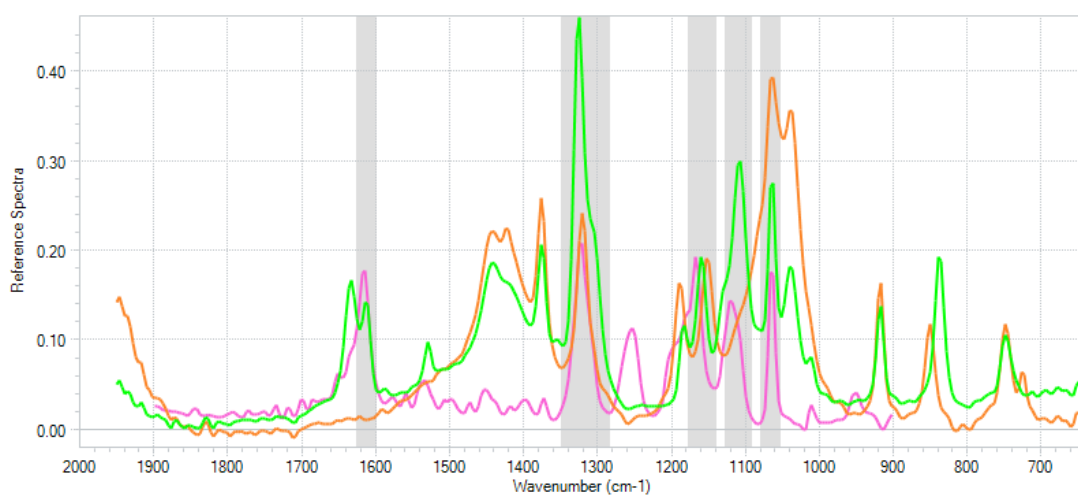
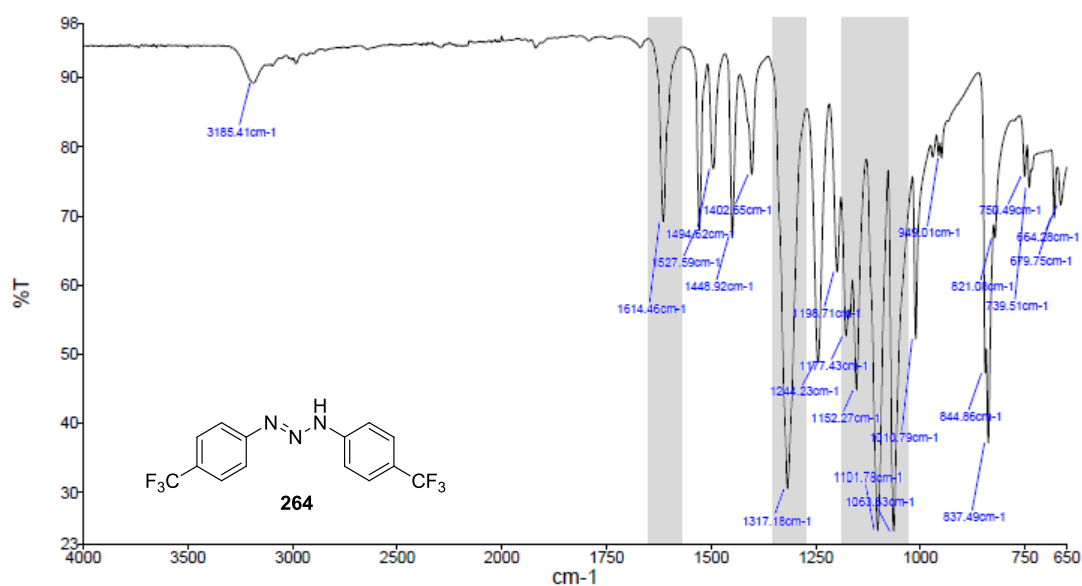
*Scheme 66: Formation of triazene intermediate **264***

It was thus decided to synthesise and characterise the triazene species **264** using a method adapted from the literature (Scheme 67)¹⁴⁸ in order to confirm this hypothesis.



*Scheme 67: Preparation of triazene intermediate **264***

The infrared spectrum of isolated compound **264** was then compared with the calculated spectrum of the predicted intermediate and both spectra were found to be extremely similar (Figure 47).



Entry	Aniline 174	Aryldiazonium 185	Simulated intermediate	Triazene 264
1	1614 cm ⁻¹	N.A.	1614 cm ⁻¹	1614 cm ⁻¹
2	1324 cm ⁻¹	1318 cm ⁻¹	1322 cm ⁻¹	1317 cm ⁻¹
3	1159 cm ⁻¹	1150 cm ⁻¹	1167 cm ⁻¹	1152 cm ⁻¹
4	1109 cm ⁻¹	N.A.	1118 cm ⁻¹	1101 cm ⁻¹
5	1064 cm ⁻¹	1064 cm ⁻¹	1064 cm ⁻¹	1063 cm ⁻¹

Figure 47: Comparison of triazene **264** with other reaction components by IR

Selected among the similarities exhibited by both spectra, a significant medium band at 1614 cm⁻¹ corresponding to the N-H bend and a strong band around 1320 cm⁻¹ corresponding to the aromatic amine C-N stretch were observed. This

result provided a strong evidence pointing towards the formation of a triazene intermediate during the transformation which can then either act as an aryldiazonium reservoir or theoretically initiate the radical decomposition (Figure 48) as supported by similar methodologies involving triazene intermediates.¹⁴⁹

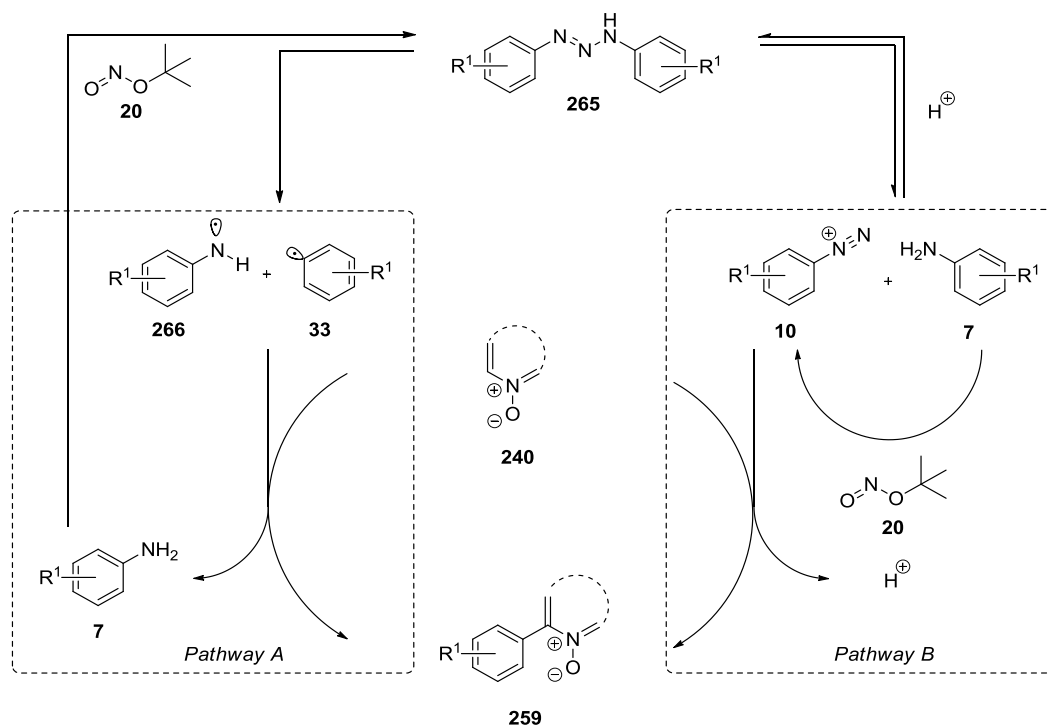
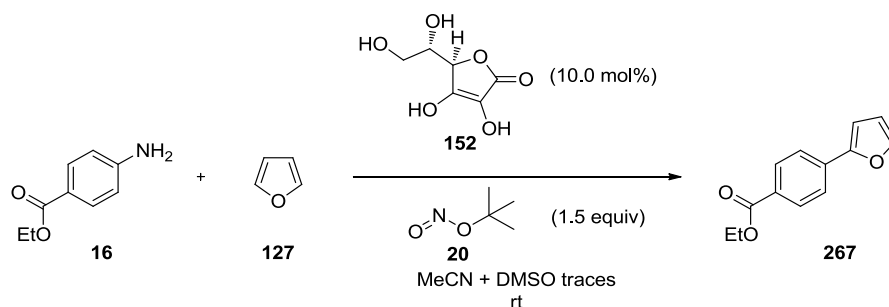


Figure 48: Postulated reaction pathways from the triazene compound **265**

While Pathway B generates an aryldiazonium species **10** which may be the reactive species leading to the arylated product in the presence of 6-methoxy-quinoline *N*-oxide, Pathway A consists of the collapse of triazene **265** to generate a reactive aryl radical **33** and a stabilised aniline radical **266**, the release of nitrogen being the driving force of this process (Figure 48). These radical species may then be involved in the radical arylation mechanism discussed in Figure 40 to generate the product of interest **259**, the aniline radical **266** being reduced throughout the process. It is noteworthy that none of these pathways requires the presence of ascorbic acid in accordance with the results obtained in this study.

In order to confirm these observations and to definitely discard the role of ascorbic acid in this radical arylation of heterocycles, it was decided to run control reactions with and without this additive and to compare the results obtained with those reported in the literature (Table 21).¹⁴³



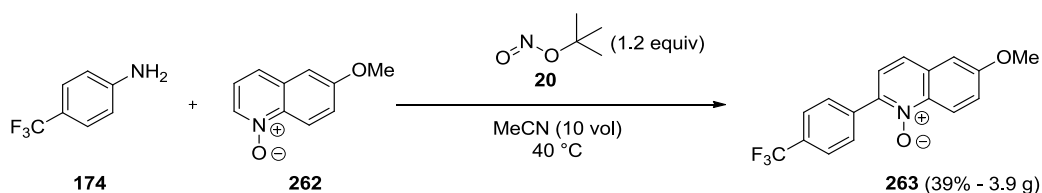
Entry	Conditions	Yield
1	Literature ¹⁴³	64%
2	With ascorbic acid 152	52%
3	Without ascorbic acid 152	53%

Table 21: Control reactions

While identical and acceptable yields were obtained regardless of the presence or absence of ascorbic acid **152** in these control reactions, this result definitely confirmed that this additive was not required for the reaction to proceed. As a conclusion of this study, all further reactions were carried out in the absence of ascorbic acid **152** including when exploring the scope of this new methodology.

III.3.vi Scale-up and calorimetry study

The true test of any new Green methodology often comes during scale-up where the sustainability advantages become increasingly important. It was therefore decided to study the calorimetry of this radical arylation in order to demonstrate the synthetic potential of this methodology while generating data which could support this mechanistic investigation. Reaction of 4-trifluoromethyl aniline **174** with 6-methoxyquinoline *N*-oxide **262** under optimised conditions (Scheme 68) was carried out on a 5 gram scale in a reaction calorimetry vessel equipped with a gas flow monitor with the aim to monitor the energy of the system and to identify potentially hazardous exothermic and gas-evolving events. It is noteworthy that the product of this arylation precipitated spontaneously from the reaction mixture and was isolated by filtration in 39% yield, thus delivering 3.9 grams of the target compound **263** (Scheme 68).



Scheme 68: Reaction for scale-up and calorimetry study

The dropwise addition of 4-trifluoromethyl aniline **174** to the mixture containing 6-methoxy quinoline *N*-oxide **262** in acetonitrile at 40 °C proved to be very mildly exothermic with a 3 °C predicted adiabatic temperature rise. Subsequent controlled addition of *tert*-butyl nitrite **20** to the reaction mixture over 10 minutes correlated with a strongly exothermic event and substantial gas evolution (Figure 49) with a calculated 81 °C predicted adiabatic temperature rise. Accumulation (of reagent or intermediates) was also a concern with 88% of the total heat output occurring after the addition of *tert*-butyl nitrite **20** was complete, implying that the reaction was intrinsically slower than the rate of addition. This issue could potentially be addressed by increasing the rate of reaction (for example by increasing reaction temperature) or by reducing the rate of *tert*-butyl nitrite **20** addition and will be examined prior to further scale-up.

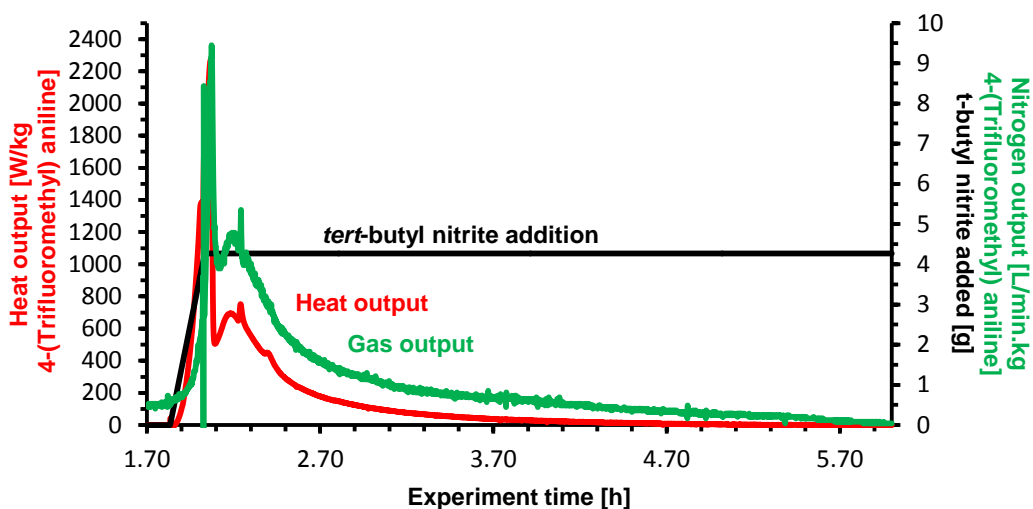


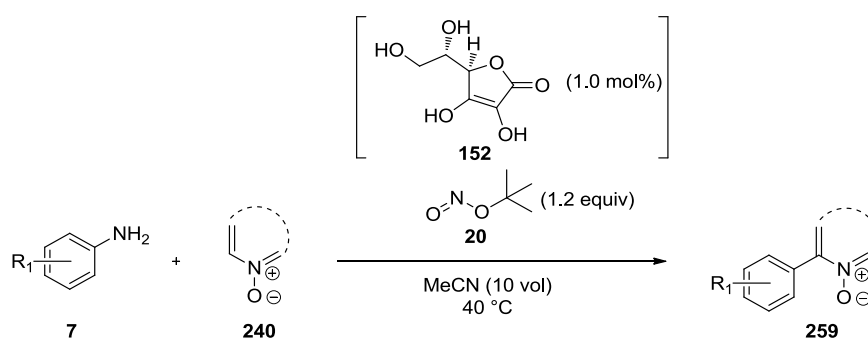
Figure 49: Gas and heat output of experiment on scheme 68

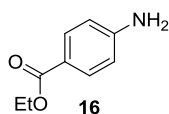
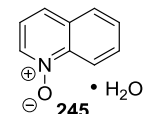
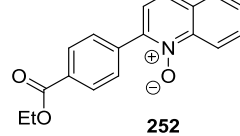
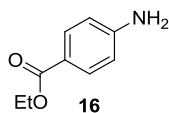
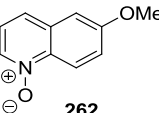
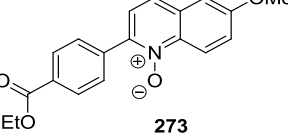
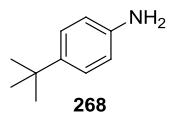
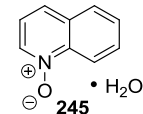
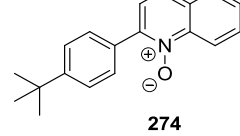
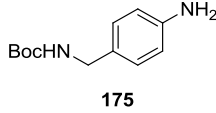
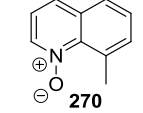
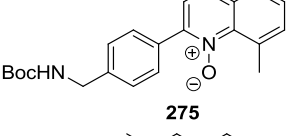
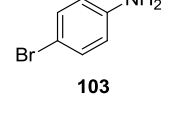
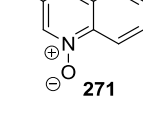
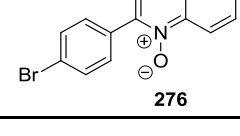
In addition to these results, the chart presented in Figure 49 is consistent with the formation of the intermediate **264** discussed in section III.3.v as two distinct peaks were observed during the calorimetry study. The sharp peak between 1.9 and 2.5 hours is believed to correspond to the direct reaction of the aryldiazonium species.

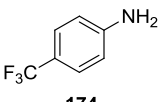
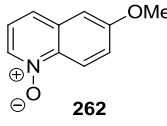
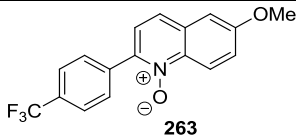
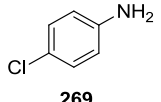
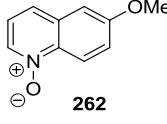
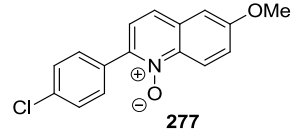
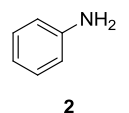
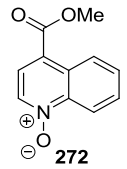
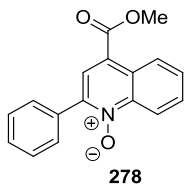
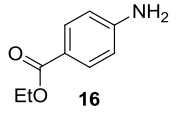
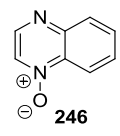
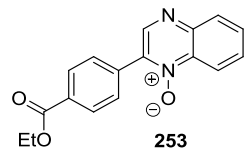
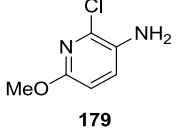
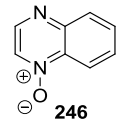
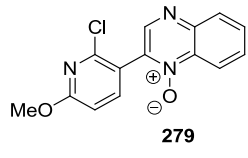
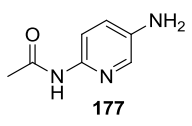
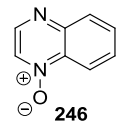
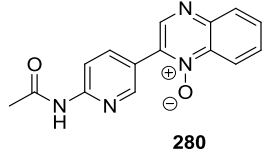
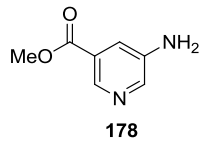
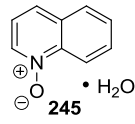
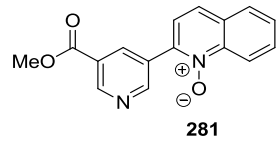
The second peak, between 1.9 and 4.7 hours, which was broader than the first, was attributed to the consumption of the triazene intermediate **264**.

III.3.vii Scope of the metal-free, ascorbic acid-free arylation

The previous studies allowed the identification of optimal reaction conditions excluding ascorbic acid **152** which were applied to a range of functionalised anilines and *N*-oxide heterocycles in order to define the scope and the limitations of this reaction (Table 22).



Entry	Aniline	<i>N</i> -oxide heterocycle	Product	Yield without 152^a	Yield with 152^a
1	 16	 245 • H ₂ O	 252	52%	53%
2	 16	 262	 273	52%	50%
3	 268	 245 • H ₂ O	 274	55%	51%
4	 175	 270	 275	44%	58%
5	 103	 271	 276	52%	51%

Entry	Aniline	<i>N</i> -oxide heterocycle	Product	Yield without 152 ^a	Yield with 152 ^a
6	 174	 262	 263	52%	50%
7	 269	 262	 277	53%	51%
8	 2	 272	 278	70%	65%
9	 16	 246	 253	74%	N.A.
10	 179	 246	 279	15%	22%
11	 177	 246	 280	43%	43%
12	 178	 245 • H ₂ O	 281	35%	34%

^aIsolated yield after chromatography.

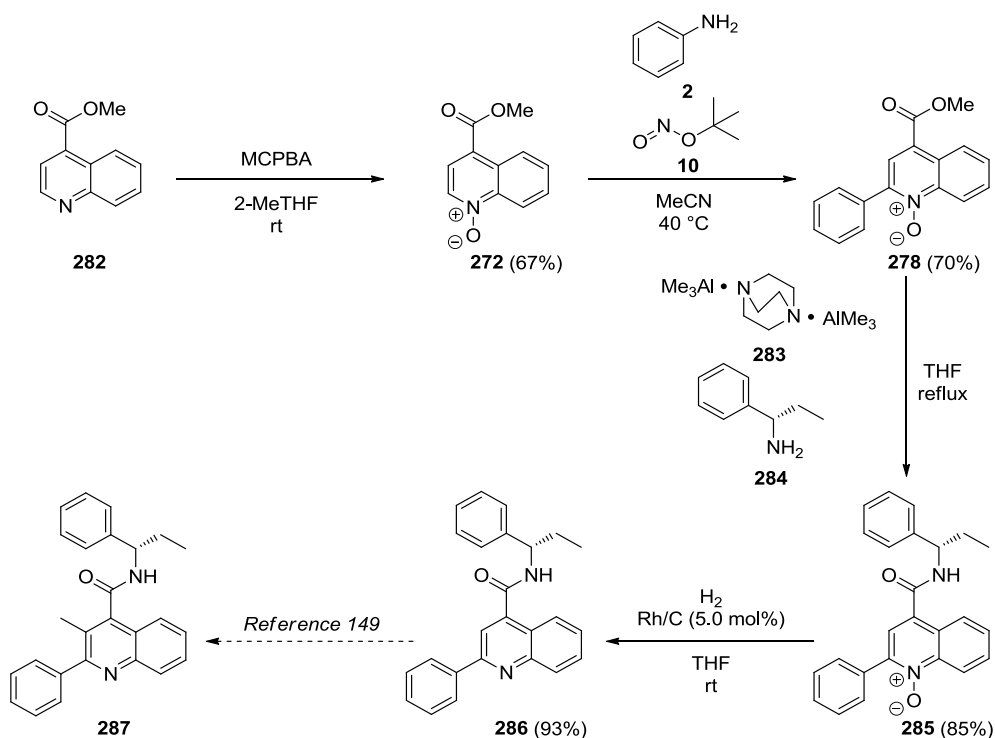
Table 22: Scope of the C-H arylation of *N*-oxide heterocycles

The electronic properties of both the aniline **7** and the *N*-oxide heterocycle **240** did not prove to affect the reaction as all combinations gave similar results with yields around 50%. Nevertheless it is noteworthy that amino-pyridine derivatives were much less efficient coupling partners compared to their otherwise similar aniline counterparts (Table 22, entries 1 and 12). This observation is consistent with pyridyldiazonium species exhibiting lower stability than the corresponding phenyldiazonium compounds as discussed in section III.1.v. In contrast, the arylation proved to be compatible with a representative range of functional groups used in medicinal chemistry such as amide (Table 22, entry 11), esters (Table 22,

entries 1, 2 and 12), a *N*-Boc protected amine (Table 22, entry 4) and halides (Table 22, entries 5 and 7), which provide significant opportunity for further elaboration. In addition, steric encumbrance on the *N*-oxide coupling partner was well tolerated (Table 22, entry 5) with the presence of an *ortho*-methyl group having no apparent impact on the yield of the transformation. This study also confirmed the observation of regioselectivity for the 2-position of the *N*-oxide heterocycle as only traces of the potential regioisomeric adducts were observed by LC/MS during this work.

III.3.viii Formal synthesis of SB222200

While arylated heterocyclic substrates could be prepared in moderate to good yields through this radical C-H arylation reaction, it was elected to apply this methodology to the pharmaceutically relevant substrate SB222200 **287**, a selective, reversible and competitive antagonist of human NK-3 receptor (Scheme 69).¹⁵⁰



Scheme 69: Formal synthesis of SB222200 **287**

The C-H arylation developed in this work required the preparation of the *N*-oxide substrate **272** which was achieved in 67% yield by oxidation using MCPBA on methyl 4-carboxyquinoline **282**. This example showed the ease of introduction of the *N*-oxide group on quinoline substrates as this compound was obtained in good yield with unoptimised reaction conditions. Subsequent arylation of *N*-oxide

heterocycle **272** was carried out in 70% yield and the methyl ester of **278** was directly converted to the corresponding amide **285** (85%) in the presence of DABAI-Me₃ **283** and enantiomerically pure amine **284**. The *N*-oxide group was then easily removed through unoptimised hydrogenation conditions catalysed by rhodium on activated charcoal and delivered the arylated quinoline **286** in 93% yield. Finally, the remaining steps to the target SB222200 **287** have been reported in the literature¹⁵¹ through deprotonation of the 3-position of the quinoline **286** and quenching with trimethyltin chloride followed by a cross-coupling with methyl iodide which was not carried out due to time constraints. This is therefore a formal synthesis of SB222200.

III.3.ix Future work

While the methodology developed in this work is dependent on the *N*-oxide group to achieve regioselectivity, the formal synthesis of SB222200 **287** showcased the ease of installation and removal of this functionality through well-established and conventional methods. The key arylation step of this sequence was successfully applied to the preparation of a relevant pharmaceutical intermediate and proved to be a viable alternative to palladium-catalysed cross-coupling methodologies.

Despite the good to moderate yields obtained during the course of this work, there is some yield unaccounted for and initial investigations pointed towards the formation of polymeric products. It may be beneficial for the transformation to study the mechanism further in order to identify the intermediates involved and design conditions to reduce the formation of these polymeric adducts.

CHAPTER IV CONCLUSION

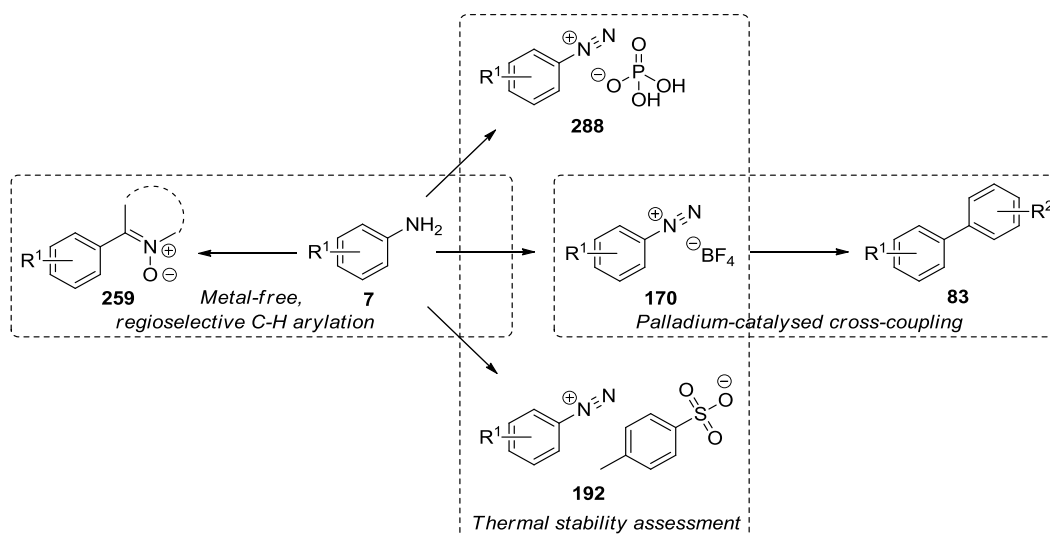


Figure 50: Research summary

Various salts of aryldiazonium species were prepared with good yields (aryldiazonium dihydrogen phosphate **288**, tetrafluoroborate **170** and tosylate **182**) and could therefore be assessed by DSC in order to determine the extent of their thermal stability. Amongst them, aryldiazonium tetrafluoroborate salts could be reliably prepared and isolated from a variety of green solvents while presenting the best thermal stability data compared to the other salts. These species have thus been shown to undergo a palladium-mediated Suzuki-Miyaura cross-coupling to afford pharmaceutically relevant biaryl systems. This methodology was optimised through the use of statistical methods including PCA and OPLS for solvent selection and DoE for the determination of the reaction conditions. Ultimately the process was applied to the multimolar-scale synthesis of an intermediate involved in the synthesis of angiotensin II inhibitors.

While all-carbon biaryl systems were afforded in good to excellent yields with this method, heterocycles did not perform well in this type of coupling and this limitation could be partially addressed through the investigation of another type of aryldiazonium reactivity. *N*-oxide heterocycles were indeed successfully coupled to aniline derivatives through their *in-situ* diazotisation thus avoiding the isolation of potentially hazardous aryldiazonium salts. This C-H arylation of *N*-oxide compounds was found to be regioselective for the 2-position and initial mechanistic investigations by ReactIR monitoring and X-ray crystallography showed that

CONCLUSION

ascorbic acid, an additive believed to be an initiator, was eventually not required for the reaction to proceed. While low yields were obtained when single core *N*-oxide species were used as substrate, fused ring systems such as quinoline and quinoxaline *N*-oxide derivatives were arylated in moderate to good yields, thus representing a viable alternative to more classical metal-catalysed couplings. Polymeric by-products were observed during the course of this work and much work is still required to avoid their formation, thus increasing the yield of this regioselective C-H arylation.

CHAPTER V EXPERIMENTAL

V.1 General experimental

All reactions were carried out under an atmosphere of nitrogen unless otherwise stated. Reagents were purchased at the highest commercial quality and used without further purification, unless otherwise stated. Where a solvent is described as “degassed” the solvent was exposed to repeated cycles of being placed under vacuum until it started to boil and then being placed under nitrogen. Yields refer to chromatographically and spectroscopically (¹H-NMR) homogeneous material, unless otherwise stated. Reactions were monitored by LC/MS and HPLC with the following conditions.

LC/MS conditions

Liquid chromatography conditions:

The liquid chromatography analysis was conducted on a Phenomenex Luna C₁₈ column (50 mm x 2.1 mm i.d. 3 μm packing diameter) at 40 °C. The solvents employed were:

A = Water + 0.05% v/v trifluoroacetic acid

B = Acetonitrile + 0.05% v/v trifluoroacetic acid

The gradient employed was:

Time (min)	Flow rate (mL/min)	% A	% B
0	1.5	100	0
8.0	1.5	5	95
8.5	1.5	5	95
8.6	1.5	100	0
10.0	1.5	100	0

The UV detection was a summed signal from wavelength of 205 nm to 400 nm.

Mass Spectrometry conditions:

MS: Waters ZQ

Ionisation mode: Positive Electrospray

Scan Range: 100 to 1000 Da

Scan Time: 1.0 second

Inter scan Delay: 0.05 seconds

HPLC conditions

The liquid chromatography analysis was conducted on a Phenomenex Luna C₁₈ column (50 mm x 2.1 mm i.d. 3 µm packing diameter) at 40 °C. The solvents employed were:

A = Water + 0.05%v/v trifluoroacetic acid

B = Acetonitrile + 0.05%v/v trifluoroacetic acid

The gradient employed was:

Time (min)	Flow rate (mL/min)	% A	% B
0	1.5	100	0
8.0	1.5	5	95
8.5	1.5	5	95
8.6	1.5	100	0
10.0	1.5	100	0

The UV detection was performed at 220 nm.

Silica gel chromatography

Silica gel chromatography purification were performed on Biotage SP4, using Biotage KP-Sil silica cartridges monitored by UV ($\lambda=254$ nm).

Mass Directed Auto-Preparative HPLC

Liquid chromatography conditions:

The HPLC separations were conducted on a XSELECT CSH C₁₈ (150 mm x 30 mm, i.d. 5 µm packing diameter) at ambient temperature. The solvents employed were:

A = Water + 0.1%v/v trifluoroacetic acid

B = Acetonitrile + 0.1%v/v trifluoroacetic acid

The gradient employed was:

Time (min)	Flow rate (mL/min)	% A	% B
0	40	70	30
3.0	40	70	30
3.5	30	70	30
24.5	30	15	85
25	30	1	99
32	30	1	99

The UV detection was for a signal wavelength at 254nm.

Mass Spectrometry conditions:

MS: Waters ZQ

Ionisation mode: Alternate-scan Positive and Negative Electrospray

Scan Range: 100 to 1000 Da

Scan Time: 0.50 second

Inter scan Delay: 0.2 seconds

Infrared spectroscopy

Infrared spectra were recorded on a Perkin-Elmer Spectrum One FT-IR Spectrometer through direct application and the data was processed using Perkin Elmer Spectrum software. Absorption frequencies of the higher intensity peaks are reported in wavenumbers (cm^{-1}). Live monitoring of experiments was achieved by a Mettler Toledo ReactIR iC 10 with MCT detector using HappGenzel apodization fitted with a DiComp (Diamond) probe connected with AgX 6mm x 2m Fiber (Silver Halide) and the data were interpreted using the software iC IR (version 4.3, Mettler Toledo).

High resolution mass spectrometry*Liquid chromatography conditions:*

The liquid chromatography analysis was conducted on a Phenomenex Luna C18 column (50 mm x 2.1mm i.d. 3.0 μm packing diameter) at 40 °C. The solvents employed were:

A = Water + 0.05% v/v trifluoroacetic acid

B = Acetonitrile + 0.05% v/v trifluoroacetic acid

The gradient employed was:

Time (min)	% A	% B
0	100	0
8	5	95
8.01	100	0
10	100	0

Mass Spectrometry conditions:

MS: Micromass Q-ToF 2 hybrid quadrupole time-of-flight mass spectrometer, equipped with a Z-spray interface

Ionisation mode: Positive Electrospray

Scan Range: 100 to 1100 Da

Scan Time: 0.9 second

Inter scan Delay: 0.1 seconds

All measured masses are accurate to within 5 ppm of the calculated mass.

Nuclear magnetic resonance spectroscopy

400 MHz ^1H NMR spectra were recorded on Bruker AV 400 NMR spectrometer. Signals are reported as : chemical shift δ /ppm (multiplicity, number of protons, coupling constants, J/Hz, assignments). Chemical shifts are reported to the nearest 0.01 ppm and coupling constant to the nearest 0.1 Hz (s = singlet; d = doublet; t = triplet; q = quartet; q = quadruplet; quint = quintuplet; sext = sextuplet; sept = septuplet; m = multiplet; a = apparent). 100 MHz ^{13}C spectra were recorded on the same spectrometers. Spectra were recorded at room temperature unless otherwise stated. DEPT135 and 2-dimensional experiments (COSY, HMBC, HMQC) were used to support assignments where appropriate.

Melting points

Melting points were measured on a Stuart automatic melting point apparatus SMP40. For compounds that decomposed over a wide temperature range, it was possible to watch a recorded video of the experiment to manually determine the melting point range. Melting points can also be observed by DSC as a sharp endothermic event.

Differential Scanning Calorimetry analysis

Samples were run in high pressure gold 40 μL crucibles from 20 $^{\circ}\text{C}$ to 350 $^{\circ}\text{C}$ at 2 $^{\circ}\text{C}/\text{min}$ on a Mettler Toledo DSC823e device.

Calorimetry Monitoring

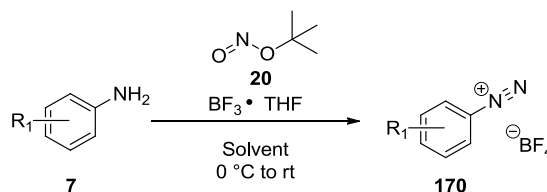
The calorimetry data were recorded using a Mettler Toledo RC1^e MidTemp 100 mL reactor and the data were exploited using iControl software version 5.

X-ray crystallography diffraction

Single crystal diffraction data were recorded on a diffractometer equipped with a cryostat using graphite monochromated Mo $\text{K}\alpha$ radiation ($\lambda(\text{Mo-K}\alpha) = 0.71073 \text{ \AA}$) radiation or on a diffractometer using Cu ($\lambda = 1.5418 \text{ \AA}$) radiation. All structures were processed and refined using SHELX-97. Selected crystallographic and refinement parameters are given in Appendix 1 and Appendix 3.

V.2 Synthesis and isolation of aryldiazonium salts

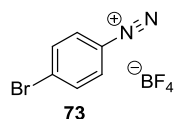
V.2.i General diazotisation procedure 1 using boron trifluoride – THF complex



To a stirred solution of the aniline derivative (1.0 equiv) in reported solvent at 0 °C was added $\text{BF}_3 \cdot \text{THF}$ complex (1.5 equiv) followed by dropwise addition of *tert*-butyl nitrite (1.2 equiv). The resulting reaction mixture was stirred at 0 °C and was then allowed to warm to room temperature. The product precipitates from solution. After careful filtration, the product was washed with TBME and dried at room temperature. When indicated, the product was purified by dissolving the crude in a minimum amount of acetone followed by precipitation by dropwise addition of TBME.

4-Bromo-benzenediazonium tetrafluoroborate 73 (223 mg, 89% yield)

73 was prepared according to the general diazotisation procedure 1 using 33 vol of ethyl acetate as solvent (30 min at 0 °C + 30 min at room temperature).



Appearance: Off-white solid

DSC: Decomposition starts at 114 °C, ends at 139 °C

FTIR: $\nu_{\text{max}} = 2286$ ($\text{N}^+\equiv\text{N}$)

^1H NMR (DMSO-d_6 , 400 MHz): $\delta = 8.58$ (d, 2H, $J = 9.0$ Hz), 8.26 (d, 2H, $J = 8.8$ Hz) ppm

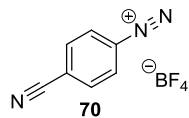
^{13}C NMR (DMSO-d_6 , 100 MHz): $\delta = 136.5$ (C_{IV}), 134.5 , 133.9 , 115.1 (C_{IV}) ppm

LCMS: $t_{\text{R}} = 0.33$ min, $[\text{M}^+]$ not available due to the early retention time

HRMS: Calculated for $\text{C}_6\text{H}_4^{79}\text{BrN}_2^+$ $[\text{M}^+]$ 182.9552, found 182.9552

4-Cyano-benzenediazonium tetrafluoroborate **70** (421 mg, 84% yield)

70 was prepared according to the general diazotisation procedure 1 using 90 vol of ethyl acetate as solvent (30 min at 0 °C + 30 min at room temperature).



Appearance: Off-white solid

DSC: Decomposition starts at 88 °C, ends at 123 °C

FTIR: $\nu_{\max} = 2290$ (C≡N + N⁺≡N) cm⁻¹

¹H NMR (DMSO-d₆, 400 MHz): $\delta = 8.84$ (d, 2H, $J = 8.5$ Hz), 8.46 (d, 2H, $J = 8.8$ Hz) ppm

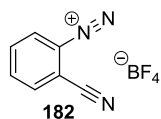
¹³C NMR (DMSO-d₆, 100 MHz): $\delta = 134.8$, 133.0, 121.8 (C_{IV}), 121.0 (C_{IV}), 116.3 (C_{IV}) ppm

LCMS: $t_R = 0.32$ min, [M⁺] not available due to the early retention time

HRMS: Calculated for C₇H₄N₃⁺ [M⁺] 130.0400 g.mol⁻¹, found 130.0399

2-Cyano-benzenediazonium tetrafluoroborate **182** (7.90 g, 86% yield)

182 was prepared according to the general diazotisation procedure 1 using 20 vol of ethanol as solvent (30 min at 0 °C + 30 min at room temperature).



Appearance: Yellow solid

DSC: Decomposition starts at 142 °C, ends at 174 °C

FTIR: $\nu_{\max} = 2297$ (C≡N + N⁺≡N) cm⁻¹

¹H NMR (DMSO-d₆, 400 MHz): $\delta = 9.00$ (dd, 1H, $J_1 = 8.3$ Hz, $J_2 = 1.0$ Hz), 8.59 (dd, 1H, $J_1 = 7.9$ Hz, $J_2 = 1.0$ Hz), 8.46 (atd, 1H, $J_1 = 7.9$ Hz, $J_2 = 1.0$ Hz), 8.32 (atd, 1H, $J_1 = 8.3$ Hz, $J_2 = 1.0$ Hz) ppm

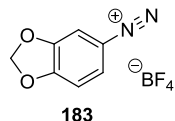
¹³C NMR (DMSO-d₆, 100 MHz): $\delta = 141.0$, 136.4, 135.6, 134.6, 118.6 (C_{IV}), 113.8 (C_{IV}), 112.4 (C_{IV}) ppm

LCMS: $t_R = 0.31$ min, [M⁺] not available due to the early retention time

HRMS: Calculated for C₇H₄N₃⁺ [M⁺] 130.0400 g.mol⁻¹, found 130.0398

3,4-Methylenedioxy-benzenediazonium tetrafluoroborate 183 (1.49 g, 87% yield)

183 was prepared according to the general diazotisation procedure 1 using 20 vol of 2-MeTHF as solvent (30 min at 0 °C + 30 min at room temperature).



Appearance: Brown solid

DSC: Decomposition starts at 92 °C, ends at 158 °C

FTIR: $\nu_{\max} = 2247$ ($\text{N}^+\equiv\text{N}$) cm^{-1}

¹H NMR (DMSO- d_6 , 400 MHz): $\delta = 8.43$ (dd, 1H, $J_1 = 8.8$ Hz, $J_2 = 2.2$ Hz), 8.06 (d, 1H, $J = 2.2$ Hz), 7.49 (d, 1H, $J = 8.8$ Hz), 6.45 (s, 2H) ppm

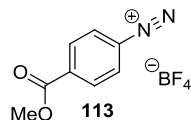
¹³C NMR (DMSO- d_6 , 100 MHz): $\delta = 158.8$ (C_{IV}), 148.5 (C_{IV}), 134.2, 110.6, 109.4, 105.5, 104.3 (C_{IV}) ppm

LCMS: $t_{\text{R}} = 0.33$ min, $[\text{M}^+]$ not available due to the early retention time

HRMS: Calculated for $\text{C}_7\text{H}_5\text{N}_2\text{O}_2^+$ $[\text{M}^+]$ 149.0351, found 149.0353

Methyl 4-benzoatediazonium tetrafluoroborate 113 (1.90 g, 77% yield)

113 was prepared according to the general diazotisation procedure 1 using 66 vol of THF as solvent (30 min at 0 °C + 30 min at room temperature). The product was purified *via* acetone/TBME reprecipitation.



Appearance: White solid

DSC: Decomposition starts at 71 °C, ends at 112 °C

FTIR: $\nu_{\max} = 2301$ ($\text{N}^+\equiv\text{N}$), 1725 ($\text{C}=\text{O}$) cm^{-1}

¹H NMR (DMSO- d_6 , 400 MHz): $\delta = 8.80$ (d, 2H, $J = 8.9$ Hz), 8.44 (d, 2H, $J = 8.9$ Hz), 3.96 (s, 3H) ppm

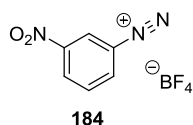
¹³C NMR (DMSO- d_6 , 100 MHz): $\delta = 163.8$ (C_{IV}), 139.2 (C_{IV}), 133.1, 131.2, 120.2 (C_{IV}), 53.4 ppm

HPLC: $t_{\text{R}} = 0.58$ min

HRMS: Calculated for $\text{C}_8\text{H}_7\text{N}_2\text{O}_2^+$ $[\text{M}^+]$ 163.0502, found 163.0502

3-Nitro-benzenediazonium tetrafluoroborate **184** (725 mg, 73% yield)

184 was prepared according to the general diazotisation procedure 1 using 20 vol of THF as solvent (30 min at 0 °C + 30 min at room temperature). The product was purified *via* acetone/TBME reprecipitation.



Appearance: White solid

DSC: Decomposition starts at 123 °C, ends at 168 °C

FTIR: $\nu_{\max} = 2306$ ($\text{N}^+\equiv\text{N}$) cm^{-1}

¹H NMR (DMSO-*d*₆, 400 MHz): $\delta = 9.61$ (s, 1H), 9.03-8.98 (m, 2H), 8.24 (at, 1H, $J = 8.4$ Hz) ppm

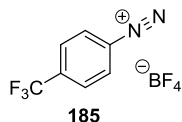
¹³C NMR (DMSO-*d*₆, 100 MHz): $\delta = 147.6$ (C_{IV}), 137.9, 135.0, 132.7, 128.1, 118.2 (C_{IV})

LCMS: $t_{\text{R}} = 0.20$ min, [M^+] not available due to the early retention time

HRMS: Calculated for $\text{C}_6\text{H}_4\text{N}_3\text{O}_2^+$ [M^+] 150.0298, found 150.0299

4-Trifluoromethyl-benzenediazonium tetrafluoroborate **185** (1.28 g, 79% yield)

185 was prepared according to the general diazotisation procedure 1 using 20 vol of TBME as solvent (30 min at 0 °C + 30 min at room temperature).



Appearance: White solid

DSC: Decomposition starts at 77 °C, ends at 114 °C

FTIR: $\nu_{\max} = 2308$ ($\text{N}^+\equiv\text{N}$) cm^{-1}

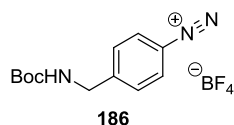
¹H NMR (DMSO-*d*₆, 400 MHz): $\delta = 8.91$ (d, 2H, $J = 8.7$ Hz), 8.42 (d, 2H, $J = 8.7$ Hz) ppm

¹³C NMR (DMSO-*d*₆, 100 MHz): $\delta = 138.1$ (C_{IV} , q, $J = 34$ Hz), 133.8, 128.2 (q, $J = 4$ Hz), 122.3 (C_{IV} , q, $J = 273$ Hz), 138.1 (C_{IV}) ppm

HPLC: $t_{\text{R}} = 0.72$ min

HRMS: Calculated for $\text{C}_7\text{H}_4\text{F}_3\text{N}_2^+$ [M^+] 173.0321, found 173.0323

4-[(N-Boc)aminomethyl]-benzenediazonium tetrafluoroborate **186** (448 mg, 90% yield) **186** was prepared according to the general diazotisation procedure 1 using 57 vol of *iso*-propanol as solvent (30 min at 0 °C + 150 min at room temperature).



Appearance: Off-white solid

DSC: Decomposition starts at 74 °C, ends at 109 °C

FTIR: ν_{\max} (cm^{-1}): 3361 (N-H), 2287 ($\text{N}^+\equiv\text{N}$), 1688 (C=O)

^1H NMR: (DMSO- d_6 , 400 MHz): δ = 8.62 (d, 2H, J = 8.6 Hz), 7.80 (d, 2H, J = 8.6 Hz), 7.67 (t, 1H, J = 5.8 Hz), 4.37 (d, 2H, J = 5.9 Hz), 1.42 (s, 9H) ppm

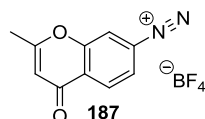
^{13}C NMR: (DMSO- d_6 , 100 MHz): δ = 155.8 (C_{IV}), 155.2 (C_{IV}), 132.9, 129.1, 113.2 (C_{IV}), 78.5 (C_{IV}), 43.6 (C_{IV}), 28.1 ppm

LCMS: t_{R} = 2.43 min, [M^+] 234

HRMS: Calculated for $\text{C}_{12}\text{H}_{16}\text{N}_3\text{O}_2^+$ [M^+] 234.1237, found 234.1242

2-Methyl-chromone-7-diazonium tetrafluoroborate **187** (3.35 g, 91% yield)

187 was prepared according to the general diazotisation procedure 1 using 30 vol of ethanol as solvent (30 min at 0 °C + 30 min at room temperature).



Appearance: Off-white solid

DSC: Decomposition starts at 103 °C, ends at 130 °C

FTIR: ν_{\max} = 2312 ($\text{N}\equiv\text{N}^+$), 1667 (C=O) cm^{-1}

^1H NMR: (DMSO- d_6 , 400 MHz): δ = 9.11 (s, 1H), 8.62 (d, 1H, J = 8.7 Hz), 8.49 (d, 1H, J = 8.7 Hz), 6.54 (s, 1H), 2.50 (s, 3H) ppm

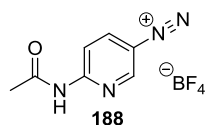
^{13}C NMR: (DMSO- d_6 , 100 MHz): δ = 174.8 (C_{IV}), 169.1 (C_{IV}), 154.2 (C_{IV}), 130.2 (C_{IV}), 128.3, 127.1, 124.2, 120.1 (C_{IV}), 111.6, 20.1 ppm

LCMS: t_{R} = 0.33 min, [M^+] not available due to the early retention time

HRMS: Calculated for $\text{C}_{10}\text{H}_7\text{N}_2\text{O}_2^+$ [M^+] 187.0502, found 187.0506

6-acetamido-pyridine-3-diazonium tetrafluoroborate 188 (905 mg, 91% yield)

188 was prepared according to the general diazotisation procedure 1 using a commercial solution of ethyl nitrite in ethanol (15-20% v/v) and 13 vol of ethanol as solvent (30 min at 0 °C + 17 h at room temperature).



Appearance: Brown solid

DSC: Decomposition starts at 109 °C, ends at 136 °C

FTIR: ν_{\max} = 3380 (N-H), 2261 (N≡N⁺), 1732 (C=O) cm⁻¹

¹H NMR: (DMSO-d₆, 400 MHz): δ = 11.83 (s, 1H), 9.52 (d, 1H, J = 2.4 Hz), 8.86 (dd, 1H, J_1 = 2.4 Hz, J_2 = 9.4 Hz), 8.48 (d, 1H, J = 9.5 Hz), 2.25 (s, 3H) ppm

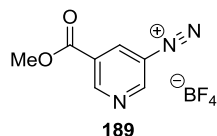
¹³C NMR: (DMSO-d₆, 100 MHz): δ = 171.1 (C_{IV}), 157.9 (C_{IV}), 155.6, 142.5, 113.2, 104.4 (C_{IV}), 24.5 ppm

LCMS: t_R = 0.33 min, [M⁺] not available due to the early retention time

HRMS: Calculated for C₇H₇N₄O⁺ [M⁺] 163.0614, found 163.0627

5-(methoxycarbonyl)-pyridine-3-diazonium tetrafluoroborate 189 (42 mg, 84% yield)

189 was prepared according to the general diazotisation procedure 1 using 65 vol of THF as solvent (30 min at 0 °C + 30 min at room temperature).



Appearance: White solid

DSC: Decomposition starts at 72 °C, ends at 93 °C

FTIR: ν_{\max} = 2303 (N⁺≡N), 1736 (C=O) cm⁻¹

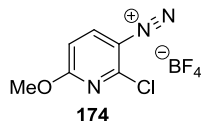
¹H NMR: (DMSO-d₆, 400 MHz): δ = 9.94 (d, 1H, J = 2.3 Hz), 9.66 (d, 1H, J = 1.8 Hz), 9.56 (d, 1H, J = 2 Hz), 4.00 (s, 3H) ppm

¹³C NMR: (DMSO-d₆, 100 MHz): δ = 162.1 (C_{IV}), 158.1, 155.8, 141.2, 126.5 (C_{IV}), 116.8 (C_{IV}), 53.5 ppm

LCMS: t_R = 0.33 min, [M⁺] not available due to the early retention time

HRMS: Unavailable due to stability issues

2-chloro-6-methoxy-pyridine-3-diazonium tetrafluoroborate 190 (885 mg, 89% yield)
190 was prepared according to the general diazotisation procedure 1 using 16 vol of THF as solvent (30 min at 0 °C + 60 min at room temperature).



Appearance: Brown solid

DSC: Decomposition starts at 136 °C, ends at 202 °C

FTIR: $\nu_{\max} = 2256$ (N≡N⁺) cm⁻¹

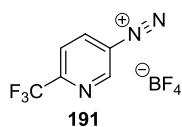
¹H NMR: (DMSO-d₆, 400 MHz): $\delta = 8.01$ (d, 1H, $J = 9.2$ Hz), 6.10 (d, 1H, $J = 9.3$ Hz), 3.85 (s, 3H) ppm

¹³C NMR: (DMSO-d₆, 100 MHz): $\delta = 169.9$ (C_{IV}), 167.9 (C_{IV}), 139.2, 111.5, (C_{IV}), 103.6, 54.5 ppm

LCMS: $t_R = 0.33$ min, [M⁺] not available due to the early retention time

HRMS: Unavailable due to stability issues

2-(trifluoromethyl)-pyridine-5-diazonium tetrafluoroborate 191 (2.25 g, 70% yield)
191 was prepared according to the general diazotisation procedure 1 using 20 volumes of ethanol as solvent (30 min at 0 °C + 30 min at room temperature).



Appearance: White solid

DSC: Decomposition starts at 63 °C, ends at 102 °C

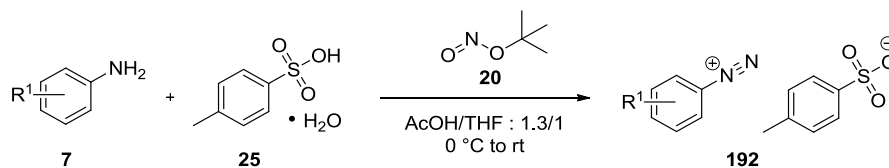
FTIR: $\nu_{\max} = 2320$ (N⁺≡N) cm⁻¹

¹H NMR: (DMSO-d₆, 400 MHz): $\delta = 9.93$ (s, 1H), 9.40 (dd, 1H, $J_1 = 8.7$ Hz, $J_2 = 1.5$ Hz), 8.60 (d, 1H, $J = 8.7$ Hz) ppm

¹³C NMR: (DMSO-d₆, 100 MHz): $\delta = 153.0$, 152.8 (q, $J = 36.3$ Hz), 144.1, 122.6 (C_{IV}), 119.9 (q, $J = 275.4$ Hz), 119.6 (C_{IV})

LCMS: $t_R = 0.33$ min, [M⁺] not available due to the early retention time

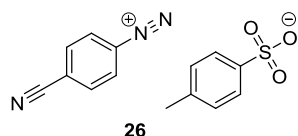
HRMS: Calculated for C₆H₃F₃N₃⁺ [M⁺] 174.0274, found 174.0276

V.2.ii General diazotisation procedure 2 using PTSA

To a stirred solution of the aniline derivative **7** (1.0 equiv) in THF and acetic acid at 0 °C was added PTSA (1.0 equiv) followed by the dropwise addition of *tert*-butyl nitrite (1.1 equiv). The resulting reaction mixture was stirred for 30 minutes at 0 °C and was allowed to warm to room temperature for 30 minutes. If the product did not precipitate spontaneously from the reaction mixture, a small amount of TBME was added until the precipitation of the product. After careful filtration, the product was washed with a small amount of TBME and dried at room temperature.

4-Cyano-benzenediazonium tosylate 26 (73 mg, 73% yield)

26 was prepared according to the general diazotisation procedure 2 using 77 vol of THF and 103 vol of acetic acid as solvent (30 min at 0 °C + 6 hours at room temperature).



Appearance: White solid

DSC: Decomposition starts at 87 °C, ends at 119 °C

FTIR: $\nu_{\text{max}} = 2307$ (C≡N + N⁺≡N) cm⁻¹

¹H NMR: (DMSO-d₆, 400 MHz): $\delta = 8.86$ (d, 2H, $J = 8.8$ Hz), 8.45 (d, 2H, $J = 8.0$ Hz), 7.46 (d, 2H, $J = 8.0$ Hz), 7.10 (d, 2H, $J = 7.8$ Hz), 2.29 (s, 3H) ppm

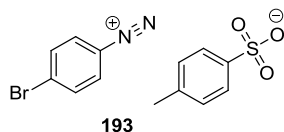
¹³C NMR: (DMSO-d₆, 100 MHz): $\delta = 145.6$ (C_{IV}), 137.6, 134.7, 133.0, 128.1, 125.5, 121.6 (C_{IV}), 121.1 (C_{IV}), 116.4 (C_{IV}), 20.8 ppm

LCMS: $t_R = 0.33$ min, [M⁺] not available due to the early retention time + 1.82 min, [M+NH₄⁺] 190 (Tosic acid)

HR MS: Calculated for C₇H₄N₃⁺ [M⁺] 130.0400, found 130.0400

4-Bromo-benzenediazonium tosylate 193 (63 mg, 63% yield)

193 was prepared according to the general diazotisation procedure 2 using 63 volumes of THF and 83 volumes of acetic acid as solvent (30 min at 0 °C + 6 hours at room temperature).



Appearance: White solid

DSC: Decomposition starts at 90 °C, ends at 131 °C

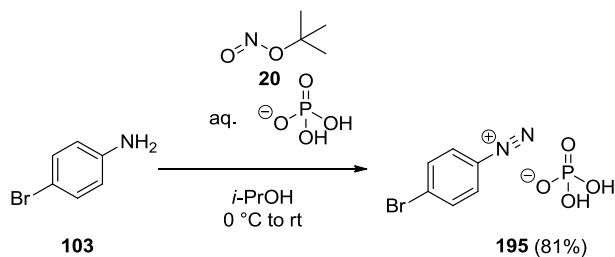
FTIR: $\nu_{\max} = 2295$ ($\text{N}^+\equiv\text{N}$) cm^{-1}

¹H NMR: (DMSO- d_6 , 400 MHz): $\delta = 8.60$ (d, 2H, $J = 8.9$ Hz), 8.24 (d, 2H, $J = 9.0$ Hz), 7.47 (d, 2H, $J = 8.0$ Hz), 7.10 (d, 2H, $J = 7.9$ Hz), 2.29 (s, 3H) ppm

¹³C NMR: (DMSO- d_6 , 100 MHz): $\delta = 145.6$ (C_{IV}), 137.6 (C_{IV}), 136.4 (C_{IV}), 134.5, 134.0, 128.0, 125.5, 115.2 (C_{IV}), 20.8 ppm

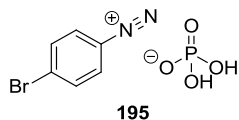
LCMS: $t_{\text{R}} = 0.32$ min, $[\text{M}^+]$ not available due to the early retention time + 1.82 min, $[\text{M}+\text{NH}_4^+]$ 190 (Tosic acid)

HRMS: Calculated for $\text{C}_6\text{H}_4^{79}\text{BrN}_2^+$ $[\text{M}^+]$ 182.9552, found 182.9556

V.2.iii Synthesis of 4-bromo-benzenediazonium dihydrogen phosphate 195

To a stirred solution of 4-bromoaniline **103** (316 mg, 1.779 mmol) in *iso*-propanol (20 mL, 63 vol.) at 0 °C was added 85% aqueous phosphoric acid (0.282 mL, 4.12 mmol) followed by *tert*-butyl nitrite **20** (0.282 mL, 2.135 mmol). The resulting reaction mixture was stirred for 30 min at 0 °C and was allowed to warm up at room temperature for 5h. The product precipitated spontaneously in solution. After careful filtration, the product **195** was washed with TBME and dried at room temperature overnight to give 4-bromo-benzenediazonium dihydrogen phosphate salt **195** (407 mg, 1.45 mmol, 81% yield).

4-Bromo-benzenediazonium dihydrogen phosphate 195 (407 mg, 81% yield)



Appearance: White solid

DSC: Decomposition starts at 105 °C, ends at 134 °C

FTIR: $\nu_{\text{max}} = 2274$ (N⁺≡N), 1555 (P=O) cm⁻¹

¹H NMR: (DMSO-d₆, 400 MHz): $\delta = 10.4$ (bs, 7H), 8.61 (d, 2H, $J = 9.0$ Hz), 8.25 (d, 2H, $J = 9.0$ Hz) ppm

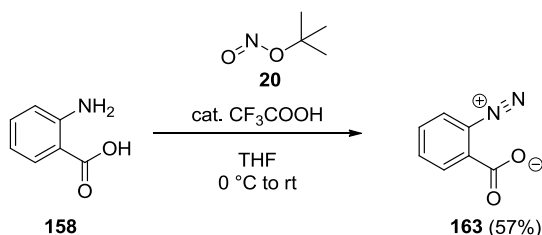
¹³C NMR: (DMSO-d₆, 100 MHz): $\delta = 136.5$ (C_{IV}), 134.5, 134.0, 115.1 (C_{IV}) ppm

LCMS: $t_R = 0.33$ min, [M⁺] not available due to the early retention time

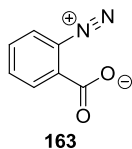
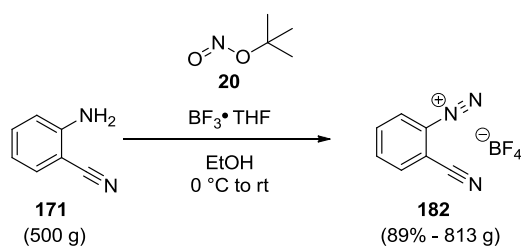
HRMS: Unavailable due to stability issues

X-ray: Appendix 1

V.2.iv Synthesis of 2-carboxylate-benzenediazonium 163



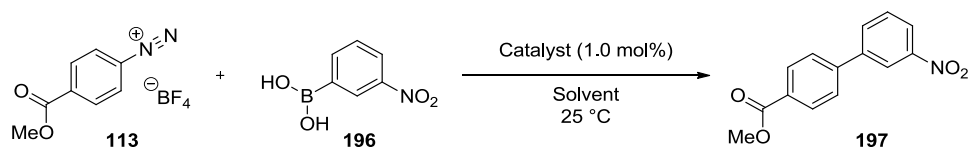
To a stirred solution of anthralinic acid **158** (50 mg, 0.365 mmol) in THF (1 mL) at 0 °C was added TFA (2.79 μ L, 0.036 mmol) followed by *tert*-butyl nitrite **20** (0.052 mL, 0.438 mmol). The resulting reaction mixture was stirred for 30 min at 0 °C and the product **163** precipitated spontaneously from the reaction mixture. After careful filtration in a plastic filter and using a plastic spatula, the product **163** was washed with THF and dried at room temperature overnight to give 2-carboxylate-benzenediazonium **163** (31 mg, 0.209 mmol, 57%).

2-Carboxylate-benzenediazonium **163** (31 mg, 57% yield)**Appearance:** Off-white solid**MP:** Unavailable due to stability issues**FTIR:** Unavailable due to stability issues**¹H NMR:** (AcOD-d₄, 400 MHz): δ = 8.53 (d, 1H, *J* = 7.6 Hz), 8.38 (d, 1H, *J* = 7.8 Hz), 8.10 (at, 1H, *J* = 7.6 Hz), 7.85 (at, 1H, *J* = 7.4 Hz) ppm**¹³C NMR:** Unavailable due to stability issues**HPLC:** t_R = Unavailable due to stability issues**HRMS:** Unavailable due to stability issues**V.2.v Scale-up of 2-Cyano-benzenediazonium tetrafluoroborate **182****

A 20 L CLR reactor fitted with an overhead stirrer was flushed with nitrogen and charged with 2-aminobenzonitrile **171** (500 g, 4.23 mol) followed by 10 L of ethanol. The solution was cooled to 0 °C and BF₃·THF complex (700 mL, 6.35 mol) was charged portionwise to the reactor without significant exotherm. *tert*-butyl nitrite **20** (673 mL, technical grade 90%, 5.08 mol) were pumped into the reactor with a peristaltic pump over 20 min and the temperature rose from - 1.2 °C to + 6.7 °C. The reaction was stirred with a mechanical stirrer for 30 minutes at 0 °C and 30 minutes at 20 °C. The product **182** precipitated from ethanol and the slurry was filtered. The resulting solid was collected and dried in a vacuum oven overnight at 20 °C to give 2-cyano-benzenediazonium tetrafluoroborate **182** (813 g, 3.75 mol, 89% yield).

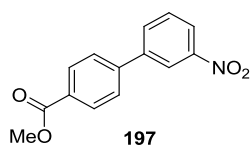
V.3 Cross-coupling of aryldiazonium salts

V.3.i Catalyst and solvent screening procedure



To a glass tube equipped with a stirrer bar were introduced 3-nitro-phenyl boronic acid **196** (56 mg, 0.335 mmol), methyl 4-benzoatediazonium tetrafluoroborate **113** (126 mg, 0.503 mmol), and palladium catalyst (1.0 mol %). The air inside was replaced by nitrogen *via* vacuum/nitrogen cycles. Solvent (5 mL) was then injected into the glass tube, and the reaction mixture was stirred under a nitrogen atmosphere at 25 °C for 24 h. Ethyl acetate was then added to the mixture and the catalyst removed by filtration over Celite. The filtrate was analysed by HPLC to determine a solution yield (Appendix 2) before being evaporated to dryness. The crude product was purified by silica gel chromatography eluting with a heptane/ethyl acetate mixture to give 4'-Methylbenzoate-3-nitro-biphenyl **197**.

4'-Methylbenzoate-3-nitro-biphenyl **197**



Appearance: White solid

MP: 146 – 148 °C

FTIR: ν_{\max} = 1712 (C=O) cm⁻¹

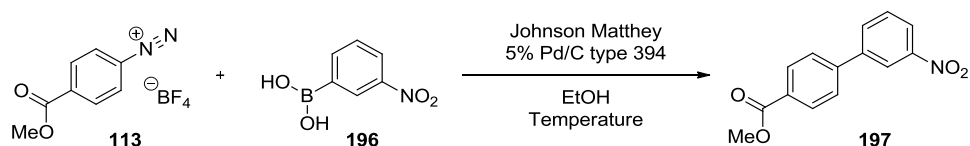
¹H NMR: (DMSO-d₆, 400 MHz): δ = 8.49 (at, 1H J = 2.0 Hz), 8.28 (dd, 1H, J_1 = 8.2 Hz, J_2 = 1.0 Hz), 8.22 (dd, 1H, J = 7.8 Hz, J_2 = 0.7 Hz), 8.08 (d, 2H, J = 8.6 Hz), 7.94 (d, 2H, J = 8.3 Hz), 7.80 (at, 1H J = 8.0 Hz), 3.90 (s, 3H) ppm

¹³C NMR: (DMSO-d₆, 100 MHz): δ = 165.9 (C_{IV}), 148.5 (C_{IV}), 142.2 (C_{IV}), 140.4 (C_{IV}), 133.5, 130.6, 129.9, 129.4 (C_{IV}), 127.4, 123.0, 121.4, 52.2 ppm

HPLC: t_R = 5.69 min

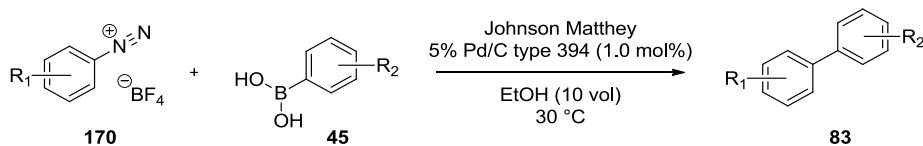
HRMS: Calculated for C₁₄H₁₁NO₄ [M + H]⁺ 258.0761, found 258.0761

V.3.ii Design of Experiments Reactions



To a glass tube equipped with a stir bar were introduced 3-nitro-phenyl boronic acid **196** (1.0 equiv), methyl 4-benzoatediazonium tetrafluoroborate **113** (Factor A) and Johnson Matthey 5% Pd/C type 394 (moisture: 56.70%) (Factor C). The air inside was replaced by nitrogen *via* vacuum/nitrogen cycles. Ethanol/water (Factor D and E) was then injected into the glass tube, and the reaction mixture was stirred under a nitrogen atmosphere at the indicated temperature (Factor B) for 24 h. Ethyl acetate was then added to the mixture, and the catalyst removed by filtration over Celite. The filtrate was analysed by HPLC to determine a solution yield according to the calibration curve in Appendix 2.

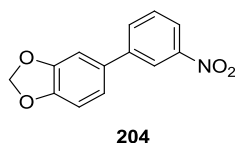
V.3.iii General cross-coupling procedure for substrate scope



To a glass tube equipped with a stir bar were introduced aryl boronic acid **45** (500 mg, 1.0 equiv), aryldiazonium tetrafluoroborate **170** (1.1 equiv), and catalyst (Johnson Matthey 5% Pd/C type 394, moisture: 56.70%, 1.0 mol %). The air inside was replaced by nitrogen *via* vacuum/nitrogen cycles. Ethanol (5 mL, 10 vol) was then injected into the glass tube, and the reaction mixture was stirred under a nitrogen atmosphere at 30 °C for 24 h. Ethyl acetate or acetone was then added to the mixture and the catalyst removed by filtration over Celite. The filtrate was evaporated to dryness, and the crude product was purified by silica gel chromatography eluting with heptane/ethyl acetate or heptane/acetone mixtures to give the biaryl product **83**.

3'-Nitro-3,4-methylenedioxy-biphenyl 204 (45 mg or 658 mg, 6% or 90% yield)

204 was prepared according to the general cross-coupling procedure.



Appearance: Beige solid

MP: 119 – 120 °C

FTIR: No characteristic bands were observed for this compound

¹H NMR: (DMSO-d₆, 400 MHz): δ = 8.33 (s, 1H), 8.14 (d, 1H, *J* = 8.1 Hz), 8.05 (d, 1H, *J* = 7.5 Hz), 7.69 (t, 1H, *J* = 7.8 Hz), 7.35 (s, 1H), 7.24 (d, 1H, *J* = 8.1 Hz), 7.02 (d, 1H, *J* = 8.1 Hz), 6.09 (s, 2H) ppm

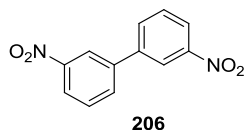
¹³C NMR: (DMSO-d₆, 100 MHz): δ = 148.3 (C_{IV}), 148.2 (C_{IV}), 147.7 (C_{IV}), 141.5 (C_{IV}), 132.9, 131.9 (C_{IV}), 130.3, 121.6, 120.9, 120.7, 108.8, 107.3, 101.4 ppm

LCMS: t_R = 5.78 min, [M+H⁺] 244

HRMS: Calculated for C₁₃H₉NO₄ [M + H]⁺ 244.0604, found 244.0602

3',3'-Dinitro-biphenyl 206 (688 mg, 94% yield)

206 was prepared according to the general cross-coupling procedure.



Appearance: White solid

MP: 207 – 208 °C

FTIR: No characteristic bands were observed for this compound

¹H NMR: (DMSO-d₆, 400 MHz): δ = 8.57 (s, 2H), 8.29 (at, 4H, *J* = 9.1 Hz), 7.83 (at, 2H, *J* = 8.0 Hz) ppm

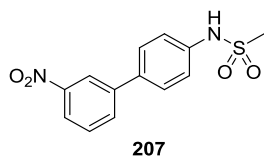
¹³C NMR: (DMSO-d₆, 100 MHz): δ = 148.5 (C_{IV}), 139.4 (C_{IV}), 133.7, 130.7, 123.2, 121.8 ppm

LCMS: t_R = 5.70 min, [M+H⁺] unavailable

HRMS: Calculated for C₁₂H₈N₂O₄ [M + H]⁺ 245.0557, found 245.0556

3'-Nitro-4-N-methylsulfonamide-biphenyl 207 (612 mg, 90% yield)

207 was prepared according to the general cross-coupling procedure.



Appearance: Beige solid

MP: 145 – 150 °C

FTIR: ν_{\max} = 3204 (N-H) cm^{-1}

$^1\text{H NMR}$: (DMSO- d_6 , 400 MHz): δ = 9.98 (s, 1H), 8.41 (t, 1H, J = 2 Hz), 8.19 (dd, 1H, J_1 = 8.2 Hz, J_2 = 1.5 Hz), 8.12 (d, 1H, J = 8.3 Hz), 7.79–7.73 (m, 3H), 7.35 (d, 2H, J = 8.7 Hz), 3.06 (s, 3H) ppm

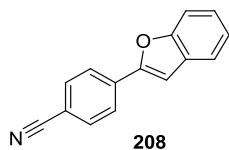
$^{13}\text{C NMR}$: (DMSO- d_6 , 100 MHz): δ = 148.5 (C_{IV}), 141.1 (C_{IV}), 138.9 (C_{IV}), 132.9 (C_{IV}), 132.8, 130.5, 128.0, 121.8, 120.6, 119.7, 39.5 ppm

LCMS: t_{R} = 4.86 min, $[\text{M} + \text{NH}_4]^+$ 310

HRMS: Calculated for $\text{C}_{13}\text{H}_{12}\text{N}_2\text{O}_4\text{S}$ $[\text{M} + \text{NH}_4]^+$ 310.0856, found 310.0854

4-(Benzofuran-2-yl)-benzonitrile 208 (237 mg, 35% yield)

208 was prepared according to the general cross-coupling procedure.



Appearance: White solid

MP: 141 – 144 °C

FTIR: 2226 ($\text{C}\equiv\text{N}$) cm^{-1}

$^1\text{H NMR}$: (DMSO- d_6 , 400 MHz): δ = 8.10 (d, 2H, J = 8.4 Hz), 7.96 (d, 2H, J = 8.6 Hz), 7.74–7.66 (m, 3H), 7.40 (ddd, 1H, J_1 = 8.0 Hz, J_2 = 8.0 Hz, J_3 = 1.3 Hz), 7.33 (ddd, 1H, J_1 = 8.0 Hz, J_2 = 8.0 Hz, J_3 = 1.3 Hz) ppm

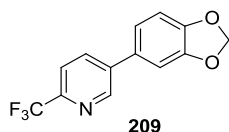
$^{13}\text{C NMR}$: (DMSO- d_6 , 100 MHz): δ = 154.6 (C_{IV}), 153.2 (C_{IV}), 133.8 (C_{IV}), 133.0, 128.4 (C_{IV}), 125.7, 125.2, 123.6, 121.8, 118.7 (C_{IV}), 111.4, 110.7 (C_{IV}), 105.3 ppm

LCMS: t_{R} = 6.10 min, $[\text{M} + \text{H}]^+$ 220

HRMS: Calculated for $\text{C}_{15}\text{H}_9\text{NO}$ $[\text{M} + \text{H}]^+$ 220.0757, found 220.0756

5-(3',4'-Methylenedioxyphenyl)-2-trifluoromethyl-pyridine **209** (53 mg, 7% yield)

209 was prepared according to the general cross-coupling procedure and purified by MDAP when Pd/C was used. **209** was also prepared in 35% yield according to the general cross-coupling procedure using palladium(II) acetate as catalyst.



Appearance: Off-white solid

MP: 117 – 125 °C

FTIR: No characteristic bands were observed for this compound

¹H NMR: (DMSO-*d*₆, 400 MHz): δ = 9.05 (s, 1H), 8.30 (d, 1H, *J* = 8.0 Hz), 7.93 (d, 1H, *J* = 8.3 Hz), 7.47 (s, 1H), 7.34 (d, 1H, *J* = 8.1 Hz), 7.09 (d, 1H, *J* = 8.3 Hz), 6.12 (s, 2H) ppm

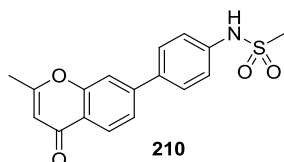
¹³C NMR: (DMSO-*d*₆, 100 MHz): δ = 148.3 (C_{IV}), 148.2 (C_{IV}), 147.9, 144.6 (C_{IV}, *q*, *J* = 33.8 Hz), 138.5 (C_{IV}), 135.5, 129.5 (C_{IV}), 121.8 (C_{IV}, *q*, *J* = 273.4 Hz), 121.5, 120.7, 109.0, 107.5, 101.5 ppm

LCMS: *t*_R = 5.47 min, [M+H⁺] 268

HRMS: Calculated for C₁₃H₈F₃NO₂ [M + H]⁺ 268.0580, found 268.0578

7-(4'-N-Methylsulfonamid-phenyl)-2-methyl-chromone **210** (705 mg, 92% yield)

210 was prepared according to the general cross-coupling procedure.



Appearance: Beige solid

MP: 226 – 228 °C

FTIR: *v*_{max} = 3100 (N-H), 1638 (C=O) cm⁻¹

¹H NMR: (DMSO-*d*₆, 400 MHz): δ = 10.00 (s, 1H), 8.01 (d, 1H, *J* = 8.3 Hz), 7.81–7.78 (m, 3H), 7.72 (d, 1H, *J* = 8.3 Hz), 7.34 (d, 2H, *J* = 8.5 Hz), 6.23 (s, 1H), 3.07 (s, 3H), 2.39 (s, 3H) ppm

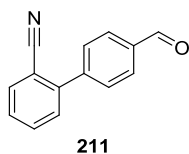
¹³C NMR: (DMSO-*d*₆, 100 MHz): δ = 176.4 (C_{IV}), 166.8 (C_{IV}), 156.4 (C_{IV}), 144.8 (C_{IV}), 139.2 (C_{IV}), 133.0 (C_{IV}), 128.2, 125.4, 123.2, 121.5 (C_{IV}), 119.5, 114.9, 110.0, 39.5, 20.0 ppm

LCMS: *t*_R = 4.31 min, [M+H⁺] 330

HRMS: Calculated for C₁₇H₁₅NO₄S [M+H]⁺ 330.0795, found 330.0794

2'-Cyano-4-formyl-biphenyl 211 (126 mg, 18% yield)

211 was prepared according to the general cross-coupling procedure. **211** was also prepared in 72% yield according to the cross-coupling scale-up procedure using palladium (II) acetate as catalyst (*vide infra*).



Appearance: White to beige solid

MP: 164 – 165 °C

FTIR: ν_{\max} = 2223 (C≡N), 1727 (C=O) cm^{-1}

¹H NMR: (DMSO- d_6 , 400 MHz): δ = 10.13 (s, 1H), 8.08 (d, 2H, J = 8.0 Hz), 8.02 (d, 1H, J = 7.8 Hz), 7.88–7.83 (m, 3H), 7.72–7.65 (m, 2H) ppm

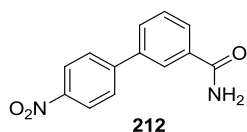
¹³C NMR: (DMSO- d_6 , 100 MHz): δ = 192.8 (C_{IV}), 143.4 (C_{IV}), 143.3 (C_{IV}), 136.0 (C_{IV}), 133.9, 133.6, 130.2, 129.7, 129.6, 129.0, 118.2 (C_{IV}), 110.2 (C_{IV}) ppm

LCMS: t_R = 4.73 min, [M+H]⁺ 208

HRMS: Calculated for C₁₄H₉NO [M + H]⁺ 208.0757, found 208.0756

3'-Carboxamido-4-nitro-biphenyl 212 (525 mg, 72% yield)

212 was prepared according to the general cross-coupling procedure.



Appearance: White solid

MP: 182 – 186 °C

FTIR: 3368 (N-H), 3177 (N-H), 1655 (C=O) cm^{-1}

¹H NMR: (DMSO- d_6 , 400 MHz): δ = 8.35 (d, 2H, J = 8.5 Hz), 8.29 (s, 1H), 8.17 (bs, 1H), 8.06 (d, 2H, J = 8.8 Hz), 7.97 (t, 2H, J = 7.6 Hz), 7.64 (t, 1H, J = 7.8 Hz), 7.50 (bs, 1H) ppm

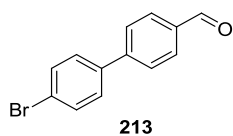
¹³C NMR: (DMSO- d_6 , 100 MHz): δ = 167.4 (C_{IV}), 146.9 (C_{IV}), 146.0 (C_{IV}), 137.8 (C_{IV}), 135.2 (C_{IV}), 130.0, 129.3, 128.1, 128.0, 126.2, 124.1 ppm

LCMS: t_R = 4.22 min, [M+H]⁺ 243

HRMS: Calculated for C₁₃H₁₀N₂O₃ [M + H]⁺ 243.0764, found 243.0761

4'-Formyl-4-bromo-biphenyl 213 (368 mg, 42% yield)

213 was prepared according to the general cross-coupling procedure.



Appearance: White solid

MP: 144 – 149 °C

FTIR: ν_{\max} = 1698 (C=O) cm^{-1}

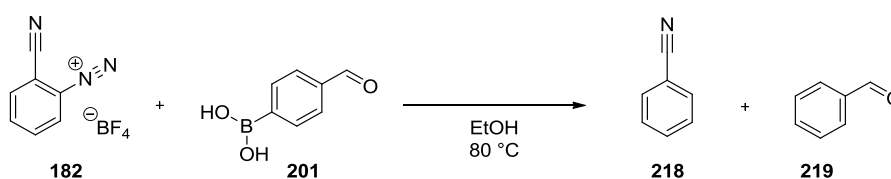
$^1\text{H NMR}$: (DMSO- d_6 , 400 MHz): δ = 10.07 (s, 1H), 8.00 (d, 2H, J = 8.3 Hz), 7.92 (d, 2H, J = 8.3 Hz), 7.75–7.70 (m, 4H) ppm

$^{13}\text{C NMR}$: (DMSO- d_6 , 100 MHz): δ = 192.7, 144.5 (C_{IV}), 137.9 (C_{IV}), 135.3 (C_{IV}), 132.0, 130.2, 129.2, 127.3, 122.2 (C_{IV}) ppm

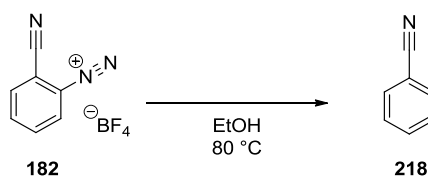
LCMS: t_{R} = 5.89 min, $[\text{M}+\text{H}^+]$ 263

HRMS: Calculated for $\text{C}_{13}\text{H}_9^{79}\text{BrO}$ $[\text{M} + \text{H}]^+$ 260.9910, found 260.9909

V.3.iv Control reactions for safety assessment



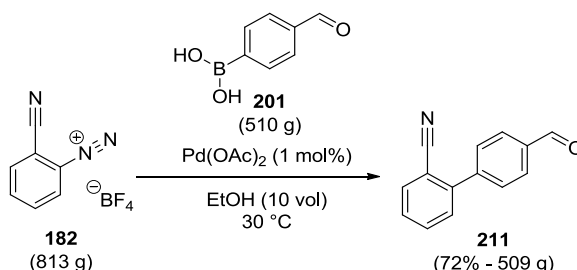
A solution of 2-cyanobenzene diazonium tetrafluoroborate **182** (51 mg, 0.235 mmol) and (4-formyl-phenyl)boronic acid **201** (32 mg, 0.213 mmol) in 320 μL of ethanol was prepared in a HPLC vial. This slurry was gradually heated to 80°C by increasing the temperature by 10°C every 10 minutes. Samples were taken every 10 minutes and it was believed that the main products formed during the decomposition were benzonitrile and benzaldehyde according to the LC/MS data. A commercial sample of benzaldehyde **219** was added to the last sample of the reaction mixture and the LC/MS trace confirmed that the product formed was benzaldehyde **219**.



A solution of 2-cyanobenzene diazonium tetrafluoroborate **182** (51 mg, 0.235 mmol) in 320 μL of ethanol was prepared in a HPLC vial. This slurry was gradually heated

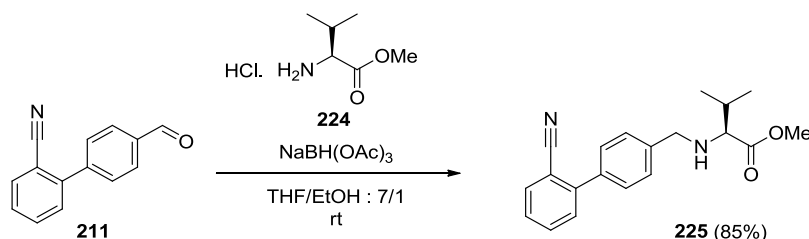
to 80°C by increasing the temperature by 10°C every 10 minutes. Samples were taken every 10 minutes and it was believed that the main product formed during the decomposition was benzonitrile according to the LC/MS data. A commercial sample of benzonitrile **218** was added to the last sample of the reaction mixture and the LC/MS trace confirmed that the product formed was benzonitrile **218**.

V.3.v Cross-coupling scale-up procedure



A 20 L CLR reactor fitted with an overhead stirrer was flushed with nitrogen and charged with 2-cyano-benzenediazonium tetrafluoroborate **182** (813 g, 3.75 mol), 4-formyl-phenylboronic acid **211** (510 g, 3.40 mol), and palladium(II) acetate (7.64 g, 34.0 mmol). Then 5.1 L of ethanol was added to the reactor at 25 °C, and the temperature rose to 43 °C; meanwhile the jacket was reset to -5 °C to control the exotherm. Once the temperature stabilised at 30 °C, the slurry was stirred at 30 °C for 24 h under a nitrogen atmosphere. Then 5.1 L of an aqueous solution of N-acetyl cysteine (55.5 g, 0.34 mol) was added to the reaction mixture, and the slurry was stirred for 2 h at 30 °C before being filtered. The resulting solid was collected and dried in a vacuum oven for 48 h at 30 °C to give 2'-cyano-4-formyl-biphenyl **211** (509 g, 2.46 mol, 72% yield).

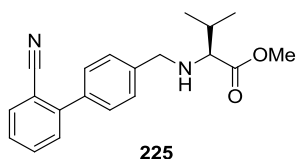
V.3.vi Synthesis of N-((2'-Cyanobiphenyl-4-yl)-methyl)-(L)-valine methyl ester **225**



To a dried round bottom flask containing 3Å molecular sieves, 2'-Cyano-4-formyl-biphenyl **211** (2.0 g, 9.65 mmol) and L-valine methyl ester hydrochloride **224** (2.427 g, 14.48 mmol) was added THF (100 mL). The reaction was stirred for 20 hours at

room temperature and was cooled down to 0 °C prior to the portionwise addition of sodium triacetoxyhydroborate (4.09 g, 19.30 mmol, 2.0 equiv) and ethanol (15 mL). The resulting slurry was stirred for 3 days at room temperature and the molecular sieves were filtered off over Celite. The reaction mixture was extracted with saturated aqueous NaHCO₃ solution and ethyl acetate. The organic layer was dried over anhydrous MgSO₄ and evaporated under reduced pressure before being purified by silica gel chromatography, eluting with heptane / ethyl acetate to give *N*-((2'-Cyanobiphenyl-4-yl)-methyl)-(L)-valine methyl ester **225** (2.659 g, 8.25 mmol, 85 % yield) as a colorless oil.

N-((2'-Cyanobiphenyl-4-yl)-methyl)-(L)-valine methyl ester **225** (2.66 g, 85% yield)¹³⁰



Appearance: Colorless oil

MP: N.A.

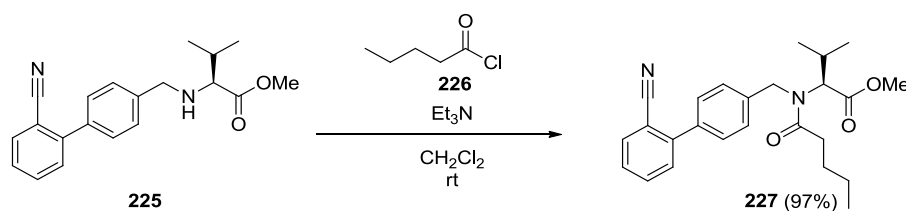
FTIR: ν_{\max} = 2960 (N-H), 2224 (C≡N), 1729 (C=O) cm⁻¹

¹H NMR: (CDCl₃, 400 MHz): δ = 7.75 (dd, 1H, J_1 = 7.8 Hz, J_2 = 1.0 Hz), 7.63 (atd, 1H, J_1 = 7.6 Hz, J_2 = 1.3 Hz), 7.53–7.40 (m, 6H), 3.90 (d, 1H, J = 13.5 Hz), 3.74 (s, 3H), 3.66 (d, 1H, J = 13.4 Hz), 3.07 (d, 1H, J = 6.2 Hz), 1.95 (sept, 1H, J = 6.4 Hz), 1.84 (bs, 1H), 0.97 (at, 6H, J = 6.5 Hz) ppm

¹³C NMR: (CDCl₃, 100 MHz): δ = 175.7 (C_{IV}), 145.4 (C_{IV}), 140.9 (C_{IV}), 136.8 (C_{IV}), 133.8, 132.8, 130.1, 128.7, 128.6, 127.4, 118.8 (C_{IV}), 111.2, 66.8, 52.2, 51.5, 31.8, 19.4, 18.7 ppm

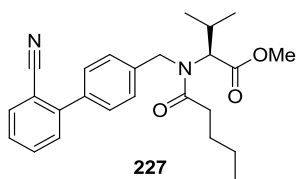
LCMS: t_R = 3.71 min, [M+H]⁺ 323

HRMS: Calculated for C₂₀H₂₂N₂O₂ [M + H]⁺ 323.1754, found 323.1759

V.3.vii Synthesis of *N*-Pentanoyl-*N*-((2'-cyanobiphenyl-4-yl)-methyl)-(L)-valine methyl ester **227**

To a round bottom flask containing *N*-[(2'-Cyanobiphenyl-4-yl)-methyl]-(L)-valine methyl ester **225** (2.4 g, 7.44 mmol) in dichloromethane (72 mL) were added triethylamine (2.59 mL, 18.61 mmol) followed by a slow addition of pentanoyl chloride **226** (2.25 mL, 18.61 mmol) over 5 minutes at 0 °C. The reaction mixture was then stirred for 15 hours at room temperature and 4 hours at 40 °C prior to being washed with a saturated solution of NaHCO_3 . The layers were separated and the organic phase was evaporated under reduced pressure. The crude product was purified by silica gel chromatography eluting with heptane / ethyl acetate to give *N*-Pentanoyl-*N*-((2'-cyanobiphenyl-4-yl)-methyl)-(L)-valine methyl ester **227** (2.92 g, 7.18 mmol, 97 % yield) as a colorless oil.

N-Pentanoyl-*N*-((2'-cyanobiphenyl-4-yl)-methyl)-(L)-valine methyl ester **227** (2.92 g, 97% yield)¹²⁹



Appearance: Colorless oil

MP: N.A.

FTIR: ν_{\max} = 2224 (C≡N), 1737 (C=O), 1650 (C=O) cm^{-1}

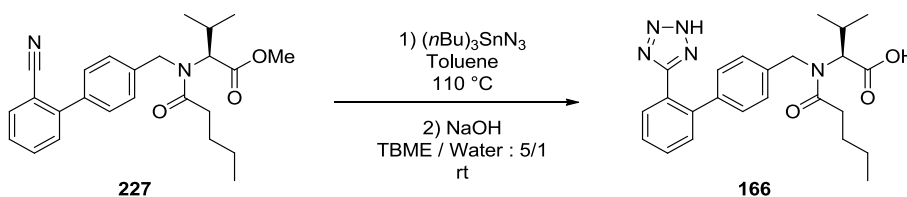
¹H NMR: (DMSO- d_6 , 400 MHz, 80 °C): δ = 7.88 (dd, 1H, J_1 = 7.6 Hz, J_2 = 0.9 Hz), 7.76 (dd, 1H, J_1 = 7.9 Hz, J_2 = 1.5 Hz), 7.62–7.48 (m, 4H), 7.34 (d, 2H, J = 7.6 Hz), 4.81 (d, 1H, J = 16.9 Hz), 4.56 (bs, 2H), 3.43 (s, 3H), 2.50–2.25 (m, 3H), 1.65–1.48 (m, 2H), 1.39–1.21 (m, 2H), 0.97 (ad, 3H, J = 6.6 Hz), 0.86 (d, 6H, J = 6.8 Hz) ppm

¹³C NMR: (DMSO- d_6 , 100 MHz): *mixture of rotamers* δ = 173.4 (C_{IV}), 170.5 (C_{IV}), 170.1 (C_{IV}), 144.4 (C_{IV}), 144.2 (C_{IV}), 138.9 (C_{IV}), 138.5 (C_{IV}), 136.4 (C_{IV}), 136.0 (C_{IV}), 133.8, 133.5, 130.0, 128.7, 128.2, 128.1, 128.0, 127.2, 126.4, 118.6 (C_{IV}), 118.5 (C_{IV}), 110.2 (C_{IV}), 110.1 (C_{IV}), 64.6, 61.8, 51.6, 51.4, 48.1, 44.6, 32.3, 32.2, 27.2, 27.0, 26.9, 21.8, 21.7, 19.8, 19.2, 18.40, 18.1 ppm

LCMS: t_R = 6.40 min, [M+H]⁺ 407

HRMS: Calculated for C₂₅H₃₁N₂O₃ [M + H]⁺ 407.2329, found 407.2338

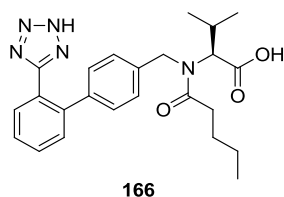
V.3.viii Synthesis of (S)-3-methyl-2-(N-[(2'-(2H-1,2,3,4-tetrazol-5-yl)biphenyl-4-yl)methyl]pentanamido)butanoic acid (Valsartan) **166**



To a round bottom flask containing *N*-Pentanoyl-*N*-[(2'-cyanobiphenyl-4-yl)-methyl]-(*L*)-valine methyl ester **227** (300 mg, 0.74 mmol) under a nitrogen atmosphere at room temperature were introduced toluene (8 mL) followed by tributyltin azide (0.40 mL, 1.48 mmol). The reaction mixture was stirred at reflux (110 °C) for 5 days. The reaction was cooled down to room temperature and distilled water (18 mL) was added to the reaction mixture, followed by an aqueous solution of NaOH (2N, 2 mL) and TBME (10 mL). The mixture was stirred at room temperature overnight and the pH of the aqueous layer was brought to pH = 1 with an aqueous solution of

hydrochloric acid (2M). The layers were separated and the aqueous layer was re-extracted with TBME. Organic layers were combined, dried over anhydrous MgSO_4 and evaporated under reduced pressure to dryness. The resulting gum was dissolved in a minimum amount of ethyl acetate and heptane was added dropwise to the solution under stirring until a precipitate was formed. The slurry was filtered and the solid was dried in a vacuum oven overnight at room temperature to give (S)-3-methyl-2-(N-([2'-(2H-1,2,3,4-tetrazol-5-yl)biphenyl-4-yl]methyl)pentanamido)butanoic acid (Valsartan) **166** (250 mg, 0.57 mmol, 78 % yield) as a white solid.

(S)-3-methyl-2-(N-([2'-(2H-1,2,3,4-tetrazol-5-yl)biphenyl-4-yl]methyl)pentanamido)butanoic acid (Valsartan) **166** (250 mg, 78% yield)¹⁵²



Appearance: White solid

MP: 107 – 114 °C

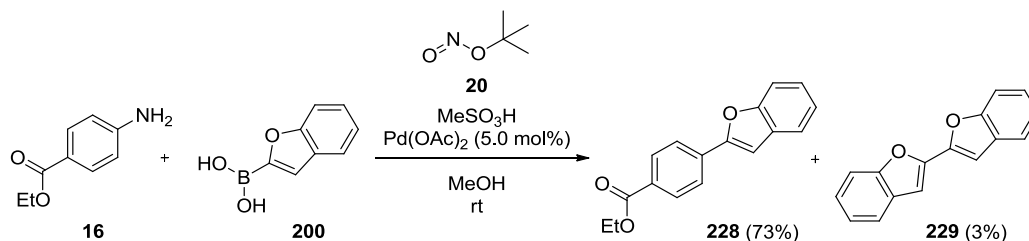
FTIR: ν_{max} = 2962.2 (O-H), 1731.7 (C=O), 1601.4 (C=O) cm^{-1}

¹H NMR: (DMSO- d_6 , 400 MHz, 120 °C): δ = 7.66–7.63 (m, 2H), 7.56–7.49 (m, 2H), 7.21 (d, 2H, J = 8.0 Hz), 7.09 (d, 2H, J = 8.0 Hz), 4.68 (d, 1H, J = 16.7 Hz), 4.54 (d, 1H, J = 16.7 Hz), 4.33 (bd, 1H, J = 9.0 Hz), 2.36–2.23 (m, 3H), 1.58–1.52 (m, 2H), 1.31 (q, 2H, J = 7.3 Hz), 1.00 (ad, 3H, J = 6.3 Hz), 0.88–0.81 (m, 6H) ppm

¹³C NMR: (DMSO- d_6 , 100 MHz): mixture of rotamers δ = 173.4 (C_{IV}), 171.9 (C_{IV}), 171.6 (C_{IV}), 155.0 (C_{IV}), 141.3 (C_{IV}), 141.2 (C_{IV}), 138.2 (C_{IV}), 137.8 (C_{IV}), 137.7 (C_{IV}), 137.1 (C_{IV}), 131.0, 130.5, 128.8, 128.3, 127.7, 127.5, 126.9, 126.2, 123.6 (C_{IV}), 123.5 (C_{IV}), 65.7, 62.9, 48.5, 45.7, 32.5, 32.4, 27.6, 27.5, 27.0, 26.8, 21.8, 21.6, 20.1, 19.4, 18.9, 18.5, 13.8, 13.7 ppm

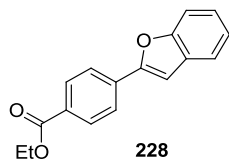
LCMS: t_R = 5.15 min, [M+H]⁺ 436

HRMS: Calculated for C₂₄H₂₉N₅O₃ [M + H]⁺ 436.2343, found 436.2345

V.3.ix One-pot synthesis of ethyl 4-(benzofuran-2'-yl) benzoate **228**

To a round bottom flask containing a stir bar, benzocaine **16** (250 mg, 1.513 mmol), palladium(II) acetate (17 mg, 0.076 mmol) and benzofuran-2-boronic acid **200** (245 mg, 1.513 mmol) under nitrogen were added methanol (12.5 mL) followed by methanesulfonic acid (0.108 mL, 1.665 mmol) and *tert*-butyl nitrite **20** (240 μ L, 1.816 mmol). The reaction mixture was stirred for 2 hours at room temperature and was evaporated under reduced pressure. The crude product was purified by silica gel chromatography eluting with heptane / ethyl acetate to give ethyl 4-(benzofuran-2'-yl) benzoate **228** (295 mg, 1.108 mmol, 73 % yield) as a white solid and 2,2'-bibenzofuran **229** (10 mg, 0.043 mmol, 3 % yield) also as a white solid.

4-(benzofuran-2'-yl) benzoate **228** (295 mg, 73% yield)



Appearance: White solid

MP: 117 – 119 °C

FTIR: ν_{\max} = 1705 (C=O) cm^{-1}

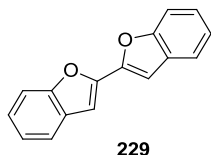
^1H NMR: (CDCl_3 , 400 MHz): δ = 8.12 (d, 2H, J = 8.6 Hz), 7.92 (d, 2H, J = 8.3 Hz), 7.61 (d, 1H, J = 7.6 Hz), 7.54 (d, 1H, J = 8.1 Hz), 7.32 (at, 1H, J = 7.2 Hz), 7.25 (at, 1H, J = 7.1 Hz), 7.15 (s, 1H), 4.41 (q, 2H, J = 7.1 Hz), 1.42 (t, 3H, J = 7.2 Hz) ppm

^{13}C NMR: (CDCl_3 , 100 MHz): δ = 166.2 (C_{IV}), 155.2 (C_{IV}), 154.7 (C_{IV}), 134.4 (C_{IV}), 130.1, 129.9 (C_{IV}), 129.0 (C_{IV}), 125.0, 124.6, 123.2, 121.3, 111.4, 103.4, 61.1, 14.4 ppm

LCMS: t_{R} = 6.76 min, $[\text{M}+\text{H}]^+$ 267

HRMS: Calculated for $\text{C}_{17}\text{H}_{15}\text{O}_3$ $[\text{M} + \text{H}]^+$ 267.1016, found 267.1025

2,2'-bibenzofuran **229** (10 mg, 3% yield)



Appearance: white solid

MP: 198 – 199 °C

FTIR: No characteristic bands were observed for this compound

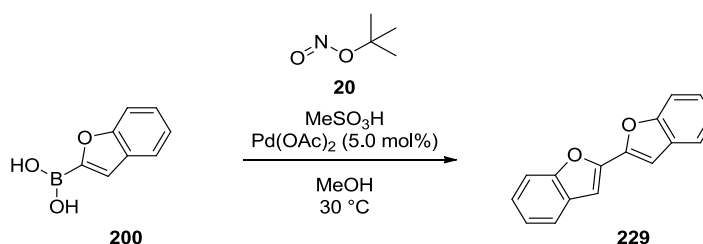
¹H NMR: (DMSO-d₆, 400 MHz): δ = 7.76 (d, 2H, *J* = 7.1 Hz), 7.71 (d, 2H, *J* = 8.3 Hz), 7.46 (s, 2H), 7.42 (atd, 2H, *J*₁ = 7.3 Hz, *J*₂ = 1.4 Hz), 7.35 (atd, 2H, *J*₁ = 7.5 Hz, *J*₂ = 0.6 Hz) ppm

¹³C NMR: (DMSO-d₆, 100 MHz): δ = 154.5 (C_{IV}), 146.7 (C_{IV}), 128.0 (C_{IV}), 125.6, 123.7, 121.7, 111.3, 104.2 ppm

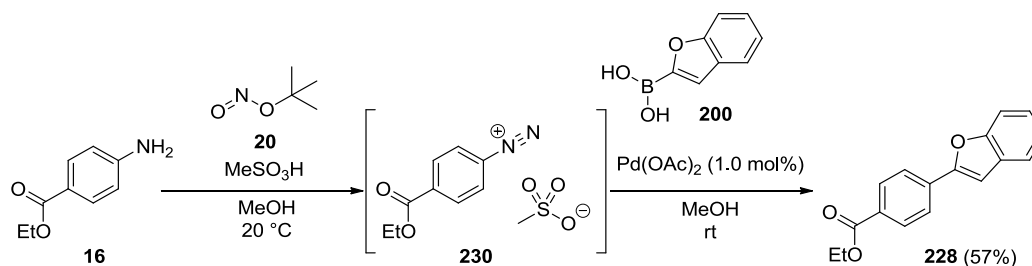
LCMS: t_R = 6.87 min, [M+H⁺] unavailable

HRMS: calculated for C₁₆H₁₁O₂ [M + H]⁺ 235.0754, found 235.0752

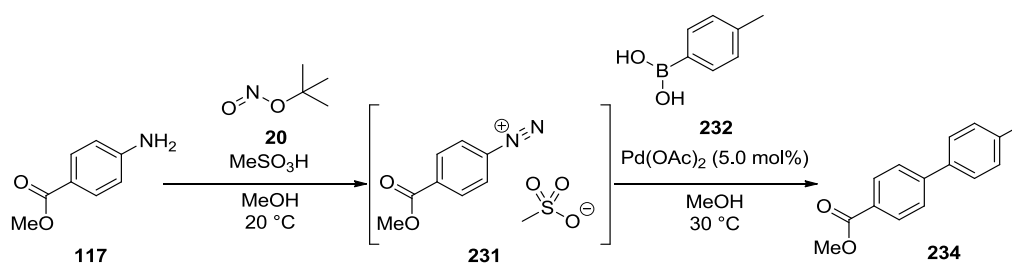
V.3.x Control reactions for oxidative coupling



To a glass tube containing a stirr bar, benzofuran-2-boronic acid **200** (300 mg, 1.852 mmol) under a nitrogen atmosphere were added methanol (16.5 mL), followed by the required components [methanesulfonic acid (0.132 mL, 2.038 mmol, *tert*-butyl nitrite **20** (0.294 mL, 2.223 mmol) and palladium(II) acetate (21 mg, 0.093 mmol)]. The reaction was stirred at 30°C for 2 hours and was analysed by LC/MS. When isolation of 2,2'-bibenzofuran **229** was required, the reaction mixture was evaporated to dryness under reduced pressure and the crude product was purified by silica gel chromatography eluting with heptane to give 2,2'-bibenzofuran **229** as a white solid.

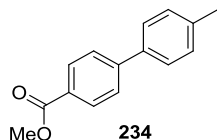
V.3.xi Sequential diazotisation / cross-coupling reaction

To a glass tube containing a stir bar and benzocaine **16** (250 mg, 1.513 mmol) under nitrogen were added methanol (12.5 mL) followed by methanesulfonic acid (0.108 mL, 1.665 mmol) and *tert*-butyl nitrite **20** (0.240 mL, 1.816 mmol). The mixture was stirred for 30 minutes at 0 °C and benzofuran-2-boronic acid **200** (245 mg, 1.513 mmol) followed by palladium(II) acetate (17 mg, 0.076 mmol) were added to the mixture. The solvent was then evaporated under reduced pressure and the crude product was purified by silica gel chromatography eluting with heptane / ethyl acetate to give 4-(benzofuran-2'-yl) benzoate **228** (228 mg, 0.856 mmol, 57 % yield) as a white solid.

V.3.xii Sequential diazotisation / cross-coupling reaction

To a round bottom flask containing a stirrer bar and methyl 4-aminobenzoate **117** (334 mg, 2.207 mmol) under a nitrogen atmosphere were added methanol (16.5 mL), followed by methanesulfonic acid (158 μ L, 2.427 mmol) and *tert*-butyl nitrite **20** (350 μ L, 2.650 mmol). The reaction was stirred at room temperature for 30 minutes and 4-tolyl boronic acid **232** (300 mg, 2.207 mmol) was added to the mixture, followed by palladium(II) acetate (25 mg, 0.110 mmol). The resulting mixture was then stirred for 24 hours at 30 °C and monitored by LC/MS. The reaction was then evaporated to dryness under reduced pressure and the crude product was purified by silica gel chromatography eluting with heptane / ethyl acetate to give methyl 4-methylbiphenyl-4'-carboxylate **234** (203 mg, 0.897 mmol, 41 % yield) as a white solid.

Methyl 4-methylbiphenyl-4'-carboxylate **234** (203 mg, 41% yield)



Appearance: White solid

MP: 119 – 121 °C

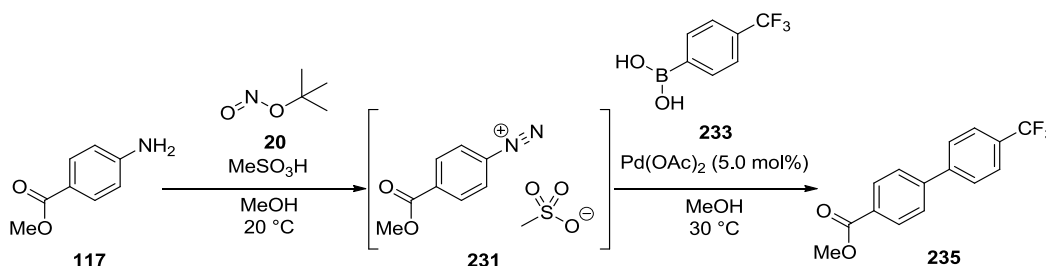
FTIR: ν_{\max} = 1713 (C=O) cm^{-1}

^1H NMR: (DMSO- d_6 , 400 MHz): δ = 8.02 (d, 2H, J = 8.5 Hz), 7.81 (d, 2H, J = 8.6 Hz), 7.65 (d, 2H, J = 8.1 Hz), 7.31 (d, 2H, J = 8.0 Hz), 3.87 (s, 1H), 2.36 (s, 1H) ppm

^{13}C NMR: (DMSO- d_6 , 100 MHz): δ = 166.1 (C_{IV}), 144.6 (C_{IV}), 137.9 (C_{IV}), 135.9 (C_{IV}), 129.8, 129.7, 128.1 (C_{IV}), 126.8, 126.6, 52.1, 20.7 ppm

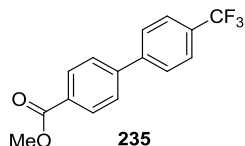
LCMS: t_{R} = 6.24 min, $[\text{M} + \text{H}]^+$ 227

HRMS: Calculated for $\text{C}_{15}\text{H}_{15}\text{O}_2$ $[\text{M} + \text{H}]^+$ 227.1067, found 227.1061



To a round bottom flask containing a stirrer bar and methyl 4-aminobenzoate **117** (239 mg, 1.580 mmol) under a nitrogen atmosphere were added methanol (16.5 mL), followed by methanesulfonic acid (113 μL , 1.738 mmol) and *tert*-butyl nitrite **20** (250 μL , 1.895 mmol). The reaction was stirred at room temperature for 30 minutes and 4-trifluoromethylphenyl boronic acid **233** (300 mg, 1.580 mmol) was added to the mixture, followed by palladium(II) acetate (18 mg, 0.079 mmol). The resulting mixture was then stirred for 24 hours at 30°C and monitored by LC/MS. The reaction was then evaporated to dryness under reduced pressure and the crude product was purified by silica gel chromatography eluting with heptane / ethyl acetate to give methyl 4-trifluoromethylbiphenyl-4'-carboxylate **235** (74 mg, 0.264 mmol, 17%) as a white solid.

Methyl 4-(trifluoromethyl)phenyl-4'-carboxylate **235** (74 mg, 17% yield)



Appearance: White solid

MP: 124 – 126 °C

FTIR: ν_{\max} = 1711 (C=O) cm^{-1}

^1H NMR: (CDCl_3 , 400 MHz): δ = 8.15 (d, 2H, J = 8.3 Hz), 7.73 (s, 4H), 7.68 (d, 2H, J = 8.3 Hz), 3.97 (s, 3H) ppm

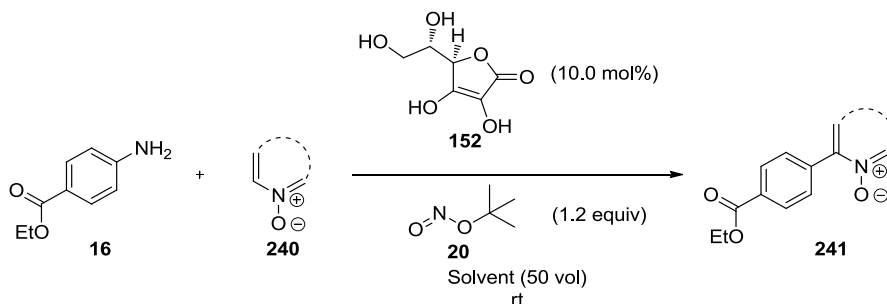
^{13}C NMR: (CDCl_3 , 100 MHz): δ = 166.7 (C_{IV}), 144.0 (C_{IV}), 143.5 (C_{IV}), 130.2, 130.1 (q, J = 32.5 Hz), 129.80 (C_{IV}), 127.6, 127.2, 125.8 (q, J = 3.6 Hz), 124.1 (q, J = 272.0 Hz), 52.2 ppm

LCMS: t_{R} = 6.47 min, $[\text{M}+\text{H}^+]$ unavailable

HRMS: Calculated for $\text{C}_{15}\text{H}_{12}\text{F}_3\text{O}_2$ $[\text{M} + \text{H}]^+$ 281.0784, found 281.0789

V.4 Radical arylation of heterocycles

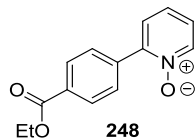
V.4.i General procedure for the screening of *N*-oxide heterocycles and solvents



To a round bottom flask containing benzocaine **16** (250 mg, 1.51 mmol), *N*-oxide heterocycle **240** (3.03 mmol) and L-ascorbic acid **152** (27 mg, 0.151 mmol) under a nitrogen atmosphere was added previously degassed solvent (12.5 mL), followed by *tert*-butyl nitrite **20** (240 μL , 1.816 mmol) and the reaction mixture was stirred for 17 hours at 20 °C. After this time the reaction mixture was then evaporated to dryness under reduced pressure and the crude product was purified by silica gel chromatography eluting with either heptane/ethyl acetate or $\text{CH}_2\text{Cl}_2/\text{MeOH}$ mixtures to yield the target compound.

2-(4'-(Ethoxycarbonyl)phenyl)-pyridine-N-oxide 248 (81 mg, 22% yield)

248 was prepared according to the general procedure of screening of *N*-oxide heterocycles in acetonitrile and purified by MDAP.



Appearance: Orange solid

MP: 119–120 °C

FTIR: ν_{\max} = 1708 (C=O) cm^{-1}

¹H NMR: (DMSO-*d*₆, 400 MHz): δ = 8.39-8.38 (m, 1H), 8.07 (d, 2H, *J* = 8.6 Hz), 8.00 (d, 2H, *J* = 8.6 Hz), 7.72-7.67 (m, 1H), 7.45-7.48 (m, 2H), 4.37 (q, 2H, *J* = 7.1 Hz), 1.36 (t, 3H, *J* = 7.1 Hz) ppm

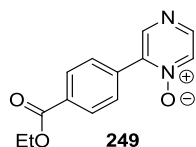
¹³C NMR: (DMSO-*d*₆, 100 MHz): δ = 165.3 (C_{IV}), 146.6 (C_{IV}), 140.2, 137.2 (C_{IV}), 130.2 (C_{IV}), 129.6, 128.7, 127.7, 126.1, 125.5, 60.9, 14.1 ppm

LCMS: t_R = 3.56 min, [M+H⁺] 244

HRMS: Calculated for C₁₄H₁₄NO₃ [M + H]⁺ 244.0968, found 244.0960

2-(4'-(Ethoxycarbonyl)phenyl)-pyrazine-N-oxide 249 (69 mg, 19% yield)

249 was prepared according to the general procedure of screening of *N*-oxide heterocycles in acetonitrile.



Appearance: beige solid

MP: 154–159 °C

FTIR: ν_{\max} = 1712 (C=O) cm^{-1}

¹H NMR: (DMSO-*d*₆, 400 MHz): δ = 8.83 (s, 1H), 8.55 (d, 1H, *J* = 4.1 Hz), 8.48 (d, 1H, *J* = 4.1 Hz), 8.08 (d, 2H, *J* = 8.5 Hz), 8.01 (d, 2H, *J* = 8.5 Hz), 4.36 (q, 2H, *J* = 7.1 Hz), 1.35 (t, 3H, *J* = 7.1 Hz) ppm

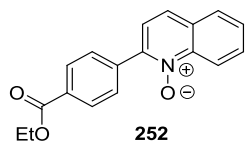
¹³C NMR: (DMSO-*d*₆, 100 MHz): δ = 165.2 (C_{IV}), 148.4, 146.9, 142.5 (C_{IV}), 134.5, 133.7 (C_{IV}), 130.9 (C_{IV}), 129.7, 128.9, 61.0, 14.1 ppm

LCMS: t_R = 3.63 min, [M+H⁺] 245

HRMS: Calculated for C₁₃H₁₃N₂O₃ [M + H]⁺ 245.0921, found 245.0924

2-(4'-(Ethoxycarbonyl)phenyl)quinoline-N-oxide 252 (264 mg, 60% yield)

252 was prepared according to the general procedure of screening of *N*-oxide heterocycles and solvents.



Appearance: Pale pink solid

MP: 196–200 °C

FTIR: ν_{\max} = 1711 (C=O) cm^{-1}

^1H NMR: (DMSO- d_6 , 400 MHz): δ = 8.67 (d, 1H, J = 8.8 Hz), 8.19 (d, 2H, J = 8.6 Hz), 8.15 (d, 1H, J = 8.6 Hz), 8.12 (d, 2H, J = 8.6 Hz), 8.05 (d, 1H, J = 8.6 Hz), 7.90 (dd, 1H, J_1 = 8.8 Hz, J_2 = 1.5 Hz), 7.81-7.78 (m, 2H), 4.39 (q, 2H, J = 7.1 Hz), 1.38 (t, 3H, J = 7.1 Hz) ppm

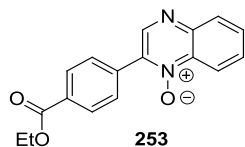
^{13}C NMR: (DMSO- d_6 , 100 MHz): δ = 165.3 (C_{IV}), 142.8 (C_{IV}), 141.5 (C_{IV}), 137.8 (C_{IV}), 130.8, 130.3 (C_{IV}), 129.9, 129.7 (C_{IV}), 128.9, 128.7, 128.6, 124.9, 123.4, 119.4, 61.0, 14.2 ppm

LCMS: t_{R} = 4.61 min, $[\text{M}+\text{H}^+]$ 294

HRMS: Calculated for $\text{C}_{18}\text{H}_{16}\text{NO}_3$ $[\text{M} + \text{H}]^+$ 294.1125, found 294.1127

2-(4'-(Ethoxycarbonyl)phenyl)-quinoline-N-oxide **253** (317 mg, 71% yield)

253 was prepared according to the general procedure of screening of *N*-oxide heterocycles and solvents.



Appearance: Beige solid

MP: 212–215 °C

FTIR: ν_{\max} = 1515 (C=O) cm^{-1}

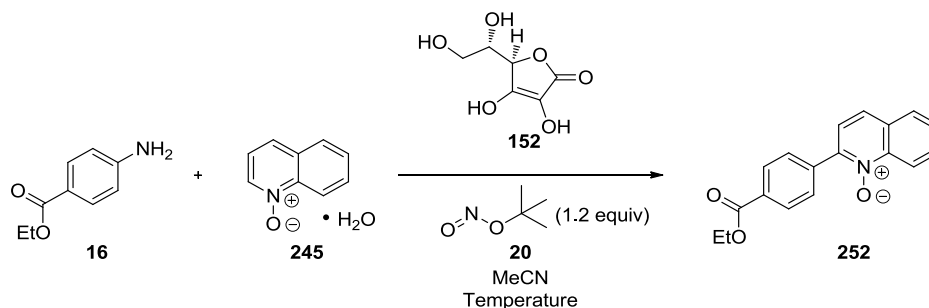
$^1\text{H NMR}$: (CDCl_3 , 400 MHz): δ = 8.93 (s, 1H), 8.70 (dd, 1H, J_1 = 8.3 Hz, J_2 = 1.2 Hz), 8.24 (d, 2H, J = 8.5 Hz), 8.18 (dd, 1H, J_1 = 8.5 Hz, J_2 = 1.4 Hz), 8.09 (d, 2H, J = 8.5 Hz), 7.89-7.80 (m, 2H), 4.45 (q, 2H, J = 7.2 Hz), 1.44 (t, 3H, J = 7.2 Hz) ppm

$^{13}\text{C NMR}$: (CDCl_3 , 100 MHz): δ = 165.9 (C_{IV}), 147.0, 144.6 (C_{IV}), 138.6 (C_{IV}), 137.6 (C_{IV}), 134.1 (C_{IV}), 132.0 (C_{IV}), 131.6, 130.7, 130.0, 129.8, 129.4, 119.4, 61.4, 14.4 ppm

LCMS: t_{R} = 4.90 min, $[\text{M}+\text{H}^+]$ 295

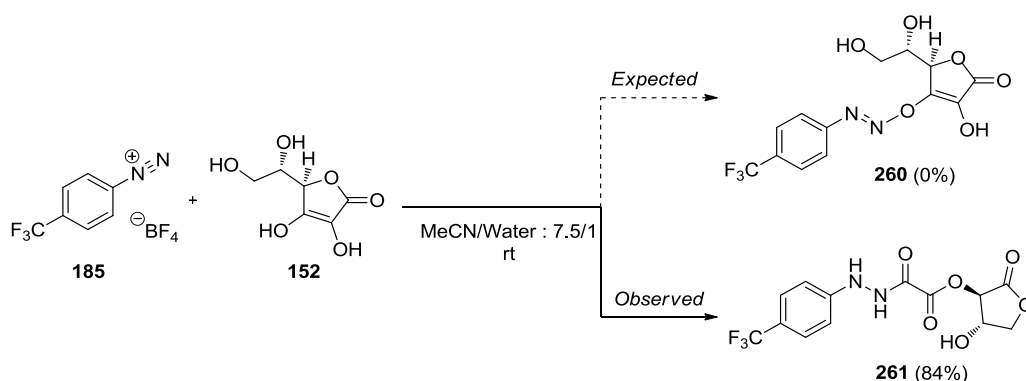
HRMS: Calculated for $\text{C}_{17}\text{H}_{15}\text{N}_2\text{O}_3$ $[\text{M} + \text{H}]^+$ 295.1077, found 295.1076

V.4.ii Design of Experiments Reactions



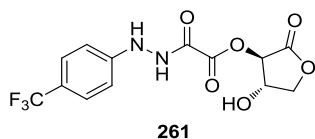
To a round bottom flask containing benzocaine **16** (250 mg, 1.513 mmol), quinoline *N*-oxide hydrate **245** (80% w/w) (Factor B) and L-ascorbic acid **152** (Factor A) under a nitrogen atmosphere was added degassed acetonitrile (Factor C), followed by *tert*-butyl nitrite **20** (240 μL , 1.816 mmol) and the reaction mixture was stirred for 17 hours at the indicated temperature (Factor D). The reaction mixture was then diluted in a 50 mL volumetric flask with ethyl acetate to dissolve the solids and the solution was analysed by HPLC to determine a solution yield according to the calibration curve established in Appendix 3.

V.4.iii Synthesis of (3R,4S)-4-hydroxy-2-oxotetrahydrofuran-3-yl-2-(2-(4'-(trifluoromethyl)phenyl)hydrazinyl)-2-oxoacetate **261**



L-ascorbic acid **152** (346 mg, 1.96 mmol) was added to a round bottom flask containing 4-(trifluoromethyl)-benzenediazonium tetrafluoroborate (510 mg, 1.96 mmol) dissolved in a mixture of acetonitrile (1 mL) and water (7.5 mL) and the resulting mixture was stirred at room temperature for 30 minutes. A precipitate was formed and was filtered off the reaction mixture to give the ascorbic acid / diazonium adduct **261** as a white solid (575 mg, 1.65 mmol, 84% yield). The solid was crystallised by diffusion of chloroform into a saturated solution of the compound in acetone and the crystals were sent to the National Crystallography Service for X-Ray analysis.

(3R,4S)-4-hydroxy-2-oxotetrahydrofuran-3-yl-2-(2-(4'-trifluoromethyl)phenyl)hydrazinyl)-2-oxoacetate **261** (575 mg, 84% yield)



Appearance: White solid

MP: 195–200 °C

FTIR: ν_{\max} = 3483 (O-H), 3362 (N-H), 3229 (N-H), 1781 (C=O), 1760 (C=O), 1694 (C=O) cm^{-1}

^1H NMR: (DMSO- d_6 , 400 MHz): δ = 11.13 (s, 1H), 8.67 (s, 1H), 7.51 (d, 2H, J = 8.5 Hz), 6.86 (d, 2H, J = 8.5 Hz), 6.17 (bs, 1H), 5.70 (d, 1H, J = 7.8 Hz), 4.71 (aq, 1H, J = 7.6 Hz), 4.52 (at, 1H, J = 8.0 Hz), 4.08 (at, 1H, J = 8.3 Hz) ppm

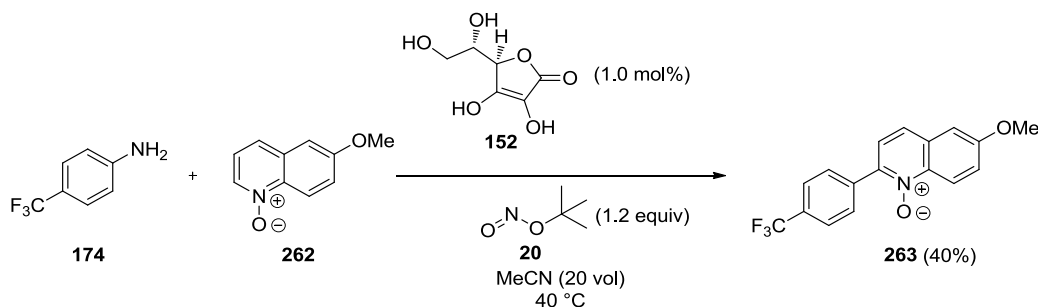
^{13}C NMR: (DMSO- d_6 , 100 MHz): δ = 170.2 (C_{IV}), 158.6 (C_{IV}), 155.9 (C_{IV}), 155.2 (C_{IV}), 126.4, 126.3, 124.9 (C_{IV} , q, J = 270.3 Hz), 118.9 (C_{IV} , q, J = 31.8 Hz), 111.7 (at, J = 29.5 Hz), 76.0, 69.4 ppm

LCMS: t_{R} = 4.03 min, $[\text{M}+\text{H}^+]$ 349

HRMS: Calculated for $\text{C}_{13}\text{H}_{12}\text{F}_3\text{N}_2\text{O}_6$ $[\text{M} + \text{H}]^+$ 349.0642, found 349.0653

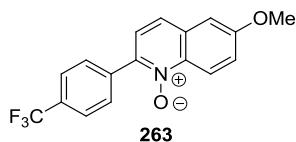
X-ray: Appendix 4

V.4.iv Procedure for IR and LC/MS monitoring experiment



To a 400 mL EasyMax 402 (Mettler Toledo) reactor fitted with a ReactIR probe (Mettler Toledo) under a nitrogen atmosphere was charged L-ascorbic acid **152** (6 mg, 0.31 mmol) diluted in previously degassed acetonitrile (100 mL), followed by 6-methoxy-quinoline *N*-oxide **262** (10.87 g, 62.1 mmol) and 4-trifluoromethyl-aniline **174** (3.91 mL, 31.0 mmol). The resulting mixture was stirred at 40 °C and monitored by IR and LC/MS for 21 hours. 6-methoxy-2-(4'-trifluoromethylphenyl)-quinoline *N*-oxide **263** precipitated spontaneously during the course of the reaction and was isolated by filtration to give a beige solid (3.92 g, 12.3 mmol, 40% yield).

6-methoxy-2-(4'-trifluoromethyl-phenyl)-quinoline N-oxide 263 (3.92 g, 40% yield)



Appearance: Beige solid

MP: 218–223 °C

FTIR: ν_{\max} = No characteristic bands were observed for this compound

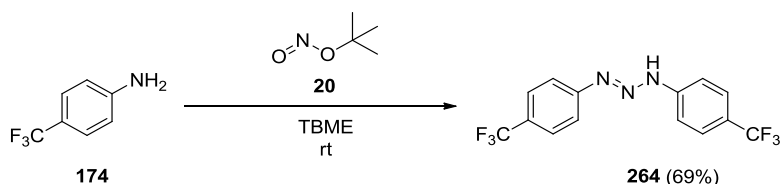
¹H NMR: (CDCl₃, 400 MHz): δ = 8.75 (d, 1H, J = 9.5 Hz), 8.09 (d, 2H, J = 8.4 Hz), 7.77 (d, 2H, J = 8.3 Hz), 7.69 (d, 1H, J = 8.6 Hz), 7.46 (d, 1H, J = 8.6 Hz), 7.43 (dd, 1H, J_1 = 9.6 Hz, J_2 = 2.7 Hz), 7.14 (d, 1H, J = 2.4 Hz), 3.98 (s, 3H) ppm

¹³C NMR: (CDCl₃, 100 MHz): δ = 159.6 (C_{IV}), 141.8, 137.80, 137.1, 131.3, 131.0 (q, J = 32.6 Hz), 130.0, 125.2 (q, J = 3.8 Hz), 124.5, 124.0 (q, J = 272.2 Hz), 123.40, 122.9, 122.0, 105.9, 55.8 ppm

LCMS: t_R = 5.28 min, [M+H]⁺ 320

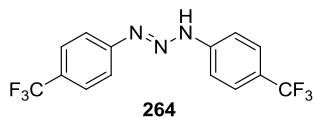
HRMS: Calculated for C₁₇H₁₃F₃NO₂ [M + H]⁺ 320.0893, found 320.0895

V.4.v Synthesis of 1,3 bis(4'-trifluoromethyl-phenyl)-triazene 264



To a round bottom flask containing a stirr bar and 4-trifluoromethyl-aniline **174** (0.195 mL, 1.552 mmol) in TBME (5 mL) was added *tert*-butyl nitrite **20** (0.123 mL, 0.931 mmol) and the resulting mixture was stirred for 2 hours at room temperature. The solvent was then removed under reduced pressure and the resulting solid was triturated in heptane. Filtration of the slurry afforded 1,3 bis(4'-trifluoromethyl-phenyl)-triazene **264** (178 mg, 0.534 mmol, 69 % yield) as an orange solid.

1,3-bis-(4' trifluoromethyl-phenyl)-triazene **264** (178 mg, 69% yield)¹⁵³



Appearance: Orange solid

MP: 114–116 °C

FTIR: ν_{max} = 3185 (N-H), 1614 (N-H), 1317 (C-F or C-N), 1152 (C-F or C-N), 1101 (C-F or C-N), 1063 (C-F or C-N) cm^{-1}

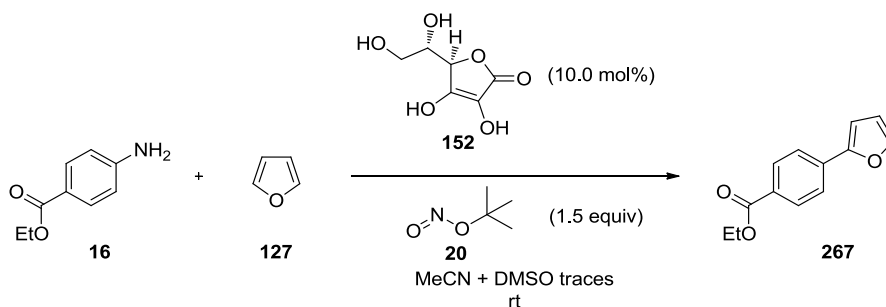
¹H NMR: (DMSO- d_6 , 400 MHz): δ = 13.07 (bs, 1H), 7.78-7.60 (m, 8H) ppm

¹³C NMR: Unavailable due to the fast proton exchange between the two nitrogens, leading to an inconsistent spectrum

LCMS: t_R = 6.91 min, $[M+H]^+$ 334

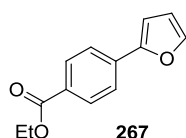
HRMS: Calculated for $C_{14}H_{10}F_6N_3$ $[M + H]^+$ 334.0773, found 334.0773

V.4.vi Control reactions – synthesis of ethyl 4-(furan-2'-yl)-benzoate **267**



To a glass tube containing benzocaine **16** (83 mg, 0.5 mmol) under a nitrogen atmosphere was added previously degassed acetonitrile (5 mL), followed by furan **127** (0.36 mL, 5.00 mmol), *tert*-butyl nitrite **20** (0.1 mL, 0.750 mmol) and a previously prepared solution of DMSO (0.1 mL) with or without L-ascorbic acid **152** (0.88 mg, 5.0 μmol). The resulting mixture was stirred for 14 hours at room temperature and was evaporated to dryness under reduced pressure. The crude product was then purified by silica gel chromatography eluting with heptane / ethyl acetate to give ethyl 4-(furan-2'-yl)-benzoate **267** (56 mg, 0.26 mmol, 52% yield with L-ascorbic acid **152**, 57 mg, 0.27 mmol, 53% yield without L-ascorbic acid **152**) as a white solid.

Ethyl 4-(furan-2'-yl)-benzoate **267** (56 mg, 52% yield with L-ascorbic acid **152**; 57 mg, 53% yield without L-ascorbic acid **152**)



Appearance: White solid

MP: 57–60 °C

FTIR: ν_{\max} = 1696 (C=O) cm^{-1}

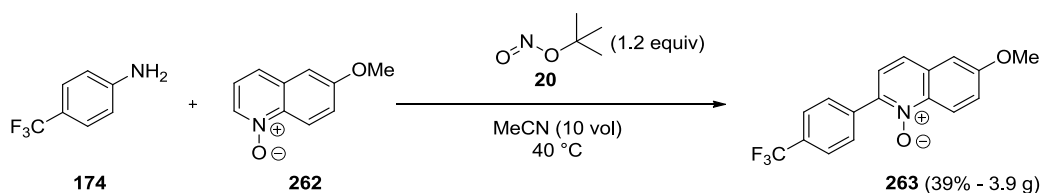
^1H NMR: (CDCl_3 , 400 MHz): δ = 8.07 (d, 2H, J = 8.6 Hz), 7.73 (d, 2H, J = 8.4 Hz), 7.53 (d, 1H, J = 1.3 Hz), 6.80 (d, 1H, J = 3.4 Hz), 6.52 (dd, 1H, J_1 = 3.5 Hz, J_2 = 1.7 Hz), 4.40 (q, 2H, J = 7.1 Hz), 1.42 (t, 3H, J = 7.1 Hz) ppm

^{13}C NMR: (CDCl_3 , 100 MHz): δ = 166.4 (C_{IV}), 153.0 (C_{IV}), 143.1, 134.7 (C_{IV}), 130.1, 129.0 (C_{IV}), 123.4, 112.0, 107.2, 61.0, 14.4 ppm

LCMS: t_{R} = 5.80 min, $[\text{M} + \text{H}]^+$ 217

HRMS: Calculated for $\text{C}_{13}\text{H}_{13}\text{O}_3$ $[\text{M} + \text{H}]^+$ 217.0859, found 217.0852

V.4.vii Scale-up and calorimetry study



To a 100 mL Reaction Calorimetry 1 (RC 1, Mettler Toledo) reactor under a nitrogen atmosphere was charged 6-methoxyquinoline *N*-oxide **262** (10.87 g, 62.1 mmol), followed by previously degassed acetonitrile (50 mL). The solution was then stirred at 40°C and a first calibration was performed ($\text{Cp} = 2221 \text{ J}/[\text{Kg.K}]$).

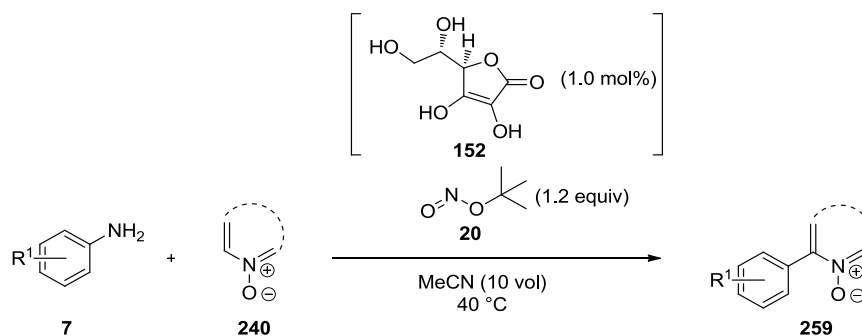
Aniline addition: 4-trifluoromethyl-aniline **174** (3.91 mL, 31.0 mmol) was added dropwise with a syringe pump over 10 minutes to the previous solution at 40°C and a second calibration was performed ($\text{Cp} = 1948 \text{ J}/[\text{Kg.K}]$). The RC 1 instrument indicated a total heat output of 0.33 kJ and a predicted adiabatic temperature rise of 3 °C. No gas output was observed during the addition of the 4-trifluoromethyl-aniline **174**.

tert-Butyl nitrite addition: *tert*-butyl nitrite **20** (4.92 mL, 37.2 mmol) was then added dropwise with a syringe pump over 10 minutes to the previous reaction mixture under nitrogen at 40°C and a third calibration was performed ($\text{Cp} = 2170 \text{ J}/[\text{Kg.K}]$)

after 19 hours. The RC 1 instrument indicated a total heat output of 10.4 kJ and a predicted adiabatic temperature rise of 81°C.

Work-up / isolation: The slurry was then stirred for 17 hours at 40°C under nitrogen before being cooled down to 20 °C. 6-methoxy-2-(4'-(trifluoromethyl)phenyl)-quinoline *N*-oxide **263** precipitated spontaneously during the course of the reaction and was isolated by filtration to give a beige solid (3.88 g, 12.15 mmol, 39% yield).

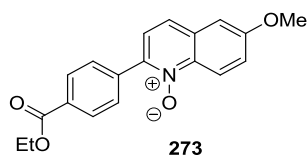
V.4.viii General procedure for the C-H arylation of *N*-oxide heterocycles



To a glass tube containing the aniline **7** (1.0 equiv), the *N*-oxide heterocycle **240** (2.0 equiv) [L-ascorbic acid **152** (1.0 mol%) when required] under a nitrogen atmosphere was added degassed acetonitrile (10 vol), followed by *tert*-butyl nitrite **20** (1.2 equiv) and the reaction mixture was stirred for 17 hours at 40 °C. The reaction mixture was then evaporated to dryness and the crude product was purified by silica gel chromatography eluting with either heptane / ethyl acetate or CH₂Cl₂ / MeOH mixtures to yield the target compound.

2-(4'-(Ethoxycarbonyl)phenyl)-6-methoxy-quinoline N-oxide 273 (252 mg, 52% yield without L-ascorbic acid **152**; 244 mg, 50% yield with L-ascorbic acid **152**)

273 was prepared according to the general procedure for the C-H arylation of N-oxide heterocycles.



Appearance: Beige solid

MP: 201–204 °C

FTIR: $\nu_{\text{max}} = 1714$ (C=O) cm^{-1}

^1H NMR: (CDCl_3 , 400 MHz): $\delta = 8.76$ (d, 1H, $J = 9.5$ Hz), 8.18 (d, 2H, $J = 8.4$ Hz), 8.05 (d, 2H, $J = 8.5$ Hz), 7.68 (d, 1H, $J = 8.5$ Hz), 7.48 (d, 1H, $J = 8.8$ Hz), 7.42 (dd, 1H, $J_1 = 9.6$ Hz, $J_2 = 2.7$ Hz), 7.14 (d, 1H, $J = 2.5$ Hz), 4.43 (q, 2H, $J = 7.1$ Hz), 3.97 (s, 3H), 1.43 (t, 3H, $J = 7.1$ Hz) ppm

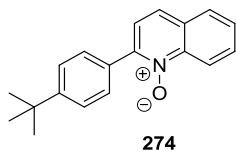
^{13}C NMR: (CDCl_3 , 100 MHz): $\delta = 166.2$ (C_{IV}), 159.6 (C_{IV}), 142.4 (C_{IV}), 137.9 (C_{IV}), 137.8 (C_{IV}), 131.3 (C_{IV}), 131.0 (C_{IV}), 129.6, 129.4, 124.6, 123.6, 122.9, 122.1, 106.0, 61.2, 55.8, 14.3

LCMS: $t_{\text{R}} = 4.84$ min, $[\text{M} + \text{H}]^+ 324$

HRMS: Calculated for $\text{C}_{19}\text{H}_{18}\text{NO}_4$ $[\text{M} + \text{H}]^+ 324.1232$, found 324.1230

2-(4'-(tert-Butyl)phenyl)-quinoline N-oxide 274 (255 mg, 55% yield without L-ascorbic acid **152**; 238 mg, 51% yield with L-ascorbic acid **152**)

274 was prepared according to the general procedure for the C-H arylation of N-oxide heterocycles.



Appearance: red solid

MP: 156–160 °C

FTIR: No characteristic bands were observed for this compound

¹H NMR: (CDCl₃, 400 MHz): δ = 8.86 (d, 1H, *J* = 8.5 Hz), 7.95 Hz (d, 2H, *J* = 8.1 Hz), 7.84 (d, 1H, *J* = 8.1 Hz), 7.77-7.75 (m, 1H), 7.72 (d, 1H, *J* = 8.8 Hz), 7.62-7.59 (m, 1H), 7.55-7.50 (m, 3H), 1.37 (s, 9H) ppm

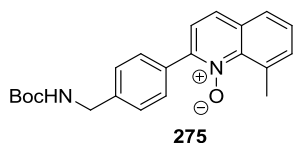
¹³C NMR: (CDCl₃, 100 MHz): δ = 152.8 (C_{IV}), 145.1 (C_{IV}), 142.3 (C_{IV}), 130.5, 129.5, 129.4, 128.3, 128.0, 125.4, 125.3, 125.3, 123.3, 120.3, 34.9 (C_{IV}), 31.3 ppm

LCMS: t_R = 5.51 min, [M + H]⁺ 278

HRMS: calculated for C₁₉H₂₀NO [M + H]⁺ 278.1539, found 278.1544

2-(4'-[(N-Boc)aminomethyl]phenyl)-8-methyl-quinoline N-oxide 275 (107 mg, 44% yield without L-ascorbic acid **152**; 236 mg, 58% yield with L-ascorbic acid **152**)

275 was prepared according to the general procedure for the C-H arylation of N-oxide heterocycles.



Appearance: Orange solid

MP: 119–123 °C

FTIR: ν_{\max} = 3320 (N-H), 1704 (C=O) cm^{-1}

$^1\text{H NMR}$: (CDCl_3 , 400 MHz): δ = 7.83 (d, 2H, J = 8.2 Hz), 7.65 (d, 2H, J = 9.0 Hz), 7.44-7.41 (m, 4H), 7.37 (d, 1H, J = 8.6 Hz), 4.91 (bs, 1H), 4.38 (d, 2H, J = 5.7 Hz), 3.20 (s, 3H), 1.47 (s, 9H) ppm

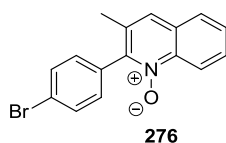
$^{13}\text{C NMR}$: (CDCl_3 , 100 MHz): δ = 155.9 (C_{IV}), 146.1 (C_{IV}), 142.1 (C_{IV}), 140.2 (C_{IV}), 134.1 (C_{IV}), 133.8, 133.2 (C_{IV}), 131.7, 129.7, 127.9, 127.4, 126.8, 125.6 (C_{IV}), 123.0, 79.6 (C_{IV}), 44.5, 28.4, 25.6 ppm

LCMS: t_{R} = 5.23 min, $[\text{M} + \text{H}]^+$ 365

HRMS: Calculated for $\text{C}_{22}\text{H}_{25}\text{N}_2\text{O}_3$ $[\text{M} + \text{H}]^+$ 365.1860, found 365.1875

2-(4'-Bromophenyl)-3-methyl-quinoline-N-oxide 276 (235 mg, 52% yield without L-ascorbic acid **152**; 233 mg, 51% yield with L-ascorbic acid **152**)

276 was prepared according to the general procedure for the C-H arylation of N-oxide heterocycles.



Appearance: Beige solid

MP: 140–143 °C

FTIR: No characteristic bands were observed for this compound

$^1\text{H NMR}$: (CDCl_3 , 400 MHz): δ = 8.71 (d, 1H, J = 8.5 Hz), 7.81 (d, 1H, J = 7.6 Hz), 7.73-7.60 (m, 5H), 7.32 (d, 2H, J = 8.6 Hz), 2.24 (s, 3H) ppm

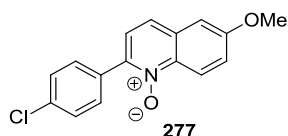
$^{13}\text{C NMR}$: (CDCl_3 , 100 MHz): δ = 146.1 (C_{IV}), 140.4 (C_{IV}), 132.2, 132.0 (C_{IV}), 131.0 (C_{IV}), 130.8, 129.8, 129.3 (C_{IV}), 128.8, 127.3, 126.0, 123.3 (C_{IV}), 120.2, 20.6 ppm

LCMS: t_{R} = 4.70 min, $[\text{M} + \text{H}]^+$ 316

HRMS: Calculated for $\text{C}_{16}\text{H}_{13}^{79}\text{BrNO}$ $[\text{M} + \text{H}]^+$ 314.0175, found 314.0188

6-methoxy-2-(4'-chloro-phenyl)-quinoline N-oxide 277 (294 mg, 53% yield without L-ascorbic acid **152**; 286 mg, 51% yield with L-ascorbic acid **152**)

277 was prepared according to the general procedure for the C-H arylation of N-oxide heterocycles.



Appearance: beige solid

MP: 169–172 °C

FTIR: No characteristic bands were observed for this compound

¹H NMR: (CDCl₃, 400 MHz): δ = 8.75 (d, 1H, *J* = 9.6 Hz), 7.94 (d, 1H, *J* = 8.6 Hz), 7.68 (d, 1H, *J* = 8.6 Hz), 7.51 (d, 2H, *J* = 8.5 Hz), 7.47 (d, 1H, *J* = 8.8 Hz), 7.44 (dd, 1H, *J*₁ = 9.6 Hz, *J*₂ = 2.7 Hz), 7.13 (d, 1H, *J* = 2.7 Hz), 3.97 (s, 3H) ppm

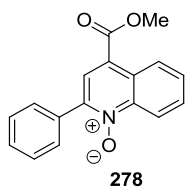
¹³C NMR: (CDCl₃, 100 MHz): δ = 159.4 (C_{IV}), 142.1(C_{IV}), 137.8 (C_{IV}), 135.2 (C_{IV}), 131.9 (C_{IV}), 131.0 (C_{IV}), 130.9, 128.5, 124.4, 123.4, 122.7, 122.0, 105.9, 55.70 ppm

LCMS: t_R = 4.76 min, [M + H]⁺ 286

HRMS: Calculated for C₁₆H₁₃³⁵ClNO₂ [M + H]⁺ 286.0629, found 286.0633

4-(Methoxycarbonyl)-2-phenyl-quinoline N-oxide 278 (251 mg, 70% yield without L-ascorbic acid **152**; 351 mg, 65% yield with L-ascorbic acid **152**)

278 was prepared according to the general procedure for the C-H arylation of N-oxide heterocycles.



Appearance: Orange solid

MP: 112–117 °C

FTIR: ν_{\max} = 1715 (C=O) cm^{-1}

^1H NMR: (CDCl_3 , 400 MHz): δ = 9.05 (dd, 1H, J_1 = 8.3 Hz, J_2 = 1.0 Hz), 8.87 (dd, 1H, J_1 = 8.6 Hz, J_2 = 1.0 Hz), 8.24 (s, 1H), 7.96 (dd, 2H, J_1 = 8.3 Hz, J_2 = 1.5 Hz), 7.80 (ddd, 1H, J_1 = 8.3 Hz, J_2 = 6.8 Hz, J_3 = 1.2 Hz), 7.74 (ddd, 1H, J_1 = 8.3 Hz, J_2 = 6.8 Hz, J_3 = 1.2 Hz), 7.57-7.46 (m, 3H), 4.02 (s, 3H) ppm

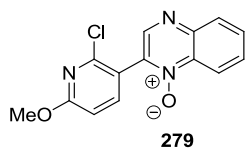
^{13}C NMR: (CDCl_3 , 100 MHz): δ = 165.4 (C_{IV}), 144.1 (C_{IV}), 143.1 (C_{IV}), 132.8 (C_{IV}), 130.6, 129.9, 129.7, 129.5, 128.5, 127.3 (C_{IV}), 126.8, 126.7, 122.4 (C_{IV}), 120.3, 52.6 ppm

LCMS: t_{R} = 4.93 min, $[\text{M} + \text{H}]^+$ 280

HRMS: Calculated for $\text{C}_{17}\text{H}_{14}\text{NO}_3$ $[\text{M} + \text{H}]^+$ 280.0968, found 280.0976

2-(2'-Chloro-6'-methoxypyridin-3'-yl)-quinoxaline N-oxide 279 (58 mg, 15% yield without L-ascorbic acid **152**; 117 mg, 22% yield with L-ascorbic acid **152**)

279 was prepared according to the general procedure for the C-H arylation of N-oxide heterocycles.



Appearance: Brown solid

MP: 174–180 °C

FTIR: No characteristic bands were observed for this compound

¹H NMR: (CDCl₃, 400 MHz): δ = 8.82 (s, 1H), 8.65 (d, 1H, *J* = 8.1 Hz), 8.18 (d, 1H, *J* = 8.3 Hz), 7.89-7.76 (m, 3H), 6.87 (d, 1H, *J* = 8.9 Hz), 4.03 (s, 3H) ppm

¹³C NMR: (CDCl₃, 100 MHz): δ = 165.5 (C_{IV}), 148.0 (C_{IV}), 147.91, 145.0 (C_{IV}), 142.5, 137.4 (C_{IV}), 136.9 (C_{IV}), 131.7, 130.5, 130.2, 119.3, 117.9 (C_{IV}), 109.8, 54.5 ppm

LCMS: *t*_R = 4.42 min, [M + H]⁺ 288

HRMS: Calculated for C₁₄H₁₁³⁵ClN₃O₂ [M + H]⁺ 288.0534, found 288.0544

2-(6'-Acetamidopyridin-3'-yl)-quinoxaline N-oxide 280 (201 mg, 43% yield without L-ascorbic acid **152**; 99 mg, 43% yield with L-ascorbic acid **152**)

280 was prepared according to the general procedure for the C-H arylation of N-oxide heterocycles.



Appearance: White solid

MP: 245–250 °C

FTIR: *v*_{max} = 3029 (N-H), 1703 (C=O) cm⁻¹

¹H NMR: (DMSO-d₆, 400 MHz): δ = 10.81 (s, 1H), 9.18 (s, 1H), 9.08 (d, 1H, *J* = 2.0 Hz), 8.56-8.53 (m, 2H), 8.26 (d, 1H, *J* = 8.8 Hz), 8.17 (dd, 1H, *J*₁ = 8.5 Hz, *J*₂ = 1.4 Hz), 7.96-7.88 (m, 2H), 2.16 (s, 3H) ppm

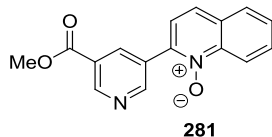
¹³C NMR: (DMSO-d₆, 100 MHz): δ = 170.2 (C_{IV}), 153.3 (C_{IV}), 149.3, 148.0, 144.4 (C_{IV}), 139.6, 137.1 (C_{IV}), 136.7 (C_{IV}), 132.0, 131.2, 130.3, 121.7 (C_{IV}), 119.2, 112.7, 24.5 ppm

LCMS: *t*_R = 3.16 min, [M + H]⁺ 281

HRMS: Calculated for C₁₅H₁₃N₄O₂ [M + H]⁺ 281.1033, found 281.1034

2-(5-Methoxycarbonyl-pyridin-3-yl)-quinoline N-oxide **281** (162 mg, 35% yield without L-ascorbic acid **152**; 158 mg, 34% yield with L-ascorbic acid **152**)

281 was prepared according to the general procedure for the C-H arylation of *N*-oxide heterocycles.



Appearance: White solid

MP: 180–183 °C

FTIR: $\nu_{\text{max}} = 1721$ (C=O) cm^{-1}

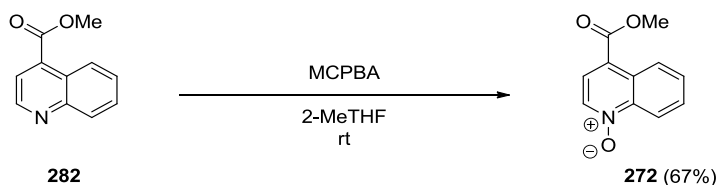
¹H NMR: (CDCl₃, 400 MHz): $\delta = 9.34$ (d, 1H, $J = 1.9$ Hz), 9.30 (d, 1H, $J = 1.4$ Hz), 9.04 (s, 1H), 8.84 (d, 1H, $J = 8.8$ Hz), 7.92 (d, 1H, $J = 8.1$ Hz), 7.85 - 7.80 (m, 2H), 7.72 - 7.68 (m, 1H), 7.56 (d, 1H, $J = 8.6$ Hz), 3.99 (s, 3H) ppm

¹³C NMR: (CDCl₃, 100 MHz): $\delta = 165.4$ (C_{IV}), 153.5 , 151.2 , 142.3 (C_{IV}), 141.1 (C_{IV}), 138.1 , 131.1 , 130.1 , 129.6 , 129.2 , 128.2 , 125.6 , 122.4 , 120.2 , 52.6 ppm. One quaternary carbon peak is missing

LCMS: $t_{\text{R}} = 3.63$ min, $[\text{M} + \text{H}]^+$ 281

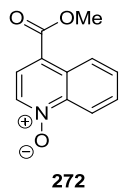
HRMS: Calculated for C₁₆H₁₃N₂O₃ $[\text{M} + \text{H}]^+$ 281.0921, found 281.0923

V.4.ix Synthesis of 4-(methoxycarbonyl)-quinoline N-oxide **272**



To a solution of methyl quinoline-4-carboxylate **282** (1.94 g, 10.36 mmol) in 2-MeTHF (100 mL) at room temperature under air was added portionwise MCPBA (1.967 g, 11.40 mmol). The resulting solution was stirred for 24 hours at room temperature and the solvent was removed under reduced pressure. The crude product was partitioned between ethyl acetate and saturated aqueous NaHCO₃ and the organic layer was dried over anhydrous Na₂SO₄ before being concentrated *in vacuo*. The crude product was then purified by silica gel chromatography eluting with dichloromethane/acetone to give 4-(methoxycarbonyl)-quinoline *N*-oxide **272** (1.40 g, 6.89 mmol, 67% yield) as a white solid.

4-(methoxycarbonyl)-quinoline N-oxide **272** (1.40 g, 67% yield)



Appearance: White solid

MP: 152–153 °C

FTIR: ν_{max} = 1716 (C=O) cm^{-1}

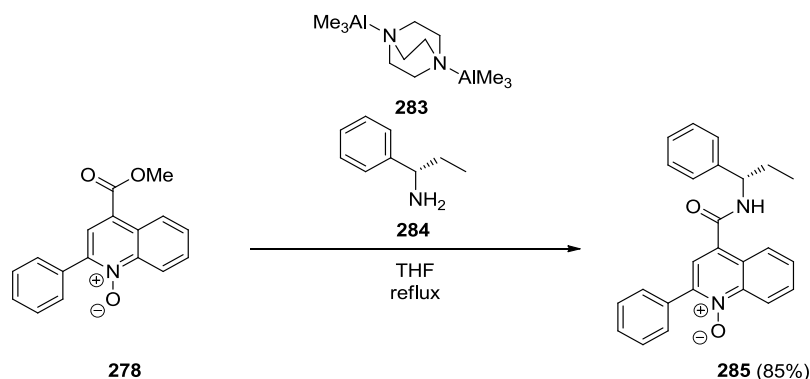
^1H NMR: (CDCl_3 , 400 MHz): δ = 9.07 (dd, 1H, J_1 = 8.1 Hz, J_2 = 1.5 Hz), 8.78 (dd, 1H, J_1 = 8.2 Hz, J_2 = 1.5 Hz), 8.55 (d, 1H, J = 6.4 Hz), 8.01 (d, 1H, J = 6.4 Hz), 7.82–7.70 (m, 2H), 4.02 (s, 3H) ppm

^{13}C NMR: (CDCl_3 , 100 MHz): δ = 165.1 (C_{IV}), 142.3 (C_{IV}), 134.4, 130.4, 130.2, 128.4 (C_{IV}), 126.8, 124.4, 123.0 (C_{IV}), 119.8, 52.6 ppm

LCMS: t_{R} = 3.36 min, $[\text{M} + \text{H}]^+$ 204

HRMS: Calculated for $\text{C}_{11}\text{H}_{10}\text{NO}_3$ $[\text{M} + \text{H}]^+$ 204.0655, found 204.0653

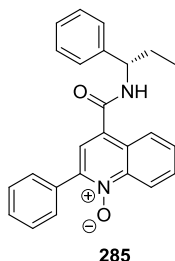
V.4.x Synthesis of 2-phenyl-4-(carboxy-(S)- α -ethylbenzylamine)-quinoline N-oxide **285**



To a stirred solution of DABAL-Me₃ **283** (193 mg, 0.75 mmol) in anhydrous THF at room temperature under nitrogen was added (S)- α -ethylbenzylamine **284** (0.108 mL, 0.75 mmol) and the resulting solution was stirred at 40°C for 1 hour. To this mixture 4-(methoxycarbonyl)-2-phenylquinoline N-oxide (140 mg, 0.50 mmol) was added and the reaction was stirred at reflux for 22 hours. The reaction mixture was cooled to ambient temperature and quenched with aqueous HCl (2 M) dropwise and was extracted with ethyl acetate. The organic phase was separated and evaporated to dryness under reduced pressure. The crude product was then purified by silica gel chromatography eluting with heptane / ethyl acetate to give (2-phenyl-4-

(carboxy-(S)- α -ethylbenzylamine)-quinoline *N*-oxide **285** (162 mg, 0.42 mmol, 85 % yield) as an off-white solid.

2-phenyl-4-(carboxy-(S)- α -ethylbenzylamine)-quinoline *N* oxide **285** (162 mg, 85% yield)



Appearance: Off-white solid

MP: 90–100 °C

FTIR: ν_{\max} = 3235 (N-H), 1638 (C=O) cm^{-1}

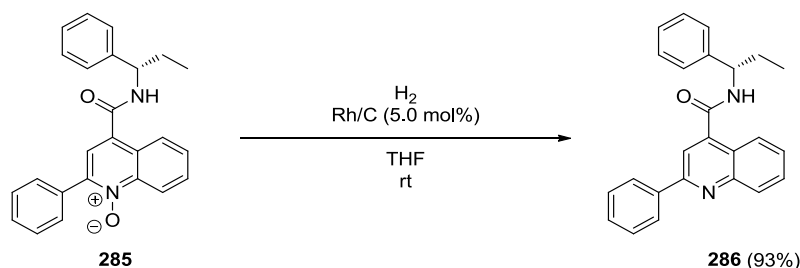
^1H NMR: (CDCl_3 , 400 MHz): δ = 9.03 (d, 1H, J = 8.3 Hz), 8.32 (d, 1H, J = 8.8 Hz), 7.76 (d, 1H, J = 8.1 Hz), 7.69 (d, 2H, J = 7.5 Hz), 7.50 (d, 2H, J = 7.1 Hz), 7.40-7.21 (m, 9H), 5.15 (q, 1H, J = 7.8 Hz), 2.20-2.00 (m, 2H), 1.07 (t, 3H, J = 7.4 Hz) ppm

^{13}C NMR: (CDCl_3 , 100 MHz): δ = 165.6 (C_{IV}), 143.6 (C_{IV}), 142.5 (C_{IV}), 141.1 (C_{IV}), 133.9 (C_{IV}), 131.7 (C_{IV}), 130.6, 130.2, 129.6, 129.0, 128.7, 128.2, 127.4, 127.1, 125.9, 125.6 (C_{IV}), 121.1, 119.5, 56.2, 29.7, 11.5 ppm

LCMS: t_{R} = 5.23 min, $[\text{M} + \text{H}]^+$ 383

HRMS: Calculated for $\text{C}_{25}\text{H}_{23}\text{N}_2\text{O}_2$ $[\text{M} + \text{H}]^+$ 383.1754, found 383.1761

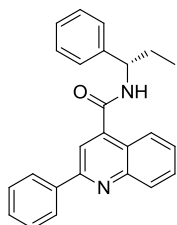
V.4.xi Synthesis of 2-phenyl-4-(carboxy-(S)- α -ethylbenzylamine)-quinoline **286**



2-phenyl-4-(carboxy-(S)- α -ethylbenzylamine)-quinoline *N*-oxide **185** (147 mg, 0.38 mmol), Johnson Matthey 5% rhodium on charcoal type 20A paste, 60% wet (99 mg, 0.02 mmol) and THF (3.5 mL) were added to a hydrogenation reactor which was purged 3 times with 5 bar of nitrogen and then 3 times with 3 bar of hydrogen. The reaction was then stirred at room temperature under 3 bar of hydrogen for 2 hours and was stopped by flushing the hydrogenation reactor with nitrogen. The

reaction mixture was then filtered through a plug of Celite to remove the catalyst and the filtrate was evaporated in vacuo. The crude product was then purified by silica gel chromatography eluting with heptane / ethyl acetate to give 2-phenyl-4-(carboxy-(S)- α -ethylbenzylamine)-quinoline **286** (131 mg, 0.36 mmol, 93 % yield) as a stable white foam.

2-phenyl-4-(carboxy-(S)- α -ethylbenzylamine)-quinoline **286** (131 mg, 93% yield)



286

Appearance: White solid

MP: 140–150 °C

FTIR: ν_{\max} = 3232 (N-H), 1635 (C=O) cm^{-1}

^1H NMR: (DMSO- d_6 , 400 MHz): δ = 9.25 (d, 1H, J = 8.5 Hz), 8.30 (d, 2H, J = 6.9 Hz), 8.13 (d, 1H, J = 8.1 Hz), 8.08 (s, 1H), 8.02 (dd, J_1 = 8.6 Hz, J_2 = 0.8 Hz), 7.82 (dd, 1H, J_1 = 7.1 Hz, J_2 = 0.5 Hz), 7.63-7.54 (m, 4H), 7.46 (d, 2H, J = 7.1 Hz), 7.38 (d, 2H, J = 7.6 Hz), 7.28 (at, 1H, J = 7.3 Hz), 5.06 (q, 1H, J = 6.6 Hz), 1.91-1.79 (m, 2H), 0.98 (t, 3H, J = 7.4 Hz) ppm

^{13}C NMR: (DMSO- d_6 , 100 MHz): δ = 166.7 (C_{IV}), 156.3 (C_{IV}), 148.4 (C_{IV}), 143.9 (C_{IV}), 143.8 (C_{IV}), 138.8 (C_{IV}), 130.6, 130.3, 130.0, 129.4, 128.8, 127.8, 127.6, 127.3, 127.0, 125.6, 123.9 (C_{IV}), 116.9, 55.5, 29.7, 11.7 ppm

LCMS: t_{R} = 5.60 min, $[\text{M} + \text{H}]^+$ 367

HRMS: Calculated for $\text{C}_{25}\text{H}_{23}\text{N}_2\text{O}$ $[\text{M} + \text{H}]^+$ 367.1805, found 367.1806

REFERENCES

- (1) Anastas, P. T.; Kirchoff, M. M. *Acc. Chem. Res.* **2002**, *35*, 686.
- (2) Carey, J. S.; Laffan, D.; Thomson, C.; Williams, M. T. *Org. Biomol. Chem.* **2006**, *4*, 2337.
- (3) Federsel, H.-J. *Drug Discov. Today* **2006**, *11*, 966.
- (4) Hogan, P. J.; Cox, B. G. *Org. Process Res. Dev.* **2009**, *13*, 875.
- (5) Griess, P. *J. Chem. Soc.* **1867**, *20*, 36.
- (6) Knoevenagel, E. *Ber. Dtsch. Chem. Ges.* **1890**, *23*, 2994.
- (7) Patai, S. *The Chemistry of Diazonium and Diazo Groups*, John Wiley & Sons: Chichester, **1978**.
- (8) Knoevenagel, E. *Ber. Dtsch. Chem. Ges.* **1895**, *28*, 2048.
- (9) Doyle, M. P.; Bryker, W. J. *J. Org. Chem.* **1979**, *44*, 1572.
- (10) Barbero, M.; Crisma, M.; Degani, I.; Fochi, R.; Perracino, P. *Synthesis* **1998**, 1171.
- (11) Filimonov, V. D.; Trusova, M.; Postnikov, P.; Krasnokutskaya, E. A.; Lee, Y. M.; Hwang, H. Y.; Kim, H.; Chi, K.-W. *Org. Lett.* **2008**, *10*, 3961.
- (12) Schiemann, G.; Winkelmueller, W. *Org. Synth.* **1933**, *13*, 52.
- (13) Gosselin, F.; Lau, S.; Nadeau, C.; Trinh, T.; O'Shea, P. D.; Davies, I. W. *J. Org. Chem.* **2009**, *74*, 7790.
- (14) Urban, P. G. *Bretherick's Handbook of Reactive Chemical Hazards*; Elsevier, Amsterdam, **2007**.
- (15) Bassan, E.; Ruck, R. T.; Dienemann, E.; Emerson, K. M.; Humphrey, G. R.; Raheem, I. T.; Tschaen, D. M.; Vickery, T. P.; Wood, H. B.; Yasuda, N. *Org. Process Res. Dev.* **2013**, *17*, 1611.
- (16) Ullrich, R.; Grewer, T. *Thermochim. Acta* **1993**, *225*, 201.
- (17) Cygler, M.; Przybylska, M.; Elofson, R. M. *Can. J. Chem.* **1982**, *60*, 2852.
- (18) Rømming, C. *Acta Chem. Scand.* **1963**, *17*, 1444.
- (19) Nielsen, M. A.; Nielsen, M. K.; Pittelkow, T. *Org. Process Res. Dev.* **2004**, *8*, 1059.
- (20) Singh, R. P.; Verma, R. D.; Meshri, D. T.; Shreeve, J. M. *Angew. Chem. Int. Ed.* **2006**, *45*, 3584.
- (21) Oger, N.; D'Halluin, M.; Le Grogneec, E.; Felpin, F.-X. *Org. Process Res. Dev.* **2014**, *18*, 1786.
- (22) Zollinger, H. *Acc. Chem. Res.* **1973**, *6*, 335.
- (23) Merino, E. *Chem. Soc. Rev.* **2011**, *40*, 3835.

- (24) Callonnec, F. Le; Fouquet, E.; Felpin, F.-X. *Org. Lett.* **2011**, *13*, 2646–2649.
- (25) Johansson Seechurn, C. C. C.; Kitching, M. O.; Colacot, T. J.; Snieckus, V. *Angew. Chem. Int. Ed.* **2012**, *51*, 5062.
- (26) Friedman, L.; Logullo, F. M. *J. Org. Chem.* **1969**, *34*, 3089.
- (27) Asao, N.; Sato, K. *Org. Lett.* **2006**, *8*, 5361.
- (28) Taniguchi, T.; Imoto, M.; Takeda, M.; Nakai, T.; Mihara, M.; Iwai, T.; Ito, T.; Mizuno, T.; Nomoto, A.; Ogawa, A. *Heteroat. Chem.* **2015**, *26*, 411.
- (29) Abele, S.; Schmidt, G.; Fleming, M. J.; Steiner, H. *Org. Process Res. Dev.* **2014**, *18*, 993.
- (30) Hernandez, M.; Cavalcanti, S. M.; Moreira, D. R.; de Azevedo Junior, W.; Leite, A. C. *Curr. Drug Targets* **2010**, *11*, 303.
- (31) Wilcken, R.; Zimmermann, M. O.; Lange, A.; Joerger, A. C.; Boeckler, F. M. *J. Med. Chem.* **2013**, *56*, 1363.
- (32) Sandmeyer, T. *Ber. Dtsch. Chem. Ges.* **1884**, *17*, 1633.
- (33) Sandmeyer, T. *Ber. Dtsch. Chem. Ges.* **1884**, *17*, 2650.
- (34) Kochi, J. K. *J. Am. Chem. Soc.* **1957**, *79*, 2942.
- (35) Hodgson, H. H. *Chem. Rev.* **1947**, *40*, 251.
- (36) Doyle, M. P.; Siegfried, B.; Dellaria, J. F. *J. Org. Chem.* **1977**, *42*, 2426.
- (37) Sigeev, A. S.; Beletskaya, I. P.; Petrovskii, P. V.; Peregudov, A. S. *Russ. J. Org. Chem.* **2012**, *48*, 1055.
- (38) Li, Y.; Pu, J.; Jiang, X. *Org. Lett.* **2014**, *16*, 2692.
- (39) Dai, J.-J.; Fang, C.; Xiao, B.; Yi, J.; Xu, J.; Liu, Z.-J.; Lu, X.; Liu, L.; Fu, Y. *J. Am. Chem. Soc.* **2013**, *135*, 8436.
- (40) Danoun, G.; Bayarmagnai, B.; Grünberg, M. F.; Gooßen, L. J. *Angew. Chem. Int. Ed.* **2013**, *52*, 7972.
- (41) Yale, H. L. *J. Med. Pharm. Chem.* **1959**, *1*, 121.
- (42) Zhang, J.; Wang, X.; Yu, H.; Ye, J. *Synlett* **2012**, *23*, 1394.
- (43) Miyaura, N.; Suzuki, A. *Chem. Rev.* **1995**, *95*, 2457.
- (44) Suzuki, A. *J. Organomet. Chem.* **1999**, *576*, 147.
- (45) Miyaura, N.; Yamada, K.; Suzuki, A. *Tetrahedron Lett.* **1979**, *20*, 3437.
- (46) Hari, D. P.; König, B. *Angew. Chem. Int. Ed.* **2013**, *52*, 4734.
- (47) Yu, J.; Zhang, L.; Yan, G. *Adv. Synth. Catal.* **2012**, *354*, 2625.
- (48) Lennox, A. J. J.; Lloyd-Jones, G. C. *Chem. Soc. Rev.* **2014**, *43*, 412.
- (49) Ishiyama, T.; Murata, M.; Miyaura, N. *J. Org. Chem.* **1995**, *60*, 7508.
- (50) Ma, Y.; Song, C.; Jiang, W.; Xue, G.; Cannon, J. F.; Wang, X.; Andrus, M. B.

- Org. Lett.* **2003**, *5*, 4635.
- (51) Berionni, G.; Maji, B.; Knochel, P.; Mayr, H. *Chem. Sci.* **2012**, *3*, 878.
- (52) Lennox, A. J. J.; Lloyd-Jones, G. C. *Angew. Chem. Int. Ed.* **2013**, *52*, 7362.
- (53) Erb, W.; Hellal, A.; Albini, M.; Rouden, J.; Blanchet, J. *Chem. - A Eur. J.* **2014**, *20*, 6608.
- (54) Erb, W.; Albini, M.; Rouden, J.; Blanchet, J. *J. Org. Chem.* **2014**, *79*, 10568.
- (55) Yamashita, R.; Kikukawa, K.; Wada, F.; Matsuda, T. *J. Organomet. Chem.* **1980**, *201*, 463.
- (56) Roglans, A.; Pla-Quintana, A.; Moreno-Mañas, M. *Chem. Rev.* **2006**, *106*, 4622.
- (57) Darses, S.; Jeffery, T.; Genet, J.-P.; Brayer, J.-L.; Demoute, J.-P. *Tetrahedron Lett.* **1996**, *37*, 3857.
- (58) Felpin, F.-X.; Fouquet, E.; Zakri, C. *Adv. Synth. Catal.* **2009**, *351*, 649.
- (59) Andrus, M. B.; Ma, Y.; Zang, Y.; Song, C. *Tetrahedron Lett.* **2002**, *43*, 9137.
- (60) Mo, F.; Qiu, D.; Jiang, Y.; Zhang, Y.; Wang, J. *Tetrahedron Lett.* **2011**, *52*, 518.
- (61) Zong, Y.; Hu, J.; Sun, P.; Jiang, X. *Synlett* **2012**, 2393.
- (62) Taylor, R. H.; Felpin, F.-X. *Org. Lett.* **2007**, *9*, 2911.
- (63) Sengupta, S.; Sadhukhan, S. K. *Tetrahedron Lett.* **1998**, *39*, 715.
- (64) Heck, R. F.; Nolley, J. P. *J. Org. Chem.* **1972**, *37*, 2320.
- (65) de Meijere, A.; Meyer, F. E. *Angew. Chem. Int. Ed. Eng.* **1995**, *33*, 2379.
- (66) Beletskaya, I. P.; Cheprakov, A. V. *Chem. Rev.* **2000**, *100*, 3009.
- (67) Kikukawa, K.; Matsuda, T. *Chem. Lett.* **1977**, *2*, 159.
- (68) Kikukawa, K.; Nagira, K.; Wada, F.; Matsuda, T. *Tetrahedron* **1981**, *37*, 31.
- (69) Yasui, S.; Fujii, M.; Kawano, C.; Nishimura, Y.; Shioji, K.; Ohno, A. *J. Chem. Soc. Perkin Trans. 2* **1994**, *2*, 177.
- (70) Nalivela, K. S.; Tilley, M.; McGuire, M. A.; Organ, M. G. *Chem. Eur. J.* **2014**, *20*, 6603.
- (71) Oger, N.; Le Grogne, E.; Felpin, F.-X. *J. Org. Chem.* **2014**, *79*, 8255.
- (72) Sonogashira, K. *J. Organomet. Chem.* **2002**, *653*, 46.
- (73) Chinchilla, R.; Nájera, C. *Chem. Rev.* **2007**, *107*, 874.
- (74) Fabrizi, G.; Goggiamani, A.; Sferrazza, A.; Cacchi, S. *Angew. Chem. Int. Ed.* **2010**, *49*, 4067.
- (75) Wu, X.-F.; Neumann, H.; Beller, M. *Chem. Commun.* **2011**, *47*, 7959.
- (76) Wu, X.-F.; Neumann, H.; Beller, M. *Angew. Chem. Int. Ed.* **2011**, *50*, 11142.

- (77) Hunt, A. J.; Farmer, T. J.; Clark, J. H. *CHAPTER 1. Elemental Sustainability and the Importance of Scarce Element Recovery*; Royal Society of Chemistry, Cambridge, **2013**.
- (78) Bonin, H.; Sauthier, M.; Felpin, F.-X. *Adv. Synth. Catal.* **2014**, *356*, 645.
- (79) Meerwein, H.; Buechner, E.; van Emster, K. *J. fur Prakt. Chemie* **1939**, *152*, 237.
- (80) Obushak, N. D.; Lesyuk, A. I.; Gorak, Y. I.; Matiichuk, V. S. *Russ. J. Org. Chem.* **2009**, *45*, 1375.
- (81) Honraedt, A.; Raux, M.-A.; Grogneq, E. Le; Jacquemin, D.; Felpin, F.-X. *Chem. Commun.* **2014**, *50*, 5236.
- (82) Paizs, C.; Tähtinen, P.; Lundell, K.; Poppe, L.; Irimie, F.-D.; Kanerva, L. T. *Tetrahedron: Asymmetry* **2003**, *14*, 1895.
- (83) V. S. Matiychuk R. Z. Lytvyn, and Yu. I. Horak, N. D. O. *Chem. Heterocycl. Compd.* **2010**, *46*, 50.
- (84) Wetzal, A.; Pratsch, G.; Kolb, R.; Heinrich, M. R. *Chem. Eur. J.* **2010**, *16*, 2547.
- (85) Heinrich, M. R.; Wetzal, A.; Kirschstein, M. *Org. Lett.* **2007**, *9*, 3833.
- (86) Chernyak, N.; Buchwald, S. L. *J. Am. Chem. Soc.* **2012**, *134*, 12466.
- (87) Hering, T.; Hari, D. P.; König, B. *J. Org. Chem.* **2012**, *77*, 10347.
- (88) Gomberg, M.; Bachmann, W. E. *J. Am. Chem. Soc.* **1924**, *46*, 2339.
- (89) Rüchardt, C.; Merz, E. *Tetrahedron Lett.* **1964**, *5*, 2431.
- (90) Beadle, J. R.; Korzeniowski, S. H.; Rosenberg, D. E.; Garcia-Slanga, B. J.; Gokel, G. W. *J. Org. Chem.* **1984**, *49*, 1594.
- (91) Molinaro, C.; Mowat, J.; Gosselin, F.; O'Shea, P. D.; Marcoux, J.-F.; Angelaud, R.; Davies, I. W. *J. Org. Chem.* **2007**, *72*, 1856.
- (92) Basavanag, U. M. V.; Dos Santos, A.; El Kaim, L.; Gámez-Montaño, R.; Grimaud, L. *Angew. Chem. Int. Ed.* **2013**, *52*, 7194.
- (93) Xia, Z.; Zhu, Q. *Org. Lett.* **2013**, *15*, 4110.
- (94) Hari, D. P.; Schroll, P.; König, B. *J. Am. Chem. Soc.* **2012**, *134*, 2958.
- (95) Zheng, D.; An, Y.; Li, Z.; Wu, J. *Angew. Chem., Int. Ed.* **2014**, *53*, 2451.
- (96) Shaaban, S.; Jolit, A.; Petkova, D.; Maulide, N. *Chem. Commun.* **2015**, *51*, 13902.
- (97) Evanochko, W. T.; Shevlin, P. B. *J. Am. Chem. Soc.* **1979**, *101*, 4668.
- (98) Meyer, V.; Lecco, M. T. *Ber. Dtsch. Chem. Ges.* **1883**, *16*, 2976.
- (99) Browne, D. L.; Baxendale, I. R.; Ley, S. V. *Tetrahedron* **2011**, *67*, 10296.

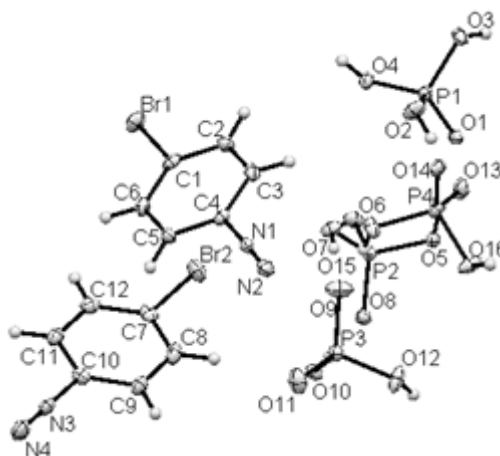
- (100) Clark, H. T.; Kirner, W. R. *Org. Synth.* **1922**, *2*, 47.
- (101) Logullo, F. M.; Seitz, A. H.; Friedman, L. *Org. Synth.* **1968**, *48*, 12.
- (102) Dach, R.; Song, J. J.; Roschangar, F.; Samstag, W.; Senanayake, C. H. *Org. Process Res. Dev.* **2012**, *16*, 1697.
- (103) Busacca, C. A.; Fandrick, D. R.; Song, J. J.; Senanayake, C. H. *Adv. Synth. Catal.* **2011**, *353*, 1825.
- (104) Curzons, A. D.; Mortimer, D. N.; Constable, D. J. C.; Cunningham, V. L. *Green Chem.* **2001**, *3*, 1.
- (105) Baumann, M.; Baxendale, I. R. *Beilstein J. Org. Chem.* **2013**, *9*, 2265.
- (106) Hassan, J.; Sévignon, M.; Gozzi, C.; Schulz, E.; Lemaire, M. *Chem. Rev.* **2002**, *102*, 1359.
- (107) Alberico, D.; Scott, M. E.; Lautens, M. *Chem. Rev.* **2007**, *107*, 174.
- (108) McGlacken, G. P.; Bateman, L. M. *Chem. Soc. Rev.* **2009**, *38*, 2447.
- (109) Wamser, C. A. *J. Am. Chem. Soc.* **1951**, *73*, 409.
- (110) Henderson, R. K.; Jiménez-González, C.; Constable, D. J. C.; Alston, S. R.; Inglis, G. G. A.; Fisher, G.; Sherwood, J.; Binks, S. P.; Curzons, A. D. *Green Chem.* **2011**, *13*, 854.
- (111) Carlson, R.; Lundstedt, T.; Albano, C.; Hordvik, A.; Wold, S.; Elguero, J. *Acta Chem. Scand.* **1985**, *39b*, 79.
- (112) Liu, J.; Yang, X.; Wang, K.; Wang, D.; Zhang, P. *Chem. Commun.* **2009**, *40*, 6080.
- (113) Oger, N.; Le Callonnec, F.; Jacquemin, D.; Fouquet, E.; Le Grogne, E.; Felpin, F.-X. *Adv. Synth. Catal.* **2014**, *356*, 1065.
- (114) Wenk, H. H.; Winkler, M.; Sander, W. *Angew. Chem. Int. Ed.* **2003**, *42*, 502.
- (115) Saito, N.; Nakamura, K.; Shibano, S.; Ide, S.; Minami, M.; Sato, Y. *Org. Lett.* **2013**, *15*, 386.
- (116) Stoessel, F. *Thermal Safety of Chemical Processes*, Wiley, New-York, **2008**.
- (117) Littke, A. F.; Fu, G. C. *Angew. Chem. Int. Ed.* **2002**, *41*, 4176.
- (118) Yin; Liebscher, J. *Chem. Rev.* **2007**, *107*, 133.
- (119) Dantas Ramos, A. L.; Alves, P. da S.; Aranda, D. A. G.; Schmal, M. *Appl. Catal. A Gen.* **2004**, *277*, 71.
- (120) Wayland, B. B.; Schramm, R. F. *Inorg. Chem.* **1969**, *8*, 971.
- (121) Willis, D. M.; Strongin, R. M. *Tetrahedron Lett.* **2000**, *41*, 6271.
- (122) Sengupta, S.; Bhattacharyya, S. *J. Org. Chem.* **1997**, *62*, 3405.
- (123) Hantzsch, A.; Jochem, E. *Ber. Dtsch. Chem. Ges.* **1901**, *34*, 3337.

- (124) Trygg, J.; Wold, S. *J. Chemometrics*. **2002**, *16*, 119.
- (125) Reichardt, C. *Angew. Chem. Int. Ed. Eng.* **1965**, *4*, 29.
- (126) Owen, M. R.; Luscombe, C.; Lai; Godbert, S.; Crookes, D. L.; Emiabata-Smith, D. *Org. Process Res. Dev.* **2001**, *5*, 308.
- (127) Caron, S.; Thomson, N. M. *J. Org. Chem.* **2015**, *80*, 2943.
- (128) Roe, A.; Graham, J. R. *J. Am. Chem. Soc.* **1952**, *74*, 6297.
- (129) Stadler, A.; Yousefi, B. H.; Dallinger, D.; Walla, P.; Eycken, E. Van Der; Kaval, N.; Kappe, C. O. *Org. Process Res. Dev.* **2003**, *7*, 707.
- (130) Goossen, L. J.; Melzer, B. *J. Org. Chem.* **2007**, *72*, 7473.
- (131) Kristensen, J.; Lysén, M.; Vedsø, P.; Begtrup, M. *Org. Lett.* **2001**, *3*, 1435.
- (132) Aalla, S.; Gilla, G.; Bojja, Y.; Anumula, R. R.; Vummenthala, P. R.; Padi, P. R. *Org. Process Res. Dev.* **2012**, *16*, 682.
- (133) Moreno-Mañas, M.; Pérez, M.; Pleixats, R. *J. Org. Chem.* **1996**, *61*, 2346.
- (134) Adamo, C.; Amatore, C.; Ciofini, I.; Jutand, A.; Lakmini, H. *J. Am. Chem. Soc.* **2006**, *128*, 6829.
- (135) Amatore, C.; Jutand, A.; Le Duc, G. *Angew. Chem. Int. Ed.* **2012**, *51*, 1379.
- (136) Amatore, C.; Le Duc, G.; Jutand, A. *Chem. Eur. J.* **2013**, *19*, 10082.
- (137) Colleville, A. P.; Horan, R. A. J.; Tomkinson, N. C. O. *Org. Process Res. Dev.* **2014**, *18*, 1128.
- (138) Neufeldt, S. R.; Jiménez-Osés, G.; Huckins, J. R.; Thiel, O. R.; Houk, K. N. *J. Am. Chem. Soc.* **2015**, *137*, 9843.
- (139) Campeau, L.-C.; Rousseaux, S.; Fagnou, K. *J. Am. Chem. Soc.* **2005**, *127*, 18020.
- (140) Campeau, L.-C.; Bertrand-Laperle, M.; Leclerc, J.-P.; Villemure, E.; Gorelsky, S.; Fagnou, K. *J. Am. Chem. Soc.* **2008**, *130*, 3276.
- (141) Campeau, L.-C.; Stuart, D. R.; Leclerc, J.-P.; Bertrand-Laperle, M.; Villemure, E.; Sun, H.-Y.; Lasserre, S.; Guimond, N.; Lecavallier, M.; Fagnou, K. *J. Am. Chem. Soc.* **2009**, *131*, 3291.
- (142) Mai, W.; Yuan, J.; Li, Z.; Sun, G.; Qu, L. *Synlett* **2012**, 145.
- (143) Crisóstomo, F. P.; Martín, T.; Carrillo, R. *Angew. Chem. Int. Ed.* **2014**, *53*, 2181.
- (144) Naylor, M. A.; Adams, G. E.; Haigh, A.; Cole, S.; Jenner, T.; Robertson, N.; Siemann, D.; Stephens, M. A.; Stratford, I. J. *Anticancer. Drugs* **1995**, *6*, 259.
- (145) Barham, H. M.; Stratford, I. J. *Biochem. Pharmacol.* **1996**, *51*, 829.
- (146) Costas-Costas, U.; Gonzalez-Romero, E.; Bravo-Diaz, C. *Helv. Chim. Acta*

- 2001**, 84, 632.
- (147) Doyle, M. P.; Nesloney, C. L.; Shanklin, M. S.; Marsh, C. A.; Brown, K. C. *J. Org. Chem.* **1989**, 54, 3785.
- (148) Hill, D. T.; Stanley, K. G.; Williams, J. E. K.; Loev, B.; Fowler, P. J.; McCafferty, J. P.; Macko, E.; Berkoff, C. E.; Ladd, C. B. *J. Med. Chem.* **1983**, 26, 865.
- (149) Kimball, D. B.; Haley, M. M. *Angew. Chem. Int. Ed.* **2002**, 41, 3338.
- (150) Sarau, H. M.; Griswold, D. E.; Bush, B.; Potts, W.; Sandhu, P.; Lundberg, D.; Foley, J. J.; Schmidt, D. B.; Webb, E. F.; Martin, L. D.; Legos, J. J.; Whitmore, R. G.; Barone, F. C.; Medhurst, A. D.; Luttmann, M. A.; Giardina, G. A.; Hay, D. W. *J. Pharmacol. Exp. Ther.* **2000**, 295, 373.
- (151) Bennacef, I.; Perrio, C.; Lasne, M.-C.; Barré, L. *J. Org. Chem.* **2007**, 72, 2161.
- (152) Potamitis, C.; Zervou, M.; Katsiaras, V.; Zoumpoulakis, P.; Durdagi, S.; Papadopoulos, M. G.; Hayes, J. M.; Grdadolnik, S. G.; Kyrikou, I.; Argyropoulos, D.; Vatougia, G.; Mavromoustakos, T. *J. Chem. Inf. Model.* **2009**, 49, 726.
- (153) Chen, N.; Barra, M.; Lee, I.; Chahal, N. *J. Org. Chem.* **2002**, 67, 2271.

APPENDIX 1 – Crystal data

Single crystal X-Ray diffraction report for $C_6H_9BrN_2O_8P_2$ **195**



Crystals were grown by slow diffusion of diethyl ether into a saturated solution of 4-bromobenzenediazonium dihydrogen phosphate **195** in acetic acid.

Empirical formula	$C_6H_9BrN_2O_8P_2$	
Formula weight (g/mol)	379.00	
Temperature (K)	123	
Wavelength (Å)	0.71073	
Crystal system	Monoclinic	
Space group	$P2_{1/c}$	
Unit cell dimensions	$a = 15.1727(4) \text{ \AA}$	$\alpha = 90^\circ$
	$b = 10.8979(3) \text{ \AA}$	$\beta = 94.824$
	$c = 15.2981(4) \text{ \AA}$	$\gamma = 90^\circ$
Cell volume (Å³)	2520.59	
Z	8	
Calculated density (Mg/m³)	1.997	
Absorption coefficient (mm⁻¹)	3.553	
F₀₀₀	1504	
Crystal size (mm³)	0.30 x 0.18 x 0.06	
Absorption correction	Semi-empirical from equivalents	
Θ range for data collection (°)	3.26 to 30.20	
Index ranges	$-21 \leq h \leq 21, -14 \leq k \leq 14, -11 \leq l \leq 20$	
Reflections measured	13940	
Independent reflections	6721 [R(int) = 0.0356]	
Refinement method	Full-matrix least-squares on F^2	
Goodness-of-fit on F^2	1.022	
R indices (all data)	$R_1 = 0.0680, wR_2 = 0.0825$	
Largest diff. peak and hole (e.Å⁻³)	0.513 and -0.616	

Table A1: Crystal data and refinement details

Atom	x	y	z	U_{equiv}
Br(1)	5858(1)	-379(1)	3734(1)	21(1)
Br(2)	8485(1)	466(1)	3874(1)	26(1)
P(1)	5896(1)	5881(1)	3413(1)	13(1)
P(2)	8471(1)	4207(1)	3747(1)	13(1)
P(3)	8929(1)	3793(1)	6397(1)	13(1)
P(4)	6509(1)	6460(1)	6464(1)	13(1)
O(1)	6792(1)	6334(2)	3201(1)	17(1)
O(2)	5727(1)	5829(2)	4363(1)	23(1)
O(3)	5166(1)	6714(2)	2938(1)	18(1)
O(4)	5774(1)	4567(2)	3016(1)	17(1)
O(5)	8324(1)	5618(2)	3725(2)	21(1)
O(6)	8301(1)	3756(2)	2801(1)	19(1)
O(7)	7750(1)	3601(2)	4262(1)	18(1)
O(8)	9389(1)	3957(2)	4158(1)	15(1)
O(9)	8018(1)	3977(2)	5954(1)	25(1)
O(10)	9531(1)	3113(2)	5770(1)	15(1)
O(11)	8974(1)	3085(2)	7242(1)	26(1)
O(12)	9363(2)	5074(2)	6619(2)	24(1)
O(13)	6621(1)	6839(2)	5530(1)	21(1)
O(14)	5621(1)	6729(2)	6785(1)	18(1)
O(15)	6690(1)	5058(2)	6573(1)	18(1)
O(16)	7251(1)	7143(2)	7049(1)	21(1)
N(1)	6610(2)	2421(2)	7066(2)	14(1)
N(2)	6736(2)	2894(2)	7696(2)	20(1)
N(3)	9120(2)	-2422(2)	7181(2)	17(1)
N(4)	9207(2)	-2913(2)	7804(2)	25(1)
C(1)	6111(2)	522(3)	4776(2)	15(1)
C(2)	5865(2)	1750(3)	4795(2)	17(1)
C(3)	6037(2)	2413(3)	5557(2)	17(1)
C(4)	6456(2)	1786(3)	6272(2)	14(1)
C(5)	6709(2)	561(3)	6269(2)	15(1)
C(6)	6527(2)	-82(3)	5503(2)	16(1)
C(7)	8693(2)	-461(3)	4909(2)	17(1)
C(8)	9074(2)	122(3)	5657(2)	21(1)
C(9)	9233(2)	-537(3)	6419(2)	19(1)
C(10)	9000(2)	-1770(3)	6391(2)	16(1)

Atom	x	y	z	U _{equiv}
C(11)	8626(2)	-2376(3)	5650(2)	18(1)
C(12)	8475(2)	-1696(3)	4896(2)	19(1)

Table A2: Atomic coordinates ($\times 10^4$) and equivalent isotropic displacement parameters ($\text{\AA}^2 \times 10^3$)

Br(1)-C(1)	1.884(3)	O(15)-H(8A)	0.845(10)
Br(2)-C(7)	1.883(3)	O(16)-H(7A)	0.849(10)
P(1)-O(2)	1.497(2)	N(1)-N(2)	1.095(3)
P(1)-O(1)	1.508(2)	N(1)-C(4)	1.400(4)
P(1)-O(4)	1.560(2)	N(3)-N(4)	1.091(3)
P(1)-O(3)	1.562(2)	N(3)-C(10)	1.401(4)
P(2)-O(8)	1.5044(18)	C(1)-C(2)	1.390(4)
P(2)-O(6)	1.529(2)	C(1)-C(6)	1.397(4)
P(2)-O(7)	1.548(2)	C(2)-C(3)	1.377(4)
P(2)-O(5)	1.553(2)	C(2)-H(2)	0.9500
P(3)-O(9)	1.501(2)	C(3)-C(4)	1.396(4)
P(3)-O(11)	1.502(2)	C(3)-H(3)	0.9500
P(3)-O(10)	1.566(2)	C(4)-C(5)	1.390(4)
P(3)-O(12)	1.569(2)	C(5)-C(6)	1.373(4)
P(4)-O(14)	1.502(2)	C(5)-H(5)	0.9500
P(4)-O(13)	1.512(2)	C(6)-H(6)	0.9500
P(4)-O(15)	1.558(2)	C(7)-C(12)	1.386(4)
P(4)-O(16)	1.565(2)	C(7)-C(8)	1.391(4)
O(2)-H(9A)	0.848(10)	C(8)-C(9)	1.373(4)
O(3)-H(1A)	0.848(10)	C(8)-H(8)	0.9500
O(4)-H(2A)	0.849(10)	C(9)-C(10)	1.389(4)
O(5)-H(3A)	0.852(10)	C(9)-H(9)	0.9500
O(6)-H(10A)	0.850(10)	C(10)-C(11)	1.392(4)
O(7)-H(4A)	0.849(10)	C(11)-C(12)	1.374(4)
O(10)-H(6A)	0.851(10)	C(11)-H(11)	0.9500
O(12)-H(5A)	0.851(10)	C(12)-H(12)	0.9500

Table A3: Bond length (\AA)

O(2)-P(1)-O(1)	116.87(11)	C(2)-C(1)-C(6)	122.8(3)
O(2)-P(1)-O(4)	108.56(13)	C(2)-C(1)-Br(1)	118.9(2)
O(1)-P(1)-O(4)	107.22(12)	C(6)-C(1)-Br(1)	118.3(2)

O(2)-P(1)-O(3)	107.48(13)	C(3)-C(2)-C(1)	119.4(3)
O(1)-P(1)-O(3)	109.10(12)	C(3)-C(2)-H(2)	120.3
O(4)-P(1)-O(3)	107.25(11)	C(1)-C(2)-H(2)	120.3
O(8)-P(2)-O(6)	114.44(12)	C(2)-C(3)-C(4)	116.6(3)
O(8)-P(2)-O(7)	112.22(11)	C(2)-C(3)-H(3)	121.7
O(6)-P(2)-O(7)	105.94(12)	C(4)-C(3)-H(3)	121.7
O(8)-P(2)-O(5)	108.28(11)	C(5)-C(4)-C(3)	125.1(3)
O(6)-P(2)-O(5)	106.62(13)	C(5)-C(4)-N(1)	116.9(2)
O(7)-P(2)-O(5)	109.11(13)	C(3)-C(4)-N(1)	118.0(3)
O(9)-P(3)-O(11)	115.56(13)	C(6)-C(5)-C(4)	117.2(3)
O(9)-P(3)-O(10)	110.42(11)	C(6)-C(5)-H(5)	121.4
O(11)-P(3)-O(10)	107.34(12)	C(4)-C(5)-H(5)	121.4
O(9)-P(3)-O(12)	109.42(14)	C(5)-C(6)-C(1)	118.9(3)
O(11)-P(3)-O(12)	106.44(13)	C(5)-C(6)-H(6)	120.6
O(10)-P(3)-O(12)	107.28(12)	C(1)-C(6)-H(6)	120.6
O(14)-P(4)-O(13)	115.50(12)	C(12)-C(7)-C(8)	122.6(3)
O(14)-P(4)-O(15)	108.15(12)	C(12)-C(7)-Br(2)	119.1(2)
O(13)-P(4)-O(15)	109.68(12)	C(8)-C(7)-Br(2)	118.3(2)
O(14)-P(4)-O(16)	110.00(12)	C(9)-C(8)-C(7)	119.3(3)
O(13)-P(4)-O(16)	106.08(12)	C(9)-C(8)-H(8)	120.3
O(15)-P(4)-O(16)	107.12(12)	C(7)-C(8)-H(8)	120.3
P(1)-O(2)-H(9A)	125(2)	C(8)-C(9)-C(10)	117.0(3)
P(1)-O(3)-H(1A)	116(3)	C(8)-C(9)-H(9)	121.5
P(1)-O(4)-H(2A)	119(3)	C(10)-C(9)-H(9)	121.5
P(2)-O(5)-H(3A)	117(3)	C(9)-C(10)-C(11)	124.7(3)
P(2)-O(6)-H(10A)	121(3)	C(9)-C(10)-N(3)	116.7(3)
P(2)-O(7)-H(4A)	113(3)	C(11)-C(10)-N(3)	118.5(3)
P(3)-O(10)-H(6A)	118(3)	C(12)-C(11)-C(10)	117.1(3)
P(3)-O(12)-H(5A)	119(2)	C(12)-C(11)-H(11)	121.4
P(4)-O(15)-H(8A)	119(2)	C(10)-C(11)-H(11)	121.4
P(4)-O(16)-H(7A)	117(2)	C(11)-C(12)-C(7)	119.3(3)
N(2)-N(1)-C(4)	178.5(3)	C(11)-C(12)-H(12)	120.4
N(4)-N(3)-C(10)	178.8(3)	C(7)-C(12)-H(12)	120.4

Table A4: Bond angles (°)

Atoms	U11	U22	U33	U23	U13	U12
Br(1)	27(1)	23(1)	15(1)	-6(1)	1(1)	-6(1)
Br(2)	31(1)	21(1)	25(1)	7(1)	2(1)	5(1)
P(1)	12(1)	13(1)	13(1)	1(1)	0(1)	-1(1)
P(2)	12(1)	12(1)	16(1)	0(1)	-1(1)	0(1)
P(3)	15(1)	13(1)	12(1)	0(1)	2(1)	0(1)
P(4)	14(1)	13(1)	13(1)	-3(1)	1(1)	-2(1)
O(1)	12(1)	17(1)	21(1)	9(1)	-1(1)	-1(1)
O(2)	25(1)	31(1)	11(1)	-3(1)	-1(1)	-9(1)
O(3)	13(1)	16(1)	23(1)	5(1)	4(1)	2(1)
O(4)	17(1)	12(1)	22(1)	-2(1)	3(1)	-1(1)
O(5)	15(1)	12(1)	36(1)	1(1)	-6(1)	-1(1)
O(6)	19(1)	25(1)	13(1)	-1(1)	-2(1)	3(1)
O(7)	15(1)	26(1)	14(1)	-2(1)	2(1)	-5(1)
O(8)	14(1)	16(1)	13(1)	3(1)	0(1)	0(1)
O(9)	17(1)	41(2)	16(1)	-6(1)	0(1)	7(1)
O(10)	16(1)	17(1)	12(1)	1(1)	2(1)	3(1)
O(11)	39(1)	22(1)	17(1)	5(1)	7(1)	-1(1)
O(12)	31(1)	17(1)	27(1)	-6(1)	16(1)	-10(1)
O(13)	30(1)	18(1)	16(1)	2(1)	0(1)	-6(1)
O(14)	15(1)	15(1)	23(1)	-7(1)	0(1)	-1(1)
O(15)	19(1)	14(1)	24(1)	1(1)	10(1)	3(1)
O(16)	14(1)	30(1)	18(1)	-12(1)	3(1)	-4(1)
N(1)	13(1)	12(1)	17(1)	2(1)	0(1)	1(1)
N(2)	18(1)	18(1)	25(2)	-2(1)	-3(1)	4(1)
N(3)	18(1)	15(1)	18(1)	-5(1)	0(1)	-4(1)
N(4)	29(2)	20(2)	24(2)	-3(1)	-3(1)	-7(1)
C(1)	13(1)	20(2)	12(1)	-2(1)	4(1)	-5(1)
C(2)	18(2)	18(2)	15(2)	2(1)	-1(1)	0(1)
C(3)	15(1)	14(2)	23(2)	2(1)	5(1)	1(1)
C(4)	14(1)	14(1)	13(2)	-4(1)	2(1)	-2(1)
C(5)	16(1)	14(2)	14(2)	1(1)	-1(1)	2(1)
C(6)	19(2)	12(1)	17(2)	-2(1)	3(1)	0(1)
C(7)	14(1)	18(2)	19(2)	4(1)	7(1)	5(1)
C(8)	23(2)	15(2)	27(2)	-3(1)	7(1)	-1(1)
C(9)	21(2)	16(2)	21(2)	-5(1)	2(1)	-3(1)
C(10)	15(1)	18(2)	14(2)	2(1)	3(1)	2(1)

Atoms	U11	U22	U33	U23	U13	U12
C(11)	17(2)	15(2)	22(2)	-3(1)	2(1)	-2(1)
C(12)	16(2)	21(2)	18(2)	-3(1)	1(1)	0(1)

Table A5: Anisotropic displacement parameters ($\text{\AA}^2 \times 10^3$)

APPENDIX 2 – Calibration curve

Solutions (in acetonitrile + 0.1% TFA v/v) were preparing by dissolving the corresponding amount of material in 25 mL volumetric flasks and analysed by HPLC.

Sample concentration (mg/mL)	HPLC Peak area (225 nm)
0	0
0.53	985.759
0.85	1540.316
1.07	2161.559
1.28	2464.461
1.55	3003.013

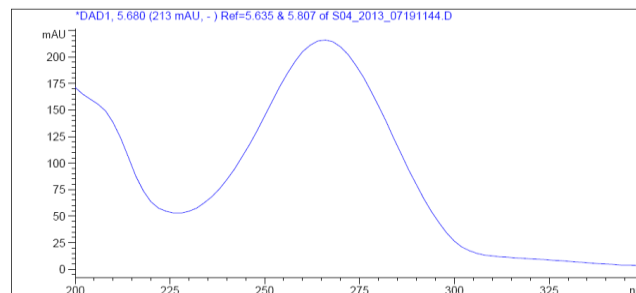
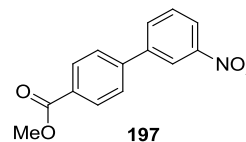


Table A1: Data used for calibration curve

Figure A1: UV spectrum of **197**

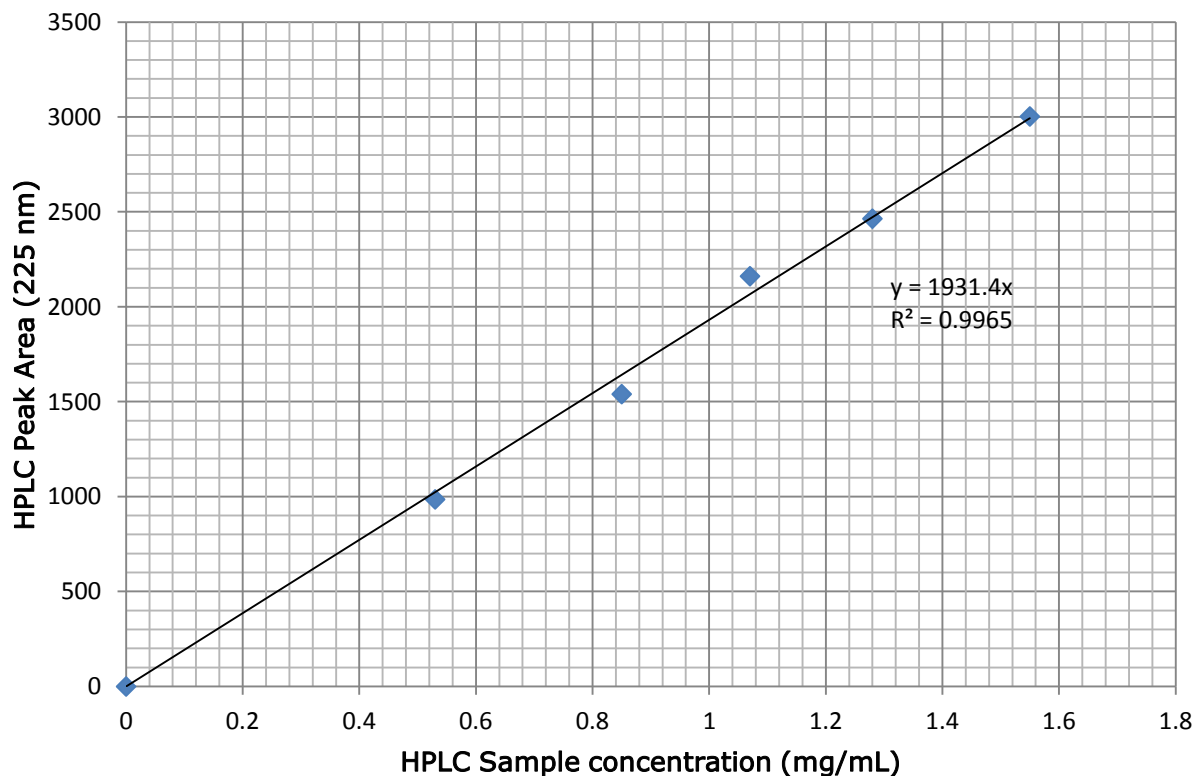
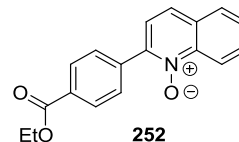


Figure A2: Caibration curve for **197**

APPENDIX 3 – Calibration curve

Solutions (in acetonitrile + 0.1% TFA v/v) were preparing by dissolving the corresponding amount of material in 25 mL volumetric flasks and analysed by HPLC.



Sample concentration (mg/mL)	HPLC Peak area (225 nm)
0	0
0.5	690.655
0.825	1067.759
1.0	1383.025
1.5	1850.923

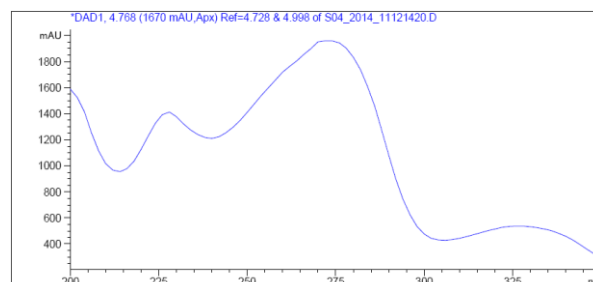


Table A1: Data used for calibration curve

Figure A1: UV spectrum of **252**

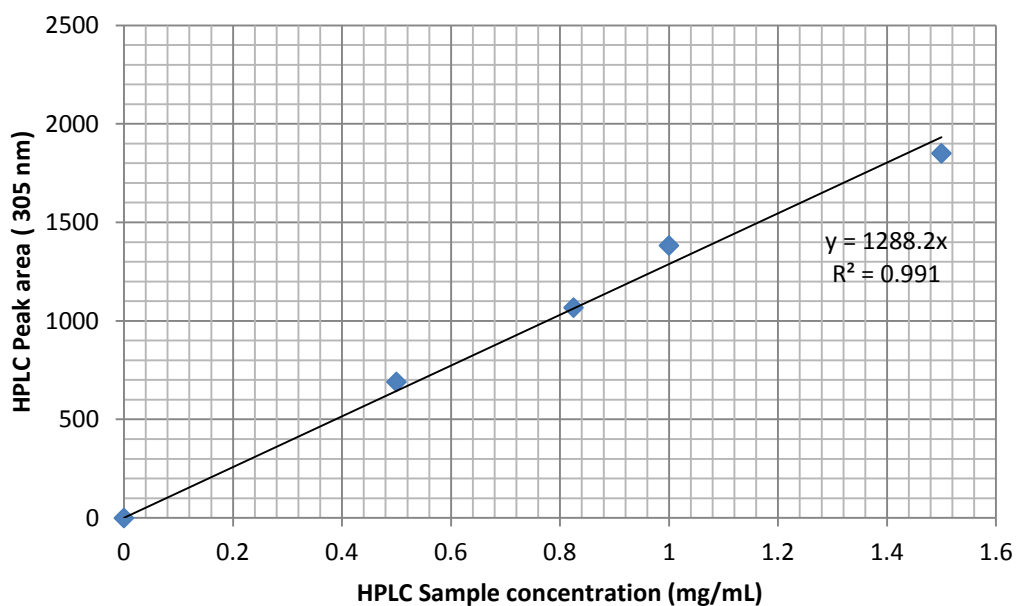
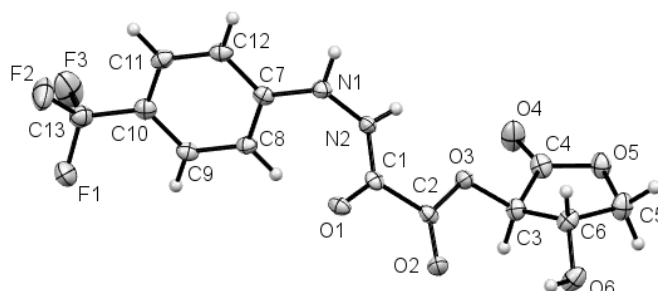


Figure A2: Calibration curve for **252**

APPENDIX 4 – Crystal data

Single crystal X-Ray diffraction report for C₁₃H₁₁F₃N₂O₆ **261**



Crystals were grown by slow diffusion of chloroform into a saturated solution of (3R,4S)-4-hydroxy-2-oxotetrahydrofuran-3-yl-2-(2-(4-(trifluoromethyl)phenyl)hydrazinyl)-2-oxoacetate **261** in acetone.

Empirical formula	C ₁₃ H ₁₁ F ₃ N ₂ O ₆	
Formula weight (g/mol)	348.24	
Temperature (K)	100	
Wavelength (Å)	0.71073	
Crystal system	Orthorhombic	
Space group	P 2 ₁ 2 ₁ 2 ₁	
Unit cell dimensions	a = 5.3216(3) Å	α = 90°
	b = 8.6808(4) Å	β = 90°
	c = 30.2575(14) Å	γ = 90°
Cell volume (Å³)	1397.77	
Z	4	
Calculated density (Mg/m³)	1.655	
Absorption coefficient (mm⁻¹)	0.156	
F₀₀₀	712	
Crystal size (mm³)	0.160 x 0.070 x 0.005	
Absorption correction	Semi-empirical from equivalents	
θ range for data collection (°)	2.441 to 27.469	
Index ranges	-4 ≤ h ≤ 6, -10 ≤ k ≤ 11, -37 ≤ l ≤ 39	
Reflections measured	10050	
Independent reflections	3198 [R(int) = 0.0348]	
Refinement method	Full-matrix least-squares on F ²	
Goodness-of-fit on F²	1.035	
R indices (all data)	R ₁ = 0.0580, wR ₂ = 0.0816	
Largest diff. peak and hole (e.Å⁻³)	0.235 and -0.193	

Table A1: Crystal data and refinement details

Atom	x	y	z	U _{equiv}
C(5)	1719(6)	6160(3)	1420(1)	29(1)
O(3)	968(3)	5411(2)	255(1)	21(1)
F(1)	1480(3)	5704(2)	-2684(1)	37(1)
O(2)	4712(4)	4334(2)	102(1)	25(1)
O(6)	4976(4)	4644(2)	1105(1)	29(1)
O(1)	2494(4)	2969(2)	-628(1)	21(1)
N(1)	-2404(5)	3601(3)	-807(1)	21(1)
N(2)	-1056(4)	4292(3)	-465(1)	19(1)
O(5)	-31(4)	7281(2)	1237(1)	26(1)
C(1)	1296(5)	3844(3)	-389(1)	19(1)
O(4)	-1164(5)	8132(2)	572(1)	37(1)
F(2)	-1716(4)	4352(2)	-2865(1)	47(1)
C(2)	2545(5)	4567(3)	15(1)	19(1)
C(7)	-2068(5)	4186(3)	-1239(1)	19(1)
C(8)	-35(5)	5106(3)	-1354(1)	20(1)
C(9)	323(5)	5517(3)	-1793(1)	21(1)
C(6)	2487(6)	5109(3)	1037(1)	23(1)
C(4)	97(6)	7299(3)	798(1)	24(1)
C(11)	-3396(5)	4137(3)	-1996(1)	23(1)
C(10)	-1339(6)	5028(3)	-2114(1)	22(1)
F(3)	-2149(4)	6739(2)	-2703(1)	55(1)
C(3)	2056(5)	6150(3)	640(1)	22(1)
C(12)	-3762(6)	3711(3)	-1562(1)	22(1)
C(13)	-931(6)	5446(3)	-2587(1)	28(1)

Table A2: Atomic coordinates ($\times 10^4$) and equivalent isotropic displacement parameters ($\text{\AA}^2 \times 10^3$)

C(5)-O(5)	1.457(3)	O(6)-H(1H)	0.87(4)
C(5)-C(6)	1.529(4)	O(1)-C(1)	1.227(3)
C(5)-H(5A)	0.9900	N(1)-N(2)	1.394(3)
C(5)-H(5B)	0.9900	N(1)-C(7)	1.412(3)
O(3)-C(2)	1.329(3)	N(1)-H(1N)	0.88(4)
O(3)-C(3)	1.450(3)	N(2)-C(1)	1.331(4)
F(1)-C(13)	1.335(4)	N(2)-H(2N)	0.83(3)
O(2)-C(2)	1.200(3)	O(5)-C(4)	1.329(3)
O(6)-C(6)	1.400(4)	C(1)-C(2)	1.527(4)

O(4)-C(4)	1.201(3)	C(6)-H(6)	1.0000
F(2)-C(13)	1.335(3)	C(4)-C(3)	1.520(4)
C(7)-C(8)	1.389(4)	C(11)-C(12)	1.379(4)
C(7)-C(12)	1.392(4)	C(11)-C(10)	1.387(4)
C(8)-C(9)	1.390(4)	C(11)-H(11)	0.9500
C(8)-H(8)	0.9500	C(10)-C(13)	1.491(4)
C(9)-C(10)	1.381(4)	F(3)-C(13)	1.342(3)
C(9)-H(9)	0.9500	C(3)-H(3)	1.0000
C(6)-C(3)	1.522(4)	C(12)-H(12)	0.9500

Table A3: Bond length (Å)

O(5)-C(5)-C(6)	106.3(2)	O(6)-C(6)-C(3)	115.5(2)
O(5)-C(5)-H(5A)	110.5	O(6)-C(6)-C(5)	108.3(2)
C(6)-C(5)-H(5A)	110.5	C(3)-C(6)-C(5)	101.8(2)
O(5)-C(5)-H(5B)	110.5	O(6)-C(6)-H(6)	110.3
C(6)-C(5)-H(5B)	110.5	C(3)-C(6)-H(6)	110.3
H(5A)-C(5)-H(5B)	108.7	C(5)-C(6)-H(6)	110.3
C(2)-O(3)-C(3)	115.4(2)	O(4)-C(4)-O(5)	123.2(3)
C(6)-O(6)-H(1H)	112(2)	O(4)-C(4)-C(3)	126.8(3)
N(2)-N(1)-C(7)	117.8(2)	O(5)-C(4)-C(3)	110.0(2)
N(2)-N(1)-H(1N)	110(2)	C(12)-C(11)-C(10)	120.4(3)
C(7)-N(1)-H(1N)	116(2)	C(12)-C(11)-H(11)	119.8
C(1)-N(2)-N(1)	119.1(2)	C(10)-C(11)-H(11)	119.8
C(1)-N(2)-H(2N)	119(2)	C(9)-C(10)-C(11)	119.7(2)
N(1)-N(2)-H(2N)	120(2)	C(9)-C(10)-C(13)	120.4(3)
C(4)-O(5)-C(5)	110.8(2)	C(11)-C(10)-C(13)	119.8(3)
O(1)-C(1)-N(2)	124.6(3)	O(3)-C(3)-C(4)	105.6(2)
O(1)-C(1)-C(2)	120.0(3)	O(3)-C(3)-C(6)	115.6(2)
N(2)-C(1)-C(2)	115.3(2)	C(4)-C(3)-C(6)	104.1(2)
O(2)-C(2)-O(3)	125.4(3)	O(3)-C(3)-H(3)	110.4
O(2)-C(2)-C(1)	121.7(2)	C(4)-C(3)-H(3)	110.4
O(3)-C(2)-C(1)	112.9(2)	C(6)-C(3)-H(3)	110.4
C(8)-C(7)-C(12)	120.0(2)	C(11)-C(12)-C(7)	119.9(3)
C(8)-C(7)-N(1)	122.4(2)	C(11)-C(12)-H(12)	120.1
C(12)-C(7)-N(1)	117.4(2)	C(7)-C(12)-H(12)	120.1
C(7)-C(8)-C(9)	119.6(2)	F(1)-C(13)-F(2)	106.3(2)
C(7)-C(8)-H(8)	120.2	F(1)-C(13)-F(3)	105.5(2)

C(9)-C(8)-H(8)	120.2	F(2)-C(13)-F(3)	106.2(2)
C(10)-C(9)-C(8)	120.4(3)	F(1)-C(13)-C(10)	113.1(2)
C(10)-C(9)-H(9)	119.8	F(2)-C(13)-C(10)	112.6(2)
C(8)-C(9)-H(9)	119.8	F(3)-C(13)-C(10)	112.6(2)

Table A4: Bond angles (°)

Atoms	U11	U22	U33	U23	U13	U12
C(5)	39(2)	24(2)	24(2)	1(1)	-2(1)	7(1)
O(3)	19(1)	24(1)	20(1)	-5(1)	0(1)	3(1)
F(1)	32(1)	52(1)	27(1)	6(1)	4(1)	-4(1)
O(2)	20(1)	33(1)	21(1)	2(1)	-1(1)	4(1)
O(6)	33(1)	24(1)	30(1)	-7(1)	-10(1)	9(1)
O(1)	18(1)	19(1)	26(1)	-4(1)	5(1)	0(1)
N(1)	17(1)	24(1)	22(1)	-3(1)	2(1)	-4(1)
N(2)	16(1)	22(1)	18(1)	-4(1)	2(1)	1(1)
O(5)	34(1)	23(1)	22(1)	-3(1)	2(1)	5(1)
C(1)	20(1)	16(1)	19(1)	3(1)	3(1)	-4(1)
O(4)	49(1)	34(1)	28(1)	2(1)	-1(1)	23(1)
F(2)	60(1)	56(1)	24(1)	-4(1)	-3(1)	-20(1)
C(2)	19(2)	19(1)	19(1)	3(1)	5(1)	0(1)
C(7)	19(2)	14(1)	23(1)	-1(1)	2(1)	4(1)
C(8)	17(1)	20(1)	23(1)	-2(1)	-1(1)	-2(1)
C(9)	19(1)	18(1)	26(2)	2(1)	2(1)	-1(1)
C(6)	26(2)	17(1)	25(1)	-2(1)	-4(1)	0(1)
C(4)	31(2)	17(1)	25(2)	-2(1)	3(1)	-1(1)
C(11)	20(2)	20(1)	27(2)	-3(1)	-4(1)	2(1)
C(10)	23(2)	17(1)	25(1)	-1(1)	0(1)	6(1)
F(3)	64(2)	56(1)	46(1)	26(1)	10(1)	32(1)
C(3)	24(2)	19(1)	22(1)	-2(1)	0(1)	0(1)
C(12)	18(1)	19(1)	29(2)	-1(1)	0(1)	1(1)
C(13)	25(2)	29(2)	29(2)	1(1)	-2(1)	4(1)

Table A5: Anisotropic displacement parameters ($\text{\AA}^2 \times 10^3$)